

Dissertation zur Erlangung des Doktorgrades
der Fakultät für Chemie und Pharmazie
der Ludwig-Maximilians-Universität München

**DnaK Functions as a Central Hub in the E. coli
Chaperone Network**

Taotao Chen

aus Henan, China

2011

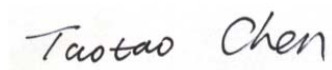
Erklärung

Diese Dissertation wurde im Sinne von §13 Absatz 3 bzw. 4 der Promotionsordnung vom 29. Januar 1998 (in der Fassung der sechsten Änderungssatzung vom 16. August 2010) von Herrn Prof. F. Ulrich Hartl betreut.

Ehrenwörtliche Versicherung

Diese Dissertation wurde selbständig, ohne unerlaubte Hilfsmittel erarbeitet.

München, am 25. 10. 2011



Taotao Chen

Dissertation eingereicht am	25. 10. 2011
1. Gutacher	Prof. Dr. F. Ulrich Hartl
2. Gutacher	Prof. Dr. Walter Neupert
Mündliche Prüfung am	12. 12. 2011

Acknowledgements

First of all, I would like to express my deepest gratitude to Prof. Dr. F. Ulrich Hartl for giving me the opportunity to study and learn the extremely interesting subject in his laboratory. I would like to thank him for the encouragement and the continual support throughout the entire period of my PhD study.

Uncountable thanks go to my direct supervisor Dr. Manajit Hayer-Hartl, Dr. Giulia Calloni, Dr. Sonya Scherrman and Dr. Roman Körner for their invaluable advice and constant support, Especially Dr. Manajit Hayer-Hartl .She is not only a good advisor of my work but also a good mentor in my personal life.

I would like to thank Prof. Dr. Walter Neupert for his help in correcting my dissertation and being the co-referee of my thesis committee.

I thank colleagues in the department of cellular biochemistry for providing accommodative environment to a foreigner like me and many helps. In particular, I would like to thank Andrea, Silke, Evelyn, Elisabeth, Emmanuel, Nadine, Albert, Romy, Andreas and Bernd Grampp for keeping the laboratory at good running. Special thanks to Nadine and Dirk for their excellent technical assistance.

Many great thanks to Andreas.Bracher, Kausik, and Martin for generously sharing their specialty opinions and many insightful discussions. Their friendships and the good working atmosphere became the main basis for the success of this work.

The deepest thanks go to my wife, Jiawen Qin, for her enormous support and patience and valuable discussions. The same deep thanks belong to my parents and my family in China for their understanding and support.

CONTENTS

1	Summary	1
2	Introduction.....	3
2.1	protein stucture.....	3
2.1.1	Protein folding and aggregation.....	5
2.2	The challenge of protein folding in the cell	8
2.3	Molecular chaperone.....	10
2.3.1	Ribosome-associated chaperone -Trigger factor	13
2.3.2	E. coli Hsp70 - DnaK.....	20
2.3.3	E. coli Chaperonin GroEL/ES.....	25
2.3.3.1	Structure and function of GroEL and GroES.....	25
2.3.3.2	Mechanisms of GroEL-mediated protein folding	27
2.3.3.3	Substrates of GroEL.....	31
2.4	Aim of the study.....	32
3	Materials and methods	33
3.1	Materials	33
3.1.1	Chemicals.....	33
3.1.2	Buffers and medium.....	34
3.1.2.1	Buffers.....	34
3.1.2.1	Medium.....	37
3.1.3	Materials and instruments	37
3.1.4	E. coli strains and plasmid	39
3.2	Methods.....	40
3.2.1	DNA analytical methods.....	40
3.2.1.1	General molecular biology methods	40
3.2.1.2	Expressing a chromosomal C-terminally His6-tagged DnaK.....	40
3.2.1.3	Electrocompetent E. coli cells and electroporation.....	41
3.2.2	Protein analytical methods	41
3.2.2.1	Apyrase purification	41
3.2.3	Quantification of proteins	42

3.2.4	SDS-PAGE	42
3.2.5	Western blotting.....	44
3.3	Biochemical and biophysical methods.....	44
3.3.1	Functional analysis of His-tagged DnaK	44
3.3.2	ATP depletion from cell lysate	44
3.3.3	In vivo isolation of DnaK/GrpE/interactor complexes.....	45
3.3.4	Fractionation of the whole cell lysate	46
3.3.5	Expression of Luc-SecM-GFP stalling sequence	46
3.3.6	GroEL/EL depletion.....	47
3.3.7	LC-MS/MS	47
3.4	Analysis of MS data.....	48
3.4.1	Determination of SILAC Ratios	48
3.4.2	Determination of the DnaK interactome.....	49
3.4.3	Determination of the DnaK interactome changes.....	50
3.4.4	Determination of substrate enrichment of DnaK (PD/Lysate SILAC).....	50
3.4.5	Determination of proteome differences between E. coli chaperone mutants	51
3.4.6	Pulse and pulse-chase SILAC.....	52
3.4.7	Bioinformatic analysis	54
4	Results.....	55
4.1	Analysis of DnaK interactome in WT	55
4.1.1	Depletion of ATP from cell lysate	55
4.1.2	Functional examination of cells with his-tagged DnaK.....	57
4.1.3	Isolation and identification of DnaK-bound proteins	59
4.1.4	Properties of DnaK interactome.....	60
4.1.5	Classification of DnaK-interactors by enrichment on DnaK.....	64
4.1.6	specific changes in proteome composition upon DnaK deletion.....	70
4.2	The Kinetics of DnaK and substrates interaction.....	74
4.2.1	DnaK functions in <i>de novo</i> folding and conformational maintenance	74
4.2.2	Protein flux through DnaK.....	78
4.3	Functional redundancy of DnaK and Trigger factor is only partial.....	79
4.4	Interplay of DnaK and GroEL/GroES	84

4.5	Proteostasis collapse upon combined deletion of DanK and TF	90
5	Discussion	101
5.1	Contribution of DnaK chaperone system to protein folding in E. coli	101
5.2	DnaK closely cooperate with Trigger factor	105
5.3	The interplay of the DanK and chaperonion systems.....	107
5.4	DnaKdnaJ and TF are involved in the biogenesis of ribosome.....	108
6	References.....	110
7	Appendices.....	121
7.1	Supplementary tables	121
7.2	List of abbreviations	160
7.3	Publication	163
7.4	Oral presentations	163
7.5	Posters.....	164
7.6	<i>Curriculum vitae</i>	164

1 Summary

Upon emerging from the ribosomal exit tunnel, folding of the polypeptide chain is necessary to form the fully functional protein. In *E. coli*, correct and efficient protein folding is mainly secured by an organized and complex chaperone system which includes two main principles: The first principle consists of the nascent binding chaperones including trigger factor (TF) and the DnaK/DnaJ system, while the second principle is represented by the downstream GroEL/ES chaperonin system. The identification of ~250 natural GroEL substrates demonstrated that GroEL/ES specifically folds a small group of proteins with complex domain topologies (Kerner et al., 2005) which include some essential proteins. Although the structural, functional and mechanistic aspects of DnaK, the *E. coli* Hsp70 chaperone, have been extensively studied, a systematic profiling of the natural DnaK substrates is still missing. Moreover, the cooperation between the two main chaperone systems remains to be elucidated.

Here we analyzed the central role of DnaK in the bacterial chaperone network and its cooperation with the ribosome-associated chaperone TF and the downstream chaperonin GroEL/GroES using SILAC-based proteomics of DnaK-pulldowns. In parallel, we also analyzed the changes at the global proteome level under conditions of single or combined chaperone deletion. Our measurements show that DnaK normally interacts with at least ~700 newly-synthesized and pre-existent proteins (~30 % of all cytosolic proteins), including ~200 aggregation-prone substrates. Individual deletion of TF or depletion of GroEL/ES at 30 °C-37 °C leads to limited but highly specific changes in the DnaK interactome and in global proteome composition. Specifically, loss of TF results in increased interaction of DnaK with ribosomal and other small, basic proteins, and in a specific defect in the biogenesis of outer membrane β -barrel proteins. While deletion of DnaK/DnaJ leads to the degradation or

aggregation of ~150 highly DnaK-dependent proteins of large size, massive proteostasis collapse is only observed upon combined deletion of the DnaK system and TF, and is accompanied by extensive aggregation of GroEL substrates and ribosomal proteins. We conclude that DnaK is a central hub in the cytosolic E. coli chaperone network, interfacing with the upstream TF and the downstream chaperonin. These three major chaperone machineries have partially overlapping and non-redundant functions.

2 Introduction

As the most abundant biological macromolecules, proteins exist in all cells and all parts of cells. Moreover, proteins are the final and essential products of the information transfer from gene to biological function. The most remarkable fact is that, by assembling the same 20 amino acids in many different sequences, cells are able to make proteins with very different properties and activities. From these building elements different organisms are able to form broadly different products, including enzymes, hormones, antibodies, transporters, muscle fibers, the lens protein of the eye, feathers, spider webs, rhinoceros horn, milk proteins, antibiotics, mushroom poisons, and a myriad other substances having diverse biological activities.

2.1 Protein structure

Proteins are bound together with covalent bonds. Moreover, the proper three-dimensional conformation is crucial for the function of a protein. There are 4 levels of protein structure: primary structure, secondary structure, tertiary structure, and quaternary structure.

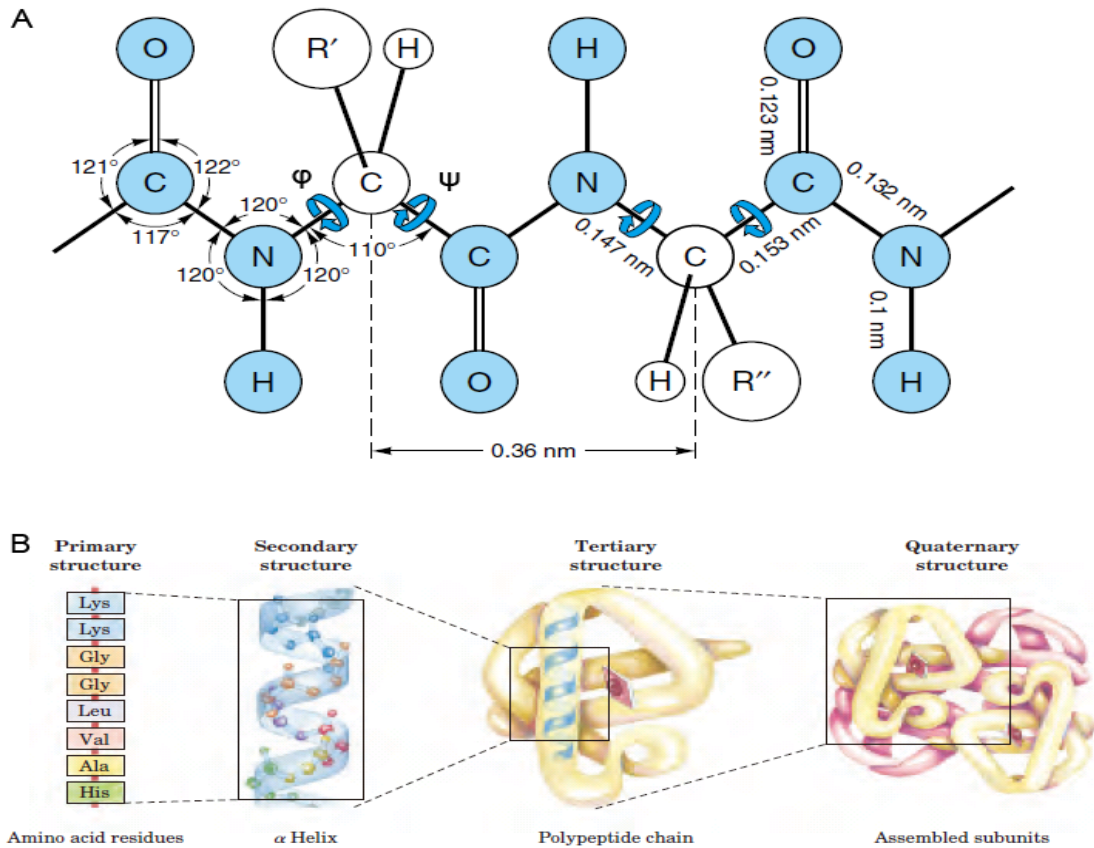


Figure 1 Relative angle in a fully extended polypeptide chain and 4 levels of protein structure.

(A) The four atoms of the peptide bond (colored blue) are coplanar. Free rotation can occur about the bonds that connect the α -carbon with the α -nitrogen and with the α -carbonyl carbon (blue arrows), which are called Φ and Ψ . R indicate the side chain residues of the corresponding amino acid. The different interatomic distances and main bond angles are shown, adapted from (Pauling et al., 1951); (B) The four structural levels of hemoglobin, adapted from (Lehninger et al., 2005).

The primary structure of a protein is its linear amino acid sequence which is translated from the genetic information. The partial double-bond character of the peptide bond between the carbonyl carbon and the nitrogen of adjacent amino acid in a peptide renders the four atoms of the peptide bond coplanar and restricts the number of potential peptide conformations. As the secondary structure is characterized by the particular

spatial arrangement of amino acids which are close in the primary sequence, it directly depends on the rotation angles around the hydrogen bonds (Figure 1). The major secondary structures are α -helix and β -sheet. Different parts of the polypeptide chain, arranged in independent secondary structures, contact each other to form the tertiary structure in three-dimensional space. The tertiary structure describes the entire three-dimensional conformation of a polypeptide.

Proteins with quaternary structure consist of two or more polypeptides interacting in a specific composition and spatial relationship, such as hemoglobin. There are two main types of quaternary structure: fibrous proteins, usually having a single type of polypeptide chain organized in long strands or sheets, and globular proteins, often having different types of polypeptide chains folded into a spherical or globular shape. The conformational stability of a protein is maintained by hydrophobic interactions, electrostatic interactions (van der Waals forces, hydrogen bonds, ionic interactions), covalent linkages (disulfide bridges) and by coordination of metals.

2.1.1 Protein folding and aggregation

In order to be functional, most proteins need to achieve a precise three-dimensional conformation. Although the amino acid sequence of each protein encodes for its spatial conformation (Anfinsen, 1973), how exactly proteins fold to their native state is still an open question.

If protein folding was a totally random event, an extremely long time would be needed for a polypeptide chain to search through every possible conformation before it reaches its native three-dimensional structure in the test tube. For a protein with 100 residues it would take 10^{20} years to try all the $\sim 10^{30}$ possible main chain conformations.

Indeed, the vast majority of proteins in the cell (~ 90%) are larger than 100 amino acids. In fact, protein folding occurs in a relative fast manner (in a second or less) (Dinner et al., 2000). This so-called “Levinthal Paradox” (Karplus, 1997) suggests that there are specific pathways through which a protein reaches its lowest energy state, the so-called “native state”.

With the development of fast mixing and high sensitive spectroscopic measurements, it became clear that even small single domain proteins (~100 amino acids) may have multiple folding pathways. Indeed, a polypeptide could not only directly fold to the native state, but also populate partially folded intermediates (Brockwell and Radford, 2007). The appearance of intermediates might be also part of the answer to the “Levinthal Paradox”. Although the existence and role of intermediates has been debated for the past 50 years, it is not yet completely understood whether they comprise native-like domain and represent stepping stones *en route* to the native state or are misfolded species which still need an extensive reorganization before achievement of the native state (Brockwell and Radford, 2007). The formation of native or non-native interactions during folding is a result of the ruggedness of the funnel-shaped folding energy landscape (Figure 2) (Hartl and Hayer-Hartl, 2009). Whether a certain polypeptide chooses a multi-downhill route or a single smooth pathway may be related to its specific amino acid sequence.

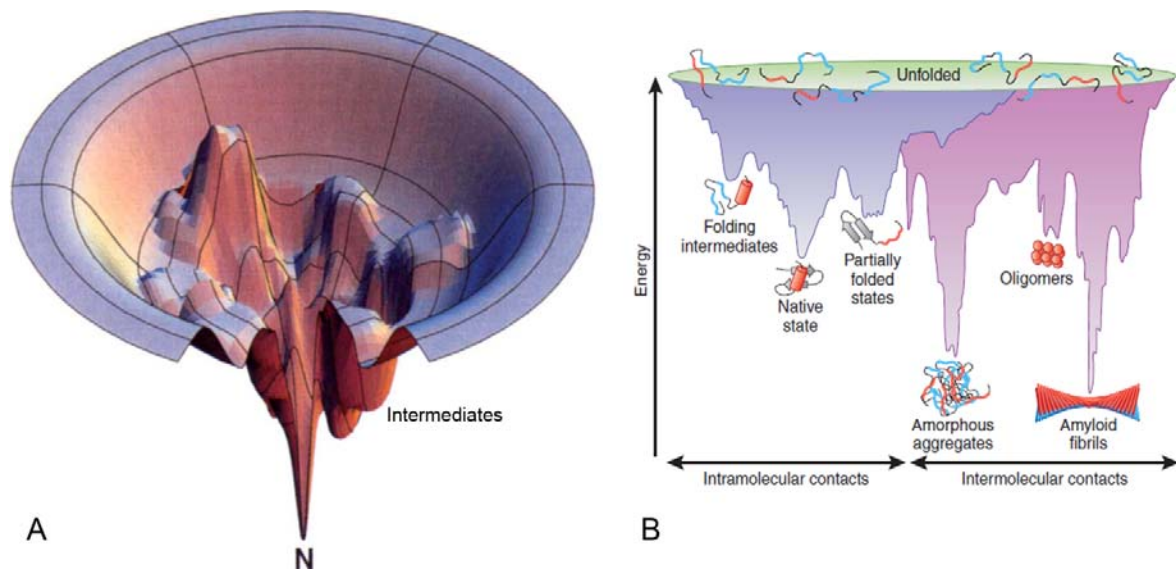


Figure 2 Energy landscape schemes of protein folding and aggregation.

(A) Multistate of protein folding adapted from (Dill and Chan, 1997). (B) The purple surface shows the multitude of conformations ‘funneling’ to the native state via intramolecular contacts and the pink area shows the conformations moving toward amorphous aggregates or amyloid fibrils via intermolecular contacts. Both parts of the energy surface overlap, adapted from (Hartl and Hayer-Hartl, 2009).

Proteins in misfolded or partially folded states tend to aggregate. Their aggregation is energetically favorable, as it is driven by the interaction of exposed hydrophobic amino acid residues and regions of the unstructured backbone which are normally buried in the core of the native state. Moreover the formation of these aggregates is often irreversible (Figure 3). Unstructured polypeptides might interact to form either amorphous aggregates (Figure 2) or highly ordered and fibril-like multimeric structures, known as amyloid, causing cellular toxicity.

2.2 The challenge of protein folding in the cell

Although protein folding can be interpreted from the point of view of physics or chemistry, the crowded environment in the cell add considerable complexity of protein folding. There are two major differences between in vivo and in vitro folding. Firstly, the cell environment is highly crowded and dynamic in comparison with the condition of folding in the test tube. In vitro folding occurs in highly diluted conditions, so that the thermodynamic properties of the unfolded polypeptide are changed and the chance of interaction between folding intermediates is quite low. Thereby spontaneous folding is possible for many proteins in the test tube. The effective concentration of macromolecules, including proteins, nucleic acids and lipids, in *E. coli* cells has been predicted to be around 300~400 mg/ml (Ellis, 2001). This extremely crowded environment gives rise to the so-called excluded volume effect, which directly enhances the formation of aggregates driven by the exposure of hydrophobic amino acids of the folding intermediates.

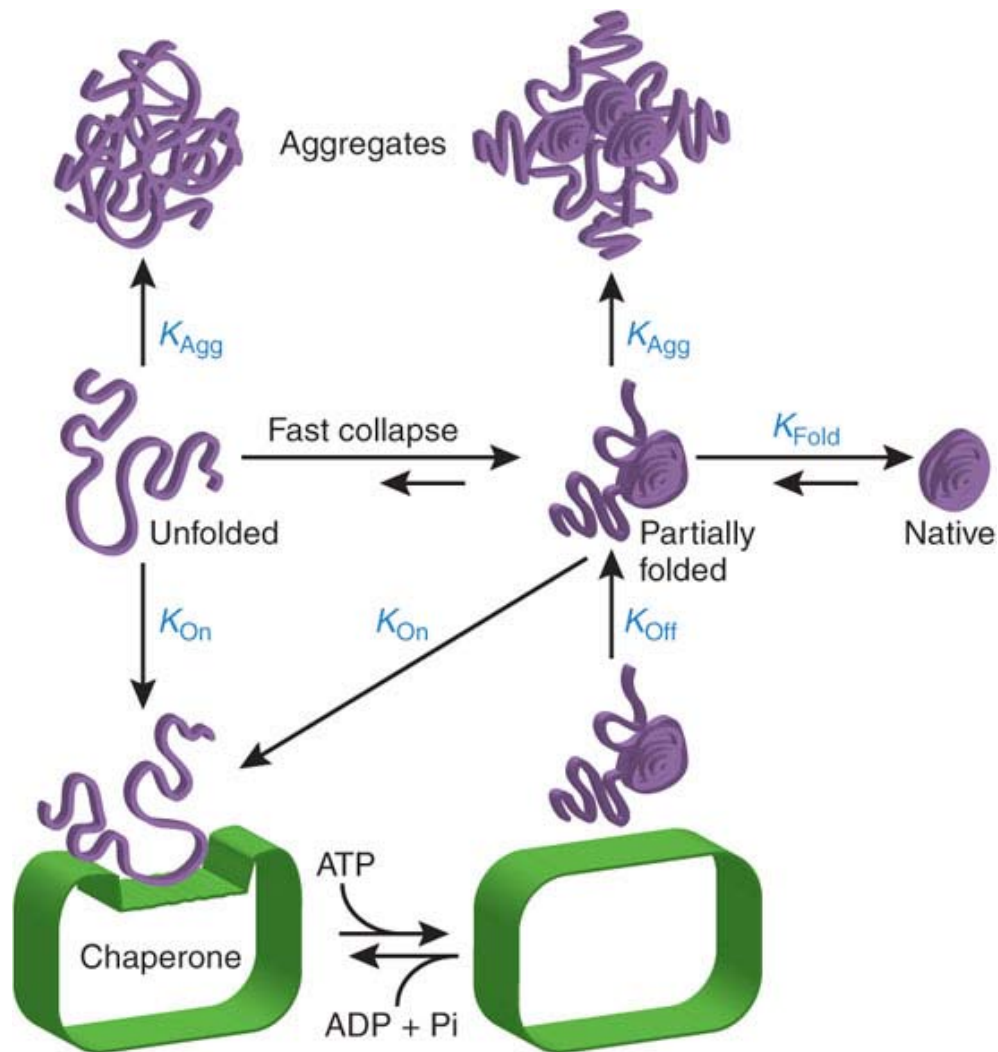


Figure 3 Model of Chaperone function of facilitating protein folding through kinetic partitioning

In the cell, protein folding is featured by mainly two kinetic orders: a. $K_{\text{Fold}} > K_{\text{On}} > K_{\text{Agg}}$; Folding is promoted and aggregation prevented when K_{Fold} is greater than K_{On} for chaperone binding (or rebinding) of partially folded states and when K_{On} is greater than intermolecular association by the higher-order rate constant K_{Agg} ; Under certain conditions (overproduction of slow folding proteins, conformational stress), K_{Agg} may become faster than K_{On} and aggregation occurs ($K_{\text{Agg}} < K_{\text{On}} < K_{\text{Fold}}$), unless chaperone expression is induced via the stress-response pathway, adapted from (Hartl and Hayer-Hartl, 2009; Hoffmann et al., 2010).

Secondly, productive folding can happen only after the complete polypeptide or at least a single domain (50~300 amino acids) has been synthesized and available outside the ribosome exit tunnel (Hartl and Hayer-Hartl, 2009). Consequently, premature (mis)folding might start already at the level of the incomplete nascent chain.

2.2 Molecular chaperone

A molecular chaperone was originally defined as a protein which interacts, stabilizes or facilitates a non-native polypeptide to achieve its native state but which is not present in the final structure (Ellis, 1987). Nowadays molecular chaperones are known to be involved in more diverse cellular processes, such as refolding or degradation of stress-denatured or aggregated proteins, assisting assembly of oligomeric complexes and protein transport. Part of the cellular proteome can reach its functional conformation only by reversible binding with a molecular chaperone. For example, DapA and MetK, which are typical substrates of GroEL in *E. coli*, are unable to fold to their native states when GroEL is depleted in the cell (Kerner et al., 2005). A chaperone system like GroEL/GroES not only supplies a favorable environment but also positively acts to optimize the efficiency of the folding process. There is a group of essential proteins in *E. coli* that are obligate substrates of this essential chaperone system. Furthermore, GroEL plays an important role in buffering the mutations accumulating in its substrate protein sequences thereby facilitating protein evolution (Tokuriki and Tawfik, 2009)

To date, a large number of chaperones have been found some of them well-studied in Bacteria, Archaea and Eukarya (Chang et al., 2007; Tang et al., 2007). More chaperones will be discovered with the advancement of technology and the increasing understanding of central biological process. Chaperones in the cell can be classified into

different groups based on various criteria. Firstly, there are constitutively expressed chaperones, mainly active in *de novo* protein folding, and chaperones induced by conformational stress, the so-called Heat Shock Proteins (HSPs) which are in charge of reducing the deleterious effect of increased aggregation of folding intermediates. DnaK (Hsp70), ClpB (Hsp100) and GroEL (Hsp60) are not only constitutively expressed chaperones but also stress induced proteins in *E. coli*. A second classification criterion names chaperones according to their molecular weight (Hsp40, Hsp60, Hsp70, Hsp90, Hsp100 and the so-called small Hsp proteins).

Additionally, chaperones can be differentiated according to their position in the folding pathway of newly synthesized proteins *in vivo*. Chaperones which bind to the translating ribosome normally contact the nascent chain earlier than other chaperones. Such ribosome-associated chaperones that interact with the large ribosomal subunit near the peptide exit tunnel belong to the upstream components of protein folding machinery and work by stabilizing the nascent chain on the ribosome and initiating protein folding (Kramer et al., 2009). Examples of this class of chaperones are trigger factor in bacteria (Figure 4), RAC (ribosome-associated complex), composed of the Hsp70 homolog of Ssb1 (or Ssb2), Ssz1 and the Hsp40 homolog zuotin in *S. cerevisiae*, Hsp70L1 and Mpp11, homologs of Ssz1 and zuotin (Hundley et al., 2005) and NAC (nascent chain-associated complex) in archaea and eukarya.

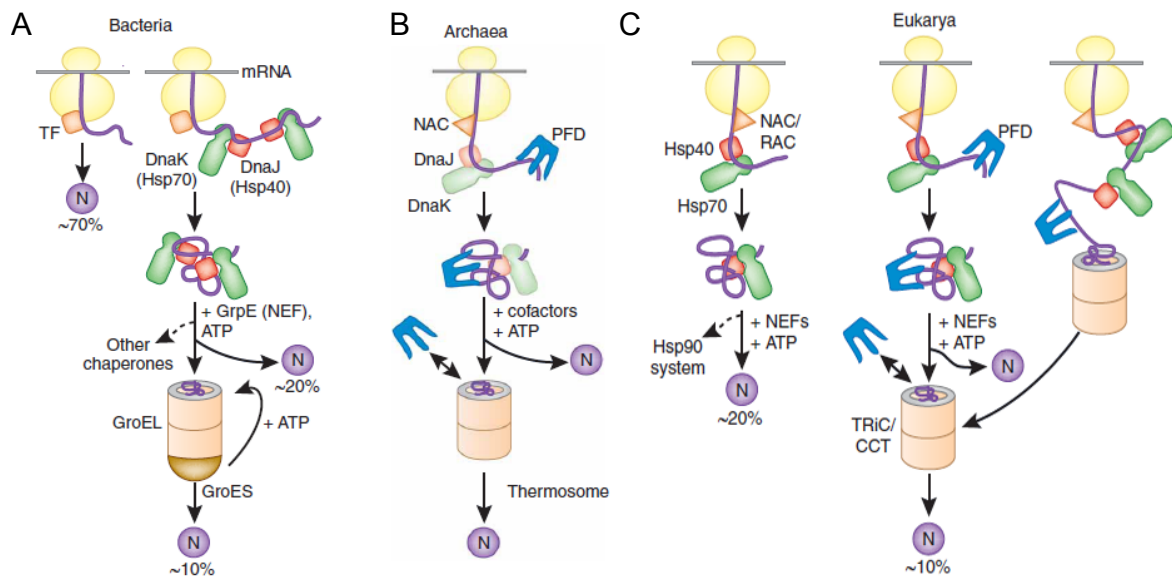


Figure 4 Models of protein folding in the cytosol with the assistance of chaperones

(A) Bacteria. Nascent chains probably interact generally with trigger factor (TF), and most small proteins (~70% of total) may fold rapidly upon synthesis without more assistance. Longer chains interact subsequently with DnaK and DnaJ (Hsp70 system) and fold upon one or several cycles of ATP-driven binding and release (~20% of total). About 10% of chains transit the chaperonin system (GroEL and GroES) for folding. N, native protein. (B) Archaea. PFD, prefoldin; NAC, nascent chain-associated complex. Only some archaeal species contain DnaK and DnaJ. (C) Eukarya. As TF, NAC probably interacts normally with nascent chains, however the role of NAC in folding is not yet clear. About 20% of chains reach their native states in a reaction assisted by RAC (ribosome-associated complex), Hsp70 and Hsp40. A fraction of these must be transferred to Hsp90 for folding. About 10% of chains are co- or post-translationally passed on to the chaperonin TRiC/CCT in a reaction mediated by Hsp70 and PFD, both of which interact directly with TRiC/CCT, adapted from (Hartl and Hayer-Hartl, 2009).

The downstream chaperones bind the nascent chain with or without replacing ribosome-associated chaperones when longer tracts of the nascent polypeptides have been translated. For example, Hsp70s, including DnaK in bacteria and Hsc70 in eukaryotes, especially facilitate multidomain protein folding by preventing premature polypeptide collapse, the reducing unwanted interdomain interactions and finally orientating the

nascent chain towards other downstream chaperones such as the chaperonins (Hsp60s) and Hsp90 (Wandinger et al., 2008). The chaperonins, such as bacterial GroEL (Tang et al., 2006) and TRiC/CCT in eukarya (Yam et al., 2008), are large cylindrical complexes that function by enclosing protein molecules, one at a time, in a cage-like isolated nanocompartment, so that folding can occur unimpaired by aggregation.

Besides the salient role in protein folding, a set of chaperones has specialized to aid the assembly of large oligomeric complexes, like in the case of RbcX, which is required for the assembly of hexadecameric Rubisco, (Ellis, 2006; Liu et al., 2010; Saschenbrecker et al., 2007). In the same line, trigger factor, DnaK and DnaJ may also involve in the assembly of ribosomal subunit in *E. coli* (Al Refaii and Alix, 2009; Karbstein, 2010; Maki et al., 2002; Martinez-Hackert and Hendrickson, 2009). In yeast, the chaperones ribosome-associated complex (RAC), nascent chain-associated complex (NAC), and Jjj1 play important roles in assisting ribosome assembly (Albanese et al., 2010; Koplín et al., 2010).

Rather than working separately, different chaperones contribute to a highly complicated and intertwined network and collaborate through specialized functions to maintain the cellular protein homeostasis (proteostasis), even in organisms as simple as Bacteria (Figure 4) (Balch et al., 2008; Teter et al., 1999).

The following sections will describe the major chaperone paradigms in *E. coli*.

2.3.1 Ribosome-associated chaperone -Trigger factor

Trigger factor (TF) is the only well-studied Ribosome-associated chaperone in bacteria. The 48 kDa protein is composed of three domains: an N-terminal ribosome-binding

domain, a peptidyl-prolyl *cis/trans* isomerase (PPIase) and a C-terminal domain TF has an overall dimension of $122 \times 59 \times 63$ Å (Ferbitz et al., 2004; Hoffmann et al., 2010).

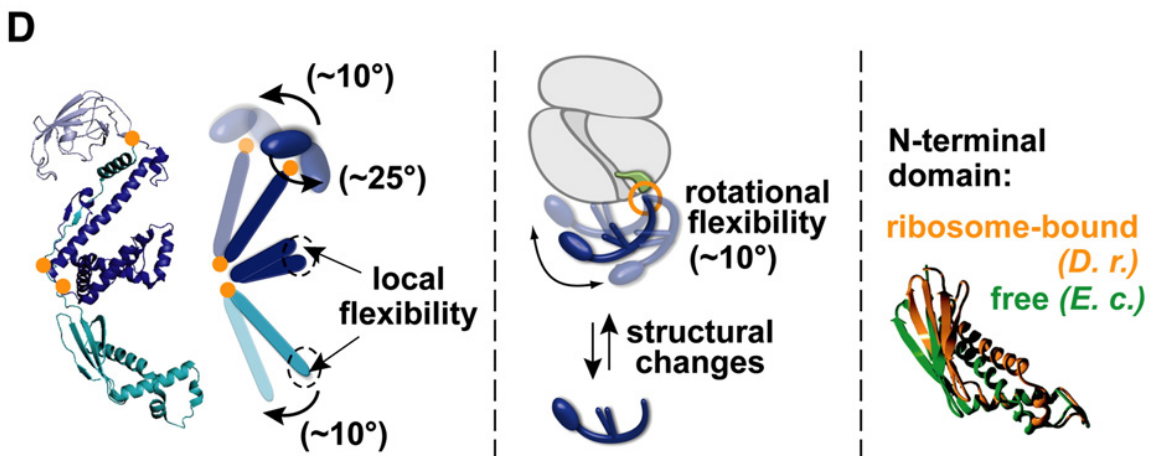
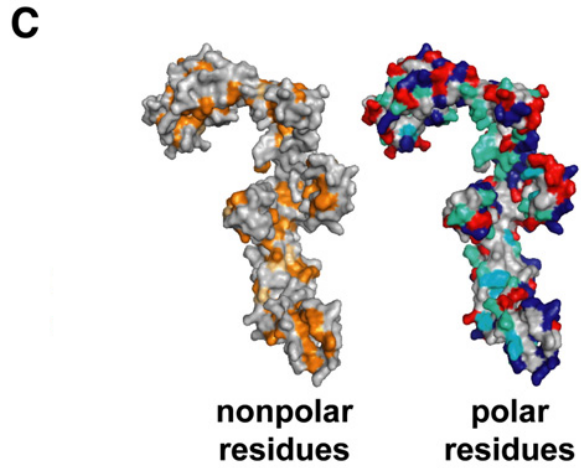
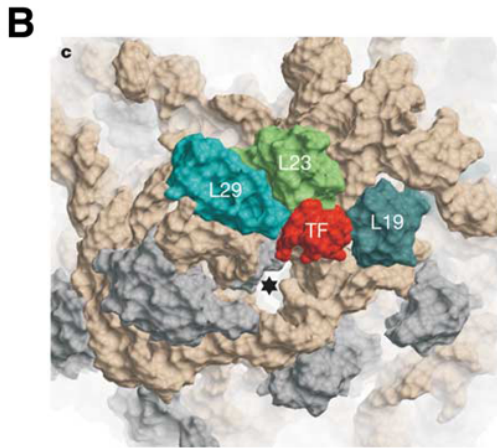
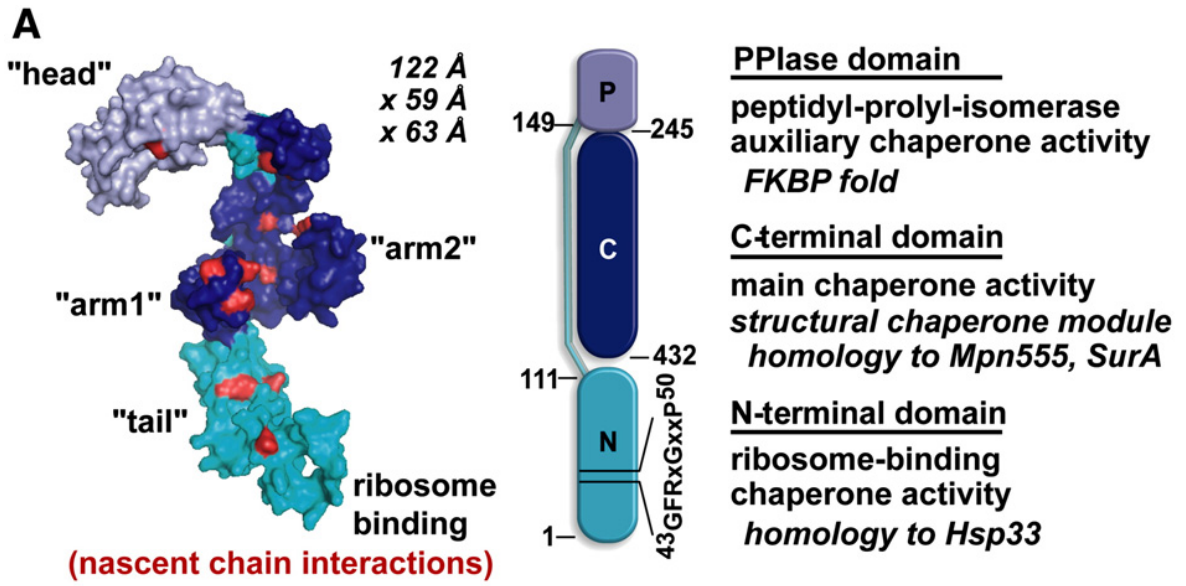


Figure 5 Structure of Trigger factor.

(A) Relative 3D position of three domains The N-terminal domain (N; cyan), the PPIase domain (P, light blue), and the C-terminal domain (C, dark blue) Identified nascent chain interaction sites are highlighted in red. The ribosome binding signature-motif (“GFRxGxxP”) is noted. (B) Bottom view of TF and ribosome complex; trigger factor fragment is shown as a red surface representation and the peptide exit tunnel is denoted with an asterisk. (C) Surface characteristics of TF (PDB 1W26). View onto the cavity-forming interaction surfaces of the N- and C-terminal domains of TF. (Left) Non-polar residues are marked in orange (Ala, Leu, Ile, Phe, Trp, Val) and light orange (Pro). (Right) Polar residues are colored in red (Asp, Glu), blue (Arg, His, Lys), greencyan (Asn, Gln, Ser, Thr) and cyan (Tyr). (D) Model of flexibility and conformational rearrangements within TF, adapted from (Ferbitz et al., 2004; Hoffmann et al., 2010).

In the 3D structure, the C-terminal domain is located between the N-terminal and PPIase domains (Figure 5A). TF signature motif (“GFRxGxxP”) located in the N-terminal domain (aa 1-110) binds to the ribosomal proteins L23 and L29 and to the 23S RNA near the polypeptide exit tunnel (Figure 5B). Although the binding site on the ribosome is crucial for efficient TF function (Schlunzen et al., 2005), TF is able to work independent of ribosome association (Martinez-Hackert and Hendrickson, 2009). After a long linker (aa 111-149), the PPIase domain (aa 150-245) is positioned at the head of the dragon-shaped TF. Even if the PPIase domain is dispensable, it does enhance the TF chaperone activity and may provide additional substrate binding sites (Kaiser et al., 2006; Kramer et al., 2004; Lakshmipathy et al., 2007). Up to date the major function of the PPIase domain still remains unclear.

The C-terminal domain (aa 246-432), which is the main chaperone module of TF, shapes an opened space with two protruding helical “arms” (Ferbitz et al., 2004). The substrate forms extensive interaction in such inner, cavity-forming space or surface rather

than binding to a particular substrate binding site (Figure 5C) (Ferbitz et al., 2004; Martinez-Hackert and Hendrickson, 2009).

TF is highly flexible in the free, substrate binding and ribosome binding states (Figure 5D) (Baram et al., 2005; Ferbitz et al., 2004; Martinez-Hackert and Hendrickson, 2009). The intradomain flexibility may facilitate substrate binding, enable the cooperation with different chaperones and allow the transition between the different functional states of TF (Hoffmann et al., 2010).

E. coli TF is very abundant, expressed constitutively and is not induced even upon considerable heat-stress (45 °C). However, recently TF was found to be strongly induced in the antarctic bacterium *Pseudoalteromonas haloplanktis* growing at a low temperature (4 °C). Under such conditions TF is the main functional chaperone (Piette et al., 2010). In the *E. coli* cytosol TF (~50 μM) is present in a ~ two-fold molar excess over ribosomes (Crooke et al., 1988). Nevertheless, TF is dispensable under normal growth conditions (Martinez-Hackert and Hendrickson, 2009).

TF associates with ribosomes in 1:1 stoichiometry, such that TF is presumably able to contact a multitude of nascent chains (Lill et al., 1988). TF performs its chaperone activity in an ATP-independent and highly dynamic cycle of binding and dissociation. In vitro ribosome-free TF is in fast dimer-monomer equilibrium with K_d of ~1 μM (Kaiser et al., 2006; Maier et al., 2003). The free TF will bind to the ribosome with a mean residence time ~ 10 s. When the nascent chain emerges from the ribosome exit tunnel, TF binds to it and promotes cotranslational folding (Figure 6).

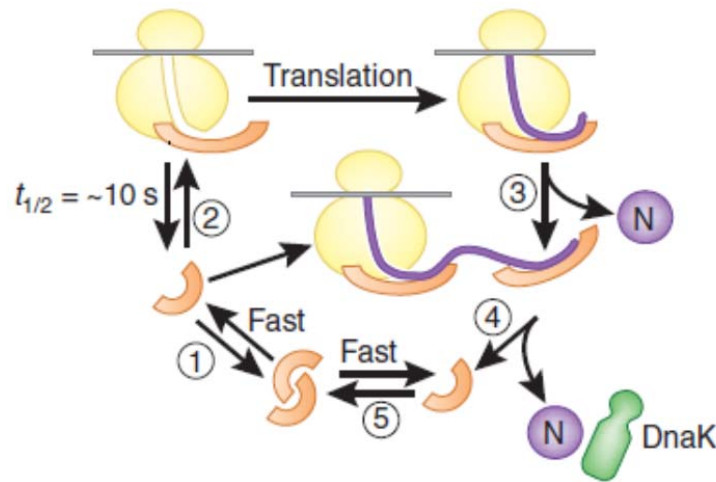


Figure 6 Model of Trigger factor functional cycle

(1) There is fast equilibrium of TF between monomeric and dimeric states. (2) Free TF monomer binds to nontranslating ribosomes with a mean time of ~ 10 s. (3) Nascent chains which bind weakly with TF might begin to compact co-translationally near TF. For certain proteins ribosome, nascent chain and TF dissociates simultaneously. (4) However multidomain protein may intact firmly with TF, even after the nascent chain has dissociated from the ribosome. Finally the nascent chain may be delivered to the downstream chaperone DnaK for further folding. (5) Released free TF monomer will join the monomer-dimer cycle, adapted from (Hartl and Hayer-Hartl, 2009).

Furthermore, for certain proteins, such as multidomain proteins, TF can continue to bind to the elongating nascent chain for an extended time (up to >30 s) in order to facilitate the entry of new free TF on the ribosome on one hand, and with the effect of retarding folding with respect to translation on the other hand (Kaiser et al., 2006). Strikingly a novel function of TF has emerged from the study of *Thermotoga maritima* TF (*tmTF*). Ribosome-free *tmTF* is able to bind and stabilize in vivo the native ribosome protein *tmS7*, and might be involved in assisting the assembly of ribosomal proteins in the large ribosome complex (Martinez-Hackert and Hendrickson, 2009).

Peptide library experiments showed that TF has high specificity for unfolded proteins and high affinity for hydrophobic amino acid sequences, especially ones containing aromatic residues and flanked by positively charged amino acids (Patzelt et al., 2001). Fluorescence Resonance Energy Transfer (FRET) studies show that the hydrophobic motif is important in modulating substrate binding to TF (Kaiser et al., 2006). Although TF does bind the highly hydrophobic signal sequences for either Sec- or Tat-mediated protein transport, it may not be crucial for the folding of these substrates, except for certain specific proteins (Eisner et al., 2003; Jong et al., 2004; Natale et al., 2008). TF may be a cofactor of SecB or SRP (Signal Recognition Particle) for directing proteins carrying signal peptide sequences to the membrane. However, the loss of TF can be compensated for by other chaperones. Recently the crystal structure of *tmTF* and *tmS7* was solved (Martinez-Hackert and Hendrickson, 2009), surprisingly showing that weak hydrophilic contacts are also important in maintaining the interaction between *tmS7* and TF.

DnaK and GroEL are well-known cooperation partners of TF in *de novo* folding. Under physiological conditions, the cellular concentration of ribosome, TF, DnaK and GroEL complex results in a ratio of 1:2:1:0.15 (Ewalt et al., 1997; Hesterkamp and Bukau, 1998; Lill et al., 1988). Although TF is dispensable under normal conditions, TF is essential above 30 °C when the cells lack DnaK (Deuerling et al., 1999; Teter et al., 1999). Furthermore, a large amount of visible aggregation was present in $\Delta dnaK dnaJ \Delta tig$ cells in comparison with only few aggregates in Δtig (Deuerling et al., 2003; Deuerling et al., 1999). Interestingly, this effect can be partly complemented by elevating the level of the GroEL/ES system (Genevaux et al., 2004; Vorderwulbecke et

al., 2005). Unlike DnaK and GroEL, the potential specific TF substrates tend to be small polypeptide chains (< 30 kDa) (Teter et al., 1999). Although a solid cooperation among TF, DnaK and GroEL has repetitively been postulated, how and when each of them hands over the folding task in *de novo* folding remains to be investigated.

2.3.2 E. coli Hsp70 – DnaK

DnaK, the major E. coli Hsp70, originally identified in DNA replication, is involved in various cellular functions including *de novo* folding, translocation, disaggregation and assembly of oligomeric complexes (Al Refaii and Alix, 2009; Glover and Lindquist, 1998; Saito and Uchida, 1978; Teter et al., 1999; Yochem et al., 1978). For its central position in the folding pathway of newly synthesized proteins, DnaK might represent the crucial hub to coordinate the cellular chaperone network in E. coli (Hartl and Hayer-Hartl, 2009; Mayer and Bukau, 2005). The function of DnaK is basically conserved in eukaryotes, with the constitutive Hsc70 and the heat shock inducible Hsp70 in mammalian cells, and Ssa1 in *Saccharomyces cerevisiae* (Daugaard et al., 2007; Hartl and Hayer-Hartl, 2009; Young, 2010). Like most Hsp70s, DnaK works with an Hsp40 co-chaperone (DnaJ) and a nucleotide-exchange factor (GrpE) that regulate the ATP-dependent DnaK functional cycle.

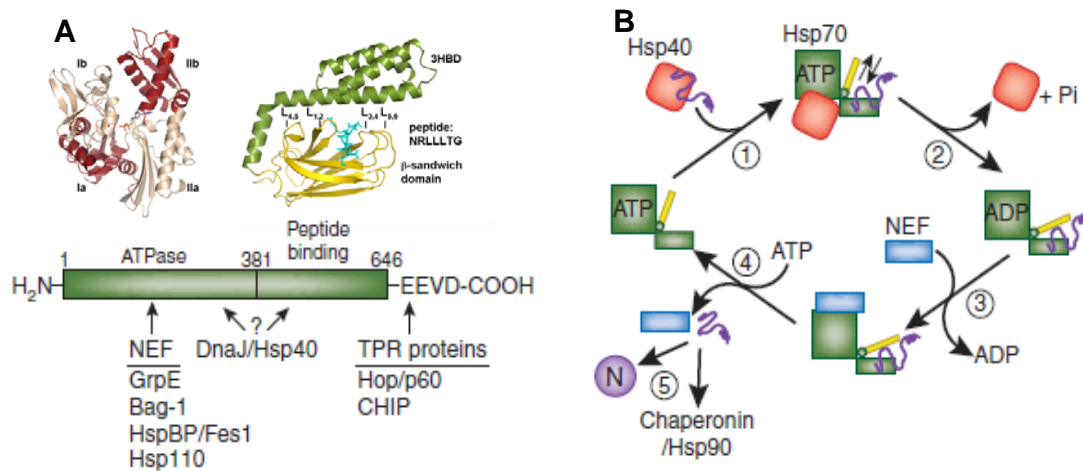


Figure 7 Hsp70 chaperone system.

(A) Structures of the nucleotide-binding domain and the substrate-binding domain of Hsp70 shown separately for DnaK. The α -helical lid of the SBD is shown in green and the extended peptide substrate as a ball-and-stick model in cyan. ATP indicates the position of the nucleotide-binding site. The amino acid sequence of the peptide is indicated. The interaction of prokaryotic and eukaryotic cofactors with Hsp70 is shown schematically. Residue numbers refer to human Hsp70. Only the Hsp70 proteins of the eukaryotic cytosol have the COOH-terminal sequence EEVD, which is involved in binding of tetratricopeptide repeat (TPR) cofactors. (B) Hsp70 reaction cycle. NEF, nucleotide-exchange factor (GrpE in case of *E. coli* DnaK; Bag, HspBP1 and Hsp110 in case of eukaryotic cytosolic Hsp70). (1) Hsp40-mediated transmission of substrate to ATP-bound Hsp70. (2) Hydrolysis of ATP to ADP, enhanced by Hsp40, results in closing of the α -helical lid and tight binding of substrate by Hsp70. Hsp40 dissociates from Hsp70. (3) Dissociation of ADP triggered by NEF. (4) Opening of the α -helical lid, induced by ATP binding, results in substrate release. (5) Released substrate either folds to native state (N), is transmitted to downstream chaperones or rebinds to Hsp70, adapted from (Hartl and Hayer-Hartl, 2009).

DnaK, which is composed of 638 amino acids, consists of two functional domains connected by a hydrophobic linker (aa 389-392): an N-terminal nucleotide-binding domain (NBD) (aa 1-388) and a C-terminal substrate binding domain (SBD) which consists of a β -sandwich subdomain and a α -helical lid segment (aa 393-638) (Hartl and

Hayer-Hartl, 2009; Swain et al., 2007). Up to date the crystal structure of full length DnaK is not available, probably because of the flexible linker region between two domains. However, the crystal structure of the two separated domains has been solved (Figure 7) (Harrison et al., 1997; Zhu et al., 1996).

Recently, the structure in solution of the full-length DnaK bound to ADP and substrate was solved by using NMR residual dipolar coupling (RDC) (Figure 8) (Bertelsen et al., 2009). The NBD and SBD are loosely linked and are able to move in cones of $\pm 35^\circ$.

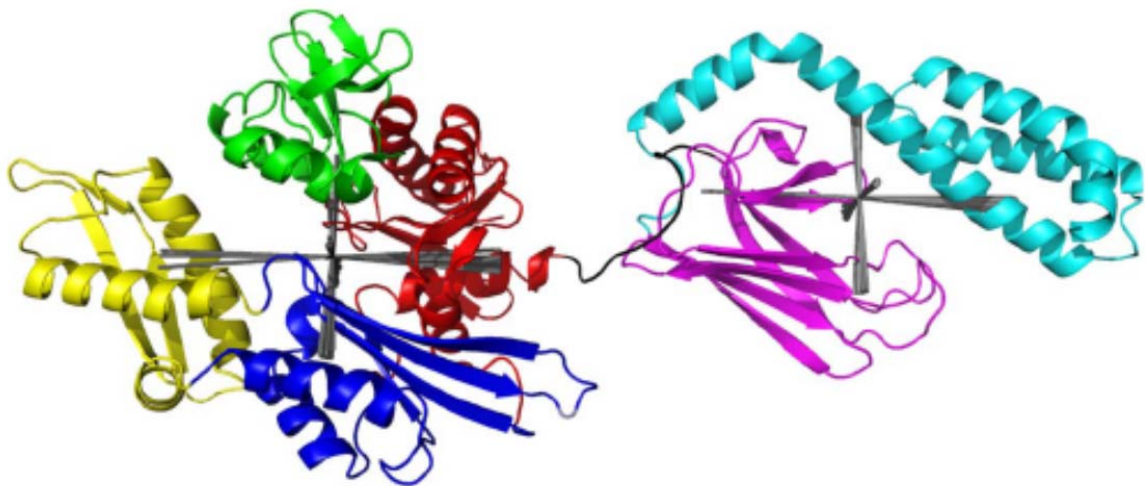


Figure 8 Hybrid NMR RDC structure of *E. coli* DnaK (1-605 with ADP), adapted from (Bertelsen et al., 2009).

DnaK never functions alone. The J domain protein DnaJ and the nucleotide exchange factor GrpE are indispensable for the proper function of DnaK (Figure 7). DnaK, as an ATPase, assists protein folding in an ATP-driven cycle of substrate binding and release. The fundamental DnaK reaction cycle has been well explained. In the ATP-bound state, DnaK has low affinity for the substrates; the exchange rate of substrate on DnaK is very high. Upon hydrolysis of ATP, the affinity for the substrate is high and the

on/off rate very slow. The conformational transition between ATP- and ADP-bound states drives the DnaK-assisted protein fold route. The hydrolysis of ATP to ADP is highly (around 1000-fold) accelerated by DnaJ (Laufen et al., 1999). Subsequently, the release of ADP is triggered by the binding of GrpE.

In the beginning of the DnaK functional cycle, DnaJ mediates the interaction between DnaK and the substrate, either an unfolded protein or a nascent polypeptide (Figure 7B) (Mayer et al., 2000; Rodriguez et al., 2008; Teter et al., 1999; Young et al., 2003). DnaJ interacts with DnaK through its J-domain and recruits substrates to the C-terminal domain of DnaK (Karzai and McMacken, 1996). The association between DnaJ and substrates is transient and fast (Gamer et al., 1996). Binding of ATP to the NBD induce a conformational change of the hydrophobic linker resulting in an open structure of the SBD (Swain et al., 2007; Vogel et al., 2006a; Vogel et al., 2006b).

Following substrate binding, the conformational change is transmitted from SBD to NBD through interdomain communication, and then ATP is hydrolyzed to ADP (Figure 7). The release of ADP is very important for the re-establishment of the starting state. In vivo, the high cytosolic ATP concentration (5 μ M) makes nucleotide release the rate limiting step.

The dissociation of ADP is triggered by the nucleotide exchange factor GrpE, which opens the nucleotide binding cleft by binding as a homodimer to the NBD of DnaK (Harrison et al., 1997). The further stabilization of the nucleotide binding cleft gives rise to the fast binding of ATP to the nucleotide-free state of DnaK (Brehmer et al., 2001). Consequently, ATP binding causes lid opening and substrate release, thereby finishing the reaction cycle (Figure 7). The released substrates can either fold or be

transferred to the downstream chaperonin GroEL/ES system, or recaptured by DnaK/DnaJ for another folding attempt.

In *E. coli*, cells deleted of DnaK are viable below 37 °C. However additional deletion of TF is lethal above 30 °C and results in the accumulation of misfolded, aggregated proteins, suggesting partially overlapping functions for TF and DnaK (Agashe et al., 2004; Teter et al., 1999). In particular, TF and DnaK may cooperate to facilitate *de novo* folding co-transnationally. The shielding or protection of exposed hydrophobic segments of nascent chain to prevent their misfolding may be the major task of DnaK. Moreover, deletion of DnaK slows ribosome biogenesis, indicating that DnaK may be involved in ribosome assembly (Al Refaii and Alix, 2009; Maki et al., 2002). Rudiger *et al* (1997) identified the probable DnaK binding motif by screening a cellulose-bound peptide library. It consists of a five-amino acid core enriched in hydrophobic residues, with a preference for Leu, but also Ile, Val, Phe and Tyr, flanked on both sides by a region where positively charged residues are preferred.

To date, a limited number (94) of DnaK substrates have been identified by rather indirect approaches (Deuerling et al., 2003). However around 30% of cytosolic proteins are thought to be DnaK interactors (reference). Thereby a large number of DnaK interactors still remain to be discovered. Furthermore, how these proteins navigate from TF to DnaK or from DnaK and to downstream chaperonin still needs to be investigated.

2.3.3 *E. coli* Chaperonin GroEL/ES

2.3.3.1 Structure and function of GroEL and GroES

In *E. coli*, the chaperonin GroEL/ES has been studied extensively from a structural, functional and mechanistic perspective. In contrast to the other chaperone systems in *E. coli*, the chaperonin GroEL, and its cofactor GroES, are unique and essential, forming an

isolated nano-cavity for protein folding (Brinker et al., 2001; Weissman et al., 1996). A small number (~ 85 proteins) of GroEL substrates have been identified, which are highly dependent on GroEL for correct folding (Kerner et al., 2005).

GroEL was first described by Costa Georgopoulos and colleagues in the 1970s. They found a mutant of the *groE* operon that blocked the assembly of bacteriophage λ heads (Georgopoulos et al., 1973). Subsequently, it was shown that GroEL and GroES, which are encoded by the same operon, are essential to the viability of *E. coli* at any temperature (Fayet et al., 1989).

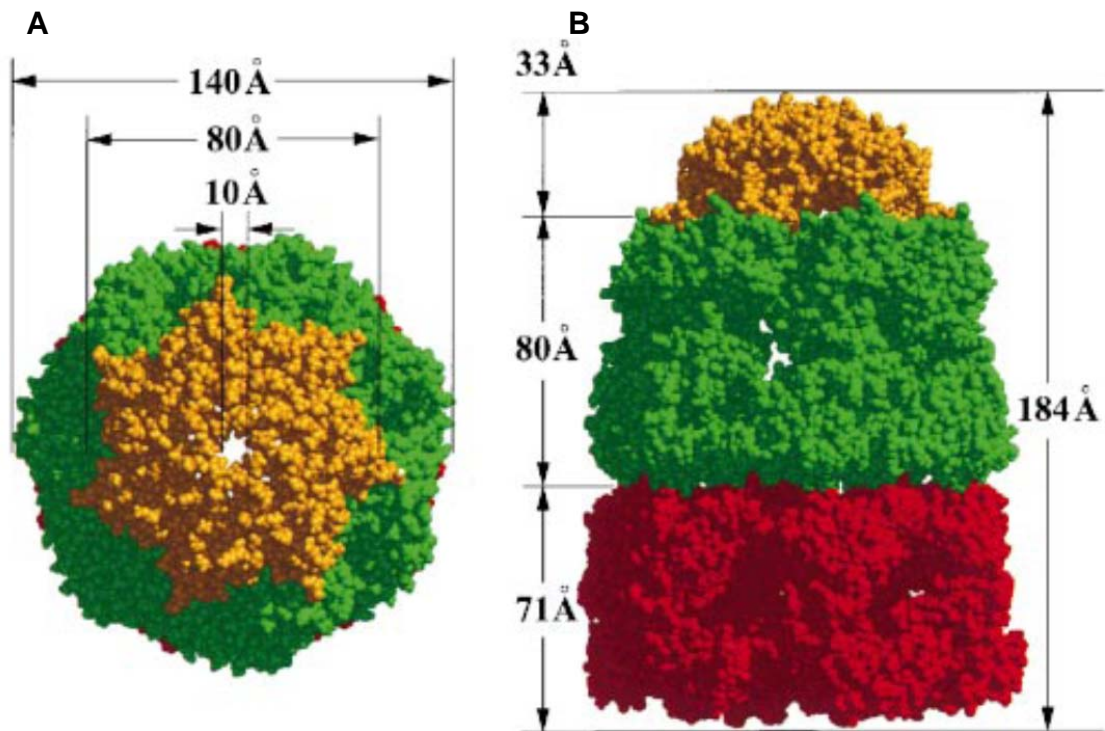


Figure 9 Architecture of the GroEL-GroES-(ADP)₇ complex

(A) Van der Waals space-filling model of the entire complex in a top view looking down from the GroES-binding (*cis*) side; (B) side view. The complex is color coded as follows: *trans* GroEL ring, red; *cis* GroEL ring, green; GroES, gold. Adapted from (Xu et al., 1997).

GroEL is a cylindrical complex consisting of two heptameric rings of ~57 kDa subunits that are stacked back-to-back. These two rings form the functionally separated active compartment (Figure 9). GroEL monomers are identical and consist of an equatorial ATPase domain, an apical domain, and an intermediate hinge domain. The equatorial domain includes the ATP/ADP binding site and forms the inter-subunit contacts between the two GroEL rings; the apical domain forms the flexible ring opening and exposes hydrophobic amino acid residues toward the central cavity for the binding of non-native substrate proteins; the intermediate domain connects the equatorial domain

and apical domain as a flexible hinge during the rearrangement of the GroEL ring when GroEL binds the substrate or the co-factor GroES (Figure 10) (Bukau and Horwich, 1998).

The co-factor GroES is a single-ring, continuous dome-shaped heptamer of identical 10 kDa subunits which cover the ends of the GroEL cylinder. GroES contains nine β -strands with one exceptionally long β -hairpin loop, the so-called mobile loop, by which GroES contacts with GroEL. GroES binds to either one of the two GroEL rings depending on the ATP or ADP bound state of GroEL. Since the hydrophobic binding regions of GroEL for polypeptide overlap with those for GroES (Fenton et al., 1994; Xu et al., 1997), the binding of GroES leads to the elevation the hydrophobic binding surface, which thereby is twisted away from the polypeptide. Consequently, the substrate is released from the GroEL apical domain into the cage for folding. The binding of GroES leads to the formation of an asymmetric complex (Figure 10). The rearrangement of apical and intermediate domains of the *cis* ring occurs by cooperative binding of seven ATP molecules to the *cis* GroEL equatorial subunits. While the domain rearrangements result in burying hydrophobic residues and hence changing the environment inside the GroEL-GroES cavity to hydrophilic (Figure 10). The cage volume is enlarged by two-fold and can accommodate up to 60 kDa polypeptides (Hartl and Hayer-Hartl, 2009).

2.3.3.2 Mechanisms of GroEL-mediated protein folding

The protein folding assisted by GroEL/GroES includes three steps: (1) the non-native polypeptide binds and is prevented from aggregation; (2) the unfolded polypeptide is released from the apical domain into the cage for subsequent folding; (3) the folded/unfolded polypeptide is released outside of the GroEL cage (Figure 11).

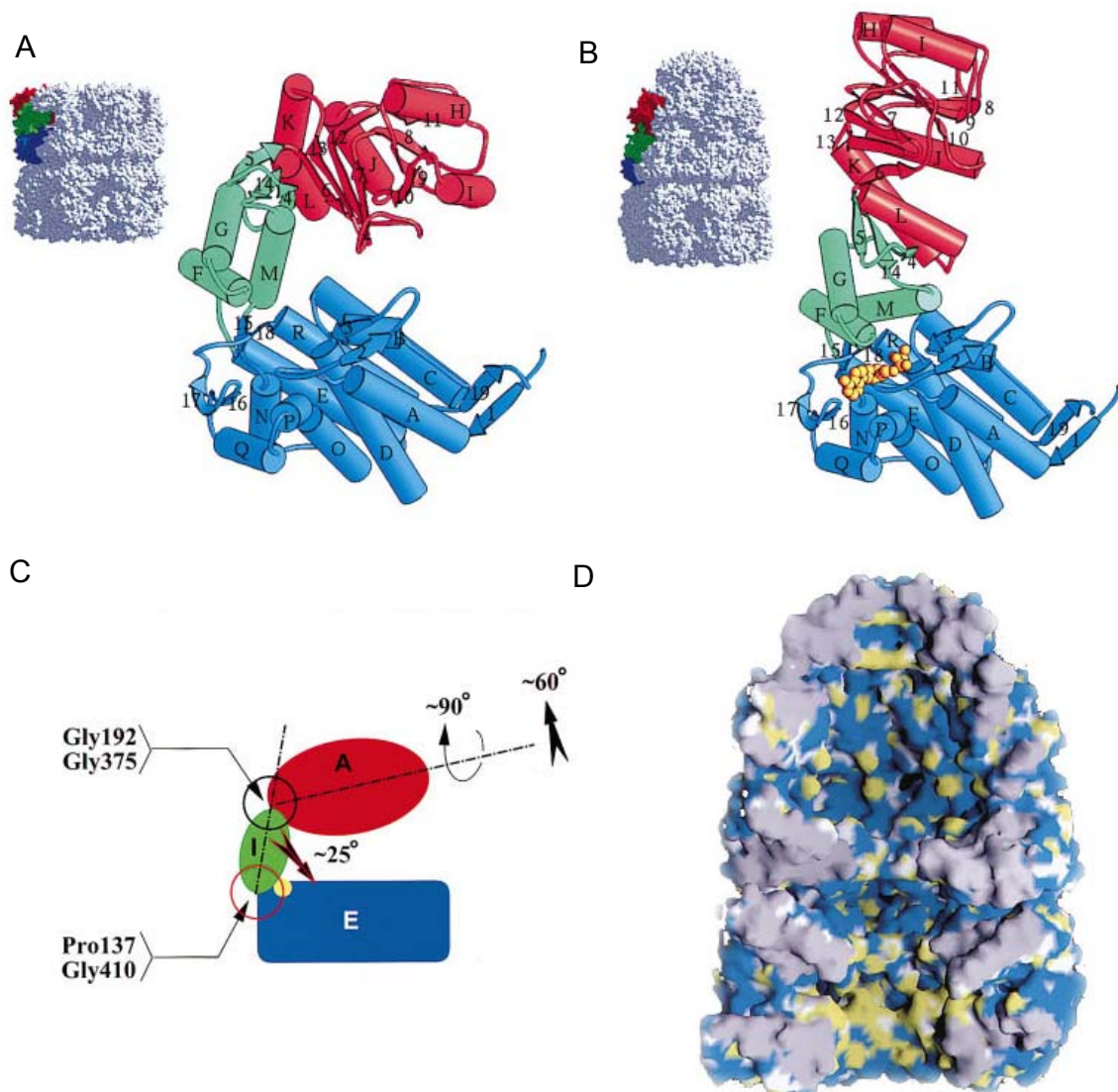


Figure 10. The structure rearrangement within individual subunits

(A, B) ribbon diagrams of an individual subunit of unliganded (A) and liganded (B) GroEL, oriented with the 7-fold axis to the right, as indicated in the space-filling models (insets). Note that GroES is not shown in the right-hand panel, to reveal more clearly the extent of motion of the apical domain. The equatorial, intermediate, and apical domains are blue, green, and red, respectively. (C) The movements that occur around the pivot points at the ends of the intermediate domain. Domains are colored as in the upper panels, and the small yellow circle on the top of the equatorial domain represents the nucleotide. (D) An interior view of four subunits

from each ring of the asymmetric structure, colored to reflect the relative hydrophobicity of the interior surface. Hydrophobic side-chain atoms are yellow; polar and charged side-chain atoms are blue; solvent-excluded surfaces at the interfaces with the missing subunits are gray; and exposed backbone atoms are white., adapted from (Bukau and Horwich, 1998).

GroEL/GroES mediated folding is started by sequestering the unfolded protein with a mechanism controlled by the ATPase activity of GroEL. After binding of the substrate to the nucleotide free GroEL ring (*trans*), ATP and GroES bind the same and newly-formed *cis* ring, thereby leading to the release of the substrate into the GroEL cavity for folding and to the dissociation of ADP and GroES from the former *cis* ring for resuming to permissive substrate-binding condition. Enclosing unfolded proteins, one molecule at a time provides a special space for protein folding during 10-15 s, the time necessary for ATP hydrolysis. Then the folded or unfolded protein leaves the cage upon GroES dissociation, which is induced by ATP binding in the opposite ring (*trans*-ring). Proteins which are not fully folded (folding intermediates) still expose extensive hydrophobic surfaces are quickly recaptured and the folding cycle is repeated until the protein reaches the native state.

Without any doubt GroEL promotes protein folding at least in part by preventing protein aggregation. However, additional mechanisms have been proposed for GroEL action, including an active catalytic function which allows the substrate protein to escape from folding traps (Brinker et al., 2001; Horwich et al., 2009; Tang et al., 2006). One model suggests that the GroEL/GroES chamber forms a passive “Anfinsen cage” that prevents folding monomers from forming reversible aggregates that limit the rate of the spontaneous folding reaction (Horwich et al., 2009). An alternative model suggests that the chaperonin plays an active role in promoting folding (Chakraborty et al., 2010; Lin et

al., 2008; Tang et al., 2006). According to this model the confinement of the GroEL/GroES cage is able to reduce entropic folding barriers, thereby promoting the formation of native contacts (Chakraborty et al., 2010).

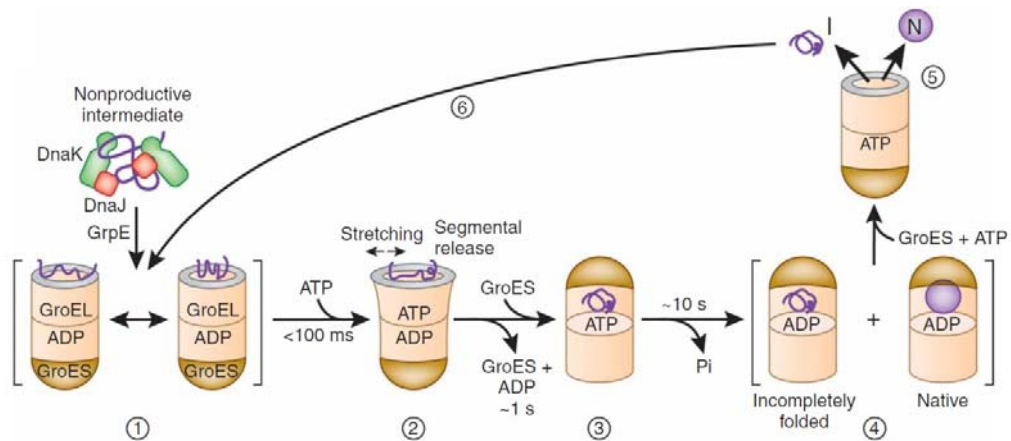


Figure 11 Schematic model of protein folding in the GroEL-GroES cavity.

(1) Substrate proteins may be delivered to GroEL by DnaK–DnaJ for further folding. Upon binding to GroEL it undergoes local unfolding to an ensemble of expanded and more compact conformations. (2) ATP-dependent domain movement of the apical GroEL domains result in stretching of tightly bound regions of substrate and in release and partial compaction of less stably bound regions. (3) Compaction is completed upon substrate encapsulation by GroES. (4) Folding in the chaperonin cage. (5) Substrate release upon GroES and ADP dissociation. (6) Rebinding of incompletely folded states. Note that binding of a second substrate molecule to the open ring of GroEL in steps (4) and (5) as well as the transient formation of a symmetrical GroEL–GroES complex is omitted for simplicity. N, native state; I, folding intermediate. Adapted from (Hartl and Hayer-Hartl, 2009).

Additionally, the forced iterative binding of the substrate, together with its conformational expansion upon initial binding to GroEL and subsequently upon ATP-dependent movements of the apical GroEL domains, may lead to reversal of kinetically trapped misfolded states (Lin et al., 2008; Sharma et al., 2008). Promotion of substrate

folding also happens during a single round of encapsulation in the chaperonin cage (GroEL single ring mutant) without such unfolding cycles (Sharma et al., 2008; Tang et al., 2006), demonstrating that the special physical cage is vital.

2.2.2.3 Substrates of GroEL

In vitro, GroEL is able to interact with many heterologous substrates such as mitochondrial malate dehydrogenase, *R. rubrum* RuBisCo and bovine rhodanese (Hartman et al., 1993; Tang et al., 2006). In vivo, 10%-15% of cytosolic protein has been found to bind to GroEL by co-immunoprecipitation (Houry et al., 1999). Subsequently with the improvement of mass spectrometry methodology and technical advancement of the instrumentation, approximately 250 proteins that interact with GroEL were identified, corresponding to ~10 % of cytosolic *E. coli* proteins (Kerner et al., 2005). Based on their chaperonin dependence, the 250 GroEL substrates were divided into three classes. Class I proteins are mainly chaperone- independent; Class II proteins are partially chaperonin dependent and cannot efficiently fold to the native state without either (DnaK/DnaJ/GrpE) or the GroEL/GroES system. Class III proteins have an obligate requirement of GroEL. Class III substrates may also interact with Hsp70 and be delivered by Hsp70 to the chaperonin for final folding (Figure 3). Recently, in Taguchi's lab (Tokyo Institute of technology, Japan), all the 250 GroEL substrates were singularly overexpressed in bacteria, confirming that ~60% of Class III proteins are absolutely dependent on GroEL, while the remaining 40%, although highly accumulated on GroEL in vivo, could also use other chaperone systems for folding (Fujiwara et al., 2010).

Most Class III proteins are between 20 kDa and 50 kDa and have complex α/β or $\alpha+\beta$ domain topologies, with a distinct enrichment of the $(\beta/\alpha)_8$ TIM barrel fold (Kerner

et al., 2005). These proteins appear to largely rely on GroEL for folding to avoid or overcome kinetically trapped states at a biologically relevant time scale.

2.2.2 Aim of the study

DnaK, the *E. coli* Hsp70 chaperone, has been studied extensively from a structural, functional and mechanistic perspective. However, its role in protein folding and proteome maintenance is not yet understood at the system level. As the central hub of the protein folding system in *E. coli*, DnaK may interact with numerous substrates which may have been handed-over by the upstream trigger factor or will be transferred to the downstream GroEL/GroES for final folding. The details of the cooperation mechanism not only between TF and DnaK but also DnaK and GroEL/GroES are still unexplored. Importantly, which kinds of proteins need specific assistance from DnaK and which are shuttled with or without assistance from TF to the GroEL system still remains to be investigated.

Here for the first time, accurately quantitative data are provided for profiling the Hsp70 interactors. Bioinformatics analysis was performed to characterize the distinct features of DnaK interactors particularly with respect to the preferential interactors. The kinetics of DnaK –substrate protein interactions were measured by Pulse-SILAC-based proteomics. Furthermore, we analyzed the role of DnaK in the bacterial chaperone network and its cooperation with the ribosome-associated chaperone trigger factor (TF) and the downstream chaperonin GroEL/GroES using SILAC-based proteomics of DnaK-pulldowns and whole proteome samples.

3 Materials and methods

3.1 Materials

3.1.1 Chemicals

Unless specified, chemicals used in this work were of pro analysis grade and purchased from Fluka (Deisenhofen, Germany), Calbiochem (Bad Soden, Germany), Merck (Darmstadt, Germany), Sigma-Aldrich (Steinheim, Germany), Roth (Karlsruhe, Germany) or Roche (Mannheim, Germany).

Amersham Pharmacia Biotech (Freiburg, Germany): ECL plus detection kit, Protein A Sepharose

BioMol (Hamburg, Germany): IPTG

Difco (Heidelberg, Germany): Bacto tryptone, Bacto yeast extract, Bacto agar

Fermentas (St. Leon-Rot, Germany): GeneRuler 1kb DNA Ladder, GeneRuler 100bp DNA Ladder

Merck (Darmstadt, Germany): Ampicillin, Acetonitrile, Methanol, Ethanol, Formic acid, Trifluoroacetic acid, Isopropanol.

New England Biolabs (Frankfurt a. Main, Germany): Restriction endonucleases, T4 DNA Ligase, Calf Intestinal Alkaline Phosphatase (CIP)

Roche (Basel, Switzerland): Benzonase, EDTA free Complete Protease Inhibitor, 10% NP-40, ATP Bioluminescence Assay Kit CLS II. ATP,

Schleicher & Schuell (Dassel, Germany): Protran Nitrocellulose Transfer Membrane.

Promega (Wisconsin, USA): Trypsin, ProteaseMAX surfactant

Wako (Osaka, Japan): Lysyl Endopeptidase

Cambridge Isotope Laboratories (MA, USA): arginine- $^{13}\text{C}_6$, lysine-4,4,5,5-d $_4$, arginine- $^{13}\text{C}_6$, $^{15}\text{N}_4$ and lysine- $^{13}\text{C}_6$, $^{15}\text{N}_2$

3.1.2 Buffers and medium

3.1.2.1 Buffers

Buffers were prepared with deionized water (electrical resistance 18.2 M Ω ·cm).

Antibiotic solutions (1000\times):	100 mg/ml ampicillin 25 mg/ml chloramphenicol 25 mg/ml kanamycin
Buffer A:	50 mM Tris-HCl pH 8.0 300 mM NaCl 20 mM MgCl ₂ 50 mM KCl
Buffer B:	20 mM Tris-HCl pH 7.5 1 \times EDTA free Complete Protease Inhibitor 50 mM NaCl
Cell resuspending buffer:	0.1 M Tris/Ac pH 8.0 0.5 M sucrose 5 mM EDTA
Cell washing buffer:	0.05 M Tris/Ac pH 8.0 0.25 M sucrose 10 mM MgSO ₄ 7H ₂ O
2\times Lysis buffer:	20 mM Tris/HCl pH 8.0 20 mM MgCl ₂ 6H ₂ O 0.2 % Triton X100 25 U/ml Benzonase 2 \times EDTA free Complete Protease Inhibitor
Column washing buffer:	50 mM Tris/HCl pH 8.0 300 mM NaCl 20 mM MgCl ₂ 6H ₂ O 50 mM KCl
Column elution buffer:	50 mM Tris/HCl pH 8.0 300 mM NaCl

	20 mM MgCl ₂ ·6H ₂ O
	50 mM KCl
	100 mM imidazole
Coomassie destaining solution:	10 % (v/v) ethanol
	10 % (v/v) acetic acid
Coomassie staining solution:	0.1 % (w/v) Serva Coomassie Blue R250
	40 % (v/v) ethanol
	10 % (v/v) acetic acid
DNA-loading buffer (6×):	0.25 % (w/v) bromophenol blue
	0.25 % (w/v) xylene cyanol FF
	40 % (w/v) sucrose in H ₂ O
ECL solution I:	100 mM Tris-HCl pH 8.8
	2.5 mM luminol (3-aminophthalhydrazid; stock: 250 mM in DMSO, dark, 4 °C)
	0.4 mM p-coumaric acid (stock: 90 mM in DMSO, dark, 4 °C)
ECL solution II:	100 mM Tris-HCl pH 8.5
	5.4 mM H ₂ O ₂
PBS (10×):	92 mM Na ₂ HPO ₄ ·2H ₂ O
	16 mM NaH ₂ PO ₄ ·H ₂ O
	1.5 M NaCl
	adjust pH 7.2 with NaOH
PBST:	1× PBS
	0.1 % (v/v) Tween 20
Ponceau S stain:	0.2 % (w/v) Ponceau S
	3 % (v/v) trichloro acetic acid
SDS-loading buffer (2×):	100 mM Tris-HCl pH 6.8
	4 % (w/v) SDS
	200 mM DTT
	20 % (v/v) glycerol
	0.2 % (w/v) bromphenolblue

SDS-running buffer (10×):	250 mM Tris 2.5 M glycine 1 % (w/v) SDS
TAE buffer (50×):	2 M Tris-acetate 50 mM EDTA pH 8.0
TBS (10×):	500 mM Tris-HCl pH 8.0 1.37 M NaCl 27 mM KCl
TBST (10×):	200 mM Tris-HCl pH 7.5 1.37 M NaCl 1 % (v/v) Tween 20
Western Blot buffer:	50 mM Tris 20 % (v/v) methanol 192 mM Glycine
Digestion buffer:	50 mM NH ₄ HCO ₃
Digestion destaining buffer:	50 mM NH ₄ HCO ₃ 50% ethanol
Digestion reduction buffer:	10 mM dithiothreitol 50 mM NH ₄ HCO ₃
Digestion alkylation buffer:	55 mM iodoacetamide 50 mM NH ₄ HCO ₃
Extraction solution:	3% trifluoroacetic acid 30% acetonitrile
Denaturation buffer:	10 mM HEPES pH8.0 6 M urea 2 M thiourea 1% n –octylglucoside (w/v)
C18 Equilibration solution:	0.1% TFA
C18 Elution buffer:	0.1% TFA, 80% acetonitrile.

3.1.2.2 Medium

LB medium

10 g/l bacto tryptone, 5 g/l bacto yeast extract, 10 g/l NaCl, pH adjusted to 7.0 with NaOH

LB agar

15 g/l Bacto agar dissolved in LB medium

M63 medium:

2 g/l (NH₄)₂SO₄, 13.6 g/l KH₂PO₄, 0.5 mg/l FeSO₄ x 7 H₂O. Before use, 1 ml MgSO₄ (1 M), 10 ml glucose (20 % w/v), L-amino acid mix (to 0.5 mM of each amino acid final) were added per 1 l medium and filter sterilized

SILAC medium:

To prepare L, M, and H media, the respective amino acids in M63 medium were exchanged by respective labelled amino acids, for L: Arg0 and Lys0 (arginine and lysine, Sigma), for M: Arg6 and Lys4 (arginine-¹³C₆ and lysine-4,4,5,5-d₄, Cambridge Isotope Laboratories), for H: Arg10 and Lys8 (arginine-¹³C₆, ¹⁵N₄ and lysine-¹³C₆, ¹⁵N₂, Cambridge Isotope Laboratories).

3.1.3 Materials and Instrumentation

B. Braun Melsungen AG (Melsungen, Germany): Orbital shaker Certomat R

Beckman Coulter GmbH (Krefeld, Germany):

- Centrifuges (GS-6R, Allegra-6R, Avanti J-25 with rotors JLA 10.500 and JA 25.50, J6-MI with rotor JS 4.2)
- DU 640 UV/VIS Spectrophotometer
- DU 800 UV/VIS Spectrophotometer
- Optima LE 80K ultracentrifuge with rotor 45 Ti, 70Ti

Berthold (Huntsville, USA): Luminometer LB9507

Biometra (Göttingen, Germany): PCR thermocycler

Bio-Rad (München, Germany):

- Gene Pulser Xcell electroporation system with electroporation cuvettes (0.1 cm)
- Horizontal agarose gel electrophoresis system (Wide) Mini-SUB CELL GT
- Mini Protean II electrophoresis cell

- Power Pac 300

BioScience, Inc. (Salt Lake City, USA): Pre-lubricated Sorenson safe seal microcentrifuge tubes, RNase/DNase-free

Eppendorf (Hamburg, Germany):

- Centrifuges (5415D and 5417R)
- Pipettes (2.5, 10, 20, 100, 200, 1000 μ l)
- Thermomixer comfort

Fisher Scientific (Schwerte, Germany): Accumet Basic pH meter

Fuji/Raytest (Straubenhardt, Germany):

- Fuji-LAS3000 luminescence and densitometry system with Image Reader LAS-3000
- Gel imaging software: AIDA v.3.5.0

GE Healthcare (München, Germany):

- Äkta Purifier
- Electrophoresis Power Supply – EPS 600
- Ettan LC
- Prepacked chromatography columns (Superdex 75 10/300; HiTrap-blue HP 5 ml)

Heidolph (Schwabach, Germany): Heatable magnetic stirrer

Jasco (Groß-Umstadt, Germany): HPLC system LC2000

Mettler Toledo (Gießen, Germany): Balances (AG285 and PB602)

Millipore (Schwalbach, Germany):

- Centriprep concentrators (10.000 and 30.000 Da MWCO)
- Steritop Filtration System (pore size 0.22 μ m)

Misonix (Farmingdale, USA): Sonicator 3000

MPI for Biochemistry (Martinsried, Germany): Western Blot system (semi-dry)

MWG AG Biotech (Ebersberg, Germany): Gel documentation system

New Brunswick Scientific (Nürtingen, Germany): Innova 44 incubator shaker

RM Business Service (Kirchseeon-Buch, Germany): Savant SpeedVac SPD121P

Sartorius (Göttingen, Germany):

- Laboratory water purification system Arium
- Sterile filters Minisart (pore size 0.22 and 0.45 μ m)
- Vivaspin 500 concentrators (10.000 and 30.000 Da MWCO)

- Vivaspin 20 concentrators (10.000 and 30.000 Da MWCO)

Scientific Industries, Inc. (Bohemia, USA): Vortex-Genie 2

Thermo-Fisher (Waltham, MA, USA):

- Ultra LTQ-FT ICR
- LTQ-Obri trap
- Proxeon EASY-nLC

Whatman GmbH (Dassel, Germany): Whatman Protran nitrocellulose transfer membrane

Waters (Massachusetts, USA): Nano Acquity UPLC

YMC (Kyoto, Japan): YMC-Pack PVA-SIL-NP 250X 10mml.D. S-5 μ m, 12nm

3.1.4 E. coli strains and Plasmid

E. coli strains

Experiments were carried out in E. coli MC4100 strain background. MC4100 $\Delta dnaK dnaJ::Kan^R$ (ΔKJ) and $\Delta dnaK dnaJ::Kan^R \Delta tig::Cm^R$ (ΔKJT) (Genevaux et al., 2004), Δtig (ΔT) and $\Delta secB::Cm^R \Delta tig$ (ΔBT) (Ullers et al., 2007) or MC4100 SC3 Kan^R with *groELS* under arabinose promoter (LS+ or LS-)(Kerner et al., 2005) have been described previously.

Replacement of the chromosomal *dnaK* gene by the *dnaK-His6-Kan^R* or *dnaK-His6-Cm^R* alleles was performed using the method developed by Datsenko and Wanner (2000), except that the Cm^R (or Kan^R) gene was first inserted by sequential cloning of the *dnaK-His6*, *cat* (or Kan^R) and *dnaJ* genes in a pUC18 vector. The PshAI/BsaAI digested *dnaK-His6-Cm^R-dnaJ* or *dnaK-His6-Kan^R-dnaJ* DNA fragments were then used as templates for recombination in MC4100 WT, ΔT and LS strains (Datsenko and Wanner, 2000). To construct the $\Delta secB$ (ΔB) and $\Delta secB/dnaK-His6-Cm^R$ ($\Delta B/K_{His}$) strains, the $\Delta secB::Kan^R$ mutant allele from strain JWK3584 (Keio collection) was first moved into both MC4100 or

MC4100 *dnaK-His6-Cm^R* strains by P1- mediated transduction (Miller, 1992) and the kanamycin resistance was subsequently removed using FLP recombinase as described (Datsenko and Wanner, 2000). The $\Delta secB::Cm^R \Delta tig/dnaK-His6-Kan^R$ strain ($\Delta BT/K_{His}$) was obtained by bacteriophage P1-mediated transduction of the *dnaK-His6-Kan^R* allele into MC4100 $\Delta secB::Cm^R \Delta tig$.

All constructs were verified by DNA sequencing and by Western blot analysis using appropriate antibodies.

Plasmid

The plasmid used was pBAD18 Luc-SecM-GFP Amp^R: Luc-SecM-GFP region was subcloned from the pBAD33 Luc-SecM-GFP kan^R (Brandt et al., 2009) in the pBAD18 (Agashe et al., 2004) receiving vector by *Blp* I and *Sca* II restriction endonucleases.

3.2 Methods

3.2.1 DNA analytical methods

3.2.1.1 General molecular biology methods

All routine molecular biology methods (e.g. agarose gel electrophoresis, DNA quantification, competent cell preparation and transformation of bacterial cells, etc.) were performed according to “Molecular Cloning” (Sambrook et al., 1989) unless otherwise stated. Plasmid DNA was purified from *E. coli* DH5 α cells using Miniprep kits (Promega) according to the manufacturer’s protocol. Primers for cloning were purchased from Metabion (Martinsried, Germany); DNA sequencing was performed by Medigenomix (Martinsried, Germany) or the sequencing facility (Core facility, MPI Biochemistry, Martinsried, Germany). PCR and gel purification of DNA were done with Wizard SV Gel and PCR Clean-Up System (Promega).

3.2.1.2 Expressing a chromosomal C-terminally His6-tagged DnaK

Replacement of the *dnaK* gene in the chromosome of different MC4100 strains with the *dnaK-his6* coding sequence was achieved as described (Datsenko and Wanner, 2000), with some modifications. In detail, a Cm^R cassette was generated by sequential cloning of the *dnaK-his6*, *cat* and *dnaJ* genes in a pUC18 vector. A recombination fragment of ~ 2400 bases was cut out by PshAI-BsaAI restriction digestion. The fragment generated contained the *cat* gene flanked upstream and downstream, respectively, by ~1600 bases of the 3' *dnaK-his6* and ~380 bases of the 5' *dnaJ* coding sequences. The respective *E. coli* strains expressing the λ Red recombinase from the pKD46 plasmid (0.04% arabinose for 1h, 30 °C) were transformed with the Cm^R cassette (100 ng) and recombinants were selected on LB plates containing 25 μ g/ml chloramphenicol.

3.2.1.3 Electrocompetent *E. coli* cells and electroporation

For the preparation of electrocompetent *E. coli* DH5 α cells, 100 ml of LB medium were inoculated with 1 ml of an overnight culture of the strain and grown at 37 °C to an OD₆₀₀ of 0.7. Cells were pelleted by centrifugation for 5 min at 4200 rpm, 4 °C (Beckmann centrifuge Avanti J-25 with rotor JS 4.2). Cells were washed with 500 ml of ice-cold autoclaved water. The cells were then resuspended in 10 ml water and centrifuged for 10 min at 6400 rpm and 4 °C (Beckmann centrifuge Avanti J-25 with rotor JA 25.50). Finally, cells were resuspended in 1.5 ml of 10 % (v/v) ice-cold sterile glycerol. 40 μ l aliquots were pipetted into Eppendorf tubes pre-chilled at -20 °C, immediately frozen in liquid nitrogen and stored at -80 °C.

To transform electrocompetent *E. coli* DH5 α cells, 40 μ l cells were thawed on ice, mixed with \leq 3 μ l of plasmid, and transferred to an electroporation cuvette (0.1 cm). Electroporation was performed by applying a pulse of 1250 V (25 μ F, 200 Ω ; Gene Pulser

Xcell). Immediately after the pulse, 800 μ l of LB medium was added, and the cells were incubated in a shaker at 30 °C for 1 h, centrifuged at 5000 rpm for 2 min in a table centrifuge (Eppendorf 5415D), resuspended in approximately 100 μ l of medium, spread on selective LB plates, and incubated overnight at 30 °C or 37 °C.

3.2.2 Protein analytical methods

3.2.2.1 Apyrase purification

2 kg red-skin potatoes (product name French potato) from the supermarket were peeled and cut into small pieces and mixed with 1L 10 mM thioglycolic acid and then homogenized. Impurities were removed by adding ammonium sulfate at 40% saturation and removing the precipitate. Then ammonium sulfate was added into the supernatant at 80% and the precipitate, containing apyrase, was collected. This fraction was resuspended in 25 ml buffer B and injected onto a Superdex 75 10/300 column in two separate injections of 12.5 ml each. The fraction containing apyrase was concentrated to 25 ml and injected onto a HiTrap-blue HP column. Apyrase was eluted with a gradient of 0-2 M NaCl. The fractions containing apyrase were concentrated and diluted with Buffer B for further use. The enzyme activity was tested according to a modified method from Taussky and Traverso-Cori (Taussky and Shorr, 1953; Traverso-Cori et al., 1965)

3.2.3 Quantification of proteins

The cell lysate was quantified by a colorimetric assay (Bio-Rad Protein Assay, BioRad), based on the method developed by Bradford (Bradford, 1976), according to the manufacturer's instructions

3.2.4 SDS-PAGE

SDS-Polyacrylamide gels were prepared as follows 4% stacking gels and 10 %, 12 % or 15 % separating gels were prepared according the following recipe:

Chemicals	Stacking gel		Separating gel	
	4 %	10 %	12 %	15 %
30 % Acrylamide (0.8% bis)	6.5 ml	16.7 ml	20 ml	25 ml
0.5 M Tris, pH 6.8	12.5 ml	–	–	–
1.5 M Tris, pH 8.8	–	12.5 ml	12.5 ml	12.5 ml
10 % SDS	0.5 ml	0.5 ml	0.5 ml	0.5 ml
2M Sucrose	–	12.5 ml	12.5 ml	12 ml
H ₂ O (up to 50 ml)	30.5 ml	7.8 ml	4.5 ml	–
TEMED	50 µl	25 µl	25 µl	25 µl
10% APS	500 µl	500 µl	500 µl	500 µl

SDS-PAGE was performed using a discontinuous buffer system (Laemmli, 1970) in BioRad Mini-Protean 3 electrophoresis chambers employing a constant current of 15 mA/gel in 50 mM Tris-Base, 380 mM glycine, 0.1 % SDS (pH 8.3). Protein samples were prepared for SDS-PAGE by mixing with 5× Laemmli buffer (Laemmli, 1970)(final concentration of 1x Laemmli buffer: 60 mM Tris-HCl, pH6.8, 1% SDS, 10 % glycerol, 0,01% Bromophenol blue, 0,1 mM β-mercaptoethanol) and boiling samples at 95°C for 3-5 min before loading onto the gel. After electrophoresis, gels were stained with Coomassie blue staining solution (0.1 % Coomassie brilliant blue R-250, 40 % ethanol, 7 % acetic acid) for 3 h and destained in 20 % ethanol, 7 % acetic acid.

Alternatively, NuPAGE gradient gels (4-12%) were used, which were run, fixed and stained with Colloidal Blue (Invitrogen) according to the manufacturer's instructions.

3.2.5 Western blotting

Western blotting was carried out in a semi-dry blotting unit. After separation by SDS-PAGE, proteins were transferred onto a nitrocellulose membrane by applying a constant current of ~ 2 mA/cm² gel size in transfer buffer for 1 h.

Blocking was carried out with 5% skimmed milk powder in TBS for 1 h. The membranes were then incubated with primary antibody (diluted in 5% milk-TBS) for 1 h at room temperature or overnight at 4 °C, followed by the incubation with HRP-conjugated secondary antibody (diluted 1:2500 in 5% milk-TBS) for 1 h at room temperature. Extensive washing between the incubation steps was performed with TBS and TBST. Immunodetection was carried out with the ECL system (BioRad) and developed with ImageReader (Fuji LAS-3000).

3.3 Biochemical and biophysical methods

3.3.1 Functional analysis of His-tagged DnaK

Overnight (ON) culture from each mutant was diluted into either liquid medium (Minimal or LB) or applied to a solid LB plate for a drop test. For the liquid medium the OD_{600nm} value at 30 °C or 37 °C in the shaker (New Brunswick Scientific) was measured every hour with DU 640 UV/VIS Spectrophotometer. The LB plates were incubated at 16 °C, 30 °C, 37 °C and 42 °C.

3.3.2 ATP depletion from cell lysate

Cell lysate, which was used in the pulldown, was used for this test. ATP concentration was determined by ATP Bioluminescence Assay Kit CLS II (Roche). The procedure is based on the manufacturer's instructions followed by the measurement from the output of Luminometer LB9507 (Biometra).

3.3.3 Isolation of DnaK/GrpE/interactor complexes

E. coli cells were grown at 37 °C in 0.5 l SILAC medium to exponential phase ($OD_{600nm} \sim 1$). Spheroplasts were then prepared (from ~ 1.5 g cells) at 4°C as previously described (Ewalt et al., 1997). Spheroplasts (~ 0.5 g) were resuspended in 3 ml SILAC medium supplemented with 0.25 M sucrose, 0.2% glycerol and recovered at 37°C for 15 min. Lysis was rapidly induced by dilution of the spheroplasts into an equal volume of 25°C hypo-osmotic lysis buffer (20 mM Tris-HCl pH 8, 0.2% (v/v) Triton X100, 20 mM $MgCl_2$, 25 U/ml benzonase, 2× EDTA-free protease inhibitor cocktail (Roche), 100 U/ml apyrase). Lysis was allowed to proceed for 1 min at RT and all subsequent steps were carried out at 4°C. The supernatant was cleared at 20,000 ×g for 30 min (a small aliquot was saved for SILAC MS of the whole proteome analysis) and incubated for 60 min with Talon resin (1 μ l/mg total protein as determined by Bradford assay) (Clontech) pre-equilibrated in buffer A (50 mM Tris-HCl pH 8, 300 mM NaCl, 20 mM $MgCl_2$, 50 mM KCl) for isolation by IMAC. The resin was washed with 200 fold bed volume of buffer A followed by 200 fold resin volume of buffer A with additional 10 mM imidazole. DnaK-interactor complexes were eluted with 0.25 ml of 100 mM imidazole in buffer A. The eluted sample was then diluted 1:10 in buffer A and incubated for 60 min with a 10% larger volume of Talon resin. After washing as before, DnaK-interactor complexes were eluted from the beads with an equal volume of LDS sample buffer (Invitrogen) by heating at 70 °C for 10 min. Differentially labeled eluates were mixed

at a 1:1 (v:v) ratio and separated on NuPAGE gradient gels (4-12%). Gels were fixed and stained with Colloidal Blue (Invitrogen), according to the manufacturer's instructions. Preparation of gel slices, reduction, alkylation, and in-gel protein digestion was carried out as described (Ong and Mann, 2006), unless otherwise stated. Finally, peptides were desalted, filtered, and enriched on OMIX-C18 tips (Varian).

3.3.4 Fractionation of the total cell lysate

Different mutants of *E. coli* MC4100 ($\Delta T/K_{His}$, ΔKJ , ΔKJT , $LS-/K_{His}$) were grown at 30 °C or 37 °C, as indicated, in 50 ml of the respective SILAC medium to $OD_{600nm} \sim 1$. After centrifugation, the cells were resuspended with 2 ml buffer B (20 mM Tris pH 7.5, 50 mM NaCl, 1× EDTA-free protease inhibitor cocktail) and flash frozen with liquid nitrogen. The cells were thawed and sonicated (Sonicator 3000, Misonix) on ice for eight pulses of 15 s with 1 min intervals. To remove cell debris, the lysate was cleared by centrifugation at 2000 × g for 10 min, and the protein concentration was determined. The total lysates labeled with different isotopes were mixed at a 1:1:1 ratio. Aliquots were withdrawn for LC-MS/MS of the whole proteome. After centrifugation of the remaining total lysate at 20,000 × g for 30 min, the supernatant was collected as soluble fraction. The pellet was further processed for isolation of aggregated proteins as described (Tomoyasu et al., 2001). In-solution digestion was carried out as described (Olsen and Macek, 2009). The digested peptides were separated by PVC-SIL-NP column (YMC) on a MicroLC (Jasco) or the Ettan LC (GE) with a 102 min gradient from 98% to 68% acetonitrile. Each fraction was dried completely in a vacuum centrifuge concentrator at 35°C before LC-MS/MS.

3.3.5 Expression of Luc-SecM-GFP stalling sequence

K_{His} and different mutants of *E. coli* MC4100 ($\Delta T/K_{His}$, ΔKJ , ΔKJT ,) were transformed with pBAD18 Luc-SecM-GFP Amp^R by electroporation. ON cultures of transformed clones were diluted in 50 ml of the respective SILAC medium and grown to exponential phase ($OD_{600nm} \sim 0.7$) at 30 °C. Expression of the Luc-SecM-GFP stalled sequence was induced for 30 minutes with 0.2% arabinose. Fractionation of the whole cell lysate was performed as described above. A reverse experiment was carried out by inverting the labeling isotopes. The final luciferase ratios between K_{His} and mutant strains for the different lysate fractions are reported as the mean of two biological replicates.

3.3.6 GroEL/ES depletion

The GroEL/GroES depletion strains (MC4100 SC3 Kan^R and MC4100 SC3 Kan^R *dnaK-His6* Cm^R) have the chromosomal groELS promoter replaced with the araC gene and the pBAD promoter, and a kanamycin resistance (*Kan^R*) cassette is immediately upstream of *groELS* (Kerner et al., 2005). For GroEL-depletion (LS-), cultures in SILAC medium containing 0.05 g/l kanamycin and 0.2% arabinose were diluted 1:10 in fresh medium containing 0.2% arabinose. After growth for 2 hours at 30 °C or 37 °C, cells were washed with sugar-free minimal medium and resuspended in pre-warmed SILAC medium containing 0.2% glucose to initiate GroEL depletion. Every hour, growing cells were diluted into fresh pre-warmed depletion medium to an $OD_{600nm} \sim 0.3$. After 3 h, 0.5 l or 50 ml cells ($OD_{600nm} \sim 1$) were collected for DnaK-interactor complex pulldowns or total proteome analysis, as described above. The level of GroEL was reduced by ~97% compared to non-depleted cells.

3.3.7 LC-MS/MS

Peptides from in-gel digestion were eluted from OMIX C18 tips using 50 μ l of 80 % acetonitrile/0.1 % TFA. The samples were dried in a vacuum centrifuge concentrator at 35°C

and resuspended in 6 μ l 0.1% formic acid (FA). Peptides from in-solution digestion of lysate fractions were directly suspended in 6 μ l 0.1% FA. Using an EasyLC system (Proxeon) or nanoAcquity LC (Waters), 6 μ l of sample were loaded at 0.5 μ l/min in 0.1 % FA onto a 15 cm long capillary column (75 μ m inner diameters) with a pre-pulled capillary tip (New Objective) packed with Reprosil-Pur 3 μ m or 2.4 μ m C18 material (Dr. Maisch). Peptides were eluted at 0.3 μ l/min using a 120 min gradient (pull-down eluate and pulse-chase samples), a 180 min gradient (pulse samples) or a 220 min gradient (lysate fractionation samples) from 2% to 80 % acetonitrile, in 0.1 % FA.

Peptides were directly injected into a Thermo LTQ-FT Ultra or a LTQ-Orbitrap using a nano-electrospray ion source (Proxeon) with electrospray voltages ranging from 1.5 to 2.5 kV. FT scans from m/z 330-1700 were taken at 100,000 resolution for LTQ-FT Ultra and 60,000 resolution for LTQ-Orbitrap, followed by collision induced dissociation (CID) scans in the LTQ of the 8 or 10 most intense ions with signal greater 2000 counts, and charge state larger than one. Dynamic exclusion of parent masses already fragmented was enabled. CID settings were as follows: isolation width 1, normalized collision energy 35 V, activation Q 0.250, and activation time 30 ms.

3.4 Analysis of MS data

3.4.1 Determination of SILAC Ratios

MS data were analyzed with MaxQuant version 1.0.13.13 (Cox and Mann, 2008) using the following parameters: Quant; SILAC Triplets, Medium Labels: Arg6, Lys4, Heavy Labels: Arg10, Lys8. Maximum labeled amino acids: 3. Variable modifications: Oxidation (M), Acetyl (Protein N-terminus). Fixed Modifications: Carbamidomethyl (C). Database: Ecogene, with contaminants and a decoy database added by the SequenceReverser.exe

program released with MaxQuant v. 1.0.12.4. Enzyme: Trypsin/P. MS/MS tolerance: 0.5 Da. Maximum missed cleavages: 2. Top MS/MS peaks/100 Da: 6. Mascot version 2.2 (Matrix Sciences, www.matrixsciences.com) was used to generate search results for MaxQuant. Identify; Peptide FDR: 0.01. Protein FDR: 0.01. Maximum PEP: 1. Minimum unique peptides: 1. Minimum peptide length: 6. Minimum peptides: 1. Protein Quantitation based on Razor and Unique peptides. Minimum Ratio count: 2. ‘Re-quantify’ and ‘Keep low-scoring versions of identified peptides’ were both enabled. Normalized or non-normalized ratios were used as specified below for every experimental set-up. Supplemental tables show the leading protein for each protein group; that is, the protein which best matched all of the peptides identified.

3.4.2 Determination of the DnaK interactome

Two sets of DnaK pull-down SILAC experiments, each composed of double- and triple-SILAC segments, were performed with the following designs: (i) triple-SILAC, MC4100 *dnaK wt* (L) versus K_{His} (M) versus $\Delta T/K_{His}$ (H); double-SILAC, ΔT (L) versus $\Delta T/K_{His}$ (H); (ii) triple-SILAC, MC4100 SC3 LS+ (L) versus LS+/K_{His} (M) versus LS-/K_{His} (3.5 h growth on glucose) (H); double-SILAC, LS- (L) versus LS-/K_{His} (H). 3 biological replicates were performed for each of the 2 set-ups.

DnaK interactors were determined from the triple-SILAC segment of experiment (i) by selecting the pulled-down proteins enriched a minimum of 2-fold over the background (non-normalized M/L ratio > 2) in at least two of the biological replicates. This results in a list of 674 proteins (Table S1 with a false positive rate (FPR) lower than 0.2%. The FPR inherent to the pull-down mixing procedure was estimated by a SILAC control experiment where two pull-downs were performed from H- and L-labeled MC4100 WT cells. Only 1

protein out of 410 was identified with non-normalized H/L ratio higher than 1.4, corresponding to a FPR of 0.24% (Figure 14C). Note that the identification of DnaK-interactors approached saturation, when considering consecutive pulldown experiments, the first resulting in 100% new identifications, the second in 30% and the third in 10% new identifications.

3.4.3 Determination of changes in the DnaK interactome

Experiment (i) and (ii) were used to determine changes in the DnaK interactome consequent to the deletion of TF and the depletion of GroEL/ES, respectively. To correct for changes in protein concentration that may occur due to the TF deletion or GroEL depletion, the normalized H/M ratios measured for the proteins in the pulldown were corrected for significant differences in protein abundance in the respective total lysates (Significance B calculated by MaxQuant < 0.05) before performing the statistical analysis. To this end, the H/M ratios of the mixed K_{His} and $\Delta T/K_{His}$ (or $LS-/K_{His}$) cell lysates were also measured and used to normalize the H/M ratios in the pulldowns. Significance thresholds for increased and decreased proteins in each pulldown were set at the median ± 1.5 MAD (median absolute deviation) of the distribution of the corrected, log transformed H/M ratios. Proteins were finally selected for the analysis only if found to be significantly changed in two of the biological replicates.

3.4.4 Enrichment of Interactors on DnaK

H-labeled DnaK-interactor complexes were mixed with appropriately diluted L-labeled soluble lysate (scheme in Figure 15A). The measured H/L ratio, corrected for the dilution factor and normalized to the DnaK ratio (as determined by Western blotting), resulted in the

relative enrichment factor (REF) of the interactors on DnaK with respect to their total cytosolic amount. DnaK-enriched and less-enriched interactor sets were formed by selecting proteins with $REF > 5$ and $REF < 0.2$, respectively, in at least 2 of 3 independent repeats of the experiment. These thresholds correspond to approximately 70th and 20th percentiles of the \log_{10} (median REF) distribution.

3.4.5 Determination of proteome differences between *E. coli* chaperone mutants

K_{His} , $\Delta T/K_{His}$, ΔKJ , ΔKJT and $LS-/K_{His}$ cells were grown at 30°C or 37°C, as indicated, in SILAC media as described above. M-labeled K_{His} total cell lysate was divided into equal aliquots; one aliquot was mixed with L-labeled $\Delta T/K_{His}$ and H-labeled ΔKJ lysate at a 1:1:1 ratio based on total protein concentration, while the second aliquot was mixed with H-labeled $LS-/K_{His}$ and L-labeled ΔKJT lysate. These samples were fractionated into soluble and aggregate fractions as described above. A reverse experiment was performed as a biological repeat by shuffling the labeling scheme.

At 37°C, L-labeled K_{His} total lysate was mixed with either H-labeled $\Delta T/K_{His}$ or M-labeled $LS-/K_{His}$ total lysate. In the reverse experiment H-labeled K_{His} total lysate was mixed with either L-labeled $\Delta T/K_{His}$ or L-labeled $LS-/K_{His}$ total lysate.

Proteins were selected for subsequent analysis when their levels were significantly changed in both biological replicates, according to MaxQuant Significance B ($p < 0.05$), for the total and soluble fractions. For the insoluble fractions, non-normal distributions of the mutant/ K_{His} SILAC ratios were observed due to extensive protein aggregation (especially in the ΔKJ and ΔKJT strains); therefore an arbitrary threshold of 2 was set in both biological replicates to select aggregating proteins for further analysis.

3.4.6 Pulse and pulse-chase SILAC

In the pulse-SILAC experiment, MC4100 cells expressing DnaK-His6 and MC4100 cells expressing DnaK-WT were grown at 37°C in 500 ml L and H media, respectively. During exponential phase ($OD_{600nm} \sim 1$), K_{His} L-labeled cells were collected, washed once with amino acid-free medium by centrifugation at RT, resuspended in pre-warmed M medium (0.25 mM Arg6 and Lys4, each) and incubated for 2.5 min at 37°C. H-labeled WT cells were processed in parallel but incubated for 2.5 min at 37°C in pre-warmed H medium. Cell growth was rapidly stopped by mixing with an equal volume of pre-chilled 2xPBS. Spheroplasts were prepared and lysed directly (i.e., without recovery phase at 37°C) as described above. The lysates obtained from the K_{His} cells (L→M pulse-labeled) and WT cells (H→H pulse-labeled) were mixed 1:1 based on total protein concentration (aliquots were withdrawn for LC-MS/MS analysis) and subjected to IMAC isolation of DnaK-interactors. Three biological replicates of the experiment were performed. Specific DnaK-interactors were selected for further analysis with a minimal enrichment of 2-fold above the background ($((M+L)/H \text{ ratio} > 2)$) in at least two of the repeats.

The M/L ratios measured in the pulldown were corrected to take into account the small contribution of background proteins. Since the fraction of specific binding can be expressed as

$$x = \frac{((M + L)/H) - 1}{(M + L)/H}$$

and since the background proteins will have the same isotope ratios as the lysate (M/L), the following correction factor was applied to the measured M/L (M/L_m) ratios in the pulldown:

$$\log(M/L) = \log(M/L_m) \times \left(\frac{1}{x}\right) - \log(M/L_l) \times \frac{1-x}{x}$$

Non-normalized M/L ratios were used for each of these calculations. The median of the corrected M/L ratios from the three experiments was used for the final analysis. Deviation of log of the ratio $((M/L_{\text{DnaK}})/(M/L_{\text{lysate}}))$ from 0 indicates enrichment of newly synthesized or pre-existent fraction of a protein on DnaK, respectively.

In the pulse-chase SILAC experiment, K_{His} cells were grown in 1 l of L medium at 37°C. When $OD_{600\text{nm}}$ approached 1, cells were collected, washed once with amino acid-free medium by centrifugation at RT, and resuspended in H medium (0.05 mM Arg and Lys, each). Pulse-labeling was allowed to proceed at 37°C for 2 min. The chase was started by addition of 100-fold excess of L Arg/Lys isotopes. Immediately after addition (time 0) and after 2, 4 and 8 min chase, aliquots of 250 ml were withdrawn and translation was stopped by mixing the cell culture with an equal volume of 2x cold PBS containing 2 mg/ml chloramphenicol (Sigma). All subsequent steps, from spheroplasts preparation to DnaK-interactor isolation, were performed at 4°C in the presence of 0.2 mg/ml chloramphenicol. Samples were processed for LC-MS/MS run was performed as above except that the reduction and alkylation steps were omitted. Consequently, in the Quant module of the MaxQuant software the Carbamidomethyl (C) was set as a variable modification. The non-normalized H/L ratios measured by MS were directly used for data analysis. Identified proteins selected for further analysis fulfilled the following criteria: (i) have H/L ratio measured for at least 3 time points including time point 0; (ii) the H/L ratio at time point 0 ($H/L_{0\text{min}}$) is the highest; (iii) i and ii are satisfied in at least two of the four experiment repetitions. The H/L ratios measured at different time points for each protein were normalized so that $H/L_{0\text{min}} = 1$ and the resulting kinetics were fitted to single exponential equation of the form

$$y = A \times \exp(-kt)$$

to estimate the apparent rate constant k for the dissociation of the DnaK-interactor complex.

3.4.7 Bioinformatic Analysis

Protein fold assignment was performed with SUPERFAMILY (<http://supfam.cs.bris.ac.uk/SUPERFAMILY/>) predictions according to SCOP 1.73 classification (<http://scop.mrc-lmb.cam.ac.uk/>). Functional assignment of *E. coli* proteins was derived from the COG database (Clusters of Orthologous Groups of proteins) (Tatusov et al., 1997) (<http://www.ncbi.nlm.nih.gov/COG/>). Signal peptide sequences, transmembrane helices and subcellular location of each protein were predicted, respectively, with TargetP 1.1 (Emanuelsson et al., 2007), TMHMM 2.0 (Moller et al., 2001), and pSORT 3.0 (Yu et al., 2010). The emPAI index calculation to estimate absolute protein concentration was done by Mascot version 2.2 (Ishihama et al., 2005). Theoretical isoelectric points (pI) of protein sequences were calculated based on published pK values of amino acids (Bjellqvist et al., 1993). The Grand Average of Hydropathy of protein sequences (GRAVY) was calculated as described (Kyte and Doolittle, 1982). Intrinsic aggregation propensity was calculated with the Zagg algorithm (Tartaglia and Vendruscolo, 2008). Statistical analysis was performed with the PROMPT software (Schmidt and Frishman, 2006).

4. Results

This work was performed in close collaboration with Dr. Giulia Calloni and Dr. Sonya Scherman in the laboratory of Prof. Dr. F. Ulrich Hartl.

4.1 Analysis of the DnaK interactome in WT

4.1.1 Depletion of ATP from cell lysate

In the ATP-driven DnaK protein folding cycle of binding and releasing, the high concentration of ATP (~ 5 mM) in the cytosol leads to the fast exchange of substrates on DnaK. Thereby a nucleotide-free cell lysate is crucial for the accumulation of stable DnaK-interactor complexes upon cell lysis (Figure 7B). ATP and ADP can be converted into AMP by apyrase in 10 sec in vitro at room temperature (Teter et al., 1999). For this project we optimized a protocol for extraction and purification of active apyrase (51 kDa) from red-skin potato. The in-house prepared apyrase showed very high purity compared to the commercial product from Sigma (Catalogue No. A6535) (Figure 12A) and depleted ATP from the cell lysate at 50 U/ml within ~10 second as detected with the ATP Bioluminescence Assay Kit CLS II (Roche) (Figure 12B). This apyrase preparation was used at a final concentration of 50 U/ml to halt the DnaK functional cycle and enrich the stable DnaK-interactor complexes immediately upon cell lysis. Western blotting analysis confirmed that the DnaK interactors were enriched on DnaK in the apyrase treated lysate compared to that of the non-treated lysate (data not shown). When compared to the Glucose/Hexokinase ATP depleting approach used in previous studies of chaperone interactomes (Kerner et al 2005, Hirtreiter et al 2009), the apyrase treatment proved to be ~60 times faster (data not shown).

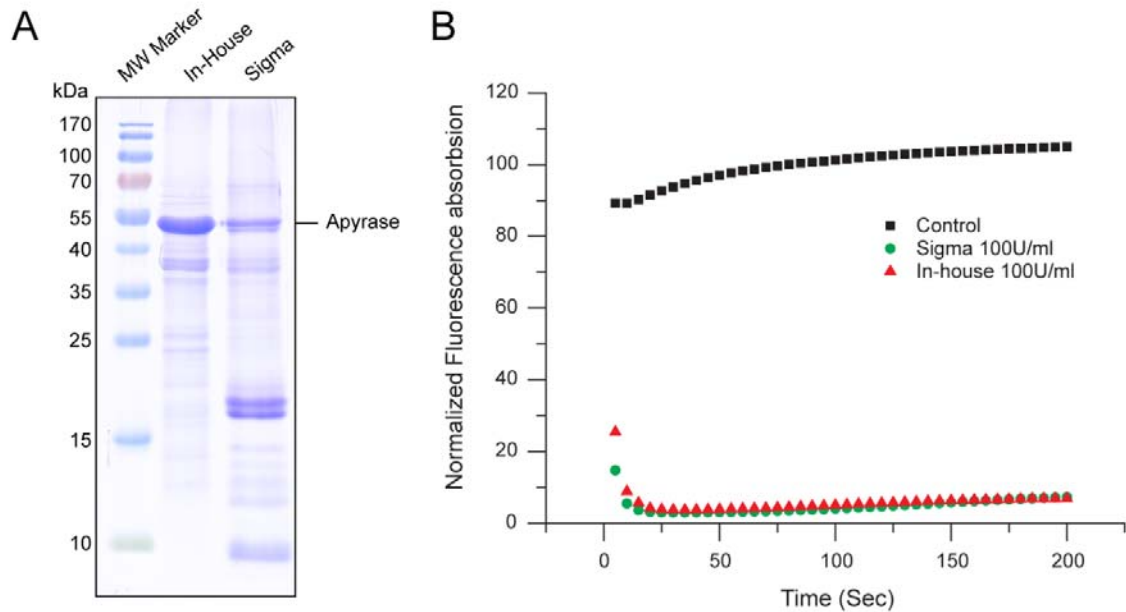


Figure 12 Depletion of ATP in cell lysate with in-house made apyrase.

(A) Equal amount of purified apyrase from red-skin potatoes (lane 2) and apyrase (Catalogue No. A6535) from Sigma (lane 3) were subjected to 15 % SDS-PAGE, followed by Coomassie blue staining. (B) In-House apyrase (red triangles) and Sigma apyrase (green circles) were used for ATP depletion in *E. coli* cell lysate. ATP concentration was measured by monitoring the intensity of luciferase fluorescence which requires ATP hydrolysis using the ATP Bioluminescence Assay Kit CLS II (Roche). Lysate sample without any additional enzyme is shown as control (black squares).

4.1.2 Functional examination of cells with his-tagged DnaK

To efficiently isolate DnaK-interactor complexes for proteomic analysis, we generated an *E. coli* MC4100 strain by homologous recombination in which the wild-type *dnaK* (WT) gene was replaced by *dnaK-His6*, expressing C-terminally His6-tagged DnaK (this strain is henceforth called K_{His}) (Figure 13A). We carefully analyzed the functionality of this construct in light of recent findings that the conserved C-terminal sequence of DnaK contributes to survival of *E. coli* under certain stress conditions (Smock et al., 2011; Smock et al., 2010). The K_{His} cells were indistinguishable from WT when grown on agar plates or in liquid culture at 30 °C and 37 °C, or under heat shock at 42°C where growth is DnaK dependent (Bukau and Walker, 1989a) (Figure 13B, C). Moreover, a quantitative proteomic analysis using SILAC (stable isotope labeling with amino acids in cell culture) (Ong and Mann, 2006) did not highlight any significant differences in protein abundance between WT and K_{His} cells among the 1021 proteins quantified (Figure 13D). DnaK-His6 also supported normal growth of TF-deleted (ΔT) where functional DnaK is strictly required at temperatures above 30 °C and of cells lacking the protein export chaperone SecB (ΔB) (Figure 13B,C) (Deuerling et al., 1999; Genevaux et al., 2004; Teter et al., 1999). Note that ΔB cells are cold sensitive and this defect is compensated by deletion of TF (Figure 13B) (Ullers et al., 2007). To sum up, DnaK-His6 is able to completely substitute WT DnaK in various genetic backgrounds in vivo.

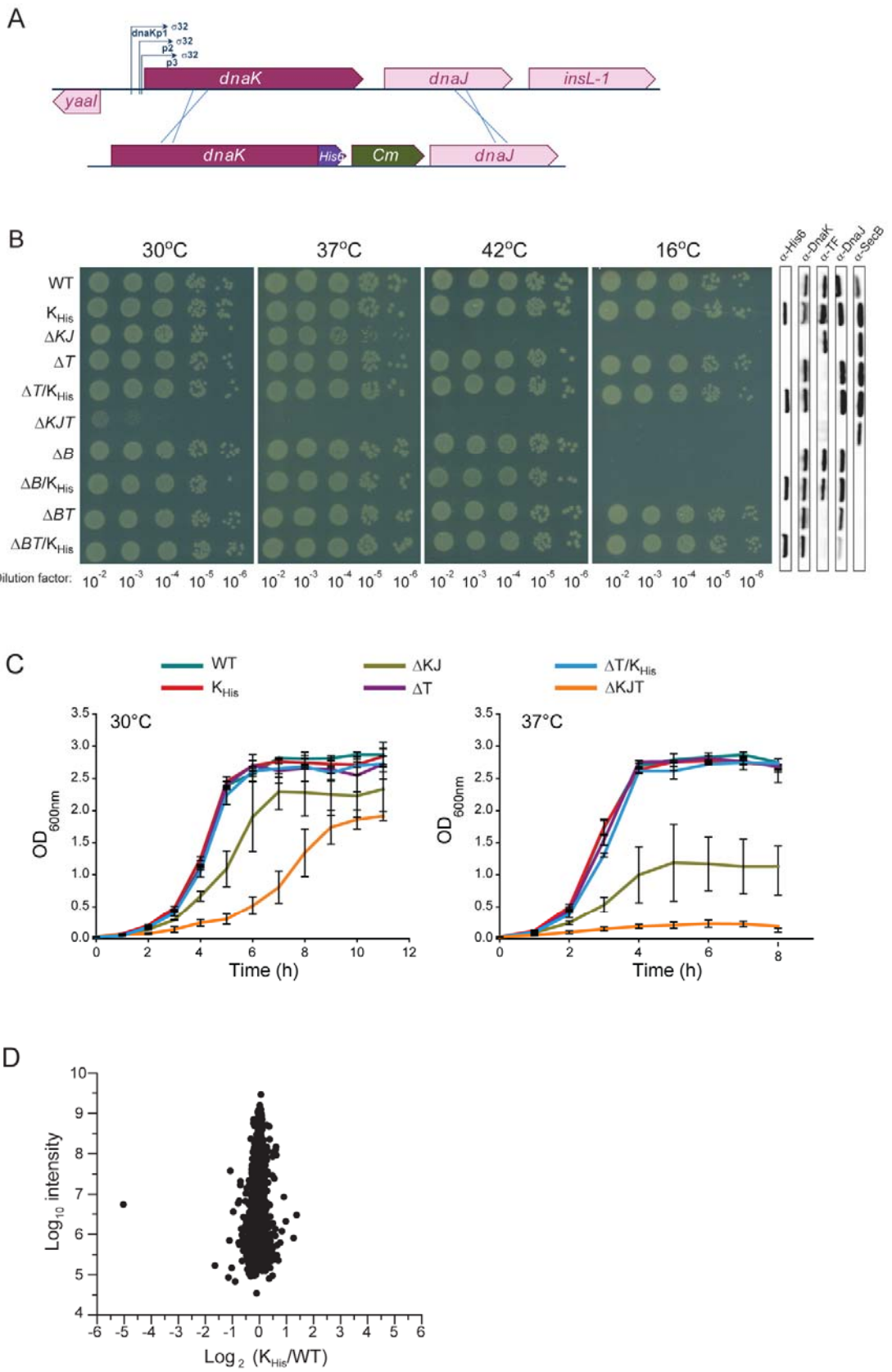


Figure 13 Examination of *E. coli* cells expressing a C-terminal his6-tagged DnaK

(A) Schematic depiction of the substitution by homologous recombination of the chromosomal *dnaK* gene with the *dnaK-His6* by using a *dnaK/Cm^R/dnaJ* cassette. (B, C) In vivo functionality of the chromosomally-encoded DnaK-His6. The *dnaK* gene (WT) was replaced with *dnaK-His6* (K_{His}) in MC4100 and the isogenic chaperone mutant strains $\Delta dnaK dnaJ$ (ΔKJ), Δtig (ΔT), $\Delta tig/dnaK-His6$ ($\Delta T/K_{His}$), $\Delta dnaK dnaJ/\Delta tig$ (ΔKJT), $\Delta secB$ (ΔB), $\Delta secB/dnaK-His6$ ($\Delta B/K_{His}$), $\Delta secB/\Delta tig$ (ΔBT) and $\Delta secB/\Delta tig/dnaK-His6$ ($\Delta BT/K_{His}$) as described above. Cells in mid-log phase were serially diluted, spotted on LB plates and incubated from 1 to 5 days at the indicated temperatures. (C) Growth of *E. coli* cells expressing WT or K_{His} in different chaperone mutant backgrounds as indicated in the figure. Cells from overnight cultures were diluted in fresh M63 medium to an OD_{600nm} of 0.025 and grown at 30°C or 37°C (D) Whole proteome comparison of MC4100 cells expressing WT or K_{His}. The x-axis shows the SILAC isotope ratios for 1021 quantified proteins in K_{His} compared to WT expressing cells of a representative experiment. The y-axis shows log₁₀ collective peptide intensity of respective proteins.

4.1.3 Isolation and identification of DnaK-bound proteins

We isolated DnaK-interactors by immobilized metal affinity chromatography (IMAC) from K_{His} cells growing exponentially at 37°C. DnaK-interactor complexes were stabilized during cell lysis by rapidly depleting ATP with apyrase to inhibit substrate cycling (Teter et al., 1999). The K_{His} cells were SILAC-labeled with medium (M) Arg/Lys isotopes. The DnaK-His6 complexes were mixed 1:1 with a background control containing proteins binding non-specifically to IMAC beads in an equivalent amount of unlabeled WT cells (light isotopes, L), followed by SDS-PAGE, in-gel digestion and peptide identification by tandem mass spectrometry (LC-MS/MS) (Figure 14A). The composition of the pulldown (PD) and background (BG) fractions prior to mixing is shown in Figure 14B. Note that under conditions of ATP depletion, the nucleotide exchange factor, GrpE, was co-isolated with

DnaK-His6 as a stoichiometric complex (Figure 14B), whereas the co-chaperone DnaJ was present only in substoichiometric amounts.

A total of 674 DnaK-interactors (Table S1) were identified with >99.8 % confidence (Figure 14C), including proteins either not identified in the BG sample or having a >2-fold enrichment (M/L ratio) in PD over BG in at least two of three independent experiments (biological repeats). For the vast majority of interactors (>95 %), the amount of co-isolated protein was strongly diminished upon incubation of the cell lysate with ATP instead of apyrase prior to pull down (Figure 14D), indicating that these proteins interact with DnaK in an ATP-regulated manner. Consistent with the functional cycle of DnaK, the interaction with GrpE was lost in the presence of ATP, while DnaJ was bound. Interestingly, besides DnaJ, the proteins that interacted with DnaK most strongly in the presence of ATP included the DnaJ homolog cbpA and the two Hsp20 chaperones, ibpA and ibpB, known to cooperate with DnaK and ClpB in reversing protein aggregation (Mogk et al., 2003).

4.1.4 Properties of the DnaK interactome

Of the ~4300 proteins predicted to be expressed in *E. coli*, a total of 1938 proteins were identified in soluble lysates from WT cells, including 623 of the 672 DnaK-interactors. For 550 DnaK-interactors the subcellular localization was predicted using the pSORT (Yu et al., 2010); ~80 % of these are predicted to be cytosolic proteins, compared to 56 % in the total proteome; 3 % of the interactors are outer membrane proteins, 3.3 % are periplasmic and 11 % inner membrane proteins (Figure 14E). Thus, the DnaK-interactors are highly enriched in cytosolic proteins, comprising ~25% of the cytosolic proteome. The molecular weight distribution of the DnaK-interactors did not differ from that of the lysate proteins (Figure 14F). Other physico-chemical properties analyzed, such as isoelectric point, average

hydrophobicity and aggregation propensity (Tartaglia and Vendruscolo, 2008), also showed no significant deviation from cytosolic lysate proteins (data not shown), indicating that DnaK has a broad substrate specificity. As discussed below, the DnaK-interactors are functionally highly diverse.

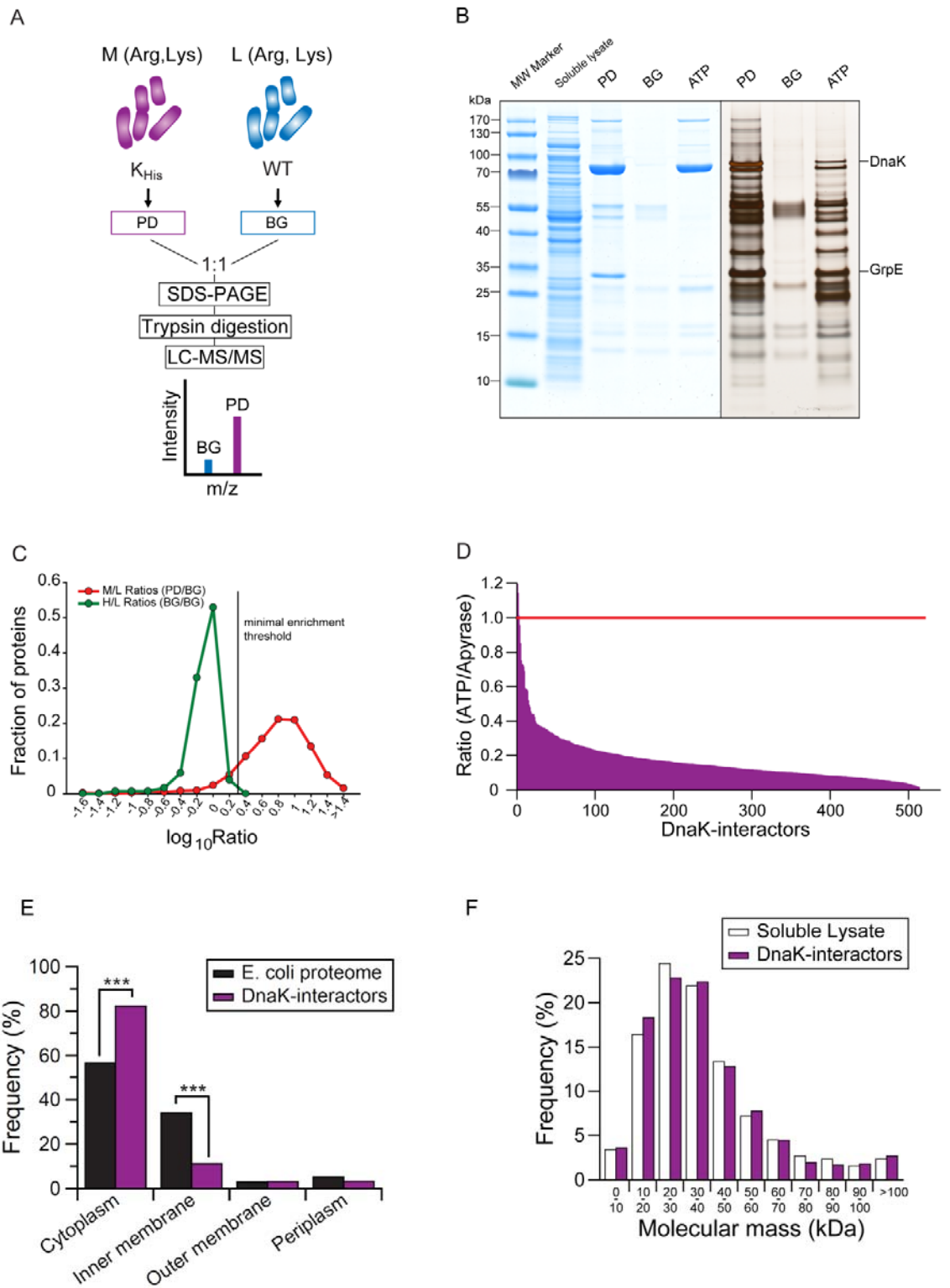


Figure 14 Isolation of DnaK-interactor complexes.

(A) Schematic of the SILAC approach used to identify DnaK-interactors. L (light) and M (medium) Arg, Lys isotope media. DnaK-interactor complexes isolated from M-labeled cells containing the DnaK-His6 (pull-down, PD) were mixed 1:1 with L-labeled proteins isolated from equal amount of cell lysate containing non-tagged DnaK (background, BG). The mixture was subsequently separated by SDS-PAGE, followed by in-gel trypsin digestion and LC-MS/MS analysis (B) Isolation of DnaK-interactor complexes. *E. coli* spheroplasts expressing DnaK-His6 were lysed in the presence of apyrase to rapidly deplete intracellular ATP. The chaperone-substrate complexes were then isolated from the soluble lysate (lane 1) by IMAC and eluted with sample buffer (lane 2&5); Fractions were subjected to 4-12% SDS-PAGE, followed by Coomassie blue staining or silver staining. To identify proteins non-specifically bound to the beads, the same pull-down procedure was performed from cells expressing the non-tagged DnaK (lane 3&6). The DnaK pull-down was performed, when *E. coli* spheroplasts expressing DnaK-His6 were lysed in the presence of ATP (lane 4&7). (C) Comparison of the H/L isotope ratio distribution of a representative DnaK-His6 pull-down (PD) relative to background (BG) (red) and of a BG/BG control sample (green). The BG/BG control sample was obtained by mixing the proteins non-specifically binding to IMAC beads from H-labeled and L-labeled MC4100 cells expressing the non-tagged DnaK (WT). The vertical line corresponds to a H/L ratio = 2, the threshold chosen as minimal enrichment of PD versus BG to select for specific DnaK-interactors. The false positive rate calculated from the BG/BG control experiment is <0.2%.

(D) ATP-dependent release of interactors from DnaK. DnaK-interactor complexes were isolated from L-labeled ATP-depleted lysate and H-labeled lysate supplemented with 5 mM ATP, mixed and subjected to LC-MS/MS analysis. The H/L ratios of the 514 quantified interactors are shown. Ratios <1 indicate a reduced interaction with DnaK in the presence of ATP. (E-F) Properties of the DnaK interactors compared to the experimental lysate and *E. coli* genome. (E) Cellular localization of DnaK-interactors compared to the genome-based *E. coli* proteome (Yu et al., 2010). ***, $p \leq 0.001$

based on chi-square test. (F) Molecular weight distribution of 1938 soluble lysate proteins and 672 DnaK-interactors.

4.1.5 Classification of DnaK-interactors by enrichment on DnaK

We next analyzed the enrichment of the DnaK-interactors relative to their abundance in soluble cell lysate, assuming that this parameter correlates with chaperone dependence, as previously observed for the substrates of the chaperonin GroEL (Kerner et al., 2005). To identify the highly enriched interactors, we measured for each individual protein the fraction of total bound to DnaK. Unlabeled cell lysate (L) was mixed at a defined proportion with DnaK-interactor complexes isolated from H-labeled cells and H/L ratios were determined by LC-MS/MS (Figure 15A). H/L ratios were obtained for 666 DnaK-interactors, reflecting their enrichment on DnaK. The relative enrichment factors (REF) displayed a broad, bimodal distribution (Figure 2A). By setting thresholds at the 20th and 70th percentiles of the distribution, we grouped 142 proteins as less-enriched, 183 proteins as enriched and 341 proteins as medium enriched on DnaK (Figure 15B and Table S1). Interestingly, the enriched proteins are of lower than average abundance (Figure 15C) but occupy ~40 % of the total DnaK capacity by mass (Figure 15D). In contrast, the less-enriched DnaK-interactors are shifted to higher than average abundance but occupy only ~13 % of DnaK capacity (Figure 15C, D). On average only $\leq 0.1\%$ of their cellular content is DnaK-bound. The medium enriched interactors occupy ~47% of the DnaK capacity, with ~1% of cellular content being bound. The enriched interactors include large proteins (Figure 15E) and cover a wide range of cellular functions, with a preference of the enriched substrates for proteins involved in DNA replication, recombination and repair (COG class L) and in cell division and chromosome partitioning (COG class D) and amino acid transport and metabolism (COG

class E) (Figure 15F). This is consistent with findings that DnaK mutant cells have defects in chromosome segregation and cell division (Bukau and Walker, 1989a, b) and are sensitive to DNA damaging antibiotics (Nichols et al., 2011). These proteins include the actin homolog MreB, the tubulin homolog FtsZ, the DNA excision repair protein UvrA, the glutamine ABC transporter component glnQ, the histidine transport ATP-binding protein hisP and the Leu/Ile/Val-binding protein livJ. The less-enriched proteins have a significant preference for proteins involved in translation, ribosomal structure and biogenesis (COG class J) and include 24 of the 32 ribosomal proteins that interact with DnaK. Accordingly, essential proteins (54 out of 142 proteins) (Gerdes et al., 2003) are more highly represented among the less-enriched substrates (Figure 16A). Enrichment correlated with a higher frequency of predicted DnaK binding sites (Van Durme et al., 2009) within protein sequences when corrected for size (Figure 16B). Furthermore, enriched interactors are more frequently part of heterooligomeric complexes than the less-enriched substrates (when ribosomal proteins are considered separately) (Figure 16C), suggesting a role for DnaK in oligomeric assembly.

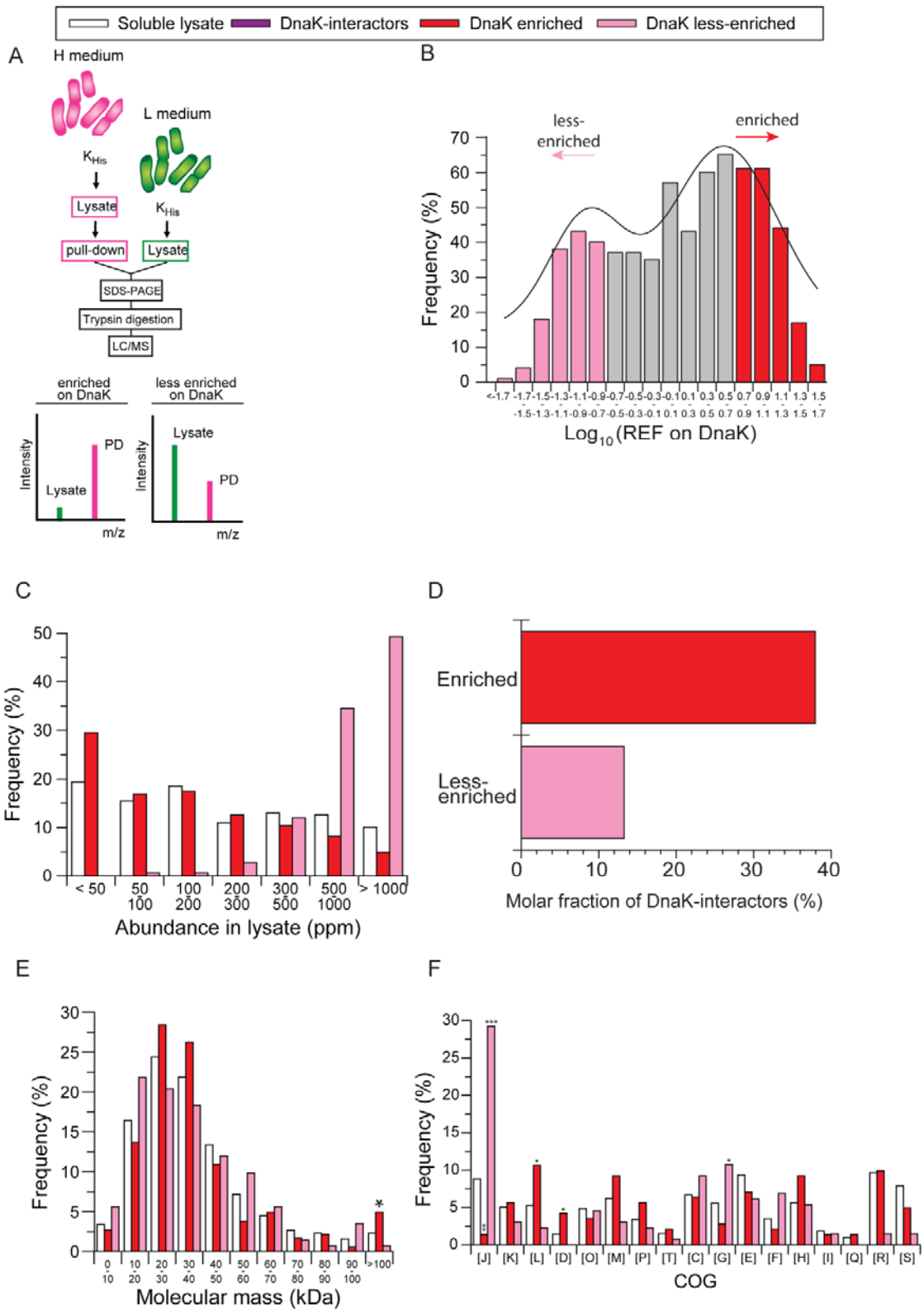


Figure 15 Properties of the DnaK enriched and less-enriched substrates (A)

(A) Scheme of the PD/Lysate SILAC experiment for the determination of highly enriched DnaK interactors. (B) Relative enrichment of interactor proteins on DnaK. The histogram shows the distribution of relative enrichment factors (REF) for 666 DnaK-interactors identified in 3 independent biological repeats. REF indicates the fraction of total cellular protein bound to DnaK. Enriched and less-enriched sets of interactors were selected at the extremes of the distribution for further analysis as described in Extended Experimental Procedures. (C) Abundance in soluble lysate determined based on cumulative abundance values (emPAI) (Ishihama et al., 2005). (D) Molar fraction of the DnaK-dependent (enriched) and less-enriched substrates identified in DnaK-interactor complexes pull-downs, as based on abundance values (emPAI) determined by MS. (E) Molecular mass distributions of soluble lysate proteome and DnaK-interacting proteins of the enriched and less-enriched sub-sets. *, $p \leq 0.05$ based on a chi-square test. (F) Functional classification according to the Categorization Of Gene products (COG). *, $p \leq 0.05$, **, $p \leq 0.01$, ***, $p \leq 0.001$ based on a chi-square test. COG function abbreviations: [J] Translation, ribosomal structure and biogenesis; [K] Transcription; [L] Replication, recombination and repair; [D] Cell cycle control, cell division, chromosome partitioning; [T] Signal transduction mechanisms; [M] Cell wall/membrane/envelope biogenesis; [O] Posttranslational modification, protein turnover, chaperones; [C] Energy production and conversion; [G] Carbohydrate transport and metabolism; [E] Amino acid transport and metabolism; [F] Nucleotide transport and metabolism; [H] Coenzyme transport and metabolism; [I] Lipid transport and metabolism; [P] Inorganic ion transport and metabolism; [Q] Secondary metabolites biosynthesis, transport and catabolism; [R] General function prediction only; [S] Function unknown.

To test whether the proteins enriched on DnaK have a higher propensity to aggregate, we took advantage of the study by Niwa et al (2009) who had analyzed the solubility of *E. coli* proteins upon in vitro translation in the reconstituted PURE system in the absence of chaperones. Indeed, we find DnaK-enriched proteins to be relatively aggregation prone in this assay, with 60% of proteins having $\leq 50\%$ solubility, while the less-enriched DnaK-interactors are more soluble than average lysate proteins (Figure 16D). The lower solubility of the former is consistent with the finding that aggregation propensity correlates inversely with abundance. Moreover, the enriched proteins frequently display pI values close to neutral

pH (Figure 16E). However, their average hydrophobicity is not increased compared to the less-enriched interactors (Figure 16F). Interestingly, ~18 % (29 proteins) of the DnaK-enriched substrates with assigned fold (159 proteins) contain at least one domain with SCOP fold c.37 (P-loop containing nucleoside triphosphate hydrolases), compared to only ~8 % of lysate proteins and ~3 % of the less-enriched DnaK-interactors (4 of 140 proteins with assigned fold) (Figure 16G). The fold c.37 is characterized by a complex alpha/beta topology, suggesting that these proteins tend to populate kinetically trapped intermediates during folding (Gromiha and Selvaraj, 2004). Indeed, their average solubility upon in vitro translation is <30% (Figure 16 D), including a number of proteins with COG class D and L functions (Figure 15G). Interestingly, it is also strongly enriched in heterooligomeric proteins (Figure 16H). The less-enriched substrates have a preference for the SCOP folds c.2 (NAD(P)-binding Rossmann-fold) and b.40 (OB-fold). These are folds commonly found in abundant metabolic enzymes and ribosomal proteins, respectively, explaining their prevalence among the less-enriched substrate and their relatively high solubility upon in vitro translation (Figure 16 D).

In summary, the enrichment of proteins on DnaK correlates with their propensity to aggregate during folding. The ~180 most enriched DnaK-interactors occupy ~40% of the DnaK capacity. They are of relatively low cellular abundance, contain more predicted DnaK binding sites than the less enriched interactors, and frequently assemble with other proteins to heterooligomeric complexes.

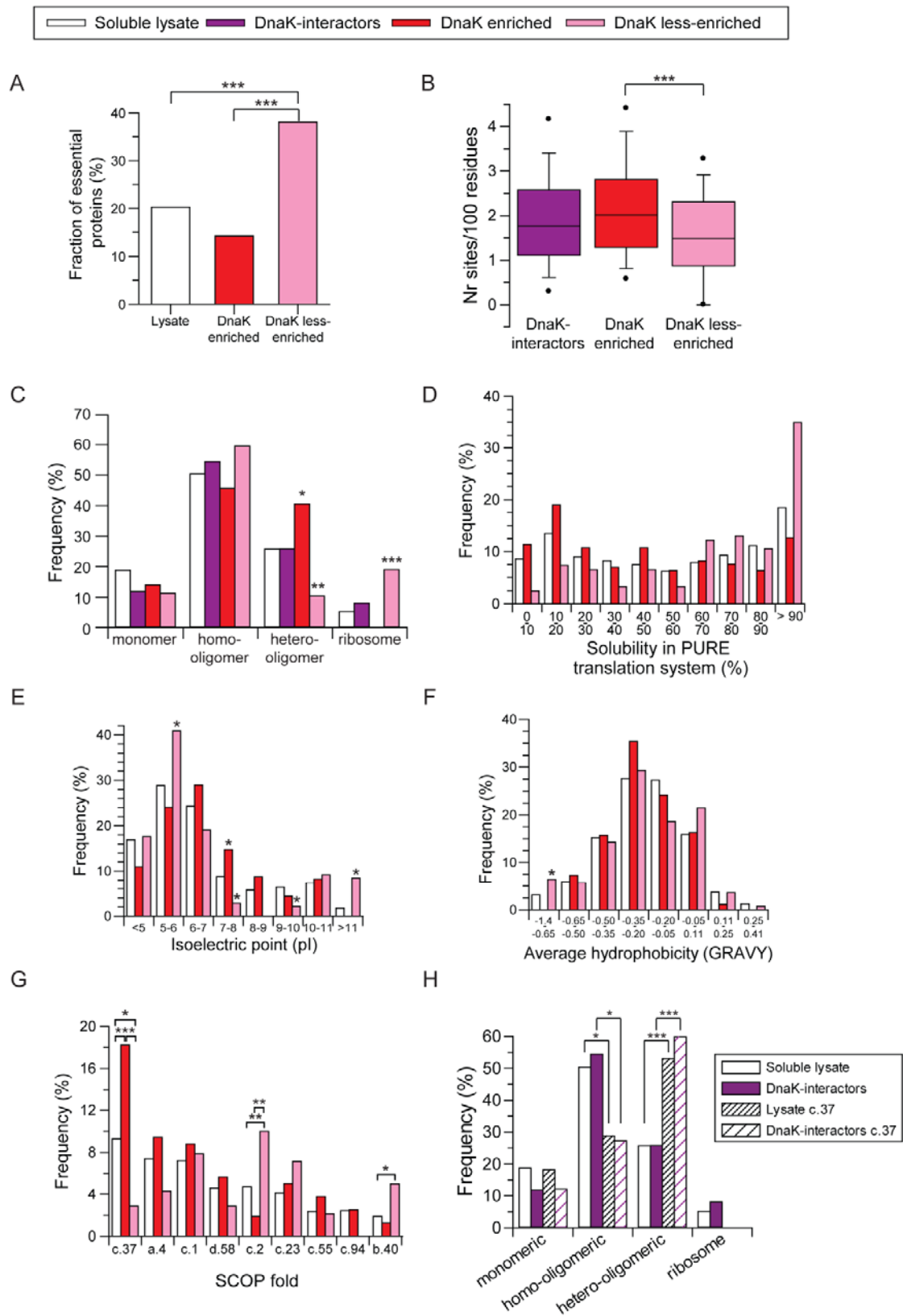


Figure 16 Properties of the DnaK enriched and less-enriched substrates (B)

(A) Fraction of essential proteins among the enriched and less-enriched DnaK interactors as compared to soluble lysate. ***, $p \leq 0.001$ based on a chi-square test. (B) Density of predicted DnaK binding sites in the sequences of enriched and less-enriched DnaK substrates as compared to the entire DnaK interactome. whisker caps and circles indicate 10th/90th and 5th/95th percentiles, respectively. ***, $p \leq 0.001$ based on a Mann-Whitney test. (C) Oligomeric state of the total, enriched and less enriched DnaK interactors compared to soluble lysate proteins. Ribosomal proteins are shown separately. *, $p \leq 0.05$, ***, $p \leq 0.001$ based on a Mann-Whitney test. (D) Solubility in PURE system of soluble lysate proteome and DnaK-interacting proteins of the enriched and less-enriched interactors. (E-G) Isoelectric point (pI), average hydrophobicity and SCOP fold distribution of the DnaK-dependent (enriched) and less-enriched interactors. *, $p \leq 0.05$, **, $p \leq 0.01$, ***, $p \leq 0.001$ based on a chi-square test. SCOP fold abbreviations: c.37, P- loop containing nucleotide triphosphate hydrolases; a.4, DNA/RNA binding 3-helical bundle; c.1, TIM β/α barrel; d.58, Ferredoxin-like; c.2, NAD(P)-binding Rossmann-fold domains; c.23, Flavodoxin-like; c.55, Ribonuclease H-like motif; c.94, Periplasmic binding protein-like II; b.40, OB-fold. (H) Oligomeric state of soluble lysate proteins, DnaK-interactors, lysate proteins with c.37 fold and DnaK-interactors with c.37 fold. *, $p \leq 0.05$, ***, $p \leq 0.001$ based on a chi-square test.

4.1.6 Limited and specific changes in proteome composition upon DnaK deletion

To analyze the consequences of deleting the DnaK chaperone system in vivo, we performed quantitative proteome analysis of SILAC labeled *dnaK-WT* (M-labeled) and $\Delta dnaK dnaJ$ (ΔKJ) cells (H-labeled) at 30 °C where deletion of DnaK and DnaJ is well tolerated (Figure 13B). Out of ~1400 proteins quantified, 105 proteins were found to be significantly increased in ΔKJ cells, presumably reflecting an adaptive response to compensate for the loss of the DnaK system. These proteins, including 42 DnaK-interactors (Table S2), also function preferentially in COG class H, as well as in carbohydrate transport and metabolism (COG class G) and in post-translational modification, protein turnover and chaperones (COG class O). Notably, the latter group of proteins include the major cytosolic

chaperones and proteases (GroEL/ES, HtpG, IbpA, IbpB, ClpB, HslU, HslV, Lon) and are 5 to >10-fold upregulated (Table S2). This correlates with a 4.5-fold increase in the level of the heat shock transcription factor rpoH (σ 32), which is negatively regulated by DnaK and DnaJ (Gamer et al., 1992)

Interestingly, only 87 proteins were reproducibly found to be decreased by ~40-95 % (median 60 %; $p < 0.05$) in the total proteome of the Δ KJ cells (Table S3). SILAC pulse-labeling demonstrated similar rates of synthesis in K_{His} and Δ KJ cells (Figure 17A), indicating that the decrease in protein abundance is largely due to degradation. Notably, 40 of the degraded proteins (4 essential proteins) were identified DnaK-interactors. Generally, these proteins are characterized by average enrichment on DnaK, lower than average protein abundance in wild-type cells and higher molecular weight (Figure 17 B-D). On average, these proteins are of lower solubility upon in vitro translation in the absence of chaperones, similar to the enriched DnaK-interactors (Figure 17E) (Niwa et al., 2009). Importantly, DnaK enriched substrates are significantly enriched in that subset, indicating that they are efficiently degraded upon misfolding (Figure 17 F). The degraded DnaK-interactors frequently function in amino acid transport and metabolism (COG class E) and in coenzyme transport and metabolism (COG class H) (Table S3).

Next, to determine the extent of protein aggregation in cells lacking DnaK/DnaJ, we analyzed the insoluble and soluble fractions of Δ KJ cells compared to K_{His} cells. In total 474 proteins, 201 of them identified DnaK-interactors (Table S4), were significantly increased in abundance in the insoluble fraction of Δ KJ cells, but only for 65 of these including 30 DnaK interactors (8 essential proteins) did aggregation result in a substantial depletion from the soluble fraction by 5-90% (median 9 %; $p < 0.05$) (Table S4). Thus, aggregation generally led

to lower levels of depletion than degradation. However, compared to the less-enriched interactors, higher levels of aggregation resulted in significant depletion from soluble fraction of some of the DnaK enriched interactors (Figure 17G). Remarkably, the aggregating proteins did not overlap with the degraded proteins. Several of the strongly aggregating DnaK interactors are very large in size (>100 kDa) (Figure 17D). They are on average somewhat less enriched on DnaK than the preferentially degraded interactors. Furthermore, they are more abundant and have higher predicted aggregation scores (Z_{agg}) (Figure 17 C and data not shown). The aggregated proteins function in coenzyme transport and metabolism (COG class H), carbohydrate transport and metabolism (COG class G), transcription (COG class K), Replication, recombination and repair (COG class L) and cell wall/membrane/envelope biogenesis (COG class M). They include the 150 kDa RNA polymerase subunits β (RpoB) and β' (RpoC), the 130 kDa transcription repair coupling factor (mfd), the 106 kDa antigen 43, the phase-variable bipartite outer membrane protein (flu) and the 103 kDa excision nuclease subunit A (UvrA). Notably, the small heat shock proteins, IbpA and IbpB, were also depleted from the soluble fraction by ~40 and ~90%, respectively, presumably due to association with the aggregates (Table S4)

These findings define a subset of DnaK-interactors as highly dependent on the presence of DnaK/DnaJ *in vivo*, experiencing either degradation or aggregation. However, the majority of aggregation-prone DnaK interactors, as defined upon translation *in vitro*, remain unaffected in ΔKJ cells, indicating that the loss of DnaK function under standard growth conditions at 30 °C is generally well compensated by other chaperones.

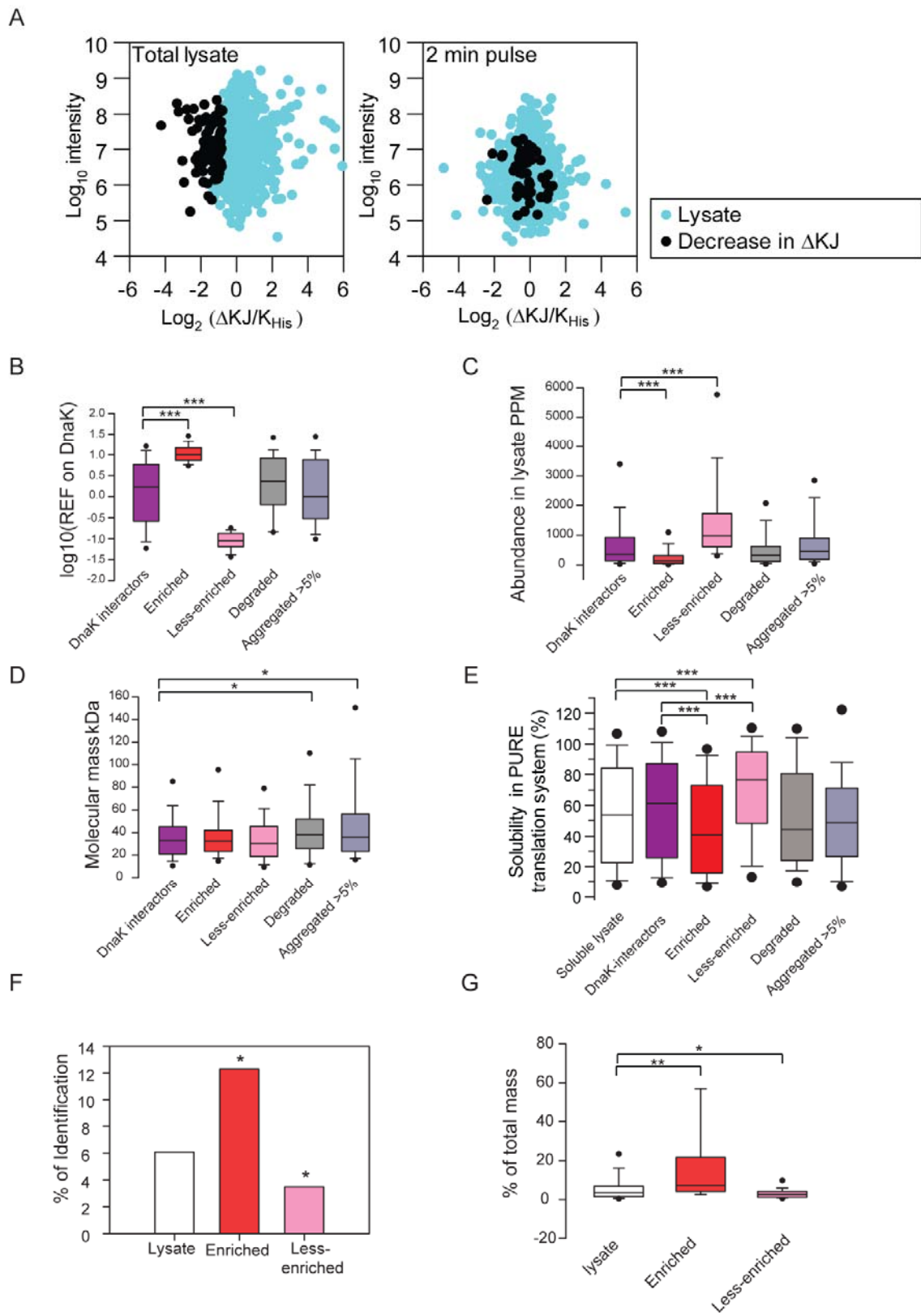


Figure 17 Limited but specific impact on proteome upon DnaK deletion

(A) Proteome change in Δ KJ cells due to degradation. Left panel: isotope ratios of proteins identified in the total cell lysate of Δ KJ cells relative to K_{His} cells, grown at 30°C, plotted against collective peptide intensity of respective proteins; black dots show the proteins significantly decreased ($p < 0.05$) in the proteome of the mutant strain. Right panel: K_{His} and Δ KJ cells growing in L medium were pulse-labeled for 2 min with M or H amino acid isotopes, respectively. The total cell lysates were mixed at a 1:1 ratio and analyzed by LC-MS/MS. The median ratios of two independent experiments are shown in the figure, indicating differences in amino acid incorporation rate in the proteins of the Δ KJ versus K_{His} cells. Proteins found to be decreased in the proteome of the Δ KJ are in black. Note that most of these proteins are synthesized with the same rate as in wild-type cells. (B-D) Box plot distribution of REF, abundance in lysate and molecular mass of degraded and aggregated preferred DnaK interactors at 30 °C. *, $p \leq 0.05$, ***, $p \leq 0.001$ based on a Mann-Whitney test. (E) Box plot distribution of solubility of degraded and aggregated preferred DnaK interactors at 30 °C. ***, $p \leq 0.001$ based on a Mann-Whitney test. (F) *, $p \leq 0.05$ based on a chi-square test. % distribution of enriched and less-enriched DnaK interactors in the degraded set of proteins in the Δ KJ strain at 30 °C compared to lysate proteins. (G) Box plots of the percentage of the total mass of proteins accumulated in the aggregated fraction and depleted from the soluble lysate in Δ KJ cells for the enriched and less-enriched DnaK interactors compared to the experimental lysate proteins. *, $p \leq 0.05$, **, $p \leq 0.01$ based on a Mann-Whitney test.

4.2 The Kinetics of DnaK and substrates interaction**4.2.1 DnaK functions in *de novo* folding and conformational maintenance**

To determine the extent to which DnaK interacts with newly-synthesized and pre-existent proteins, we performed pulse-SILAC experiments. K_{His} cells were grown at 37 °C in media containing unlabeled Arg/Lys (L) and then shifted to media containing M-labeled Arg/Lys for 2.5 min to label newly-synthesized polypeptides. WT cells grown in heavy (H) Arg/Lys served as background control. Lysates from the K_{His} and WT cells were mixed 1:1 and DnaK-interactors identified. The M/L ratio of a DnaK-interactor relative to its M/L ratio in the lysate (the latter correcting for rates of synthesis and turnover) was used to indicate

whether it bound to DnaK preferentially as a newly-synthesized or pre-existent protein (Figure 3A). Isotope ratios were obtained for ~300 DnaK-interactors (Table S5). \log_{10} M/L ratios lower than 0, indicating a preference for interaction as pre-existent protein, were observed for only 20 interactors (Figure 18A). Most other proteins bound to DnaK preferentially upon synthesis, including ~100 proteins with a strong preference for interaction as newly-synthesized polypeptides (\log_{10} M/L ratio >1). Ribosomal proteins interacted with DnaK as newly-synthesized proteins (Figure 18A), in support of the proposed role of DnaK in ribosome assembly (El Hage and Alix, 2004; Maki et al., 2002; Rene and Alix, 2011). Thus, DnaK interacts predominantly with newly-synthesized-proteins, reflecting functions in *de novo* protein folding/assembly, but many of these proteins return to DnaK for conformational maintenance.

We next compared the physico-chemical properties of the newly-synthesized DnaK-interactors (\log_{10} M/L ratio ≥ 1) and the pre-existent interactors (\log_{10} M/L ratios ≤ 0) (Figure 18A). Ribosomal proteins were analyzed separately, as their unusual size and charge properties would introduce a strong bias. The proteins that preferentially interact with DnaK upon synthesis are on average relatively large in size (Figure 18B) and less hydrophobic than the pre-existent substrates (Figure 18C). They have aggregation propensities, calculated with the Z_{agg} algorithm (Tartaglia and Vendruscolo, 2008), comparable to average lysate proteins, whereas the ribosomal proteins have very low aggregation scores (Figure 18D). Furthermore, the tendency to interact with DnaK upon synthesis correlates with a low enrichment on DnaK, suggesting that these proteins interact transiently (Figure 18E). In contrast, the pre-existent interactors are similar in size to the average of lysate proteins (Figure 18E) and are more enriched on DnaK than the newly-synthesized proteins (Figure 18E), arguing for longer

residence times on DnaK. They are also characterized by higher intrinsic aggregation propensities than the newly-synthesized interactors or the average lysate proteins ($p < 0.05$) (Figure 18D). Thus, a prominent feature of the pre-existent interactors is their intrinsic tendency to populate aggregation-prone states, explaining their requirement for conformational maintenance by DnaK. It is interesting to note that several of the DnaK-interactors that are degraded in ΔKJ cells belong to this group of proteins (Figure 16E).

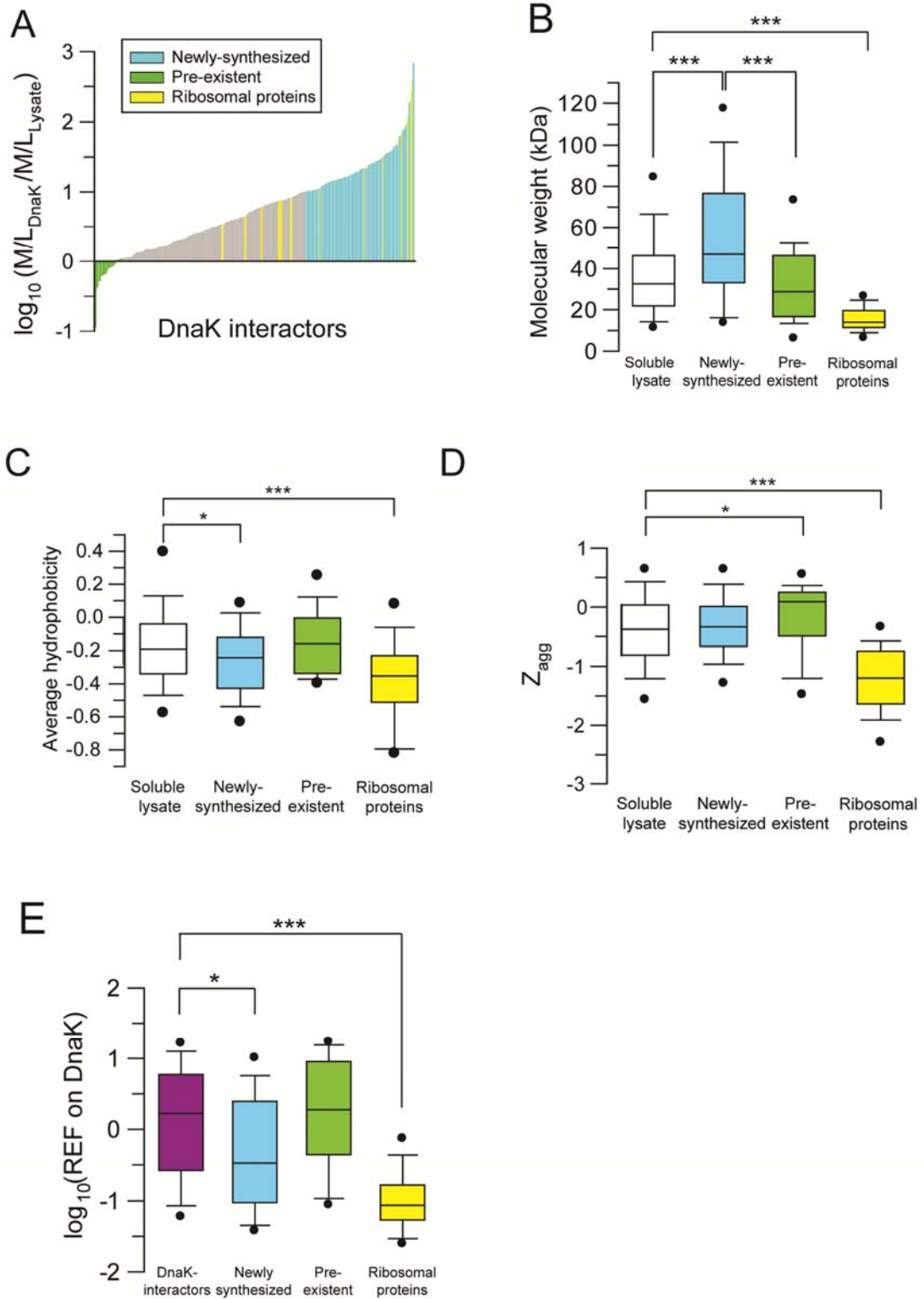


Figure 18 DnaK interacts preferentially with newly synthesized proteins

(A) Ratios of medium to light isotopes (M/L) of DnaK-interactors relative to the M/L ratios for the same proteins in soluble cell lysate. Positive values of the log transformed ratio of ratios indicate a preferential interaction with DnaK as newly-synthesized proteins. Groups of proteins selected for bioinformatic analysis are color coded. Molecular weight (B), average hydrophobicity (GRAVY) (C), intrinsic aggregation propensity, Z_{agg} (D) and relative enrichment on DnaK (REF) (E) of the substrates preferentially interacting as pre-existent or newly-synthesized polypeptides as compared to *E. coli* soluble lysate proteins and all DnaK-interactors, respectively. The ribosomal proteins among DnaK-interactors are analyzed separately. Horizontal line indicates the median, whisker caps and circles indicate 10th/90th and 5th/95th percentiles, respectively. *, $p \leq 0.05$, ***, $p \leq 0.001$ based on a Mann-Whitney test.

4.2.2 Protein flux through DnaK

To measure the residence time of interactors on DnaK directly, K_{His} cells were pulse-labeled with Arg/Lys isotopes (H) for 2.5 min, followed by a chase with excess of unlabeled amino acids (L). The decrease of the H/L ratio over time allowed us to estimate the residence time on DnaK. Interpretable time course data were collected for 91 proteins, with apparent rate constants of substrate release corresponding to half-times from ~30 s to ~25 min (Figure 19A and Table S6). Proteins with slow release rates (≤ 30 th percentile of the rate distribution; 27 proteins) include the chaperones GroEL, IbpA and SecB, presumably reflecting their functional co-operation with DnaK. Slow releasing proteins (excluding chaperones) are characterized by above average enrichment on DnaK and an average number of predicted binding sites compared to all DnaK-interactors (Figure 19B). Proteins with fast release rates (≥ 70 th percentile of the rate distribution; 27 proteins) display average enrichment on DnaK but significantly lower number of binding sites (Figure 19B). Thus, the residence time (and consequently the enrichment) on DnaK is regulated, at least in part, by the frequency of potential DnaK recognition motifs in the polypeptide chain.

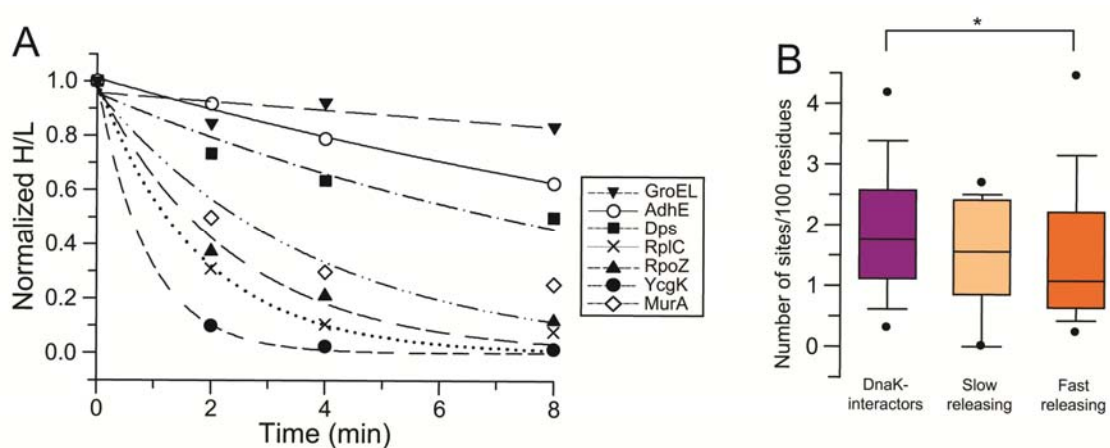


Figure 19 Kinetics of DnaK-interactor interaction

(A) Kinetics of dissociation from DnaK shown for selected proteins. Data were fitted to exponential decay. (B) Distribution of the number of predicted DnaK binding sites for the DnaK-interactor sets with fast and slow release kinetics as compared to all DnaK-interactors. Horizontal line indicates the median, whisker caps and circles indicate 10th/90th and 5th/95th percentiles, respectively. *, $p \leq 0.05$ based on Mann-Whitney test.

4.3 Functional redundancy of DnaK and Trigger factor is only partial

The chaperone components of the *E. coli* cytosol are thought to form a network of inter-related and partially overlapping functions (Hartl and Hayer-Hartl, 2009). To understand the role of DnaK within this network, we investigated how the DnaK interactome changes upon deletion of the upstream chaperone trigger factor (TF) or depletion of the downstream GroEL/ES chaperonin system.

The ribosome-bound TF and DnaK have overlapping functions in *de novo* folding, as indicated by the fact that they can be deleted individually but double deletion is lethal at temperatures above 30 °C (see Figure 13) (Deuerling et al., 1999; Genevaux et al., 2004;

Teter et al., 1999). We identified the DnaK-interactors in the Δtig strain at 37 °C by pulldown from H-labeled $\Delta tig/dnaK-His6$ ($\Delta T/K_{His}$) cells using L-labeled ΔT cells as background. The number of DnaK-interactors was increased to 998 (Table S7), exhibiting a ~95 % overlap with the 672 DnaK-interactors identified in K_{His} cells (Figure 20A). It is important to note here that DnaK levels are increased ~1.5-fold in $\Delta T/K_{His}$ cells, which may contribute to the increase in the number of identified interactors (Table S7). The additional 357 proteins have physico-chemical properties similar to the DnaK-interactors in wild-type cells, except that they tend to have higher pI values (median pI of 6.4, compared to 6.1), including additional 14 ribosomal proteins. To detect possible changes in the composition of the DnaK interactome, we performed a direct quantitative comparison of the DnaK complexes from H-labeled $\Delta T/K_{His}$ cells and M-labeled K_{His} cells. Proteins significantly increased on DnaK in the $\Delta T/K_{His}$ cells were selected from the distribution of H/M ratios by setting a threshold of minimal enrichment at the median +1.5 MAD (median absolute deviation) (corresponding to an average of ~1.5-fold enrichment). Sets of 71 and 74 proteins were increased or decreased on DnaK, respectively, in the $\Delta T/K_{His}$ cells (Table S8, S9). The proteins increasing on DnaK occupy ~10% of the DnaK capacity in K_{His} cells and ~15% in $\Delta T/K_{His}$ cells. Interestingly, these proteins are preferentially small in size (< 20 kDa) and include 17 highly basic ribosomal proteins (Table S8) as well as 10 basic non-ribosomal proteins (pI \geq 9) (Figure 20B, C), such as several secretory proteins with functions in cell envelope biogenesis and outer membrane biogenesis (Skp, AmpH, YcgK, SlyB). These proteins are medium enriched on DnaK (~1% of total cellular content in $DnaK_{His}$ cells) and interact with DnaK preferentially as newly-synthesized proteins (Table S8). The proteins decreased on DnaK in $\Delta T/K_{His}$ cells

are relatively large in size and normally have above average enrichment on DnaK. They may be partially displaced from DnaK by the small proteins (Figure 20B).

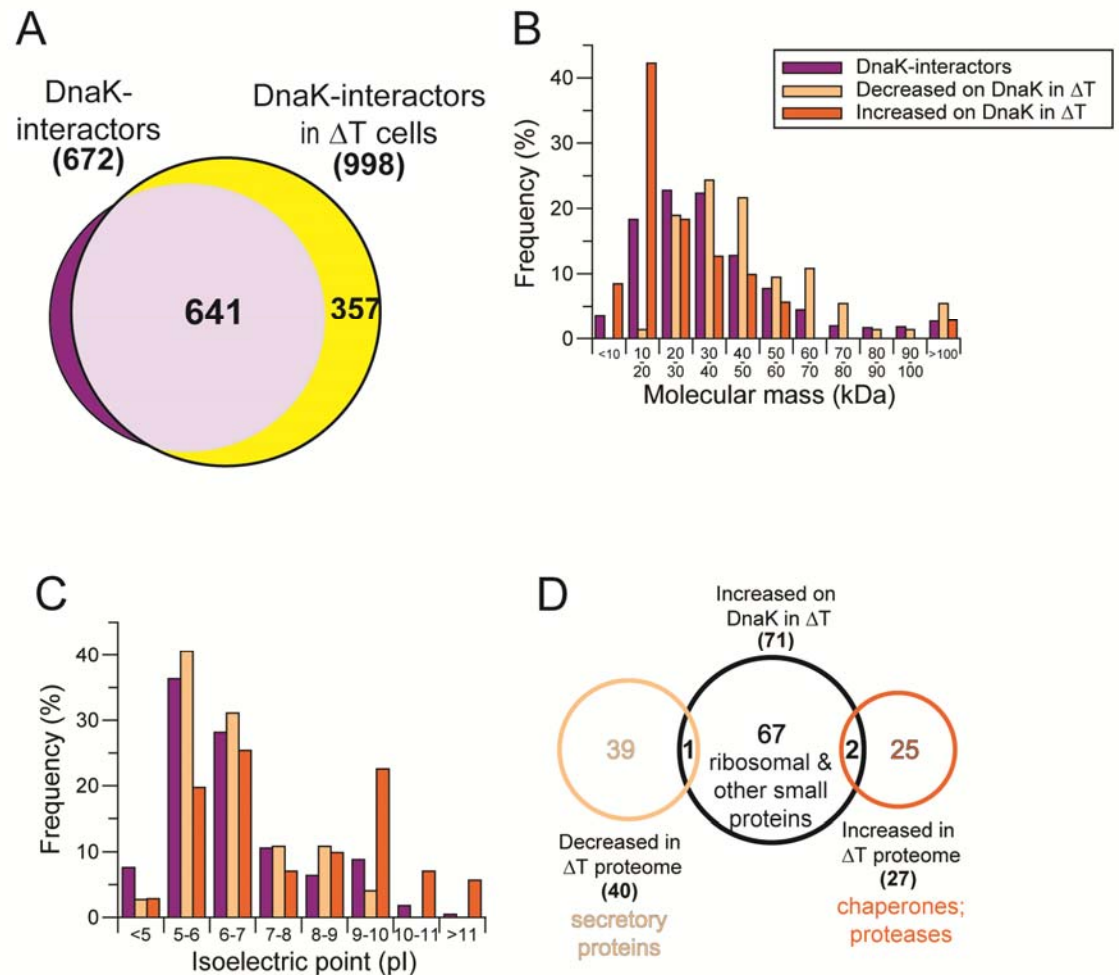


Figure 20 Specific Trigger factor substrates accumulated on DnaK in $\Delta T/K_{His}$

(A) Overlap of DnaK-interactors in K_{His} (672 proteins) and $\Delta T/K_{His}$ cells (998 proteins). (B-C) Change in the distribution of molecular weight (B) and isoelectric point (C) of the DnaK interactome in $\Delta T/K_{His}$ cells compared to all DnaK-interactors in K_{His} cells. (D) Minimal overlap of the sets of proteins significantly decreased or increased in abundance in the proteome of $\Delta T/K_{His}$ cells with the set of proteins that increased on DnaK in $\Delta T/K_{His}$ cells.

To further explore the functional interplay between TF and DnaK, we analyzed the changes of protein levels in total cell lysate and in the insoluble fraction of isotope labeled $\Delta T/K_{His}$ cells as compared to K_{His} cells. Only 40 of 1490 quantified proteins were reproducibly found to be decreased by 25-84 % ($p < 0.05$) in the TF deleted cells, and 27 proteins were increased in abundance (Figure 20D and Table S10, S12). Neither of these groups of proteins overlapped significantly with the proteins that interacted increasingly with DnaK upon TF deletion (Figure 20D). Strikingly, ~80 % of the proteins that were decreased in $\Delta T/K_{His}$ cells (31 out of 40 proteins) carry predicted signal peptide sequences (Figure 21A), although their rates of synthesis were unchanged (Figure 21B) (Table S10). These proteins include numerous outer membrane β -barrel proteins OmpA and OmpC, the β -barrel assembly components BamA (YaeT) (Kim et al., 2007), the outer membrane channel for nucleosides tsx, Outer membrane factor (OMF) of tripartite efflux pumps tolC, as well as the periplasmic chaperone DegP (Sklar et al., 2007), involved in β -barrel protein folding, and the periplasmic PPIase FkpA (Bothmann and Pluckthun, 2000). These findings suggested that $\Delta T/K_{His}$ cells have a defect in the structural integrity of the outer membrane. Indeed, $\Delta T/K_{His}$ cells proved to be sensitive to treatment with detergents like as deoxycholate, and high molecular weight antibiotics, such as vancomycin, which is indicative of a weakening of the outer membrane (Freire et al., 2006; Heidrich et al., 2002; Nichols et al., 2011; Sampson et al., 1989) (Figure 21C). Only 2 of the β -barrel proteins, OmpC and TolC, were identified as enriched DnaK-interactors (Table S1). Interestingly, OmpA, OmpC and TolC decreased on DnaK in ΔT cells (Table S9). The proteins that increased in abundance in $\Delta T/K_{His}$ cells include chaperones (DnaK, GroEL/ES, ClpA, ClpB, ClpX, ClpP, HtpG, and IbpA), the secretory ATPase SecA and the proteases Lon and HslU. These factors are moderately

increased ~ 1.5 -fold, presumably reflecting a compensatory up-regulation in response to the loss of TF. Only few proteins were found to be increased in the insoluble fraction of $\Delta T/K_{His}$ cells (Table S11), without resulting in depletion, indicating that loss of TF function at $37^\circ C$ does not result in significant protein aggregation.

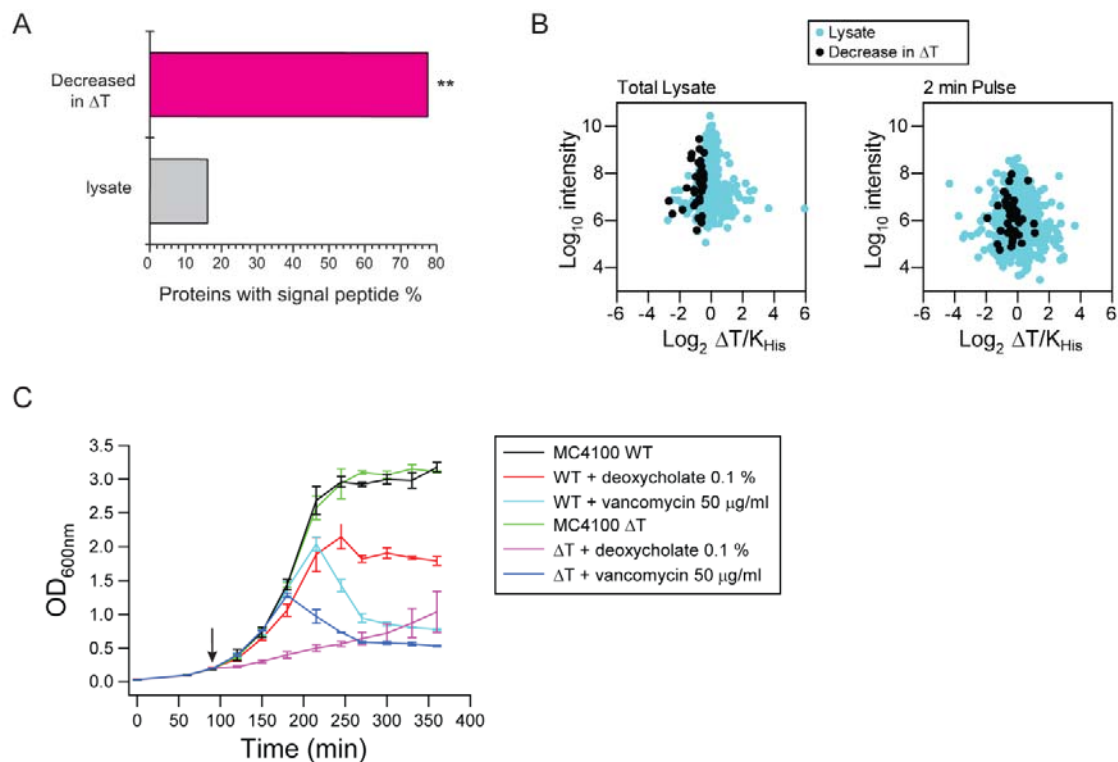


Figure 21 The subset of secretory proteins degraded upon deletion of Trigger factor

(A) * * $p < 0.005$ based on a chi-square test. Signal peptide prediction for the proteins significantly decreased in the $\Delta T/K_{His}$ total lysate. (B) Proteome change in $\Delta T/K_{His}$ cells due to degradation. Left panel: isotope ratios of proteins identified in the total cell lysate of $\Delta T/K_{His}$ cells relative to K_{His} cells, grown at $37^\circ C$, plotted against collective peptide intensity of respective proteins; black dots show the proteins significantly decreased ($p < 0.05$) in the proteome of the mutant strain. Right panel: K_{His} and $\Delta T/K_{His}$ cells growing in L medium were pulse-labeled for 2 min with M or H amino acid isotopes, respectively. The total cell lysates were mixed at a 1:1 ratio and analyzed by LC-MS/MS. The median ratios of two independent experiments are shown in the figure, indicating differences in amino acid

incorporation rate in the proteins of the $\Delta T/K_{His}$ versus the K_{His} cells. Proteins found to be decreased in the proteome of the $\Delta T/K_{His}$ are in black. Note that most of these proteins are synthesized with the same rate as in wild-type cells. (C) Outer membrane destabilization in $\Delta T/K_{His}$ cells. Growth curves at 37°C of K_{His} and $\Delta T/K_{His}$ cells in the presence and absence of 0.1% deoxycholate or 50 µg/ml vancomycin. Arrow indicates the time of addition of deoxycholate or vancomycin after dilution of an overnight culture in fresh M63 medium at an OD_{600nm} of 0.025.

These results indicate a functional overlap of TF and DnaK in the folding/assembly of ribosomal and other small, basic proteins. In addition, TF has a specific role in the biogenesis of outer membrane β -barrel proteins. This function is only partially replaced by other chaperones and by up-regulation of the secretory ATPase SecA, resulting in outer membrane destabilization.

4.4 Interplay of DnaK and GroEL/GroES

In both ΔKJ and $\Delta T/K_{His}$ cells the chaperonin GroEL and its cofactor GroES are increased in abundance by ~8 and 1.5-fold, respectively (Tables S3 and S11), suggesting that these chaperone systems form a functional network. Indeed, we find that 119 of the 248 previously identified GroEL substrates (Kerner et al., 2005) were also identified as DnaK-interactors and this number increases to 152 when TF is deleted, occupying ~27% of the DnaK capacity (Figure 22A and Tables S1 and S7). 42 of these DnaK-interactors are obligate GroEL-dependent (class III) and thus must be delivered to GroEL for folding, while 80 belong to class II and 30 to class I (Figure 22B) (Fujiwara et al., 2010; Kerner et al., 2005). Class II substrates are highly chaperone dependent but can utilize either GroEL/ES or DnaK/DnaJ for folding in vitro, whereas class I proteins have a lower chaperone dependence. To investigate how the loss of GroEL/ES affects the spectrum of DnaK-interactors, we isolated DnaK-

interactor complexes from cells (LS-/K_{His}) in which GroEL/ES was depleted. To this end, MC4100 cells expressing DnaK-His6 and carrying the *groELS* operon under arabinose control (Kerner et al., 2005; McLennan and Masters, 1998) were shifted from arabinose (LS+/K_{His}) to glucose containing medium for 4 hours at 37°C (LS-/K_{His}), resulting in a depletion of GroEL/ES by ~97 %. Note that the cells grow normally during the first 5 h of GroEL/ES depletion (data not shown). DnaK-interactor complexes from LS+/K_{His} cells (H-labeled) were analyzed in comparison to DnaK complexes from LS+/K_{His} cells of the same strain under non-depleting conditions (M-labeled). 92 proteins were reproducibly increased on DnaK by ≥ 2 -fold upon GroEL depletion and 54 proteins were decreased. The proteins increased on DnaK include 38 previously identified GroEL substrates of which 19 (50 %) (Figure 22B) belong to class III (Table S12, S13). They are enriched in domains with SCOP fold c.1 (TIM-barrel), in molecular mass 30-50 kDa and pI 6-7 (Figures 22 C-E), which are prominent features of the obligate GroEL/ES substrates (Kerner et al., 2005). On the other hand, the proteins reduced on DnaK included only 11 GroEL substrates of which the majority belong to class II (data not shown), comprising proteins predicted to utilize either DnaK/DnaJ or GroEL/ES for folding (Kerner et al., 2005). This would suggest that in the absence of GroEL, misfolded class III substrates compete with other proteins for DnaK binding.

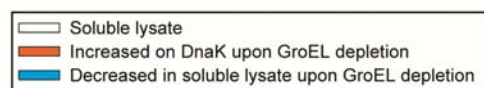
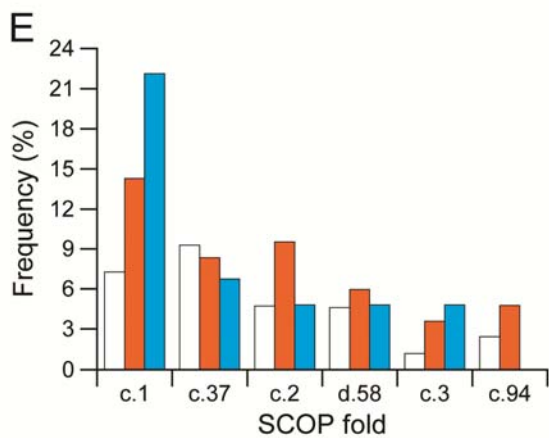
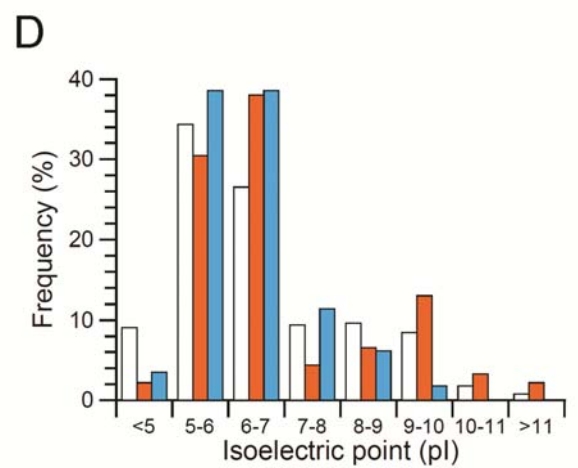
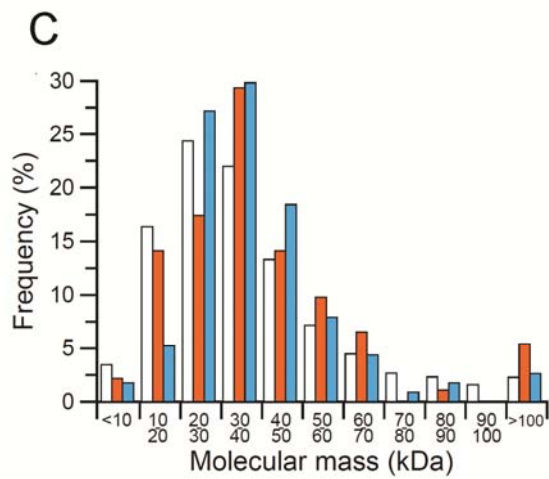
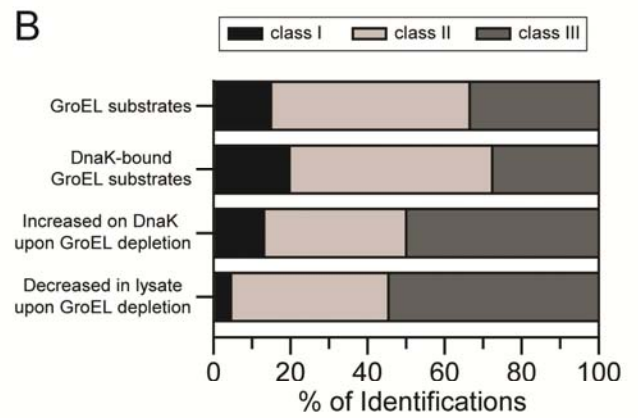
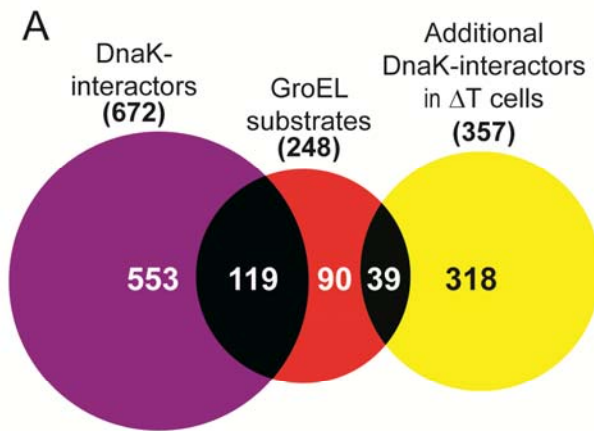


Figure 22 Obligate GroEL substrates accumulated on DnaK upon GroEL depletion

(A) Overlap of previously identified GroEL substrates (248 proteins) (Kerner et al., 2005) with DnaK-interactors in K_{His} (672 proteins) and $\Delta T/K_{His}$ (357 additional DnaK-interactors). (B) Class distribution of the GroEL substrates (Kerner et al., 2005) compared to the class distribution of GroEL substrates bound to DnaK in K_{His} cells, increased on DnaK upon GroEL-depletion and class distribution of GroEL substrates that are partially degraded in total cell lysate upon GroEL-depletion. Class I, chaperone independent; class II, chaperone dependent; class III, obligate GroEL substrates. (C-E) Molecular weight (C), isoelectric point (pI) (D) and SCOP fold distribution (E) of proteins increased on DnaK and decreased in total cell lysate in $LS-/K_{His}$ cells compared to the SCOP fold distribution of proteins in soluble lysate of $LS+/K_{His}$ cells. SCOP abbreviations: c.1, TIM β/α barrel; c.2, NAD(P) binding Rossmann fold domains; c.3, FAD/NAD(P) binding domain; c.37, P loop containing nucleotide triphosphate hydrolases; d.58, ferredoxin-like; c.94, Periplasmic binding protein-like II.

The consequences of GroEL depletion were also analyzed at the proteome level at 37°C. GroEL depletion reproducibly resulted in a ~35 to ~95 % decrease in abundance of 114 proteins and a ≥ 2 -fold increase of 95 proteins in total cell lysate (Table S14). The latter group again comprised chaperones and proteases, including DnaK, DnaJ and GrpE (Table S14). 19 of these 95 proteins are GroEL substrates, including 8 Class III substrates of which 6 found to be extensively aggregated upon GroEL depletion (11%-60%), suggesting that their up-regulation may be a mechanism to compensate for the loss of functional protein by aggregation. The observed reduction in protein abundance was due to degradation, because there was no apparent difference in the rates of protein synthesis between GroEL depleted and non-depleted cells (Figure 23A). The degraded proteins include 44 GroEL substrates, 24 of which (~55 %) are class III proteins (Figure 22B, 23C).

Strikingly, 18 of these GroEL substrates are nevertheless increased on DnaK (Figure 23B), suggesting that DnaK stabilizes GroEL substrates that are unable to fold for

degradation. However, analysis of the insoluble fraction of GroEL-depleted cells revealed that loss of GroEL function not only resulted in degradation but also in aggregation. In total, 527 proteins were found to increase significantly in the insoluble fraction of GroEL-depleted cells at 37 °C, including ~70 % of all the previously identified class III GroEL substrates, ~45 % of the class II and ~23 % of the class I substrates (100 of the 239 identified GroEL substrates) (Figure 23D). On average 27% of total of the class III proteins, ~23% of the class II proteins and only ~9 % of class I proteins were recovered as aggregates (Figure 23E). Again, the proteins degraded or aggregated upon GroEL depletion were strongly enriched in proteins with SCOP fold c.1 (TIM-barrel) domains (Figures 22C-E). Notably, only 4 (<6 %) of the 68 predicted class III substrates aggregated upon GroEL depletion at 30 °C (Figure 23D and Table S14). Instead, 21 class III substrates were degraded by ~ 50 % under these conditions (Figure 23D). Apparently, at the lower temperature, these relatively low abundance proteins are efficiently stabilized by other chaperones, such as the DnaK system, and are rapidly delivered for degradation.

In summary, about half of the known GroEL substrates, including ~40 % of class III proteins, also interact with DnaK, which transiently stabilizes them and transfers them to GroEL. Upon depletion of GroEL, obligate GroEL substrates accumulate further on DnaK and are stabilized in non-aggregated states for subsequent degradation, which is efficient at 30 °C. However, upon GroEL depletion at 37 °C, the extent of protein misfolding exceeds the capacity of the upstream chaperone and protease systems. As a consequence, a large fraction of the GroEL substrates aggregate.

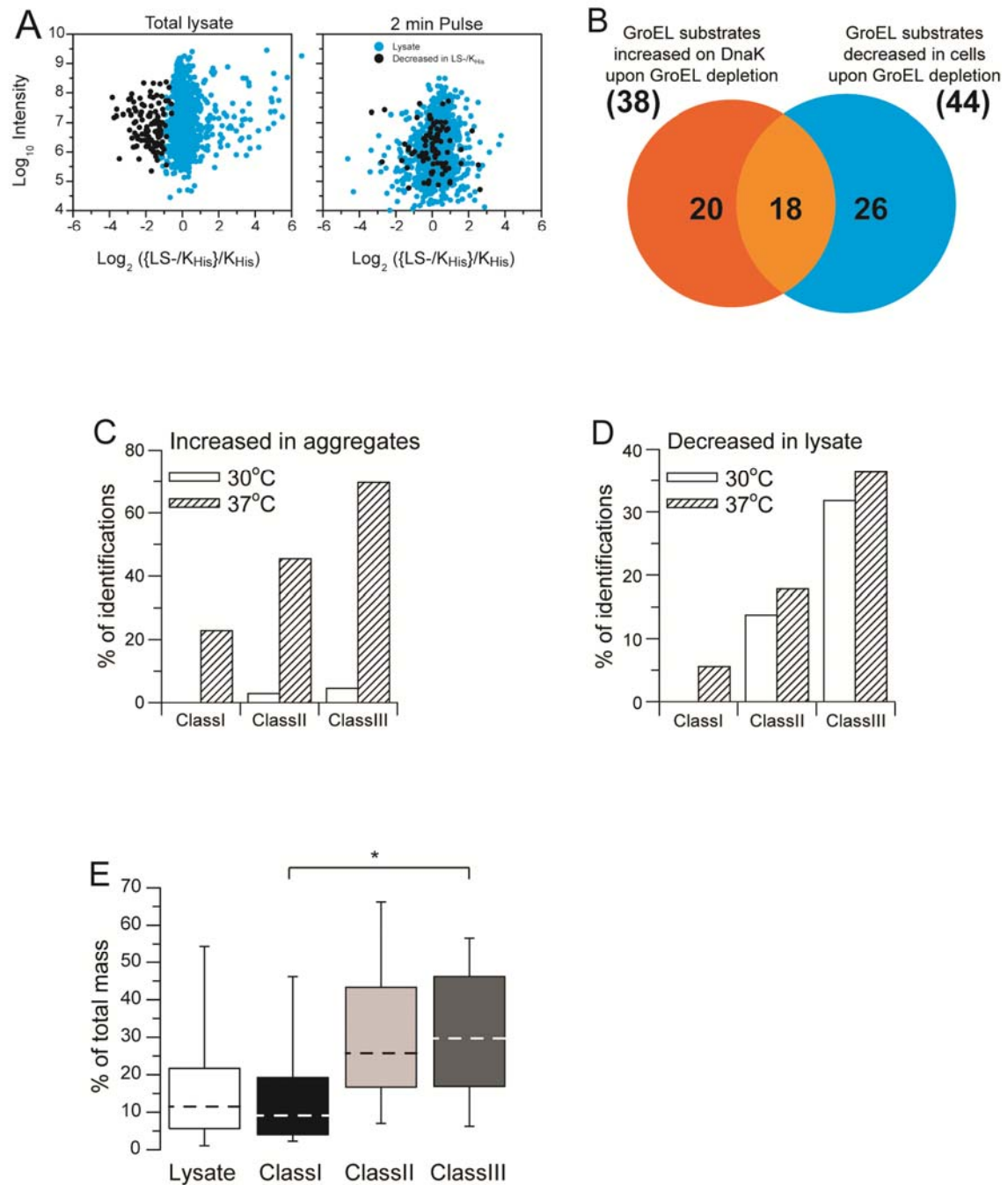


Figure 23 Proteomics analysis of GroEL-depleted cells

(A) Proteome change in LS-/K_{His} cells due to degradation. Left panel: isotope ratios of proteins identified in the total cell lysate of LS-/K_{His} cells relative to K_{His} cells, grown under the same

conditions at 37°C, plotted against protein intensity; black dots show the proteins significantly decreased ($p < 0.05$) upon GroEL depletion. Right panel: K_{His} and $LS-/K_{\text{His}}$ cells growing in L medium were pulse-labeled for 2 min with M or H amino acid isotopes, respectively. The total cell lysates (see Extended Experimental Procedures) were mixed at a 1:1 ratio and analyzed by LC-MS/MS. The median ratios of two independent experiments are shown in the figure, indicating differences in amino acid incorporation rate in the proteins of the $LS-/K_{\text{His}}$ versus the K_{His} cells. Proteins found to be decreased in the proteome upon GroEL/ES depletion are in black. Note that most of these proteins are synthesized with the same rate as in K_{His} cells. (B) Intersect between the groups of GroEL substrates increased on DnaK and GroEL substrates significantly decreased in the total lysate upon GroEL depletion. (C) Class distribution of GroEL substrates identified at 37°C in the aggregate fraction of $LS-/K_{\text{His}}$ cells and of GroEL substrates decreased in the total proteome of $LS-/K_{\text{His}}$ cells due to degradation. (D) Box plot of aggregation levels of GroEL substrates in GroEL depleted cells at 37 °C. (E) Box plots of the percentage of the total mass of proteins of different classes accumulated in the aggregated fraction and depleted from the soluble lysate upon GroEL depletion at 37 °C, GroEL substrates of different classes among the significantly aggregated proteins in the GroEL-depleted cells at 37 °C. *, $p < 0.05$, based on a Mann-Whitney test.

4.5 Proteostasis collapse upon combined deletion of DnaK and TF

Prevention of protein aggregation is one of the most fundamental functions of chaperones in proteostasis maintenance. To define the relative contribution of the different chaperone systems to aggregation prevention, we performed a comparative analysis of the aggregated proteomes upon individual and combined chaperone deletion at 30 °C, where cells lacking DnaK/DnaJ and TF (ΔKJT) still grow, albeit slowly (Figure 13B,C). As described above, 474 proteins were found to aggregate in ΔKJ cells, corresponding to ~ 0.8% of total cellular protein by mass, while only 15 proteins aggregated in $\Delta T/K_{\text{His}}$ cells (<0.1% of total protein by mass) and 33 proteins in $LS-/K_{\text{His}}$ cells (~0.4 % of total protein by mass) (Figure 24 A-D,E). This indicates a major role of the DnaK chaperone system in aggregation prevention. Notably, upon combined deletion of DnaK/DnaJ and TF, the number of proteins detected in

the insoluble fraction increased to 1087, including 403 identified DnaK interactors and amounting to ~ 3.9 % of total protein mass (Figure 24E). As expected, almost all (94 %) of the proteins found to aggregate in Δ KJ cells also aggregated in Δ KJT cells (Figure 25A, Table S4 and S15). Moreover, whereas in Δ KJ cells only 65 proteins (15 essential proteins) were >5 % depleted from the soluble fraction due to aggregation, 254 proteins aggregated to >5 % of total upon additional loss of TF, including 72 essential proteins (Figure 24E). Among these substantially aggregated proteins are 151 identified DnaK interactors. As in Δ KJ cells, many of these proteins were >80 kDa in size (Table S4 and S15), but they were more extensively aggregated, resulting in a median depletion by ~15 % compared to ~9 % in Δ KJT cells (Table S4 and S15). Moreover, from Δ KJ cells to Δ KJT cells, the degradation levels were similar in terms of numbers of degraded proteins in both mutants (Figure 25B).

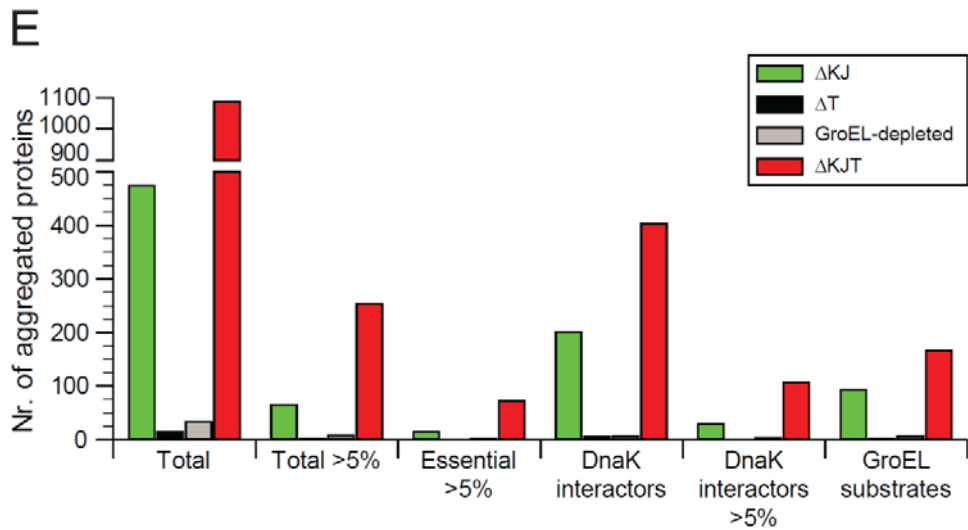
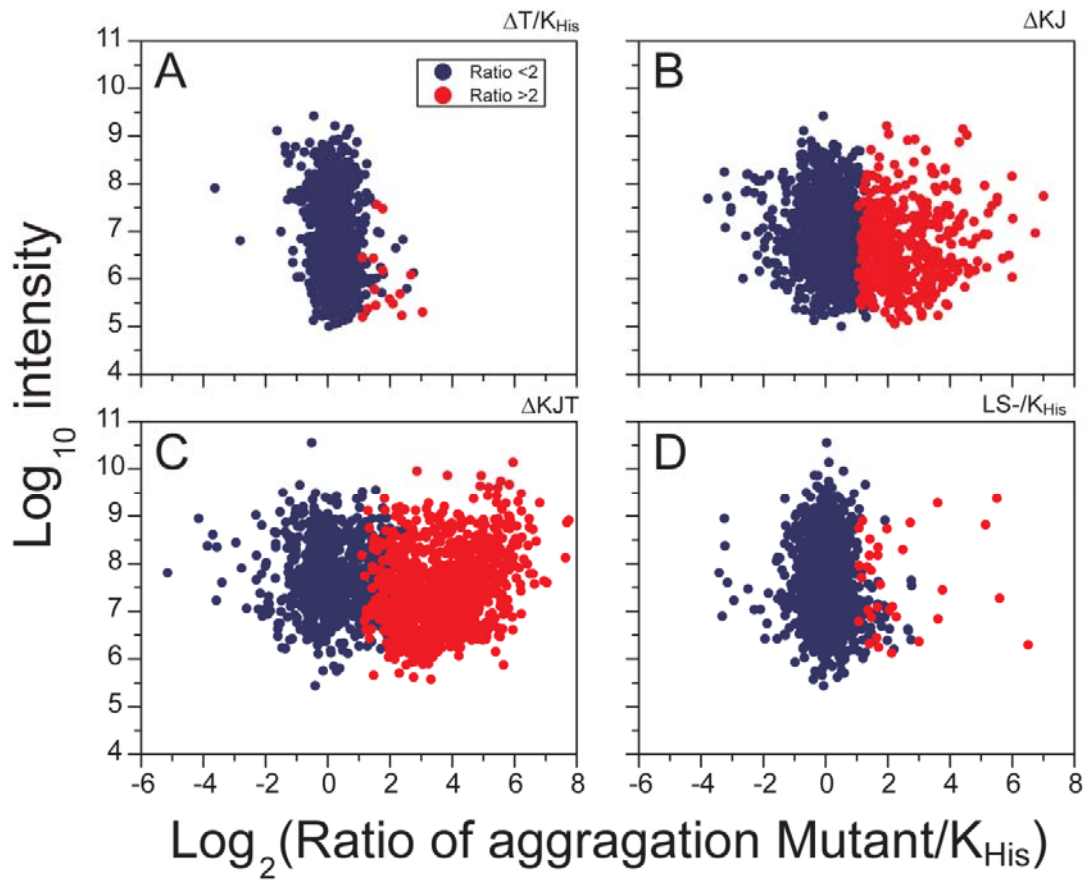


Figure 24 Functional proteomics analysis of aggregation in mutants

(A) Proteomic analysis of the aggregated fraction of cells with different chaperone deficiencies, including ΔT (A), ΔKJ (B), ΔKJT (C) and $LS-K_{His}$ cells (D). The y-axis shows \log_{10} collective peptide intensity of respective proteins. Red dots indicate the proteins significantly accumulated in the aggregates of the mutant strains as compared to the K_{His} . (E) Protein aggregation in ΔKJ , $\Delta T/K_{His}$, $LS-K_{His}$ and ΔKJT cells. The number aggregated proteins were analyzed according to the following categories: total, aggregated to greater than 5% (Total >5%), essential proteins aggregated to greater than 5% (Essential >5%), DnaK-interactors, DnaK-interactors aggregated to greater than 5% and GroEL substrates.

Interestingly, 167 (67%) of the ~250 GroEL substrates (Kerner et al., 2005) were also recovered in the aggregate fraction of ΔKJT cells, including 58 class III substrates of which 14 were strongly depleted from the soluble fraction (Figure 25C). Aggregation of GroEL substrates was less pronounced in ΔKJ cells and not detectable in the ΔT strain at 30 °C (Figure 25C). The pronounced aggregation of GroEL substrates in ΔKJT cells is surprising when one takes into consideration that GroEL/ES, along with numerous other chaperones, is ~10-fold increased in abundance relative to wild-type cells (data not shown). Thus, substrate delivery to GroEL critically depends on the upstream chaperones DnaK and TF.

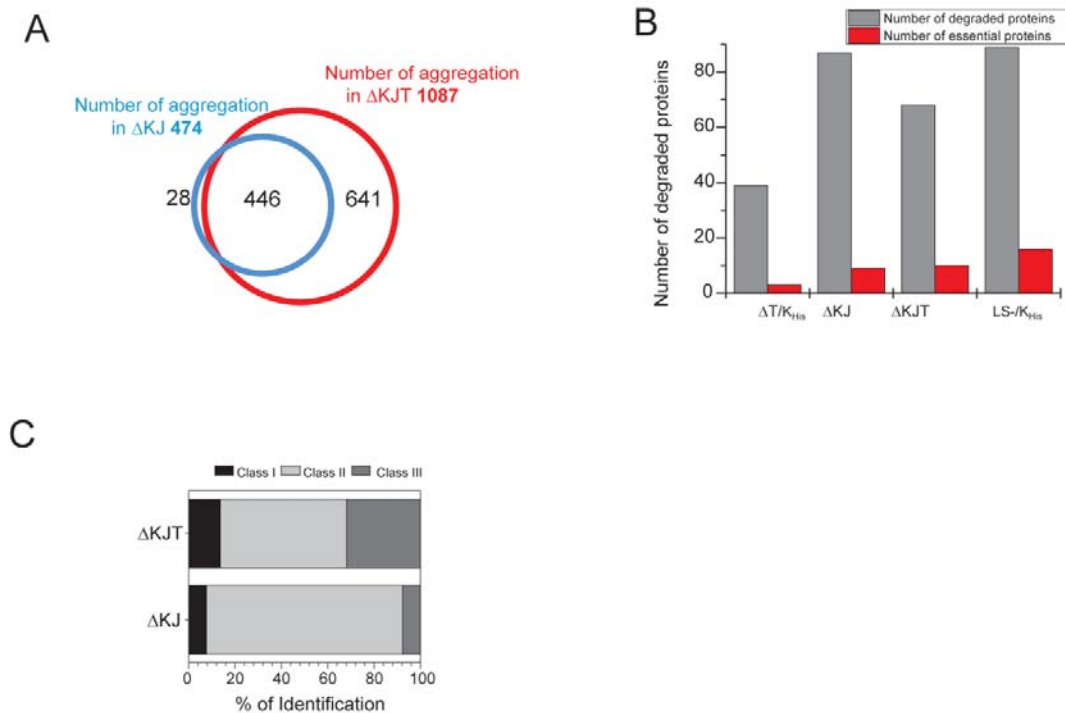


Figure 25 Functional proteomics analysis of aggregation in mutants

(A) Overlap between aggregating proteins in ΔKJ and ΔKJT cells at 30 °C. (B) Number of degraded proteins (gray) and of essential proteins degraded (red) in $\Delta T/K_{His}$, ΔKJ , and ΔKJT and $LS-/K_{His}$ cells at 30 °C. (C) GroEL substrate distribution in the aggregated fraction (>5%) of ΔKJ and ΔKJT cells at 30 °C.

Pulse labeling experiments with amino acid isotope showed that both preexistent and newly-synthesized proteins aggregated in ΔKJT cells (Figure 26A), demonstrating the importance of the chaperone system in conformational maintenance. Quantitative data were obtained for 231 of the proteins that aggregated to >5 % of total. We compared the physico-chemical properties of the 48 proteins with the highest and 45 proteins with the lowest propensity to aggregate as newly-synthesized, respectively. Interestingly, proteins of the first group tended to be less abundant, smaller in size, contained less essential proteins and had

substantially lower solubility upon translation in the absence of chaperones (Figure 26B-E). These proteins also had a greater number of predicted DnaK interaction sites and pI values closer to neutral than the preexistent proteins in the aggregate fraction (Figure 26F, G). Thus, the proteins that aggregate upon synthesis are similar in properties to the proteins that are normally highly enriched on DnaK (Figure 16) and interact with DnaK both upon synthesis and for conformational maintenance (Figure 18).

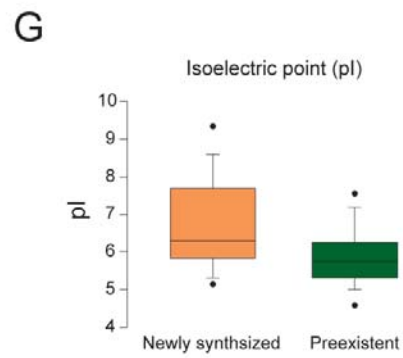
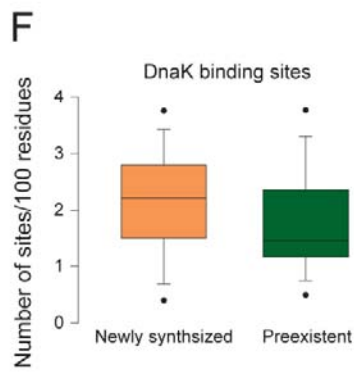
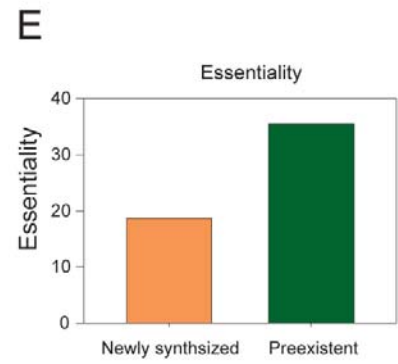
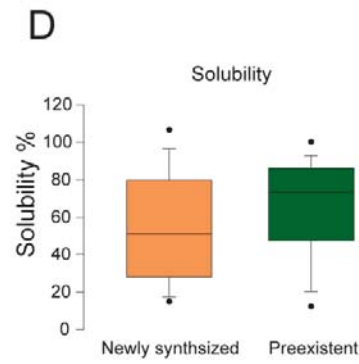
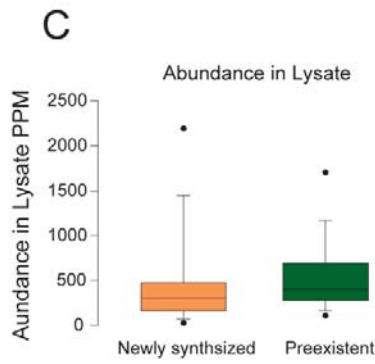
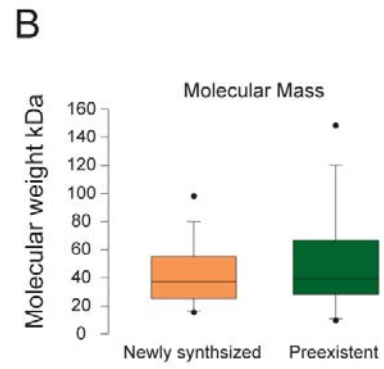
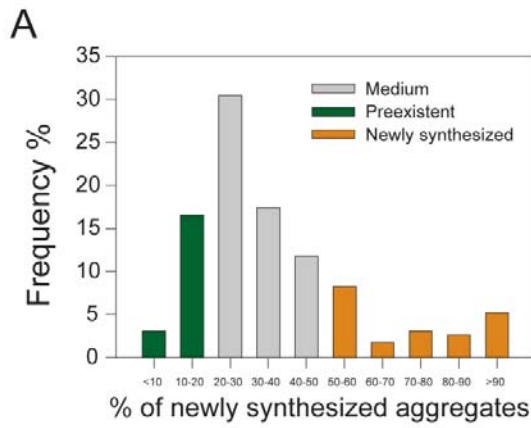


Figure 26 Pulse labeling analysis of aggregated proteins in Δ KJT cells

(A) Histogram of the percentage of newly synthesized aggregates in Δ KJT cells. 48 and 45 proteins at the extremes of the distribution were selected as preferentially aggregating as newly synthesized (orange) or preexistent proteins (dark green), respectively. (B) Comparison of the properties of newly synthesized and preexistent aggregating proteins in terms of molecular mass, isoelectric point, solubility in the PURE system, essentiality, DnaK binding site per 100 residue and abundance in lysate.

Notably, 42 ribosomal proteins, 24 from the large subunit and 18 from the small subunit, were also found to accumulate in the insoluble fraction of Δ KJT cells, almost all (39) of which were identified as DnaK-interactors. However, aggregation of these proteins did not result in a significant depletion from the soluble fraction. Deletion of DnaK/DnaJ alone had only resulted in the detectable aggregation of 3 ribosomal proteins and no ribosomal protein aggregated in Δ T cells. Isotope labeling showed that both preexistent and newly-synthesized ribosomal proteins were recovered in aggregates. These results suggested the possibility that Δ KJT cells may have a defect in ribosomal biogenesis. Indeed, a quantitative proteome analysis revealed that the abundance of numerous ribosomal proteins was moderately but significantly reduced by 10-30% in Δ KJT in comparison to K_{His} cells and the single chaperone deletions (Figure 27A). Interestingly, two small ribosomal proteins (RpsQS17 and RpsT S20) were increased in abundance, an effect that was also detected in Δ KJ cells (Figure 27A). A defect in ribosomal biogenesis was corroborated by sucrose density gradient analysis which demonstrated that the concentration of 70S ribosomes was substantially reduced in Δ KJT cells (Figure 27B).

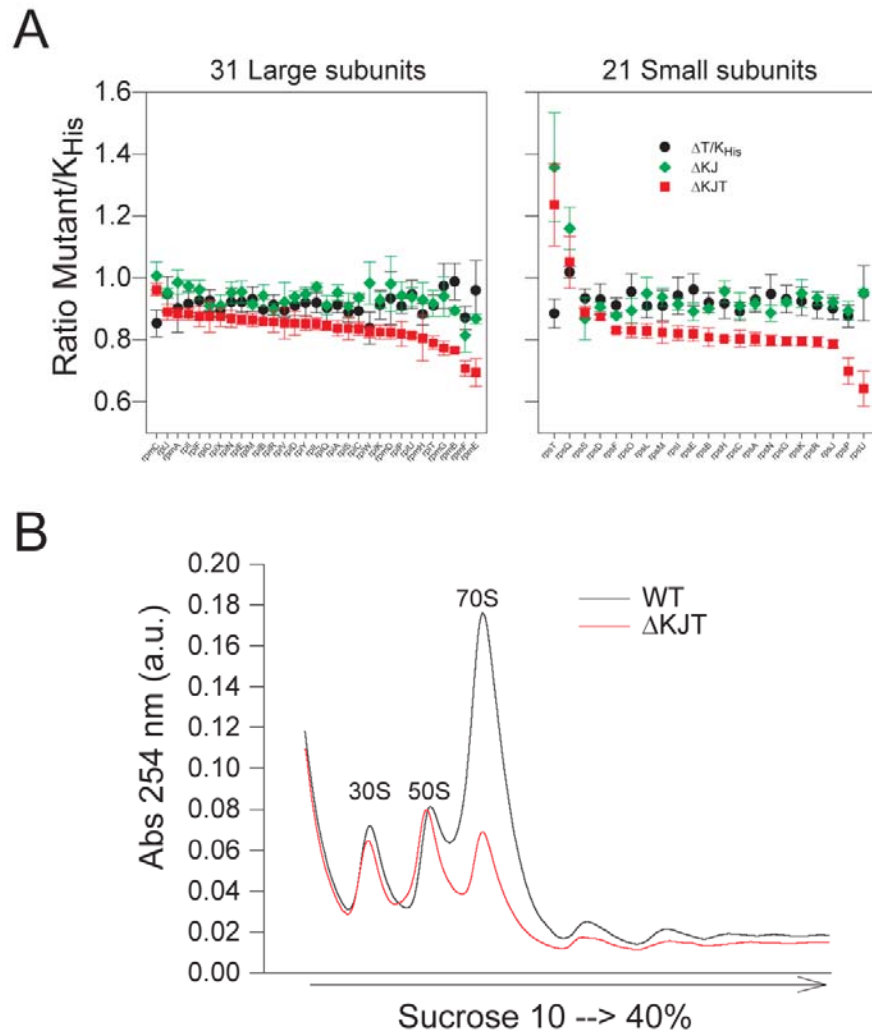


Figure 27 Impaired ribosome biogenesis in ΔKJT

(A) Changes in abundance of small and large ribosomal proteins in ΔKJ , $\Delta T/K_{His}$ and ΔKJT relative to K_{His} cells. SILAC ratios (mutant/ K_{His}) are shown with standard deviations from 3 independent biological repeats for 21 small and 31 large ribosomal proteins. (B) Sucrose gradient analysis of ribosome fractions in WT and ΔKJ cells.

The appearance of ribosomal proteins in the insoluble fraction could be a consequence of the aggregation of nascent polypeptide chains in the absence of these chaperones. To investigate whether ribosome-bound polypeptides aggregated, the model

protein Luciferase-SecM-GFP was expressed from an arabinose-inducible plasmid (Brandt et al., 2009) in K_{His} , ΔT , ΔKJ and ΔKJT cells (Figure 28). Stalling was highly efficient, as no read-through resulting in the synthesis of full-length Luciferase-SecM-GFP fusion protein occurred. The presence of the SecM stalling sequence (Evans et al., 2005; Ito et al., 2010; Nakatogawa and Ito, 2002) allowed us to monitor the fate of the ribosome-nascent chain complexes by following the partitioning of luciferase between the soluble and insoluble cell fractions. While the luciferase nascent chains were soluble upon DnaK/DnaJ or TF deletion, ~30% of the total expressed luciferase in the ΔKJT was found in the aggregate fraction. This demonstrates that protein aggregation can initiate at the nascent chain level and is effectively prevented by DnaK/DnaJ and TF.

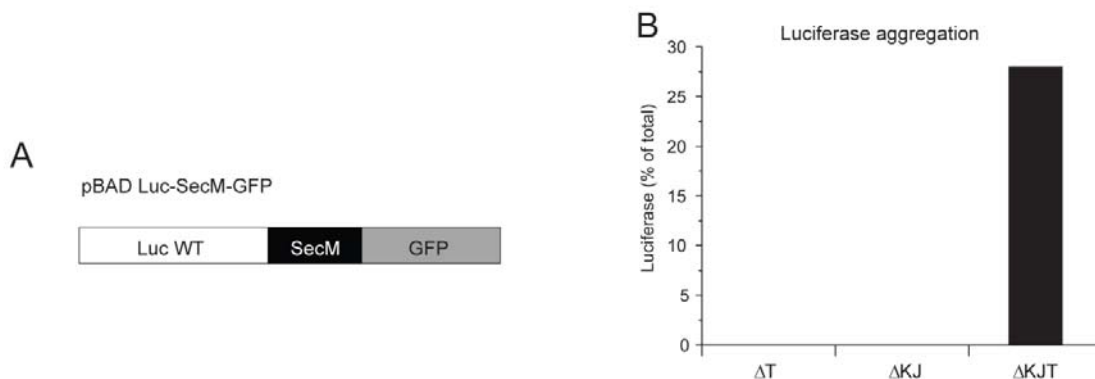


Figure 28 DnaK and TF cooperate in preventing Co-translational aggregation.

(A) Schematic of the arabinose inducible construct pBAD-18 Luc-SecM-GFP. (B) After inducing the expression of Luc-SecM-GFP with arabinose for 30 min, aggregated luciferase significantly accumulated only in ΔKJT strain.

In summary, the combined loss of DnaK/DnaJ and TF results in a dramatic proteostasis collapse characterized by massive protein aggregation, disruption of proper

protein flux through GroEL/ES and defective ribosomal biogenesis. These findings explain the strong growth defect of the cells at 30 °C and their inability to grow at higher temperatures.

5 Discussion

The results of this study provide quantitative insights into the organization of the chaperone network that operates in the bacterial cytosol in *de novo* protein folding and proteome maintenance. The DnaK (Hsp70) chaperone system is identified as a central hub of this network, normally interacting with more than 25% of cytosolic proteins and functionally cooperating with the upstream TF and the downstream GroEL/ES chaperonin. Surprisingly, upon growth at 30°C, the loss or down-regulation of individual chaperone modules –DnaK/DnaJ, TF or GroEL/ES– is remarkably well compensated at a global proteome level, leading only to limited changes in proteome composition due to degradation or aggregation of misfolded proteins. However, only the loss of the DnaK-system causes a massive stress response with a ~10-fold increase in the concentration of rpoH regulated chaperones and proteases, consistent with the role of DnaK/DnaJ in attenuating rpoH (Yura and Nakahigashi, 1999). Proteostasis collapse occurs when at least two chaperone modules fail. This is exemplified by the combined deletion of DnaK/DnaJ and TF, which results not only in extensive and substantial protein aggregation but also in a dramatic impairment of the essential GroEL/ES function, even though the chaperonin is strongly upregulated, thus signifying the failure of the entire chaperone network.

5.1 Contribution of DnaK chaperone system to protein folding in *E. coli*

The DnaK interactome characterized here is extensive, comprising at least ~700 proteins in WT cells and ~1000 proteins in TF-deleted cells. Most of the interactors (~80%) are cytosolic, but DnaK also interacts with a small subset of proteins of the inner membrane, periplasm and outer membrane. The DnaK substrates generally bind to DnaK upon synthesis, reflecting an eminent role of the Hsp70 system in *de novo* protein folding, but many proteins

return to DnaK during their life time for conformational maintenance. By measuring for each protein the fraction of total bound to DnaK we defined a set of ~180 interactors that are highly enriched on DnaK and occupy about 40% of the DnaK chaperone capacity, with ~5% of total of each protein being bound to DnaK at 37°C.

Enrichment of proteins on DnaK generally correlates inversely with their cellular abundance, solubility upon translation in the absence of chaperones (Niwa et al., 2009) and essential function, and is positively correlated with higher than average size, the number of predicted DnaK binding sites and assembly into heterooligomeric complexes. Enriched substrates bind DnaK with higher affinity, as reflected in their slower dissociation from DnaK compared to less enriched substrates, and utilize the chaperone more extensively for conformational maintenance. The higher propensity of enriched DnaK substrates to aggregate corresponds with isoelectric point values closer to 7.5, the physiological pH of the *E. coli* cytosol, and their larger size, but is not due to overall higher sequence hydrophobicity, as measured by GRAVY. We noted, however, that the enriched interactors contain a greater than average fraction of amino acid residues with low burial potential, which may result in greater structural flexibility. Interestingly, ~18% of the DnaK-enriched substrates contain at least one domain with SCOP fold c.37 (P-loop containing nucleoside triphosphate hydrolases). Proteins with this complex alpha/beta topology have to form many long-range interactions during folding and are thus likely to populate kinetically trapped folding intermediates (Gromiha and Selvaraj, 2004). Many proteins with c.37 domains must assemble into heterooligomeric complexes and thus may cycle on DnaK until they interact productively with partner subunits. Our results are in line with the view that protein abundance correlates inversely with solubility (Kerner et al., 2005; Tartaglia and Vendruscolo, 2008) and

demonstrate that proteins of relatively lower solubility interact more extensively with chaperones.

The DnaK substrates have a wide range of cellular functions. DnaK and its co-chaperone DnaJ are not essential under standard growth conditions up to 37°C, consistent with the lower than average preponderance of proteins with essential functions among the DnaK-enriched substrates. A similar trend was noted for the proteins that depend on GroEL and probably reflects the evolutionary pressure to optimize the folding properties of essential proteins (Kerner, et al., 2005). However, our proteomic analysis helps to explain the decrease in fitness of the DnaK deletion strain under a variety of growth conditions that deviate from standard laboratory conditions (Nichols et al., 2011). For example, the sensitivity of $\Delta dnaK$ cells to antibiotics causing DNA damage is consistent with our finding that proteins of COG class L (DNA replication, recombination and repair) are overrepresented among the DnaK-enriched substrates (Figure S2). 5 of the 64 proteins found to aggregate extensively (>5% of total) in ΔKJ cells belong to this class, including the 105 kDa UvrA nucleotide excision repair protein, a heterooligomeric, DnaK-enriched interactor with two c.37 domains that aggregates extensively in the absence of DnaK already at 30°C (~30% of total). The sensitivity of $\Delta dnaK$ cells to antibiotics that inhibit protein synthesis (Nichols et al., 2011) would correlate with our finding that DnaK interacts with many ribosomal proteins. Moreover, several DnaK-interactors of COG class E (amino acid transport and metabolism) are 45-90% degraded in ΔKJ cells, including amino acid synthases (thrC, metE, metH; gltD, gltB, argG) and periplasmic amino acid binding proteins for leucine, arginine and branched-chain amino acids (livK, artJ, livG, livJ and livF). The sensitivity of $\Delta dnaK$ cells to acidic conditions is consistent with the 80-97% degradation in ΔKJ cells of the glutamate-GABA

antiporter, *gadC*, involved in glutamate-dependent acid resistance, and of the periplasmic chaperone of acid-denatured proteins, *hdeB*.

Is any protein an obligate substrate of DnaK in vivo and what is its behavior in ΔKJ ? DnaK is not a necessary folding factor for any essential protein in *E. coli* at 30 °C. However, 14 proteins of the identified 140 enriched DnaK substrates are significantly degraded (> ~50%) in the ΔKJ cells (Table S3). Similarly to the GroEL obligate substrates in the GroEL-depleted cells (Figure 23C), these 14 proteins may be obligate DnaK substrates, which are degraded because of the inability of other chaperone systems to compensate for the DnaK function. These proteins are characterized by a much higher median MW and a much lower solubility in the PURE system than all the enriched substrates, indicating an even greater dependence on DnaK. However there is only one essential protein (*ubiE*, Ubiquinone/menaquinone biosynthesis methyltransferase), explaining why DnaK is dispensable under physiological conditions. Interestingly, there is virtually no overlap between the 87 degraded proteins and the 474 aggregated proteins in ΔKJ cells, indicating the existence of different groups of DnaK substrates having distinct fate upon DnaK deletion. On the other hand, the extent of aggregation of the DnaK substrates is also positively correlated with their enrichment on DnaK (Figure 17), suggesting a major role for DnaK in preventing aggregation of the more dependent proteins. The loss of DnaK results in the extensive aggregation (> 5% of the protein recovered in the aggregates) of 10 enriched interactors for which other upregulated chaperones cannot compensate the loss of the DnaK function. In conclusion, 14 degraded and 8 aggregated enriched DnaK interactors in the ΔKJ cells may represent obligate DnaK interactors with the highest dependence on DnaK for folding or assembly.

The major role of DnaK in *de novo* folding of newly-synthesized proteins (Deuerling et al., 1999; Teter et al., 1999) is also confirmed by our pulse-SILAC DnaK pulldown experiments. Distinct physical-chemical properties dictate the preferential binding to DnaK of the preexistent or newly-synthesized form of the substrate proteins. The fact that ~50% of DnaK capacity is occupied by preexistent interactors, demonstrates that DnaK functions not only in *de novo* folding but also in proteome maintenance. Interestingly the ribosomal proteins interact with DnaK predominantly as newly synthesized proteins (Figure 18A), indicating the important role of DnaK in ribosome assembly and fast turnover rate of ribosomal proteins in vivo (Rene and Alix, 2011).

5.2 DnaK closely cooperates with Trigger factor

Our analysis of the DnaK-interactome in cells lacking TF or GroEL/ES assigns the DnaK system a central hub position in the chaperone network and demonstrates that TF and DnaK closely cooperate in the *de novo* folding of newly-synthesized proteins. However the functional overlap between them is only partial. TF may interact with most of the nascent polypeptides emerging from ribosome exit tunnel (Hartl and Hayer-Hartl, 2009). Nevertheless the deletion of TF does not result in any severe aggregation, degradation or growth defect (Figure 13A B, Figure 24A, and Figure 25B). The modest upregulation of other chaperones (~1.5 fold) and proteases (~ 1.2 fold) could compensate for most of the TF functions. The increase of a subset of DnaK substrates on DnaK in the absence of TF defines in a quantitative manner the functional overlap between these two chaperone systems suggested earlier (Teter et al., 1999; Deuerling et al., 1999). These proteins occupy normally ~10% of the DnaK capacity and increase to ~15% in ΔT cells. Interestingly, they comprise mostly ribosomal and other small (<20 Kda), positively charged proteins of higher than

average solubility and extensive structural disorder (in the case of ribosomal proteins). Indeed, TF has a negative net charge, which may facilitate its interaction with positively charged nascent polypeptides, and role of TF in the folding/assembly of ribosomal proteins has been suggested (Martinez-Hackert and Hendrickson, 2009). Importantly, DnaK can efficiently assist the folding of this group of TF substrates in the ΔT strain and compensating the loss of TF by cooperating with other chaperone system.

However, global proteome analysis indicated that TF deletion does not result in a folding defect for these proteins, suggesting that DnaK efficiently replaces TF function. In contrast, DnaK/DnaJ are unable to replace the role of TF in the biogenesis of a set of ~40 proteins, including mostly secretory proteins, with β -barrel proteins of the outer membrane being prominently represented. These proteins undergo partial degradation in ΔT cells. While some of them were also identified as DnaK-interactors, they do not increase on DnaK in the absence of TF but rather decrease in abundance. These findings suggest a specific role of TF in maintaining the precursors of outer membrane proteins, including BamA, the protein required for their assembly into the outer membrane, in a loosely-folded conformation competent for translocation across the inner membrane. This unexpected function of TF is consistent with the identification of TF as an *in vitro* chaperone of proOmpA translocation (Crooke et al., 1988) and the recent demonstration that TF interacts with the mature sequence of proOmpA on the ribosome (Lakshminpathy et al., 2010). Recently, SecA was found to be able to co-transnationally mediate the targeting of nascent substrates to post-translational translocation (Huber et al., 2011). The increased amount of SecA consequent to the TF deletion may rescue the loss of TF, although not completely. As described in the Results section, secretory proteins are underrepresented in the DnaK interactome. Thus, DnaK cannot

fully replace the role of TF in assisting the folding of this second group of TF substrates which are mainly secretory proteins.

15 and 474 proteins aggregated in ΔT and ΔKJ cells at 30 °C, respectively. However, 1087 proteins aggregated upon the additional deletion of TF in the ΔKJ background indicating that the cooperation between TF and DnaK is essential to prevent massive aggregation even at a permissive temperature. When and where TF and DnaK exert their control on protein aggregation is still an open question. The expression of Luciferase-SecM-GFP demonstrates that the aggregation can initiate at the nascent chain level and that DnaK and TF cooperate to prevent nascent chain aggregation (Figure 28). Indeed, our pulse-SILAC experiment results indicate that not only preexistent proteins aggregate in ΔKJT cells but also newly synthesized proteins (Figure 26A), again proving the essential role of DnaK and TF in *de novo* folding, aggregation prevention of newly synthesized and nascent chains and conformational maintenance.

5.3 Interplay of the DnaK and chaperonin systems

The fact that in both ΔKJ and ΔT cells, the chaperonin system is upregulated, and that the DnaK system is upregulated upon the depletion of GroEL/ES strongly suggests their mutual functional relevance. The DnaK-interactome also overlaps extensively with the set of ~250 proteins that utilize GroEL/ES for folding, including 41% of the obligate GroEL substrates (class III), occupying nearly 30% of the DnaK capacity. Indeed, our data suggest that the majority of these proteins reach GroEL via DnaK. From the modest increase in identifications of GroEL substrates on DnaK in the absence of TF, we estimate that only ~20% of proteins circumvent DnaK and are transferred to GroEL directly from TF. When GroEL and GroES are downregulated, this results in the substantial degradation or

aggregation of GroEL class III substrates (at 37°C), with degradation being the preferred fate at 30°C. Notably, despite their overall decrease in abundance due to degradation, numerous GroEL substrates increase on DnaK, reflecting the role of DnaK in stabilizing these proteins until GroEL is available or in transferring them to the proteolytic system (Figure 23).

The aggregation of GroEL substrates is less prominent in Δ KJ cells and even not detected in Δ T/ K_{His} cells, indicating that the other chaperone could compensate for the defect. However, 167 of the ~250 GroEL substrates aggregated in Δ KJT cells (Figure 25), showing that the upstream chaperones are important for substrate delivery to GroEL.

5.4 DnaK and TF are involved in the biogenesis of ribosome

DnaK and TF are involved in the late stages of ribosome biogenesis as their deletion results in the accumulation of ribosome subunit precursors under non-permissive growth conditions (Al Refaii and Alix, 2009; Rene and Alix, 2011). Furthermore, a recent study shows that DnaK not only interacts with unfolded extended polypeptides but can also interact with folded proteins (Schlecht et al., 2011) opening the possibility that DnaK may facilitate the assembly of fully folded ribosomal proteins. TF may also be involved in ribosome assembly as suggested by the recent finding that ribosome-free TF is found in association with a number of putative substrates, including the ribosomal protein S7 (Martinez-Hackert and Hendrickson, 2009). Our results showed that ribosomal proteins are substrates of DnaK and TF, and are preferentially bound by DnaK soon after their synthesis with fast releasing kinetics. Furthermore, DnaK can take over these ribosomal protein substrates upon the deletion of TF, explaining why no severe degradation or aggregation of ribosomal proteins is observed in Δ KJ or Δ T cells. A pronounced reduction in abundance of ribosomal proteins of both the small and large subunits is indeed only observed in Δ KJT cells. Moreover, the

dramatic reduction of the 70S ribosomes confirms the defect of ribosome biogenesis in the Δ KJT cells due to the loss of cooperation between DnaK and TF.

6 REFERENCES

- Agashe, V.R., Guha, S., Chang, H.C., Genevaux, P., Hayer-Hartl, M., Stemp, M., Georgopoulos, C., Hartl, F.U., and Barral, J.M. (2004). Function of trigger factor and DnaK in multidomain protein folding: increase in yield at the expense of folding speed. *Cell* *117*, 199-209.
- Al Refaii, A., and Alix, J.H. (2009). Ribosome biogenesis is temperature-dependent and delayed in *Escherichia coli* lacking the chaperones DnaK or DnaJ. *Mol Microbiol* *71*, 748-762.
- Albanese, V., Reissmann, S., and Frydman, J. (2010). A ribosome-anchored chaperone network that facilitates eukaryotic ribosome biogenesis. *J Cell Biol* *189*, 69-81.
- Anfinsen, C.B. (1973). Principles that govern the folding of protein chains. *Science* *181*, 223-230.
- Balch, W.E., Morimoto, R.I., Dillin, A., and Kelly, J.W. (2008). Adapting proteostasis for disease intervention. *Science* *319*, 916-919.
- Baram, D., Pyetan, E., Sittner, A., Auerbach-Nevo, T., Bashan, A., and Yonath, A. (2005). Structure of trigger factor binding domain in biologically homologous complex with eubacterial ribosome reveals its chaperone action. *Proceedings of the National Academy of Sciences of the United States of America* *102*, 12017-12022.
- Bertelsen, E.B., Chang, L., Gestwicki, J.E., and Zuiderweg, E.R. (2009). Solution conformation of wild-type *E. coli* Hsp70 (DnaK) chaperone complexed with ADP and substrate. *Proceedings of the National Academy of Sciences of the United States of America* *106*, 8471-8476.
- Bjellqvist, B., Hughes, G.J., Pasquali, C., Paquet, N., Ravier, F., Sanchez, J.C., Frutiger, S., and Hochstrasser, D. (1993). The focusing positions of polypeptides in immobilized pH gradients can be predicted from their amino acid sequences. *Electrophoresis* *14*, 1023-1031.
- Bothmann H, Pluckthun A. (2000). The periplasmic *Escherichia coli* peptidylprolyl isomerase FkpA-I. Increased functional expression of antibody fragments with and without cis-prolines. *J Biol Chem* *275*(22):17100–17105.
- Bradford, M.M. (1976). A rapid and sensitive method for the quantitation of microgram quantities of protein utilizing the principle of protein-dye binding. *Analytical biochemistry* *72*, 248-254.
- Brandt, F., Etchells, S.A., Ortiz, J.O., Elcock, A.H., Hartl, F.U., and Baumeister, W. (2009). The native 3D organization of bacterial polysomes. *Cell* *136*, 261-271.
- Brehmer, D., Rudiger, S., Gassler, C.S., Klostermeier, D., Packschies, L., Reinstein, J., Mayer, M.P., and Bukau, B. (2001). Tuning of chaperone activity of Hsp70 proteins by modulation of nucleotide exchange. *Nat Struct Biol* *8*, 427-432.

- Brinker, A., Pfeifer, G., Kerner, M.J., Naylor, D.J., Hartl, F.U., and Hayer-Hartl, M. (2001). Dual function of protein confinement in chaperonin-assisted protein folding. *Cell* *107*, 223-233.
- Brockwell, D.J., and Radford, S.E. (2007). Intermediates: ubiquitous species on folding energy landscapes? *Curr Opin Struct Biol* *17*, 30-37.
- Bukau, B., and Horwich, A.L. (1998). The Hsp70 and Hsp60 chaperone machines. *Cell* *92*, 351-366.
- Bukau, B., and Walker, G.C. (1989a). Cellular defects caused by deletion of the *Escherichia coli* dnaK gene indicate roles for heat shock protein in normal metabolism. *J Bacteriol* *171*, 2337-2346.
- Bukau, B., and Walker, G.C. (1989b). Delta dnaK52 mutants of *Escherichia coli* have defects in chromosome segregation and plasmid maintenance at normal growth temperatures. *J Bacteriol* *171*, 6030-6038.
- Chakraborty, K., Chatila, M., Sinha, J., Shi, Q., Poschner, B.C., Sikor, M., Jiang, G., Lamb, D.C., Hartl, F.U., and Hayer-Hartl, M. (2010). Chaperonin-catalyzed rescue of kinetically trapped states in protein folding. *Cell* *142*, 112-122.
- Chang, H.C., Tang, Y.C., Hayer-Hartl, M., and Hartl, F.U. (2007). SnapShot: molecular chaperones, Part I. *Cell* *128*, 212.
- Cox, J., and Mann, M. (2008). MaxQuant enables high peptide identification rates, individualized p.p.b.-range mass accuracies and proteome-wide protein quantification. *Nat Biotechnol* *26*, 1367-1372.
- Crooke, E., Guthrie, B., Lecker, S., Lill, R., and Wickner, W. (1988). ProOmpA is stabilized for membrane translocation by either purified *E. coli* trigger factor or canine signal recognition particle. *Cell* *54*, 1003-1011.
- Datsenko, K.A., and Wanner, B.L. (2000). One-step inactivation of chromosomal genes in *Escherichia coli* K-12 using PCR products. *Proceedings of the National Academy of Sciences of the United States of America* *97*, 6640-6645.
- Daugaard, M., Rohde, M., and Jaattela, M. (2007). The heat shock protein 70 family: Highly homologous proteins with overlapping and distinct functions. *FEBS Lett* *581*, 3702-3710.
- Deuerling, E., Patzelt, H., Vorderwulbecke, S., Rauch, T., Kramer, G., Schaffitzel, E., Mogk, A., Schulze-Specking, A., Langen, H., and Bukau, B. (2003). Trigger Factor and DnaK possess overlapping substrate pools and binding specificities. *Mol Microbiol* *47*, 1317-1328.
- Deuerling, E., Schulze-Specking, A., Tomoyasu, T., Mogk, A., and Bukau, B. (1999). Trigger factor and DnaK cooperate in folding of newly synthesized proteins. *Nature* *400*, 693-696.

- Dill, K.A., and Chan, H.S. (1997). From Levinthal to pathways to funnels. *Nat Struct Biol* 4, 10-19.
- Dinner, A.R., Sali, A., Smith, L.J., Dobson, C.M., and Karplus, M. (2000). Understanding protein folding via free-energy surfaces from theory and experiment. *Trends Biochem Sci* 25, 331-339.
- Eisner, G., Koch, H.G., Beck, K., Brunner, J., and Muller, M. (2003). Ligand crowding at a nascent signal sequence. *J Cell Biol* 163, 35-44.
- El Hage, A., and Alix, J.H. (2004). Authentic precursors to ribosomal subunits accumulate in *Escherichia coli* in the absence of functional DnaK chaperone. *Mol Microbiol* 51, 189-201.
- Ellis, J. (1987). Proteins as molecular chaperones. *Nature* 328, 378-379.
- Ellis, R.J. (2001). Macromolecular crowding: an important but neglected aspect of the intracellular environment. *Curr Opin Struct Biol* 11, 114-119.
- Ellis, R.J. (2006). Molecular chaperones: assisting assembly in addition to folding. *Trends Biochem Sci* 31, 395-401.
- Emanuelsson, O., Brunak, S., von Heijne, G., and Nielsen, H. (2007). Locating proteins in the cell using TargetP, SignalP and related tools. *Nat Protoc* 2, 953-971.
- Evans, M.S., Ugrinov, K.G., Frese, M.A., and Clark, P.L. (2005). Homogeneous stalled ribosome nascent chain complexes produced *in vitro*. *Nat Methods* 2, 757-762.
- Ewalt, K.L., Hendrick, J.P., Houry, W.A., and Hartl, F.U. (1997). Observation of polypeptide flux through the bacterial chaperonin system. *Cell* 90, 491-500.
- Fayet, O., Ziegelhoffer, T., and Georgopoulos, C. (1989). The groES and groEL heat shock gene products of *Escherichia coli* are essential for bacterial growth at all temperatures. *J Bacteriol* 171, 1379-1385.
- Fenton, W.A., Kashi, Y., Furtak, K., and Horwich, A.L. (1994). Residues in chaperonin GroEL required for polypeptide binding and release. *Nature* 371, 614-619.
- Ferbitz, L., Maier, T., Patzelt, H., Bukau, B., Deuerling, E., and Ban, N. (2004). Trigger factor in complex with the ribosome forms a molecular cradle for nascent proteins. *Nature* 431, 590-596.
- Freire, P., Vieira, H.L., Furtado, A.R., de Pedro, M.A., and Arraiano, C.M. (2006). Effect of the morphogene bolA on the permeability of the *Escherichia coli* outer membrane. *FEMS Microbiol Lett* 260, 106-111.
- Fujiwara, K., Ishihama, Y., Nakahigashi, K., Soga, T., and Taguchi, H. (2010). A systematic survey of obligate chaperonin-dependent substrates. *EMBO J* 29, 1552-1564.

- Gamer, J., Multhaup, G., Tomoyasu, T., McCarty, J.S., Rudiger, S., Schonfeld, H.J., Schirra, C., Bujard, H., and Bukau, B. (1996). A cycle of binding and release of the DnaK, DnaJ and GrpE chaperones regulates activity of the Escherichia coli heat shock transcription factor sigma32. *EMBO J* 15, 607-617.
- Gamer, J., Bujard, H., and Bukau, B. (1992). Physical interaction between heat shock proteins DnaK, DnaJ, and GrpE and the bacterial heat shock transcription factor sigma 32. *Cell* 69, 833-842.
- Genevaux, P., Keppel, F., Schwager, F., Langendijk-Genevaux, P.S., Hartl, F.U., and Georgopoulos, C. (2004). analysis of the overlapping functions of DnaK and trigger factor. *EMBO Rep* 5, 195-200.
- Georgopoulos, C.P., Hendrix, R.W., Casjens, S.R., and Kaiser, A.D. (1973). Host participation in bacteriophage lambda head assembly. *Journal of molecular biology* 76, 45-60.
- Gerdes, S.Y., Scholle, M.D., Campbell, J.W., Balazsi, G., Ravasz, E., Daugherty, M.D., Somera, A.L., Kyrpides, N.C., Anderson, I., Gelfand, M.S., *et al.* (2003). Experimental determination and system level analysis of essential genes in Escherichia coli MG1655. *J Bacteriol* 185, 5673-5684.
- Glover, J.R., and Lindquist, S. (1998). Hsp104, Hsp70, and Hsp40: a novel chaperone system that rescues previously aggregated proteins. *Cell* 94, 73-82.
- Gromiha, M.M., and Selvaraj, S. (2004). Folding mechanism of all-beta globular proteins. *Prep Biochem Biotechnol* 34, 13-23.
- Harrison, C.J., Hayer-Hartl, M., Di Liberto, M., Hartl, F., and Kuriyan, J. (1997). Crystal structure of the nucleotide exchange factor GrpE bound to the ATPase domain of the molecular chaperone DnaK. *Science* 276, 431-435.
- Hartl, F.U., and Hayer-Hartl, M. (2009). Converging concepts of protein folding in vitro and . *Nat Struct Mol Biol* 16, 574-581.
- Hartman, D.J., Surin, B.P., Dixon, N.E., Hoogenraad, N.J., and Hoj, P.B. (1993). Substoichiometric amounts of the molecular chaperones GroEL and GroES prevent thermal denaturation and aggregation of mammalian mitochondrial malate dehydrogenase in vitro. *Proceedings of the National Academy of Sciences of the United States of America* 90, 2276-2280.
- Heidrich, C., Ursinus, A., Berger, J., Schwarz, H., and Holtje, J.V. (2002). Effects of multiple deletions of murein hydrolases on viability, septum cleavage, and sensitivity to large toxic molecules in Escherichia coli. *J Bacteriol* 184, 6093-6099.
- Hesterkamp, T., and Bukau, B. (1998). Role of the DnaK and HscA homologs of Hsp70 chaperones in protein folding in E. coli. *EMBO J* 17, 4818-4828.

- Hoffmann, A., Bukau, B., and Kramer, G. (2010). Structure and function of the molecular chaperone Trigger Factor. *Biochim Biophys Acta* 1803, 650-661.
- Horwich, A.L., Apetri, A.C., and Fenton, W.A. (2009). The GroEL/GroES cis cavity as a passive anti-aggregation device. *FEBS Lett* 583, 2654-2662.
- Houry, W.A., Frishman, D., Eckerskorn, C., Lottspeich, F., and Hartl, F.U. (1999). Identification of substrates of the chaperonin GroEL. *Nature* 402, 147-154.
- Huber, D., Rajagopalan, N., Preissler, S., Rocco, M.A., Merz, F., Kramer, G., and Bukau, B. (2011). SecA interacts with ribosomes in order to facilitate posttranslational translocation in bacteria. *Molecular cell* 41, 343-353.
- Hundley, H.A., Walter, W., Bairstow, S., and Craig, E.A. (2005). Human Mpp11 J protein: ribosome-tethered molecular chaperones are ubiquitous. *Science* 308, 1032-1034.
- Ishihama, Y., Oda, Y., Tabata, T., Sato, T., Nagasu, T., Rappsilber, J., and Mann, M. (2005). Exponentially modified protein abundance index (emPAI) for estimation of absolute protein amount in proteomics by the number of sequenced peptides per protein. *Mol Cell Proteomics* 4, 1265-1272.
- Ito, K., Chiba, S., and Pogliano, K. (2010). Divergent stalling sequences sense and control cellular physiology. *Biochem Biophys Res Commun* 393, 1-5.
- Jong, W.S., ten Hagen-Jongman, C.M., Genevaux, P., Brunner, J., Oudega, B., and Luirink, J. (2004). Trigger factor interacts with the signal peptide of nascent Tat substrates but does not play a critical role in Tat-mediated export. *Eur J Biochem* 271, 4779-4787.
- Kaiser, C.M., Chang, H.C., Agashe, V.R., Lakshmipathy, S.K., Etchells, S.A., Hayer-Hartl, M., Hartl, F.U., and Barral, J.M. (2006). Real-time observation of trigger factor function on translating ribosomes. *Nature* 444, 455-460.
- Karbstein, K. (2010). Chaperoning ribosome assembly. *J Cell Biol* 189, 11-12.
- Karplus, M. (1997). The Levinthal paradox: yesterday and today. *Fold Des* 2, S69-75.
- Karzai, A.W., and McMacken, R. (1996). A bipartite signaling mechanism involved in DnaJ-mediated activation of the Escherichia coli DnaK protein. *J Biol Chem* 271, 11236-11246.
- Kerner, M.J., Naylor, D.J., Ishihama, Y., Maier, T., Chang, H.C., Stines, A.P., Georgopoulos, C., Frishman, D., Hayer-Hartl, M., Mann, M., *et al.* (2005). Proteome-wide analysis of chaperonin-dependent protein folding in Escherichia coli. *Cell* 122, 209-220.
- Kim, S., Malinverni, J.C., Sliz, P., Silhavy, T.J., Harrison, S.C., and Kahne, D. (2007). Structure and function of an essential component of the outer membrane protein assembly machine. *Science* 317, 961-964.

- Koplin, A., Preissler, S., Ilina, Y., Koch, M., Scior, A., Erhardt, M., and Deuerling, E. (2010). A dual function for chaperones SSB-RAC and the NAC nascent polypeptide-associated complex on ribosomes. *J Cell Biol* 189, 57-68.
- Kramer, G., Boehringer, D., Ban, N., and Bukau, B. (2009). The ribosome as a platform for co-translational processing, folding and targeting of newly synthesized proteins. *Nat Struct Mol Biol* 16, 589-597.
- Kramer, G., Patzelt, H., Rauch, T., Kurz, T.A., Vorderwulbecke, S., Bukau, B., and Deuerling, E. (2004). Trigger factor peptidyl-prolyl cis/trans isomerase activity is not essential for the folding of cytosolic proteins in *Escherichia coli*. *J Biol Chem* 279, 14165-14170.
- Kyte, J., and Doolittle, R.F. (1982). A simple method for displaying the hydrophobic character of a protein. *Journal of molecular biology* 157, 105-132.
- Laemmli, U.K. (1970). Cleavage of structural proteins during the assembly of the head of bacteriophage T4. *Nature* 227, 680-685.
- Lakshmiopathy, S.K., Gupta, R., Pinkert, S., Etschells, S.A., and Hartl, F.U. (2010). Versatility of trigger factor interactions with ribosome-nascent chain complexes. *J Biol Chem*.
- Lakshmiopathy, S.K., Tomic, S., Kaiser, C.M., Chang, H.C., Genevoux, P., Georgopoulos, C., Barral, J.M., Johnson, A.E., Hartl, F.U., and Etschells, S.A. (2007). Identification of nascent chain interaction sites on trigger factor. *J Biol Chem* 282, 12186-12193.
- Laufen, T., Mayer, M.P., Beisel, C., Klostermeier, D., Mogk, A., Reinstein, J., and Bukau, B. (1999). Mechanism of regulation of hsp70 chaperones by DnaJ cochaperones. *Proceedings of the National Academy of Sciences of the United States of America* 96, 5452-5457.
- Lehninger, A.L., Nelson, D.L., and Cox, M.M. (2005). *Lehninger principles of biochemistry*, 4th edn (New York, W.H. Freeman).
- Lill, R., Crooke, E., Guthrie, B., and Wickner, W. (1988). The "trigger factor cycle" includes ribosomes, presecretory proteins, and the plasma membrane. *Cell* 54, 1013-1018.
- Lin, Z., Madan, D., and Rye, H.S. (2008). GroEL stimulates protein folding through forced unfolding. *Nat Struct Mol Biol* 15, 303-311.
- Liu, C., Young, A.L., Starling-Windhof, A., Bracher, A., Saschenbrecker, S., Rao, B.V., Rao, K.V., Berninghausen, O., Mielke, T., Hartl, F.U., *et al.* (2010). Coupled chaperone action in folding and assembly of hexadecameric Rubisco. *Nature* 463, 197-202.
- Maier, R., Eckert, B., Scholz, C., Lilie, H., and Schmid, F.X. (2003). Interaction of trigger factor with the ribosome. *Journal of molecular biology* 326, 585-592.
- Maki, J.A., Schnobrich, D.J., and Culver, G.M. (2002). The DnaK chaperone system facilitates 30S ribosomal subunit assembly. *Mol Cell* 10, 129-138.

- Martinez-Hackert, E., and Hendrickson, W.A. (2009). Promiscuous substrate recognition in folding and assembly activities of the trigger factor chaperone. *Cell* *138*, 923-934.
- Mayer, M.P., and Bukau, B. (2005). Hsp70 chaperones: cellular functions and molecular mechanism. *Cell Mol Life Sci* *62*, 670-684.
- Mayer, M.P., Rudiger, S., and Bukau, B. (2000). Molecular basis for interactions of the DnaK chaperone with substrates. *Biol Chem* *381*, 877-885.
- McLennan, N., and Masters, M. (1998). GroE is vital for cell-wall synthesis. *Nature* *392*, 139.
- Mogk, A., Deuerling, E., Vorderwulbecke, S., Vierling, E., and Bukau, B. (2003). Small heat shock proteins, ClpB and the DnaK system form a functional triade in reversing protein aggregation. *Mol Microbiol* *50*, 585-595.
- Moller, S., Croning, M.D., and Apweiler, R. (2001). Evaluation of methods for the prediction of membrane spanning regions. *Bioinformatics* *17*, 646-653.
- Nakatogawa, H., and Ito, K. (2002). The ribosomal exit tunnel functions as a discriminating gate. *Cell* *108*, 629-636.
- Natale, P., Bruser, T., and Driessen, A.J. (2008). Sec- and Tat-mediated protein secretion across the bacterial cytoplasmic membrane--distinct translocases and mechanisms. *Biochim Biophys Acta* *1778*, 1735-1756.
- Nichols, R.J., Sen, S., Choo, Y.J., Beltrao, P., Zietek, M., Chaba, R., Lee, S., Kazmierczak, K.M., Lee, K.J., Wong, A., *et al.* (2011). Phenotypic landscape of a bacterial cell. *Cell* *144*, 143-156.
- Olsen, J.V., and Macek, B. (2009). High accuracy mass spectrometry in large-scale analysis of protein phosphorylation. *Methods Mol Biol* *492*, 131-142.
- Ong, S.E., and Mann, M. (2006). A practical recipe for stable isotope labeling by amino acids in cell culture (SILAC). *Nat Protoc* *1*, 2650-2660.
- Patzelt, H., Rudiger, S., Brehmer, D., Kramer, G., Vorderwulbecke, S., Schaffitzel, E., Waitz, A., Hestekamp, T., Dong, L., Schneider-Mergener, J., *et al.* (2001). Binding specificity of Escherichia coli trigger factor. *Proceedings of the National Academy of Sciences of the United States of America* *98*, 14244-14249.
- Pauling, L., Corey, R.B., and Branson, H.R. (1951). The structure of proteins; two hydrogen-bonded helical configurations of the polypeptide chain. *Proceedings of the National Academy of Sciences of the United States of America* *37*, 205-211.
- Piette, F., D'Amico, S., Struvay, C., Mazzucchelli, G., Renaut, J., Tutino, M.L., Danchin, A., Leprince, P., and Feller, G. (2010). Proteomics of life at low temperatures: trigger factor is the primary chaperone in the Antarctic bacterium *Pseudoalteromonas haloplanktis* TAC125. *Mol Microbiol* *76*, 120-132.

- Rene, O., and Alix, J.H. (2011). Late steps of ribosome assembly in *E. coli* are sensitive to a severe heat stress but are assisted by the HSP70 chaperone machine. *Nucleic Acids Res* *39*, 1855-1867.
- Rodriguez, F., Arsene-Ploetze, F., Rist, W., Rudiger, S., Schneider-Mergener, J., Mayer, M.P., and Bukau, B. (2008). Molecular basis for regulation of the heat shock transcription factor sigma32 by the DnaK and DnaJ chaperones. *Mol Cell* *32*, 347-358.
- Rudiger, S., Germeroth, L., Schneider-Mergener, J., and Bukau, B. (1997). Substrate specificity of the DnaK chaperone determined by screening cellulose-bound peptide libraries. *EMBO J* *16*, 1501-1507.
- Saito, H., and Uchida, H. (1978). Organization and expression of the dnaJ and dnaK genes of *Escherichia coli* K12. *Mol Gen Genet* *164*, 1-8.
- Sambrook, J., Fritsch, E.F., and Maniatis, T. (1989). *Molecular cloning: a laboratory manual*. Cold Spring Harbor Laboratory.
- Sampson, B.A., Misra, R., and Benson, S.A. (1989). Identification and characterization of a new gene of *Escherichia coli* K-12 involved in outer membrane permeability. *Genetics* *122*, 491-501.
- Saschenbrecker, S., Bracher, A., Rao, K.V., Rao, B.V., Hartl, F.U., and Hayer-Hartl, M. (2007). Structure and function of RbcX, an assembly chaperone for hexadecameric Rubisco. *Cell* *129*, 1189-1200.
- Schlecht, R., Erbse, A.H., Bukau, B., and Mayer, M.P. (2011). Mechanics of Hsp70 chaperones enables differential interaction with client proteins. *Nature structural & molecular biology* *18*, 345-351.
- Schlunzen, F., Wilson, D.N., Tian, P., Harms, J.M., McInnes, S.J., Hansen, H.A., Albrecht, R., Buerger, J., Wilbanks, S.M., and Fucini, P. (2005). The binding mode of the trigger factor on the ribosome: implications for protein folding and SRP interaction. *Structure* *13*, 1685-1694.
- Schmidt, T., and Frishman, D. (2006). PROMPT: a protein mapping and comparison tool. *BMC Bioinformatics* *7*, 331.
- Sharma, S., Chakraborty, K., Muller, B.K., Astola, N., Tang, Y.C., Lamb, D.C., Hayer-Hartl, M., and Hartl, F.U. (2008). Monitoring protein conformation along the pathway of chaperonin-assisted folding. *Cell* *133*, 142-153.
- Sklar, J.G., Wu, T., Kahne, D., and Silhavy, T.J. (2007). Defining the roles of the periplasmic chaperones SurA, Skp, and DegP in *Escherichia coli*. *Genes Dev* *21*, 2473-2484.
- Smock, R.G., Blackburn, M.E., and Gierasch, L.M. (2011). The conserved, disordered C-terminus of DnaK enhances its in vitro chaperone function and cellular survival upon stress. *The Journal of biological chemistry*.

- Smock, R.G., Rivoire, O., Russ, W.P., Swain, J.F., Leibler, S., Ranganathan, R., and Gierasch, L.M. (2010). An interdomain sector mediating allostery in Hsp70 molecular chaperones. *Mol Syst Biol* 6, 414.
- Swain, J.F., Dinler, G., Sivendran, R., Montgomery, D.L., Stotz, M., and Gierasch, L.M. (2007). Hsp70 chaperone ligands control domain association via an allosteric mechanism mediated by the interdomain linker. *Mol Cell* 26, 27-39.
- Tang, Y.C., Chang, H.C., Hayer-Hartl, M., and Hartl, F.U. (2007). SnapShot: molecular chaperones, Part II. *Cell* 128, 412.
- Tang, Y.C., Chang, H.C., Roeben, A., Wischnewski, D., Wischnewski, N., Kerner, M.J., Hartl, F.U., and Hayer-Hartl, M. (2006). Structural features of the GroEL-GroES nano-cage required for rapid folding of encapsulated protein. *Cell* 125, 903-914.
- Tartaglia, G.G., Pechmann, S., Dobson, C.M., and Vendruscolo, M. (2007). Life on the edge: a link between gene expression levels and aggregation rates of human proteins. *Trends Biochem Sci* 32, 204-206.
- Tartaglia, G.G., and Vendruscolo, M. (2008). The Zyggregator method for predicting protein aggregation propensities. *Chem Soc Rev* 37, 1395-1401.
- Tatusov, R.L., Koonin, E.V., and Lipman, D.J. (1997). A genomic perspective on protein families. *Science* 278, 631-637.
- Tausky, H.H., and Shorr, E. (1953). A microcolorimetric method for the determination of inorganic phosphorus. *J Biol Chem* 202, 675-685.
- Teter, S.A., Houry, W.A., Ang, D., Tradler, T., Rockabrand, D., Fischer, G., Blum, P., Georgopoulos, C., and Hartl, F.U. (1999). Polypeptide flux through bacterial Hsp70: DnaK cooperates with trigger factor in chaperoning nascent chains. *Cell* 97, 755-765.
- Tomoyasu, T., Mogk, A., Langen, H., Goloubinoff, P., and Bukau, B. (2001). Genetic dissection of the roles of chaperones and proteases in protein folding and degradation in the *Escherichia coli* cytosol. *Mol Microbiol* 40, 397-413.
- Traverso-Cori, A., Chaimovich, H., and Cori, O. (1965). Kinetic Studies and Properties of Potato Apyrase. *Arch Biochem Biophys* 109, 173-184.
- Ullers, R.S., Ang, D., Schwager, F., Georgopoulos, C., and Genevoux, P. (2007). Trigger Factor can antagonize both SecB and DnaK/DnaJ chaperone functions in *Escherichia coli*. *Proceedings of the National Academy of Sciences of the United States of America* 104, 3101-3106.

- Van Durme, J., Maurer-Stroh, S., Gallardo, R., Wilkinson, H., Rousseau, F., and Schymkowitz, J. (2009). Accurate prediction of DnaK-peptide binding via homology modelling and experimental data. *PLoS Comput Biol* 5, e1000475.
- Vogel, M., Bukau, B., and Mayer, M.P. (2006a). Allosteric regulation of Hsp70 chaperones by a proline switch. *Mol Cell* 21, 359-367.
- Vogel, M., Mayer, M.P., and Bukau, B. (2006b). Allosteric regulation of Hsp70 chaperones involves a conserved interdomain linker. *J Biol Chem* 281, 38705-38711.
- Vorderwulbecke, S., Kramer, G., Merz, F., Kurz, T.A., Rauch, T., Zachmann-Brand, B., Bukau, B., and Deuerling, E. (2005). Low temperature of GroEL/ES overproduction permits growth of *Escherichia coli* cells lacking trigger factor DnaK. *FEBS Lett* 579, 181-187.
- Wandinger, S.K., Richter, K., and Buchner, J. (2008). The Hsp90 chaperone machinery. *J Biol Chem* 283, 18473-18477.
- Weissman, J.S., Rye, H.S., Fenton, W.A., Beechem, J.M., and Horwich, A.L. (1996). Characterization of the active intermediate of a GroEL-GroES-mediated protein folding reaction. *Cell* 84, 481-490.
- Xu, Z., Horwich, A.L., and Sigler, P.B. (1997). The crystal structure of the asymmetric GroEL-GroES-(ADP)₇ chaperonin complex. *Nature* 388, 741-750.
- Yam, A.Y., Xia, Y., Lin, H.T., Burlingame, A., Gerstein, M., and Frydman, J. (2008). Defining the TRiC/CCT interactome links chaperonin function to stabilization of newly made proteins with complex topologies. *Nat Struct Mol Biol* 15, 1255-1262.
- Yochem, J., Uchida, H., Sunshine, M., Saito, H., Georgopoulos, C.P., and Feiss, M. (1978). Genetic analysis of two genes, *dnaJ* and *dnaK*, necessary for *Escherichia coli* and bacteriophage lambda DNA replication. *Mol Gen Genet* 164, 9-14.
- Young, J.C. (2010). Mechanisms of the Hsp70 chaperone system. *Biochem Cell Biol* 88, 291-300.
- Young, J.C., Barral, J.M., and Ulrich Hartl, F. (2003). More than folding: localized functions of cytosolic chaperones. *Trends Biochem Sci* 28, 541-547.
- Yu, N.Y., Wagner, J.R., Laird, M.R., Melli, G., Rey, S., Lo, R., Dao, P., Sahinalp, S.C., Ester, M., Foster, L.J., *et al.* (2010). PSORTb 3.0: improved protein subcellular localization prediction with refined localization subcategories and predictive capabilities for all prokaryotes. *Bioinformatics* 26, 1608-1615.
- Yura, T., and Nakahigashi, K. (1999). Regulation of the heat-shock response. *Curr Opin Microbiol* 2, 153-158.

Zhu, X., Zhao, X., Burkholder, W.F., Gragerov, A., Ogata, C.M., Gottesman, M.E., and Hendrickson, W.A. (1996). Structural analysis of substrate binding by the molecular chaperone DnaK. *Science* 272, 1606-1614.

7 APPENDICES

7.1 Supplementary tables

Supplementary Table S1 DnaK interactors

DnaK interactors (DnaJ and GrpE are excluded from table S1) sorted according to their enrichment above the background binding (PD/BG ratio), from high to low ratios. PD/BG ratio, enrichment of the DnaK-interactors compared to the background as measured by SILAC MS; REF, the relative enrichment factors; DnaK-enriched less-enriched substrates are highlighted in yellow and blue, respectively; Essential proteins are in bold (1).

EG	Gene Name	PD/BG ratio	REF	EG	Gene Name	PD/BG ratio	REF	EG	Gene Name	PD/BG ratio	REF
EG10230	dksA	22.57	3.95	EG50001	rplU	6.75	0.08	EG10370	ispG	4.42	0.48
EG10978	sspB	19.76	9.26	EG10164	crp	6.72	35.37	EG12108	norR	4.39	3.69
EG10841	fliD	19.28		EG10585	metF	6.72	1.75	EG10953	sodA	4.38	0.10
EG12899	yheO	19.17	4.96	EG11647	accA	6.72	0.59	EG12967	yciO	4.37	0.41
EG10893	rpoA	18.46	0.22	EG13937	rsxG	6.71	12.34	EG10873	rplL	4.35	0.05
EG11827	rpiB	17.55	9.41	EG12144	pgm	6.71	0.04	EG11485	hemG	4.35	13.45
EG10100	atpC	17.49	0.49	EG10338	fruR	6.71	0.89	EG11059	usg	4.35	0.71
EG13395	iscU	17.15	4.80	EG13442	nagK	6.71	2.32	EG11885	opgG	4.34	2.87
EG10439	hha	16.66	13.86	EG10088	asd	6.69	0.12	EG10915	rpsP	4.33	0.09
EG12642	pdxK	16.63	15.71	EG12930	hslO	6.69	1.45	EG13469	yphH	4.32	7.10
EG11747	panD	16.19	0.31	EG10509	katE	6.69	10.03	EG13226	ftsK	4.32	6.71
EG10091	asnA	15.73	13.23	EG11666	moaC	6.67	10.98	EG10859	rne	4.31	1.63
EG10684	pal	15.56	3.74	EG11529	ftsN	6.67	0.68	EG10154	moeB	4.31	5.26
EG10539	livJ	15.12	49.68	EG13893	ycgL	6.66	1.72	EG10877	rplP	4.30	0.10
EG10047	apaG	15.04	7.57	EG10546	lpxB	6.64	7.00	EG11324	ubiH	4.30	13.07
EG10986	tag	14.86	8.89	EG10643	narL	6.57	0.32	EG10815	rbsB	4.30	5.41
EG12119	yehJ	14.61	10.02	EG11124	ompW	6.57	12.40	EG11437	plsX	4.29	2.05
EG11390	uspA	14.38	0.73	EG11320	nrdR	6.56	13.77	EG10238	dnaE	4.28	2.01
EG10937	secB	14.37	0.41	EG10404	gltD	6.53	0.83	EG10103	atpF	4.27	0.20
EG10165	err	13.94	0.81	EG12479	rsgA	6.53	0.92	EG10543	lpd	4.27	0.20
EG10897	rpoH	13.57	4.36	EG13657	miaB	6.52	6.20	EG11031	trxA	4.27	0.04
EG10389	glnQ	13.45	12.41	EG10547	lrp	6.50	0.09	EG13408	slyA	4.27	0.09
EG10884	rplX	13.43	0.14	EG13066	guaD	6.49	2.29	EG10818	rbsK	4.25	0.14
EG11009	tolC	12.96	11.64	EG11456	rffA	6.48	0.31	EG13658	ubiF	4.23	2.52
EG50003	acpP	12.82	0.24	EG12903	yheS	6.45	5.28	EG11226	leuA	4.22	0.20
EG10270	era	12.76	20.42	EG11450	yifE	6.45	0.07	EG10904	rpsE	4.22	0.43
EG10823	recA	12.74	10.48	EG11128	yciH	6.43	2.45	EG13656	ybeZ	4.22	0.09

EG14069	thiM	12.39	4.72	EG11979	rfbC	6.43	0.12	EG11609	evgA	4.21	0.66
EG11569	lptD	12.38	5.61	EG10456	hmp	6.42	1.75	EG10977	sspA	4.21	0.04
EG12111	nlpD	12.27	5.14	EG10752	potD	6.42	3.06	EG13892	ycgK	4.20	32.59
EG11835	yihI	12.20		EG11067	valS	6.42	0.03	EG12382	fxsA	4.20	4.41
EG10587	metH	12.00	13.27	EG12171	yjiI	6.42	2.75	EG13969	ydiJ	4.20	9.64
EG11527	narP	11.81	18.37	EG11487	pdxH	6.41	1.67	EG10096	aspC	4.19	0.04
EG12319	can	11.71	27.14	EG12685	ygfZ	6.38	0.33	EG10931	sdhA	4.18	6.98
EG10567	manX	11.55	21.49	EG11623	sdaB	6.37	2.31	EG11372	tadA	4.18	7.92
EG11505	holE	11.25	12.80	EG40003	insC	6.37	4.27	EG11013	topA	4.17	0.35
EG10811	pyrI	11.08	4.64	EG10876	rplO	6.36	0.07	EG10599	groL	4.14	0.14
EG13173	queF	11.03	7.44	EG10790	purA	6.35	2.49	EG10874	rplM	4.14	0.18
EG10403	gltB	10.92	6.31	EG11699	gpmA	6.35	0.03	EG10300	ffh	4.13	2.21
EG12712	luxS	10.79	1.41	EG11478	tatA	6.34	1.30	EG10638	narG	4.13	9.53
EG10316	lpxD	10.75	0.42	EG10372	gdhA	6.34	0.71	EG11427	tktA	4.11	0.06
EG11539	pyrH	10.66	0.04	EG10024	aceE	6.33	1.19	EG11738	rsd	4.10	22.08
EG10670	ompC	10.63	10.10	EG12069	mqo	6.30	1.16	EG11621	metN	4.10	8.56
EG14062	fbaB	10.61	0.23	EG10789	ptsI	6.29	0.40	EG12412	rfbB	4.09	0.11
EG11398	hdeA	10.55		EG13433	nagZ	6.28	0.22	EG10798	purM	4.09	0.13
EG12343	yjiK	10.49	1.12	EG11879	rraA	6.27	0.27	EG13416	rfaE	4.08	0.28
EG13142	dinJ	10.49	6.51	EG10432	hemL	6.27	0.38	EG12336	yacH	4.07	0.61
EG11399	hdeB	10.44	12.06	EG13685	ybjP	6.27	3.72	EG11853	yiiD	4.06	1.80
EG10518	kdsA	10.44	0.07	EG10703	pgk	6.21	0.07	EG10800	purR	4.05	0.11
EG10386	glnH	10.41	3.29	EG11001	thrS	6.20	12.03	EG12401	rlmN	4.04	4.56
EG11012	tonB	10.40	7.43	EG10673	ompT	6.20	6.44	EG10631	nadB	4.02	29.59
EG10239	dnaG	10.39	6.65	EG11131	relE	6.20	3.80	EG10930	sdaA	4.02	0.96
EG12089	nuoI	10.33	4.68	EG12193	cbpA	6.18	5.24	EG13693	ybjX	4.00	8.38
EG11385	ahpF	10.27	0.61	EG10770	proS	6.16	0.28	EG10801	putA	3.99	1.66
EG10367	gapA	10.18	0.94	EG10887	rpmC	6.12	0.08	EG11281	mutL	3.99	15.23
EG10275	accB	10.06	1.65	EG14209	yfgM	6.10	0.27	EG13022	ygiT	3.98	11.19
EG13611	yajO	10.06	0.97	EG12181	grxD	6.10	0.14	EG40008	insH	3.97	16.73
EG11332	upp	10.03	0.67	EG11206	yjaA	6.09	2.71	EG10870	rplI	3.95	0.06
EG10428	hemB	10.00	0.09	EG13752	ydcI	6.09	16.12	EG11284	fabZ	3.94	0.21
EG13838	ydfZ	10.00	0.04	EG12686	flu	6.07	2.84	EG12677	iscS	3.94	0.60
EG14397	yibT	10.00	4.26	EG11117	yceB	6.07	0.94	EG10754	poxB	3.93	1.72
EG10223	deoR	10.00	2.11	EG10274	fabB	6.07	0.09	EG13252	queC	3.91	2.15
EG10463	degP	10.00	1.22	EG10744	pntA	6.06	0.20	EG14207	der	3.91	3.65
EG11575	leuD	10.00	1.03	EG11291	yggG	6.06	2.04	EG11610	evgS	3.88	5.50
EG10452	hisP	9.98	31.36	EG11132	ydiA	6.04	1.30	EG13900	dhaL	3.88	0.69
EG13325	ybiT	9.98	0.82	EG11404	yehF	6.03	2.17	EG10668	ogt	3.87	9.41
EG11592	ybeD	9.96	4.01	EG10600	groS	6.02	0.06	EG10574	mcrB	3.86	3.09
EG10571	mazE	9.91		EG11889	dctR	6.01	3.05	EG12347	yecC	3.86	8.95
EG12083	nuoB	9.89	8.50	EG10411	gnd	6.01	0.06	EG11351	rfaB	3.85	1.02

EG11288	mak	9.83	2.11	EG13472	gsiA	6.01	2.45	EG10137	cdd	3.84	2.40
EG10277	fabH	9.83	0.04	EG10836	relB	6.01	3.20	EG10908	rpsI	3.82	0.07
EG10831	recN	9.68	12.74	EG11030	trpS	5.99	0.11	EG14111	yfcH	3.80	3.29
EG10244	dnaT	9.54	3.22	EG12878	zapA	5.99	2.15	EG10731	phoP	3.80	0.39
EG10596	minC	9.52	4.51	EG12762	agaR	5.97	1.11	EG10159	clpX	3.78	3.02
EG13690	ltaE	9.48	0.18	EG10776	pspA	5.95	1.02	EG12352	ppiC	3.78	1.67
EG14287	ycaR	9.44	7.07	EG11830	yihD	5.95	1.85	EG10609	mreC	3.77	4.58
EG12474	blc	9.36	13.13	EG11094	sbcD	5.94	7.09	EG12957	glk	3.76	0.13
EG10248	dppA	9.20	2.20	EG13464	yphC	5.92	12.11	EG10119	bioC	3.74	9.06
EG10669	ompA	9.18	3.72	EG12855	yebG	5.92	1.95	EG10735	phoU	3.72	0.80
EG12826	tldD	9.17	0.89	EG10465	ribB	5.90	0.54	EG10533	lexA	3.71	1.54
EG11192	yicC	9.15	0.37	EG11630	potG	5.90	5.46	EG10245	dnaX	3.71	3.98
EG12273	yiaF	9.13	3.24	EG10709	pheS	5.88	0.16	EG10222	deoD	3.70	0.05
EG10387	glnL	9.12	6.91	EG10068	argG	5.87	0.65	EG11436	yjgB	3.70	13.81
EG12332	erpA	9.10	1.76	EG10667	nusG	5.86	3.24	EG10457	hns	3.69	0.04
EG13678	ybjI	9.09	5.83	EG12345	ydfG	5.85	1.68	EG10906	rpsG	3.69	0.04
EG14129	yfcZ	9.08	1.18	EG11369	ubiC	5.85	14.98	EG11318	fabG	3.68	0.05
EG11897	rpoE	9.05	0.77	EG12473	yjeK	5.84	9.48	EG10318	fldA	3.68	0.05
EG10317	fis	9.04	0.15	EG12615	torR	5.82	5.69	EG10806	pyrC	3.68	5.27
EG12296	gpmM	9.03	0.41	EG10021	yjiA	5.80	2.03	EG11140	uvrY	3.65	15.34
EG13530	yqaB	8.98	13.15	EG11590	thiH	5.78	6.17	EG13935	rsxC	3.65	7.55
EG10973	gutQ	8.86	0.90	EG10505	infB	5.77	0.26	EG13727	etp	3.64	18.47
EG11490	gadB	8.69	14.20	EG10794	purF	5.77	0.49	EG13478	rimO	3.63	16.22
EG13290	yqgF	8.60	0.07	EG10946	serC	5.76	0.06	EG10552	lysS	3.62	0.28
EG11574	thiB	8.57	2.52	EG10867	rplD	5.75	0.34	EG11884	tehB	3.62	0.48
EG13305	ybgI	8.57	1.53	EG10768	proB	5.70	0.28	EG11984	wbbJ	3.61	4.06
EG10899	rpoZ	8.49	2.24	EG10420	guaA	5.69	0.14	EG13683	ybjN	3.60	3.62
EG13929	ydgH	8.48	9.91	EG10066	argD	5.69	1.42	EG10178	cyoA	3.60	0.49
EG11092	crl	8.48	1.07	EG12690	rarA	5.67	3.57	EG13397	iscR	3.59	2.97
EG11929	zur	8.41	12.02	EG12099	efp	5.65	0.09	EG10595	miaA	3.58	3.33
EG11723	yieF	8.38	0.15	EG12928	yrfG	5.64	14.84	EG10661	nrdB	3.58	0.42
EG11321	ribD	8.35	1.47	EG11045	udp	5.64	0.15	EG11391	osmY	3.56	11.87
EG10961	speC	8.35	1.11	EG11531	cfa	5.61	3.83	EG10687	parE	3.54	1.19
EG10347	ftsZ	8.33	7.61	EG10194	cysN	5.60	7.77	EG10660	nrdA	3.54	3.66
EG10611	mrp	8.25	0.89	EG12972	scpB	5.60	21.28	EG10265	lpxC	3.53	4.29
EG10603	mprA	8.24	0.18	EG10530	lepB	5.59	0.92	EG11799	hybA	3.53	5.87
EG12102	feoB	8.24	7.89	EG10885	rplY	5.59	0.55	EG10220	deoB	3.52	0.17
EG11680	lptB	8.23	7.70	EG10943	selD	5.58	1.62	EG11422	inaA	3.52	8.78
EG11415	dps	8.22	1.93	EG10821	rcsB	5.58	2.61	EG10418	gshA	3.51	0.05
EG12006	yehT	8.21	3.71	EG12503	flkB	5.58	0.15	EG11438	yceF	3.50	1.10
EG10707	pheA	8.17	3.20	EG10830	recJ	5.55	10.41	EG12502	ytfB	3.49	7.70
EG13625	mhpF	8.15	2.71	EG11143	ubiG	5.55	3.88	EG10087	ascG	3.48	1.73

EG11467	yigI	8.14	6.19	EG13931	ydgJ	5.55	1.53	EG10608	mreB	3.48	12.09
EG10258	eno	8.13	0.21	EG10425	hdhA	5.54	0.09	EG12627	dppD	3.47	1.76
EG13295	frmB	8.11	3.29	EG10217	accD	5.53	0.84	EG10231	dld	3.47	16.92
EG11701	udk	8.07	14.04	EG13440	lolD	5.52	15.02	EG13547	ivy	3.46	0.36
EG12419	gatY	8.06	2.98	EG13578	galF	5.52	0.93	EG11837	typA	3.46	3.39
EG13357	tteA	8.05	5.07	EG11116	yeeA	5.52	26.83	EG13443	cobB	3.46	2.09
EG10671	ompF	8.05	18.58	EG11589	thiG	5.47	0.32	EG14060	yegQ	3.45	1.07
EG11586	thiE	8.03	7.31	EG10889	rpmE	5.46	0.55	EG10128	btuD	3.44	15.02
EG10450	hisH	7.99	0.20	EG12666	lpxH	5.45	3.35	EG10749	potA	3.44	0.45
EG10421	guaB	7.96	0.07	EG12086	nuoE	5.44	25.59	EG11314	purB	3.44	0.08
EG13431	yefM	7.95	15.67	EG10441	ihfB	5.44	0.71	EG13964	sufC	3.43	2.62
EG11331	ribA	7.90	2.70	EG14199	yfgC	5.42	4.61	EG11986	wbbL	3.43	15.50
EG11204	murI	7.88	1.03	EG10994	tdk	5.42	12.94	EG10576	mdh	3.43	0.03
EG10497	ilvE	7.88	0.21	EG11178	rbfA	5.41	0.61	EG12182	yajG	3.42	1.02
EG10976	ssb	7.88	0.33	EG11003	tig	5.41	0.04	EG13134	uup	3.38	2.40
EG12207	rlmA	7.83	30.56	EG10081	aroK	5.40	0.22	EG12739	exuR	3.38	3.27
EG10883	rpIW	7.82	0.07	EG10360	fusA	5.39	0.26	EG10948	maeA	3.36	0.19
EG12803	kdsD	7.81	13.71	EG11881	hslU	5.38	1.92	EG10803	pykA	3.35	0.13
EG10032	adk	7.80	0.07	EG11473	ubiE	5.38	10.08	EG10097	aspS	3.35	0.08
EG10924	ruvB	7.80	11.22	EG13190	rstA	5.37	4.57	EG10200	cytR	3.35	3.93
EG10544	lpp	7.79	0.74	EG10532	leuS	5.36	0.15	EG10451	hisI	3.32	0.33
EG10161	cpsB	7.79	5.05	EG13031	yqiC	5.35	2.88	EG10025	aceF	3.29	0.07
EG12418	gatZ	7.75	35.24	EG10407	gltX	5.34	0.44	EG10981	sucC	3.29	0.04
EG12167	smtA	7.74	1.96	EG10031	adhE	5.30	4.88	EG14364	yheV	3.29	1.46
EG10597	minD	7.72	6.07	EG10900	rpsA	5.28	0.17	EG12743	yqiD	3.28	0.37
EG10233	dmsB	7.72	4.43	EG11978	rfaA	5.26	0.11	EG10409	glyQ	3.27	0.62
EG12130	hscA	7.71	2.12	EG11241	ycaC	5.26	13.56	EG13716	yebX	3.26	2.85
EG11587	thiF	7.70	11.27	EG12676	bamA	5.24	4.38	EG10492	ileS	3.26	0.52
EG11556	talB	7.70	0.05	EG10959	speA	5.23	0.13	EG10205	dapA	3.25	0.30
EG10895	rpoC	7.69	3.54	EG13026	qseB	5.22	12.94	EG11504	metQ	3.23	0.33
EG10879	rpIR	7.68	0.11	EG10589	metK	5.19	0.10	EG11171	ygiD	3.23	1.25
EG11549	pepT	7.65	0.37	EG10666	nusB	5.19	0.27	EG10918	rpsS	3.23	0.04
EG11384	ahpC	7.64	0.93	EG10408	glyA	5.18	0.23	EG12983	yggW	3.22	6.97
EG10236	dnaB	7.60	2.52	EG10783	pstB	5.15	7.95	EG12298	yibQ	3.22	7.57
EG10804	pykF	7.59	0.38	EG12218	dcrB	5.14	0.90	EG10902	rpsC	3.18	0.08
EG11358	murA	7.58	9.67	EG13148	yafK	5.13	4.91	EG11246	uspE	3.17	0.25
EG13410	csgD	7.56	9.27	EG12447	speG	5.13	0.84	EG11785	yfiE	3.16	8.82
EG11518	fpr	7.56	0.19	EG10891	rpmG	5.12	0.10	EG11874	yiiQ	3.11	5.08
EG10495	ilvC	7.54	0.15	EG14322	tatB	5.12	1.19	EG10157	clpB	3.10	0.30
EG13385	yeeR	7.54	2.15	EG12674	uspF	5.11	4.63	EG10975	srmB	3.10	0.08
EG11048	ugpC	7.52	7.23	EG13256	cueR	5.10	4.09	EG11033	tsf	3.09	0.11
EG10462	htpX	7.52	0.79	EG11535	ibpB	5.09	12.71	EG12263	bcsE	3.09	11.79

EG10449	hisG	7.50	0.94	EG11595	moaA	5.05	16.54	EG12313	yacF	3.08	5.62
EG13324	ybiS	7.49	9.37	EG10050	appY	5.04	7.24	EG10434	hemY	3.08	2.05
EG11022	trmA	7.44	1.92	EG10466	hupA	5.03	0.04	EG10689	pcm	3.08	0.99
EG10261	entC	7.44	10.38	EG10861	rnhB	5.03	8.25	EG10805	pyrB	3.07	0.21
EG11540	wrbA	7.43	0.29	EG10117	bioA	5.02	3.25	EG10134	carA	3.05	0.10
EG10207	dapD	7.42	0.13	EG10781	pssA	4.99	4.44	EG10810	pyrG	3.04	0.12
EG12221	acpT	7.38	31.53	EG10489	icd	4.99	0.11	EG12434	htrG	3.04	1.24
EG10894	rpoB	7.37	5.83	EG13759	ydcP	4.99	21.45	EG12606	fabF	3.03	0.14
EG12591	opgB	7.35	2.86	EG10260	entB	4.98	8.35	EG11286	argE	3.01	6.83
EG10331	frdB	7.33	5.63	EG10979	sucA	4.97	1.92	EG10156	clpA	3.01	3.66
EG12678	znuA	7.33	6.11	EG11189	rfaC	4.97	2.44	EG10328	folD	3.01	0.07
EG12524	yjgF	7.32	0.06	EG12242	gadW	4.96	10.92	EG13050	xdhB	2.98	22.45
EG12135	ompX	7.31	1.10	EG10866	rplC	4.94	0.41	EG10120	bioD	2.98	5.45
EG10844	rhlB	7.30	3.27	EG12628	dppF	4.94	2.36	EG11786	yfiF	2.97	1.27
EG12939	rtcB	7.30	5.61	EG10909	rpsJ	4.93	0.81	EG50011	folP	2.96	0.15
EG11387	amyA	7.27	6.96	EG10218	dedD	4.92	2.91	EG10663	nadE	2.96	0.03
EG12457	ydgA	7.27	1.14	EG40012	insL	4.92	8.88	EG10506	infC	2.96	0.04
EG12316	acnB	7.26	0.16	EG10125	bolA	4.92	0.65	EG12084	nuoC	2.95	10.18
EG10598	minE	7.26	0.77	EG11311	dusB	4.90	8.89	EG10529	lepA	2.93	7.99
EG10104	atpG	7.26	0.20	EG12123	lrhA	4.90	1.58	EG10672	ompR	2.92	0.82
EG11015	tpiA	7.25	0.06	EG10701	pflB	4.90	0.78	EG10340	ftsE	2.87	10.46
EG11296	radA	7.25	16.86	EG10674	oppA	4.90	0.48	EG14101	yfbQ	2.84	13.28
EG10282	fbaA	7.24	0.08	EG10954	sodB	4.88	0.08	EG13355	ydaM	2.83	4.93
EG14107	yfcD	7.22	0.69	EG10201	dacA	4.85	0.93	EG10880	rplS	2.82	0.12
EG11252	mukE	7.20	1.81	EG10064	argB	4.85	2.02	EG10919	rpsT	2.82	0.07
EG14132	gtrB	7.19	0.90	EG10807	pyrD	4.85	0.54	EG10653	nirB	2.81	7.42
EG14108	yfcE	7.18	0.98	EG10869	rplF	4.84	0.11	EG10771	proV	2.79	3.43
EG10834	recR	7.16	2.51	EG11000	thrC	4.84	0.20	EG10809	pyrF	2.78	0.07
EG11784	yfiD	7.15	1.51	EG12101	feoA	4.84	21.41	EG10741	pmbA	2.78	0.71
EG12789	yhbT	7.14	6.17	EG10098	atpA	4.83	4.94	EG10888	rpmD	2.78	0.05
EG10677	oppD	7.14	8.19	EG12752	yhaM	4.81	3.84	EG10484	hypB	2.78	13.01
EG13186	ldhA	7.14	0.07	EG11212	nsrR	4.81	2.41	EG10868	rplE	2.77	0.07
EG12777	yraL	7.11	0.90	EG13409	slyB	4.80	2.13	EG11315	yhdH	2.76	0.19
EG10872	rplK	7.10	0.24	EG10325	fnr	4.79	1.29	EG10390	glnS	2.74	0.07
EG11585	thiC	7.10	3.04	EG13132	znuC	4.79	36.82	EG11221	zwf	2.74	0.15
EG14222	bamD	7.10	5.87	EG11591	lipB	4.78	2.57	EG10756	ppc	2.71	0.09
EG10742	pncB	7.10	0.88	EG10330	frdA	4.77	2.62	EG10871	rplJ	2.70	0.11
EG10158	clpP	7.08	9.05	EG11319	galU	4.77	1.81	EG12841	yrdD	2.69	15.13
EG10196	cysS	7.05	0.11	EG10838	rfaD	4.77	0.09	EG10710	pheT	2.69	0.08
EG11306	lipA	7.05	16.38	EG10383	glnA	4.72	0.13	EG11857	fdoH	2.66	5.26
EG11673	folB	7.05	0.25	EG11981	glf	4.69	1.14	EG11730	viaA	2.64	8.32
EG10584	metE	7.03	0.96	EG10094	asnS	4.68	0.08	EG12179	cspE	2.63	0.02

EG10980	sucB	7.03	0.16	EG11061	uvrA	4.65	7.28	EG13413	csgG	2.62	8.82
EG11809	purT	7.02	0.57	EG10455	skp	4.63	0.29	EG11596	moaB	2.59	0.16
EG11447	csrA	7.02	0.54	EG10854	rlpA	4.62	6.05	EG10203	dacC	2.58	0.83
EG10101	atpD	7.02	3.04	EG10118	bioB	4.62	2.69	EG10243	dnaQ	2.58	3.78
EG12589	yjjM	7.01	2.60	EG11433	msrA	4.61	1.34	EG13161	dsdC	2.57	9.88
EG11534	ibpA	7.00	9.22	EG11899	recT	4.61	22.28	EG20173	pta	2.56	0.39
EG13146	lpcA	6.99	0.06	EG10795	purH	4.60	0.09	EG14105	yfbU	2.56	0.91
EG14200	yfgD	6.99	0.45	EG10905	rpsF	4.58	0.14	EG11528	fabI	2.56	0.23
EG10061	arcA	6.99	0.09	EG12087	nuoG	4.58	16.01	EG10073	aroA	2.54	0.14
EG10499	ilvH	6.96	2.70	EG10461	htpG	4.57	0.55	EG12664	flgM	2.53	15.15
EG12624	yiaG	6.95	18.00	EG10281	fadR	4.57	0.52	EG12867	ampH	2.52	3.54
EG10864	rplA	6.94	0.30	EG10982	sucD	4.56	0.78	EG10034	alaS	2.51	0.12
EG10092	asnB	6.92	1.28	EG12597	yjjU	4.56	1.61	EG11440	def	2.51	0.23
EG12727	ygiP	6.91	20.52	EG12935	nfuA	4.54	0.15	EG12851	ybeL	2.50	
EG10368	epd	6.91	0.33	EG12866	proQ	4.52	0.17	EG10755	ppa	2.49	0.04
EG10791	purC	6.90	1.27	EG10192	cysK	4.52	0.22	EG13537	ybdR	2.49	
EG11198	glmU	6.87	0.32	EG10696	pepN	4.52	0.09	EG10385	glnG	2.47	4.32
EG11119	yceD	6.86	3.91	EG12253	kdgK	4.51	0.87	EG10683	pabB	2.47	1.88
EG10797	purL	6.85	0.41	EG10724	phnO	4.50	27.21	EG10130	btuR	2.45	2.22
EG10944	serA	6.85	0.78	EG11261	nfsA	4.49	0.08	EG10356	fumA	2.41	0.17
EG50010	frmA	6.84	12.57	EG14031	exoX	4.49	8.61	EG11580	ybiB	2.39	0.35
EG10699	pfkA	6.83	0.12	EG12132	iscA	4.47	0.12	EG13200	rnlA	2.38	7.95
EG10630	nadA	6.80	1.06	EG10947	serS	4.46	0.08	EG13612	dxs	2.35	3.82
EG10284	fdhE	6.79	9.75	EG12188	ptsP	4.46	9.02	EG10702	pgi	2.34	0.12
EG10174	cydB	6.79	0.06	EG10107	avtA	4.45	0.99	EG14018	kdgR	2.33	0.13
EG13502	yeaP	6.77	7.73	EG14165	yfeX	4.45	0.16	EG10467	hupB	2.32	0.07
EG10273	fabA	6.77	0.11	EG10498	ilvG	4.44	16.22	EG10184	cysB	2.22	1.13
EG10692	pdxB	6.77	0.08	EG11581	ybiC	4.44	0.64	EG13007	yghW	2.20	2.01
EG11345	hflD	6.75	3.94	EG10353	fucR	4.44	11.00	EG11425	rfaY	2.07	7.56

1. Essential proteins (Gerdes et al., 2003)

Supplementary Table S2 Proteins significantly increased in the Δ KJ proteome

Significantly ($p < 0.05$) decreased proteins in the Δ KJ proteome compared to WT, ordered by fold change from high to low. MW, molecular weight in kDa; E, essentiality. All DnaK interactors are in bold; DnaK enriched and less-enriched interactors are highlighted in yellow and blue, respectively.

EG	Gene Name	MW(kDa)	E	Fold change	EG	Gene Name	MW(kDa)	E	Fold change
EG11535	ibpB	16		169.22	EG10932	sdhB	26.7		3.41
EG12414	gatA	16.9		71.48	EG12586	yjiY	77.3		3.38
EG12418	gatZ	47.1		69.15	EG10326	folA	18	E	3.33
EG12416	gatC	48.3		63.43	EG12679	yeaD	32.6		3.28
EG11534	ibpA	15.7		47.96	EG10982	sucD	29.7		3.27
EG12417	gatD	37.3	E	47.10	EG12495	ulaC	17.2		3.13
EG10221	deoC	27.7		41.37	EG10510	rpoS	37.9		3.12
EG10219	deoA	47.2		31.59	EG10980	sucB	44	E	3.10
EG10157	clpB	95.5		28.27	EG11009	tolC	53.7		3.10
EG12686	flu	106.8		19.27	EG10981	sucC	41.3		3.08
EG12822	aaeB	73.5		12.50	EG10921	ftnA	19.4		2.98
EG12870	ycjF	39.3	E	12.23	EG11969	zntR	16.1		2.96
EG10461	htpG	71.4		12.16	EG13156	dgsA	44.3		2.93
EG11676	hslV	19		11.84	EG10979	sucA	105	E	2.93
EG11881	hslU	49.5		10.86	EG11746	panC	31.5		2.89
EG13921	ycjX	52.6		10.52	EG12316	acnB	93.4		2.88
EG13385	yeeR	57.2		8.88	EG10934	sdhD	12.8		2.88
EG10416	grpE	21.7	E	8.62	EG10691	pdxA	35.1		2.82
EG10600	groS	10.3	E	8.14	EG12935	nfuA	20.9		2.74
EG10599	groL	57.3	E	7.66	EG12312	coaE	22.6	E	2.74
EG13261	ybbN	31.7		7.62	EG11511	mog	21.2	E	2.72
EG11441	prlC	77.1		6.90	EG12392	ychM	59.4		2.70
EG11592	ybeD	9.8		6.64	EG11081	ispH	34.7	E	2.69
EG13186	ldhA	36.5		6.37	EG10011	yaaA	29.5		2.67
EG12816	nanE	24		5.84	EG10367	gapA	35.5	E	2.64
EG10542	lon	87.4		5.81	EG10095	aspA	52.3		2.62
EG11717	dgoK	31.3		5.53	EG11589	thiG	26.8		2.61
EG12752	yhaM	45.3		5.29	EG12838	yrdA	20.2		2.57
EG11005	tnaA	52.7		5.15	EG12142	sdaC	46.9		2.56
EG10220	deoB	44.3		5.12	EG11675	panB	28.2		2.56
EG12419	gatY	30.8		5.10	EG12313	yacF	28.2		2.53
EG12545	yjhC	41.3		5.10	EG10805	pyrB	34.4		2.51

EG11187	yibA	31.8	E	4.86	EG10815	rbsB	30.9		2.50
EG12930	hslO	32.5		4.78	EG11506	ftsH	70.7		2.49
EG50011	folP	30.6		4.77	EG10048	apaH	31.2		2.49
EG13656	ybeZ	39		4.76	EG11574	thiB	36.1		2.49
EG13655	ybeY	17.5	E	4.75	EG10512	kbl	43.1		2.49
EG11619	mfd	129.9		4.71	EG11596	moaB	18.6		2.47
EG13407	ugd	43.6		4.58	EG10814	rbsA	55		2.41
EG10897	rpoH	32.4	E	4.45	EG13547	ivy	16.8		2.41
EG13181	hslJ	15.1	E	4.33	EG11585	thiC	70.8		2.36
EG11083	hepA	109.7		4.26	EG10492	ileS	104.2	E	2.33
EG10422	guaC	37.3		4.18	EG11079	ribF	34.7	E	2.33
EG10931	sdhA	64.4		4.15	EG11322	ribE	16.1	E	2.32
EG13875	ymdC	53.6		4.15	EG11572	thiQ	25		2.31
EG10035	aldA	52.2		3.92	EG11556	talB	35.2		2.29
EG10593	mglB	35.7	E	3.92	EG13200	rnlA	40		2.29
EG12844	yefM	9.3		3.81	EG11598	moaE	16.9		2.26
EG11448	acs	72		3.78	EG11934	aphA	26.1		2.24
EG11586	thiE	23		3.59	EG10137	cdd	31.5		2.16
EG12233	yhiQ	26.9		3.52	EG10021	yjiA	35.6		2.16
EG11507	rlmE	23.3		3.42	EG13393	yeeZ	29.6		2.13
					EG10993	tdh	37.2		2.07

Supplementary Table S3 Proteins significantly decreased in the Δ KJ proteome

Significantly ($p < 0.05$) decreased proteins in the Δ KJ proteome compared to WT, ordered by fold change from low to high. MW, molecular weight in kDa; E, essentiality. All DnaK interactors are in bold; DnaK enriched and less-enriched interactors are highlighted in yellow and blue, respectively.

EG	Gene Name	MW(kDa)	E	Fold change	EG	Gene Name	MW(kDa)	E	Fold change
EG10999	thrB	33.6		0.06	EG11628	artJ	26.8		0.40
EG10998	thrA	89.1		0.10	EG11823	amiA	31.4		0.40
EG11000	thrC	47.1		0.11	EG12627	dppD	35.8		0.40
EG11398	hdeA	11.8		0.13	EG12628	dppF	37.5		0.41
EG12456	gadC	55		0.13	EG13964	sufC	27.5		0.41
EG10584	metE	84.6		0.15	EG12309	yjtD	25.2		0.42
EG11490	gadB	52.6		0.16	EG10603	mprA	20.5		0.42
EG13317	fiu	81.9		0.17	EG12215	zntA	76.8		0.44
EG11399	hdeB	12		0.19	EG10066	argD	43.7		0.44
EG10495	ilvC	54		0.20	EG13935	rsxC	80.1		0.45
EG10264	entF	141.9		0.21	EG10166	cspA	7.4		0.45
EG11394	fabR	24.4		0.21	EG10073	aroA	46		0.46
EG11890	slp	20.9	E	0.22	EG10740	plsB	91.3		0.46
EG10261	entC	42.9		0.23	EG12102	feoB	84.4		0.46
EG13965	sufB	54.7		0.24	EG10585	metF	33.1		0.46
EG10404	gltD	52		0.24	EG11333	visC	44.2		0.47
EG50009	gadA	52.6		0.24	EG12159	yaiE	10.2		0.47
EG11784	yfiD	14.2	E	0.27	EG10537	livG	28.4		0.47
EG40003	insC	13.4		0.28	EG10944	serA	44.1		0.48
EG10260	entB	32.5		0.28	EG12165	mukF	50.5	E	0.48
EG13193	yfjG	17.7	E	0.29	EG12817	nanR	29.5	E	0.48
EG11761	pptA	8.6		0.29	EG10536	livF	26.3		0.49
EG10271	exbB	26.2		0.29	EG11554	stpA	15.3		0.49
EG10403	gltB	161.9		0.30	EG10539	livJ	39		0.50
EG10460	hsdS	51.3		0.30	EG13905	yeiT	27.6		0.50
EG13247	ybaS	32.9		0.30	EG11143	ubiG	26.5	E	0.50
EG10317	fis	11.2	E	0.31	EG12263	bcxE	59.4		0.51
EG13397	iscR	17.3		0.32	EG11606	kch	46		0.52
EG11473	ubiE	28	E	0.32	EG11422	inaA	25.2		0.53
EG12240	mdtE	41.1		0.33	EG10745	pntB	48.7		0.53
EG10649	ndh	47.3		0.33	EG12794	yhbY	10.7		0.53
EG11223	argH	50.3		0.33	EG10744	pntA	54.6		0.53

EG12807	yrbL	24.3		0.33	EG10248	dppA	60.2		0.53
EG11886	opgH	96.9		0.34	EG10215	deaD	70.5		0.54
EG13546	nemA	39.5		0.34	EG11261	nfsA	26.8		0.55
EG10540	livK	39.3		0.35	EG12820	yhcN	9.1		0.55
EG12241	mdtF	111.5		0.35	EG11576	leuC	49.8		0.55
EG10587	metH	135.9		0.36	EG10496	ilvD	65.5		0.56
EG12743	yqjD	11		0.37	EG10230	dksA	17.5		0.56
EG10272	exbD	15.5		0.37	EG10673	ompT	35.5		0.56
EG11116	yceA	39.7		0.37	EG10463	degP	49.3		0.56
EG10079	aroG	38		0.39	EG10068	argG	49.8		0.57
EG13185	elaB	11.3		0.39	EG10027	ackA	43.2	E	0.59
					EG10497	ilvE	34		0.61

Supplementary Table S4 Proteins aggregated in Δ KJ cells

Significantly increased (> 2 fold) proteins in the Δ KJ insoluble fraction compared to WT are ordered alphabetically according to gene name. Dep (%): depletion percentage of total mass. All DnaK interactors are in bold; DnaK enriched and less-enriched interactors are highlighted in yellow and blue, respectively.

EG	Gene Name	Dep (%)	EG	Gene Name	Dep (%)	EG	Gene Name	Dep (%)	EG	Gene Name	Dep (%)
EG12825	aaeR		EG10407	gltX	1.74	EG10703	pgk		EG11587	thiF	1.91
EG10022	aceA	2.16	EG11787	gmd		EG10707	pheA		EG11589	thiG	0.81
EG10024	aceE		EG13415	gmr		EG10709	pheS		EG11590	thiH	4.11
EG10025	aceF		EG10411	gnd		EG10710	pheT	0.85	EG13273	thiI	11.21
EG11325	acnA	4.39	EG11699	gpmA	3.90	EG10728	phoB		EG11573	thiP	
EG12316	acnB		EG10413	gpp		EG10731	phoP	2.65	EG11572	thiQ	
EG11942	actP		EG10414	gpt		EG10738	pldA		EG11001	thrS	4.03
EG10031	adhE	13.30	EG10599	groL		EG10742	pncB	2.01	EG11002	thyA	
EG11384	ahpC		EG10600	groS		EG10743	pnp	0.44	EG11427	tktA	0.80
EG10034	alaS	3.77	EG10416	grpE		EG10755	ppa		EG12100	tktB	
EG10035	aldA	3.33	EG12181	grxD	1.19	EG10758	ppiB		EG11005	tnaA	2.00
EG10039	amn		EG10418	gshA	2.48	EG11510	ppk	24.25	EG11013	topA	5.41

EG11387	amyA	42.17	EG11102	gsk	4.11	EG11403	ppx	4.32	EG12672	tpx	
EG10045	ansA		EG12882	gsp	7.87	EG12114	prfC	1.30	EG11019	trkA	
EG10051	apt	2.82	EG10420	guaA	4.15	EG12365	prkB		EG11023	trmD	
EG10071	argS		EG10422	guaC		EG11441	prlC	1.10	EG13452	trmJ	7.20
EG14091	arnA		EG10423	gyrA		EG10770	proS	2.30	EG11030	trpS	0.59
EG10074	aroB	3.01	EG10428	hemB	2.33	EG13766	prp		EG11031	trxA	
EG10092	asnB	1.91	EG10431	hemH		EG10774	prs	0.24	EG11032	trxB	2.10
EG10093	asnC		EG11083	hepA	0.60	EG10781	pssA		EG11036	tufA	2.34
EG10094	asnS		EG10437	hflX	6.06	EG10785	pth		EG11837	typA	4.80
EG10096	aspC	3.31	EG10438	hfq		EG11004	ptrB		EG11039	tyrA	
EG10097	aspS		EG10444	hisA	3.06	EG10788	ptsH	1.95	EG11043	tyrS	1.63
EG11668	atoC		EG10446	hisC	0.97	EG10792	purD	1.14	EG11396	ubiD	
EG10113	bfr	17.78	EG10447	hisD	1.79	EG10793	purE		EG13658	ubiF	
EG13079	bglA	2.37	EG10453	hisS		EG10797	purL	0.80	EG11324	ubiH	
EG10121	bioF		EG20098	hpt	6.27	EG10799	purN		EG13407	ugd	
EG10123	birA		EG12329	hrpB		EG10800	purR	2.56	EG11061	uvrA	28.56
EG10130	btuR		EG10458	hsdM	8.80	EG11819	purU	10.13	EG11064	uvrD	
EG12319	can	16.35	EG10459	hsdR		EG13908	puuA		EG11067	valS	1.42
EG10134	carA	2.57	EG10460	hsdS	22.67	EG10803	pykA	1.01	EG11423	waaU	
EG10135	carB		EG13181	hsJ		EG10804	pykF		EG11985	wbbK	
EG11531	cfa	1.40	EG12930	hslO		EG10805	pyrB		EG11986	wbbL	
EG10157	clpB		EG11881	hslU		EG10810	pyrG	0.83	EG13566	wza	
EG10158	clpP		EG11676	hslV		EG11539	pyrH		EG11146	xapR	
EG10159	clpX	3.60	EG10461	htpG		EG10811	pyrI		EG11072	xseA	8.01
EG10922	coaA		EG11188	htrL		EG12690	rarA	0.10	EG11098	xseB	
EG10164	crp	3.76	EG11534	ibpA	43.34	EG11178	rbfA	0.42	EG11073	xthA	5.98
EG10165	err	4.11	EG11535	ibpB	88.53	EG10814	rbsA		EG10011	yaaA	3.57
EG13410	csgD		EG10489	icd	1.42	EG10815	rbsB		EG11089	yacC	
EG13413	csgG		EG10492	ileS		EG10817	rbsD		EG12313	yacF	
EG12204	cspC	2.94	EG11422	inaA		EG10822	resC		EG11749	yadE	
EG10167	cstA		EG40012	insL		EG12158	rdgC	4.63	EG11100	ybaB	1.12
EG10184	cysB	5.67	EG11783	intA		EG10825	recC		EG13218	ybaO	
EG10192	cysK	0.08	EG13885	iraM		EG11351	rfaB		EG13261	ybbN	
EG11408	dadX		EG10017	ispB		EG10838	rfaD	3.80	EG11255	ybeB	5.57
EG10207	dapD		EG10370	ispG	0.07	EG11978	rfaA	2.50	EG11592	ybeD	
EG10208	dapE	7.88	EG11081	ispH		EG12412	rfaB		EG13655	ybeY	
EG10212	dcp		EG10512	kbl	3.61	EG11979	rfaC	9.70	EG13656	ybeZ	
EG12464	deuR		EG14018	kdgR	1.05	EG12411	rfaD	2.78	EG11521	ybfA	
EG10214	ddlB		EG10518	kdsA	4.32	EG11451	rffE		EG11580	ybiB	
EG10219	deoA		EG10519	kdsB	1.21	EG11406	ribC		EG11581	ybiC	6.88
EG10220	deoB		EG13186	ldhA		EG11322	ribE		EG13325	ybiT	2.27
EG10221	deoC		EG10532	leuS	0.10	EG11079	ribF		EG13678	ybjI	14.24

EG10222	deoD		EG11548	lhr		EG12483	rlmB	0.56	EG13689	ybjT	
EG10223	deoR		EG11591	lipB		EG11507	rlmE		EG13699	ycaO	1.06
EG14207	der	1.38	EG11963	lldD		EG13725	rlmI	6.10	EG13718	yebZ	
EG13156	dgsA		EG10542	lon		EG13717	rlmL		EG11430	yefD	0.53
EG13901	dhaK	3.45	EG13146	lpcA		EG11472	rmuC		EG12444	yefJ	
EG11357	dinG		EG10543	lpd		EG10857	rnc		EG13434	yefP	
EG10236	dnaB	4.67	EG10316	lpxD	10.22	EG11299	rng	1.44	EG13887	yegF	
EG10238	dnaE		EG10547	lrp		EG13200	rnlA		EG12119	yehJ	
EG10242	dnaN	10.76	EG10948	maeA	1.31	EG11259	rnr		EG12392	yehM	
EG11932	dusA		EG14193	maeB	0.56	EG10863	rph		EG11121	yecA	
EG11311	dusB		EG11288	mak		EG10868	rpIE	1.49	EG12870	yecF	24.51
EG10251	dut		EG10562	malT		EG10893	rpoA	5.28	EG13921	yecX	
EG14031	exoX		EG10566	manA		EG10894	rpoB	5.49	EG13183	ydbK	
EG10273	fabA		EG10570	map		EG10895	rpoC	7.82	EG13752	ydcI	
EG10274	fabB		EG10572	mazG		EG10896	rpoD	4.22	EG13759	ydcP	2.87
EG10277	fabH		EG10576	mdh		EG10897	rpoH		EG13793	yddV	
EG11394	fabR	18.68	EG11368	menB		EG10510	rpoS	11.95	EG11643	ydeH	
EG11284	fabZ		EG10579	menD		EG10902	rpsC	4.21	EG13931	ydgJ	
EG10278	fadA		EG10586	metG	0.52	EG10904	rpsE	3.20	EG13420	ydhF	
EG10279	fadB		EG11619	mfd	11.09	EG11879	rraA	2.87	EG11132	ydiA	
EG13145	fadE		EG10592	mglA		EG13177	rseB		EG13969	ydiJ	
EG14127	fadJ		EG11596	moaB		EG10523	rsmA		EG12679	yeaD	0.56
EG10282	fbaA		EG11666	moaC	5.58	EG12596	rsmC		EG13493	yeaG	
EG10283	fbp	1.26	EG13227	modE		EG11623	sdaB		EG13506	yeaT	
EG10318	fldA	4.06	EG11511	mog	9.23	EG12142	sdaC		EG13405	yecM	
EG12686	flu	21.77	EG11085	mraW	4.21	EG10931	sdhA		EG13382	yeeN	2.08
EG11268	fnt		EG10616	mtlD	1.08	EG10932	sdhB		EG13385	yeeR	
EG10328	folD		EG11090	mtn	24.35	EG10933	sdhC		EG13393	yeeZ	
EG11375	folE		EG10617	mtr		EG10934	sdhD		EG12396	yegE	
EG50011	folP		EG11358	murA	4.96	EG10937	secB	8.26	EG14060	yegQ	
EG14263	folX	20.19	EG10621	murE	2.22	EG10941	selA	4.00	EG14087	yfaY	
EG10334	fire	3.60	EG10622	murF		EG10944	serA	0.34	EG14105	yfbU	
EG13295	frmB		EG11204	murI		EG10947	serS	5.89	EG14198	yfdZ	
EG10335	frr		EG10329	mutM		EG12094	sgrR		EG14165	yfeX	11.40
EG11091	frsA	6.48	EG10631	nadB	9.17	EG11782	smpB		EG14224	yfiQ	
EG10338	fruR	17.46	EG10663	nadE		EG10953	sodA		EG13197	yfjK	
EG10921	ftnA		EG11335	nadR		EG10954	sodB	1.35	EG11794	ygdE	0.55
EG10339	ftsA	9.33	EG12815	nanK		EG10958	soxS		EG11323	ygfB	
EG10356	fumA		EG11527	narP		EG10959	speA	3.65	EG12685	ygfZ	6.04
EG10360	fusA		EG10648	narZ		EG10960	speB	2.16	EG13019	ygiQ	17.42
EG12382	fxsA		EG10650	ndk		EG10961	speC	0.01	EG12749	yhaJ	
EG12242	gadW	12.14	EG20151	nfsB	0.24	EG10962	speD		EG12752	yhaM	

EG10367	gapA		EG12935	nfuA	5.20	EG12447	speG		EG12234	yhiR	3.60
EG12414	gatA		EG11078	nhaR		EG10966	spoT	23.40	EG11762	yibF	
EG12415	gatB		EG11519	nikR		EG10976	ssb		EG11192	yicC	7.32
EG12416	gatC		EG10660	nrdA		EG11600	sseA	2.98	EG11195	yidA	5.71
EG12417	gatD	24.50	EG11702	nudC		EG10977	sspA	4.71	EG11467	yigI	
EG12419	gatY		EG12926	nudE	8.88	EG11428	sthA		EG12473	yjeK	
EG12418	gatZ		EG12795	obgE	3.38	EG10979	sucA		EG12544	yjhB	
EG10372	gdhA		EG10677	oppD		EG10980	sucB		EG10021	yjiA	
EG13869	ghrA		EG11675	panB		EG10981	sucC	1.15	EG12579	yjiR	
EG12272	ghrB	1.49	EG11746	panC		EG10982	sucD		EG12586	yjiY	
EG11981	glf	1.93	EG10688	pck	1.08	EG10985	surA		EG12309	yjtD	
EG10379	glgC	10.57	EG11088	pdhR		EG10986	tag		EG13481	yliJ	
EG10380	glgP	16.01	EG10691	pdxA	2.95	EG11556	talB		EG13988	yniC	2.36
EG10381	glgX		EG10692	pdxB	0.89	EG13093	tas		EG13513	yoaA	
EG12957	glk		EG11487	pdxH		EG10993	tdh		EG14049	yodA	
EG11553	glmM	0.42	EG10694	pepA	0.78	EG10994	tdk	23.33	EG12024	yohK	
EG10382	glmS	1.71	EG10695	pepD	2.17	EG11884	tehB	6.95	EG14168	ypeA	
EG10383	glnA	2.81	EG10696	pepN	0.63	EG10995	tesB		EG13469	yphH	
EG10384	glnB	1.80	EG11549	pepT		EG10996	tgt	5.36	EG13097	yqeF	
EG11411	glnD		EG10699	pfkA	5.47	EG11574	thiB		EG12838	yrdA	
EG10390	glnS	2.13	EG10700	pfkB	7.05	EG11585	thiC	0.05	EG12878	zapA	
EG10402	gltA	5.59	EG10702	pgi		EG11586	thiE		EG11969	zntR	
									EG11929	zur	
									EG11221	zwf	7.31

Supplementary Table S5 DnaK interactors selected in the Pulse SILAC experiment

DnaK interactors identified above the background in the Pulse SILAC experiment of proteins to interact with DnaK as newly-synthesized or pre-existent proteins. High and low ratios correspond to strong tendency to interact as new and pre-existent proteins, respectively. The proteins are ordered from high to low ratios (Pulse M/L ratio).

EG	Gene Name	Pulse M/L ratio	EG	Protein Name	Pulse M/L ratio	EG	Gene Name	Pulse M/L ratio	EG	Protein Name	Pulse M/L ratio
EG13892	yecK	676.16	EG10317	fis	14.29	EG12111	nlpD	5.61	EG10939	secE	1.95
EG10866	rplC	391.74	EG10872	rplK	14.10	EG12316	acnB	5.48	EG11178	rbfA	1.93
EG10901	rpsB	267.07	EG10576	mdh	14.08	EG10158	clpP	5.36	EG10173	cydA	1.92
EG10913	rpsN	198.92	EG10710	pheT	14.04	EG10998	thrA	5.15	EG10245	dnaX	1.91
EG14263	folX	185.61	EG10455	skp	13.63	EG11385	ahpF	5.12	EG10433	hemX	1.81
EG10902	rpsC	119.21	EG10870	rplI	13.51	EG10533	lexA	5.10	EG10649	ndh	1.78

EG10906	rpsG	100.42	EG10895	rpoC	13.37	EG10451	hisI	4.91	EG10118	bioB	1.74
EG10755	ppa	89.05	EG11699	gpmA	13.00	EG10423	gyrA	4.76	EG12197	seqA	1.70
EG10903	rpsD	79.41	EG11314	purB	12.74	EG12434	htrG	4.60	EG10701	pflB	1.70
EG10552	lysS	78.54	EG11005	tnaA	12.42	EG10891	rpmG	4.44	EG11286	argE	1.68
EG10670	ompC	71.58	EG10489	icd	12.16	EG13406	cld	4.33	EG13173	queF	1.67
EG10867	rplD	68.53	EG12676	bamA	12.08	EG10791	purC	4.32	EG11527	narP	1.66
EG10908	rpsI	61.79	EG10079	aroG	11.46	EG10101	atpD	4.30	EG13478	rimO	1.63
EG11067	valS	61.76	EG10907	rpsH	11.35	EG11198	glmU	4.29	EG11478	tatA	1.62
EG10888	rpmD	54.74	EG10864	rplA	10.92	EG12296	gpmM	4.26	EG10597	minD	1.61
EG10845	rho	46.11	EG10316	lpxD	10.81	EG12690	rarA	4.15	EG10936	secA	1.60
EG10883	rplW	45.85	EG10797	purL	10.60	EG10859	rne	4.07	EG11306	lipA	1.58
EG10221	deoC	44.88	EG10360	fusA	10.57	EG10179	cyoB	4.03	EG11647	accA	1.55
EG11221	zwf	43.54	EG10596	minC	10.49	EG10103	atpF	4.01	EG11128	yciH	1.51
EG10105	atpH	39.81	EG10684	pal	10.43	EG12343	yjjK	3.93	EG11140	uvrY	1.50
EG10904	rpsE	39.37	EG10810	pyrG	10.36	EG13969	ydiJ	3.93	EG12130	hscA	1.49
EG11984	wbbJ	37.55	EG10532	leuS	10.34	EG10509	katE	3.89	EG11597	moaD	1.49
EG10912	rpsM	37.33	EG10873	rplL	10.30	EG10466	hupA	3.87	EG11415	dps	1.48
EG10589	metK	35.89	EG10157	clpB	10.26	EG11096	yajC	3.84	EG13357	tteA	1.47
EG10915	rpsP	35.69	EG10790	purA	10.18	EG12182	yajG	3.69	EG11060	ushA	1.47
EG11981	glf	35.01	EG10879	rplR	10.12	EG10192	cysK	3.67	EG10598	minE	1.47
EG11569	lptD	33.52	EG10457	hns	10.05	EG12095	secG	3.67	EG11183	damX	1.47
EG10436	hflK	32.39	EG10599	groL	9.87	EG11293	lolB	3.65	EG10529	lepA	1.45
EG10881	rplT	31.44	EG11985	wbbK	9.84	EG12419	gatY	3.42	EG10608	mreB	1.45
EG10878	rplQ	30.15	EG10025	aceF	9.77	EG13929	ydgH	3.40	EG12899	yheO	1.43
EG10893	rpoA	29.44	EG10403	gltB	9.68	EG10900	rpsA	3.38	EG10844	rhlB	1.37
EG11001	thrS	28.45	EG10282	fbaA	9.64	EG11197	yidC	3.38	EG11061	uvrA	1.35
EG11810	gcvP	27.84	EG10702	pgi	9.39	EG12447	speG	3.37	EG12683	uspG	1.34
EG14193	maeB	27.58	EG10420	guaA	9.32	EG10159	clpX	3.28	EG12855	yebG	1.34
EG10740	plsB	27.05	EG10707	pheA	9.02	EG12273	viaF	3.26	EG11473	ubiE	1.33
EG10094	asnS	26.39	EG11556	talB	8.88	EG10756	ppc	3.20	EG10223	deoR	1.33
EG10884	rplX	26.19	EG10618	mukB	8.61	EG10165	ctr	3.15	EG10156	clpA	1.31
EG10135	carB	25.56	EG10034	alaS	8.58	EG10766	secY	3.10	EG11534	ibpA	1.29
EG11009	tolC	25.36	EG12193	cbpA	8.52	EG11296	radA	3.09	EG10823	recA	1.27
EG10107	avtA	24.98	EG10899	rpoZ	8.20	EG10619	murC	3.09	EG10898	rpoN	1.23
EG10880	rplS	24.65	EG10871	rplJ	8.06	EG12597	yjjU	3.02	EG10505	infB	1.17
EG10953	sodA	23.97	EG12082	nuoA	8.06	EG13226	ftsK	3.02	EG12417	gatD	1.14
EG50001	rplU	23.87	EG10674	oppA	8.05	EG10201	dacA	2.93	EG12614	yhcB	1.13
EG10754	poxB	21.60	EG10238	dnaE	7.96	EG10461	htpG	2.91	EG10347	ftsZ	1.12
EG11358	murA	21.57	EG11160	mscS	7.77	EG10789	ptsI	2.89	EG50009	gadA	1.11
EG10868	rplE	21.42	EG14105	yfbU	7.65	EG10031	adhE	2.87	EG12418	gatZ	1.11
EG10890	rpmF	21.25	EG10801	putA	7.58	EG12341	rseA	2.82	EG11212	nsrR	1.10
EG10600	groS	21.23	EG10631	nadB	7.56	EG10264	entF	2.71	EG12263	bcse	1.10

EG12677	iscS	20.95	EG10542	lon	7.49	EG10798	purM	2.67	EG11116	yceA	1.10
EG10358	fumC	20.41	EG10905	rpsF	7.44	EG13249	ppiD	2.65	EG10510	rpoS	1.09
EG10096	aspC	19.60	EG10937	secB	7.40	EG10424	gyrB	2.63	EG10178	cyoA	1.08
EG10274	fabB	19.08	EG10885	rplY	7.30	EG13031	yqiC	2.62	EG11986	wbbL	1.05
EG12900	fkpA	18.96	EG10184	cysB	7.30	EG11504	metQ	2.57	EG10068	argG	1.04
EG10024	aceE	18.81	EG11427	tktA	7.27	EG10587	metH	2.56	EG12642	pdxK	1.03
EG10948	maeA	18.79	EG11384	ahpC	7.18	EG10170	cyaA	2.54	EG11305	tatE	1.02
EG10909	rpsJ	17.85	EG10203	dacC	7.01	EG10771	proV	2.52	EG10567	manX	0.99
EG10959	speA	17.75	EG10411	gnd	6.97	EG11529	ftsN	2.46	EG11281	mutL	0.94
EG10886	rpmB	17.53	EG20173	pta	6.95	EG14049	yodA	2.45	EG14322	tatB	0.91
EG10375	mmnG	17.23	EG10441	ihfB	6.90	EG14166	yfeY	2.42	EG40003	insC	0.86
EG10894	rpoB	16.44	EG11411	glnD	6.80	EG14033	cmoA	2.35	EG11413	holC	0.86
EG10882	rplV	16.40	EG10609	mreC	6.67	EG12295	yibN	2.34	EG10353	fucR	0.83
EG10408	glyA	16.32	EG10386	glnH	6.56	EG13657	miaB	2.32	EG10947	serS	0.83
EG10421	guaB	16.19	EG10098	atpA	6.48	EG11881	hslU	2.26	EG11747	panD	0.82
EG10979	sucA	16.08	EG12089	nuoI	6.48	EG10821	rcsB	2.16	EG13397	iscR	0.76
EG11013	topA	16.02	EG10435	hflC	6.30	EG10465	ribB	2.15	EG11490	gadB	0.69
EG10543	lpd	15.57	EG10367	gapA	6.17	EG12218	derB	2.14	EG10273	fabA	0.67
EG10380	glgP	15.32	EG10671	ompF	6.16	EG10743	pnp	2.09	EG10590	metL	0.66
EG11983	wbbI	15.27	EG10869	rplF	5.99	EG10462	htpX	2.06	EG13395	iscU	0.65
EG11033	tsf	15.11	EG10804	pykF	5.89	EG10243	dnaQ	2.03	EG10206	dapB	0.62
EG11003	tig	15.07	EG10931	sdhA	5.87	EG10217	accD	2.03	EG12382	fxsA	0.61
EG10669	ompA	14.91	EG10703	pgk	5.80	EG10562	malT	2.01	EG10275	accB	0.53
EG12524	yjgF	14.42	EG10944	serA	5.71	EG10092	asnB	1.99	EG10550	lysC	0.53
EG11008	tolB	14.39	EG12457	ydgA	5.61	EG10896	rpoD	1.96	EG11784	yfiD	0.43
									EG10258	eno	0.41
									EG11426	rfaZ	0.11

Supplementary Table S6 Half times of the DnaK-interactor interactions

Half time of the DnaK-interactor interaction was obtained for 91 proteins in a Pulse-chase SILAC experiment. The proteins are sorted from short to long half times. Rate constant, rate of the DnaK-interactor interaction release; $t_{1/2}$, half time of the DnaK-interactor interaction in minutes; The two groups of fast and slow releasing proteins selected for the analysis are highlighted in light orange and light red, respectively.

EG	Protein Name	Rate constant (min ⁻¹)	t _{1/2} (min)	Pulse M/L ratio	EG	Protein Name	Rate constant (min ⁻¹)	t _{1/2} (min)	Pulse M/L ratio
EG11009	tolC	1.329	0.521	1.40	EG10909	rpsJ	0.160	4.327	1.25
EG13892	ycgK	1.123	0.617	2.83	EG12418	gatZ	0.159	4.365	0.04
EG10906	rpsG	0.763	0.908	2.00	EG10869	rplF	0.149	4.637	0.78
EG10358	fumC	0.705	0.984	1.31	EG10230	dksA	0.142	4.870	

EG10671	ompF	0.643	1.077	0.79	EG12664	flgM	0.141	4.911	
EG10897	rpoH	0.616	1.125		EG10270	era	0.133	5.217	
EG10670	ompC	0.590	1.174	1.85	EG10135	carB	0.129	5.385	1.41
EG12130	hscA	0.494	1.404	0.17	EG10101	atpD	0.118	5.888	0.63
EG10879	rplR	0.490	1.413	1.01	EG10953	sodA	0.108	6.442	1.38
EG10899	rpoZ	0.467	1.485	0.91	EG10367	gapA	0.103	6.736	0.79
EG10866	rplC	0.444	1.560	2.59	EG10872	rplK	0.103	6.744	1.15
EG10596	minC	0.434	1.599	1.02	EG11198	glmU	0.101	6.833	0.63
EG10273	fabA	0.418	1.657	-0.17	EG10461	htpG	0.097	7.131	0.46
EG13031	yqiC	0.396	1.750	0.42	EG11178	rbfA	0.096	7.195	0.29
EG12111	nlpD	0.354	1.957	0.75	EG11415	dps	0.092	7.528	0.17
EG10631	nadB	0.343	2.022	0.88	EG10771	proV	0.091	7.640	0.40
EG10905	rpsF	0.332	2.086	0.87	EG11005	tnaA	0.089	7.779	1.09
EG12457	ydgA	0.312	2.218	0.75	EG10024	aceE	0.088	7.894	1.27
EG12524	yjgF	0.307	2.257	1.16	EG10098	atpA	0.086	8.104	0.81
EG10884	rplX	0.293	2.365	1.42	EG11505	holE	0.082	8.419	
EG10275	accB	0.289	2.401	-0.28	EG10544	lpp	0.076	9.100	
EG10316	lpxD	0.288	2.404	1.03	EG12336	yaeH	0.076	9.147	
EG10543	lpd	0.287	2.419	1.19	EG10871	rplJ	0.074	9.398	0.91
EG12642	pdxK	0.285	2.429	0.01	EG40008	insH	0.074	9.417	
EG10908	rpsI	0.282	2.462	1.79	EG10466	hupA	0.068	10.199	0.59
EG10465	ribB	0.279	2.485	0.33	EG10165	crr	0.060	11.553	0.50
EG13937	rsxG	0.276	2.515		EG13478	rimO	0.058	11.902	0.21
EG10192	cysK	0.274	2.533	0.57	EG10031	adhE	0.057	12.124	0.46
EG11358	murA	0.262	2.648	1.33	EG10811	pyrI	0.057	12.241	
EG10913	rpsN	0.261	2.652	2.30	EG10867	rplD	0.055	12.681	1.84
EG12624	yiaG	0.250	2.769		EG14322	tatB	0.053	13.005	-0.04
EG10282	fbaA	0.245	2.832	0.98	EG14049	yodA	0.053	13.030	0.39
EG11504	metQ	0.242	2.867	0.41	EG11534	ibpA	0.053	13.085	0.11
EG12083	nuoB	0.237	2.925		EG10599	groL	0.050	13.860	0.99
EG10797	purL	0.236	2.942	1.03	EG10937	secB	0.048	14.305	0.87
EG10667	nusG	0.224	3.094		EG11306	lipA	0.048	14.307	0.20
EG10274	fabB	0.222	3.127	1.28	EG10386	glnH	0.035	19.899	0.82
EG50001	rplU	0.220	3.156	1.38	EG10243	dnaQ	0.034	20.183	0.31
EG10158	clpP	0.213	3.257	0.73	EG40003	insC	0.034	20.214	-0.07
EG10506	infC	0.212	3.261		EG10068	argG	0.033	20.738	0.02
EG10873	rplL	0.205	3.376	1.01	EG11747	panD	0.033	20.962	-0.09
EG10236	dnaB	0.195	3.553		EG10731	phoP	0.031	22.029	
EG10893	rpoA	0.195	3.560	1.47	EG10703	pgk	0.031	22.554	0.76
EG11738	rsd	0.173	4.011		EG10567	manX	0.029	24.241	0.00
EG12319	can	0.169	4.098		EG10587	metH	0.028	24.422	0.41
EG10669	ompA	0.163	4.248	1.17					

Supplementary Table S7 Additional DnaK interactors identified upon Trigger factor deletion

Additional interactors pulled down upon the deletion of TF are sorted according to their enrichment above the background binding (PD/BG ratio). PD/BG ratio, enrichment of the DnaK-interactors above the background.

EG	Gene Name	PD/BG ratio	EG	Gene Name	PD/BG ratio	EG	Gene Name	PD/BG ratio	EG	Gene Name	PD/BG ratio
EG12813	yhcG	46.31	EG13079	bglA	10.00	EG12414	gatA	7.99	EG10793	purE	5.13
EG50009	gadA	41.10	EG13093	tas	10.00	EG12682	erfK	7.97	EG11160	mscS	5.10
EG10478	hycE	33.41	EG13156	dgsA	10.00	EG13085	mltA	7.93	EG10903	rpsD	5.07
EG12449	prmB	27.02	EG13171	truC	10.00	EG10916	rpsQ	7.92	EG12838	yrdA	5.06
EG12693	nudL	20.92	EG13292	mhpE	10.00	EG10788	ptsH	7.88	EG10740	plsB	4.95
EG12417	gatD	20.01	EG13418	csiE	10.00	EG13849	ynfK	7.85	EG10237	dnaC	4.94
EG11153	rimM	18.57	EG13451	caiF	10.00	EG10494	ilvB	7.81	EG11411	glnD	4.91
EG13247	ybaS	16.55	EG13493	yeaG	10.00	EG11443	rpiA	7.79	EG10491	iclR	4.89
EG12329	hrpB	16.28	EG13691	hcr	10.00	EG12240	mdtE	7.77	EG10758	ppiB	4.86
EG13377	mtfA	15.68	EG13851	cusR	10.00	EG11096	yajC	7.76	EG11548	lhr	4.83
EG11100	ybaB	14.66	EG13963	sufD	10.00	EG11810	gevP	7.72	EG10292	fecR	4.77
EG10957	soxR	14.63	EG14045	yedW	10.00	EG11801	hybC	7.72	EG11083	hepA	4.77
EG10459	hsdR	14.44	EG14066	yegW	10.00	EG10335	frf	7.72	EG13434	yefP	4.71
EG12362	menF	14.39	EG14102	yfbR	10.00	EG10648	narZ	7.70	EG14091	arnA	4.71
EG14201	hda	14.27	EG20098	hpt	10.00	EG10453	hisS	7.68	EG10896	rpoD	4.60
EG13766	prf	13.62	EG50007	eutC	10.00	EG13216	cof	7.60	EG12516	ytfP	4.60
EG10371	gcvH	12.73	EG10290	fecE	10.00	EG10998	thrA	7.54	EG10636	nagC	4.55
EG10458	hsdM	12.64	EG10592	mglA	10.00	EG11414	holD	7.50	EG10586	metG	4.55
EG11966	adiY	12.35	EG10939	secE	10.00	EG10510	rpoS	7.38	EG10500	ilvI	4.54
EG10334	fre	12.31	EG10968	sppA	10.00	EG11620	rnv	7.36	EG10845	rho	4.53
EG12717	mug	12.21	EG11506	ftsH	10.00	EG11495	hdeD	7.29	EG13120	queD	4.53
EG11413	holC	12.15	EG11624	artP	10.00	EG12779	yraN	7.22	EG10327	folC	4.50
EG10826	recD	11.72	EG11703	acrA	10.00	EG13015	dkgA	7.20	EG10027	ackA	4.42
EG13420	ydhF	11.41	EG12041	yejF	10.00	EG12860	yebK	7.11	EG11544	gadE	4.41
EG14233	cusC	11.09	EG12115	yjjG	10.00	EG10213	ddlA	7.06	EG10570	map	4.41
EG11797	talA	10.99	EG12217	yhhQ	10.00	EG10695	pepD	6.96	EG11023	trmD	4.40
EG11969	zntR	10.94	EG12801	yrbF	10.00	EG12452	rspB	6.95	EG11036	tufA	4.39
EG11492	qorA	10.83	EG13654	ybeX	10.00	EG10828	recF	6.95	EG13870	yedX	4.35
EG12672	tpx	10.70	EG13897	emtA	10.00	EG10486	hypD	6.94	EG10936	secA	4.34
EG13006	hybO	10.55	EG10321	fliC	10.00	EG12224	yhiI	6.90	EG10886	rpmB	4.33
EG11317	fabD	10.52	EG11502	rcsF	10.00	EG11458	rffM	6.87	EG10682	pabA	4.33

EG11731	ravA	10.41	EG12875	ybhC	10.00	EG10039	amn	6.87	EG11019	trkA	4.28
EG11191	slmA	10.40	EG11008	tolB	10.00	EG10423	gyrA	6.82	EG11619	mfd	4.28
EG11088	pdhR	10.26	EG11735	efeB	10.00	EG10173	cydA	6.81	EG13672	ybhP	4.25
EG13223	yaeQ	10.24	EG12781	yraP	10.00	EG11449	hdfR	6.78	EG11650	yafD	4.25
EG10812	queA	10.23	EG14015	ynhG	10.00	EG12454	ybaK	6.68	EG11341	rfaQ	4.24
EG10102	atpE	10.19	EG10520	waaA	10.00	EG11322	ribE	6.64	EG13968	ydiI	4.24
EG10083	aroM	10.00	EG10955	sohA	10.00	EG12120	rssA	6.62	EG10562	malT	4.16
EG10095	aspA	10.00	EG11097	yajD	10.00	EG10993	tdh	6.60	EG10329	mutM	4.16
EG10113	bfr	10.00	EG11158	ygfA	10.00	EG11305	tatE	6.60	EG11037	tufB	4.14
EG10166	cspA	10.00	EG11183	damX	10.00	EG12045	yejH	6.60	EG10851	rimJ	4.03
EG10256	eda	10.00	EG11199	mioC	10.00	EG11350	rfaS	6.60	EG13688	ybjS	4.02
EG10361	gabT	10.00	EG11659	yedD	10.00	EG10215	deaD	6.56	EG13616	allR	3.97
EG10379	glgC	10.00	EG11684	yieH	10.00	EG12902	kefG	6.55	EG10375	mnmG	3.96
EG10400	glpR	10.00	EG11823	amiA	10.00	EG14149	ypdB	6.54	EG10625	mutS	3.91
EG10422	guaC	10.00	EG11855	yiiF	10.00	EG11721	yidZ	6.53	EG11025	trpB	3.91
EG10482	zraR	10.00	EG11936	yjbR	10.00	EG14068	thiD	6.53	EG12295	yibN	3.85
EG10519	kdsB	10.00	EG12042	yejG	10.00	EG11068	vsr	6.52	EG13289	yqgE	3.81
EG10620	murD	10.00	EG12411	rfbD	10.00	EG11363	amiB	6.32	EG11677	modF	3.80
EG10693	pdxJ	10.00	EG12554	sgcA	10.00	EG12595	fhuF	6.32	EG10882	rplV	3.76
EG10700	ptkB	10.00	EG12742	yqjC	10.00	EG10542	lon	6.31	EG10762	prfB	3.74
EG10743	pnp	10.00	EG12844	yefM	10.00	EG10170	cyaA	6.25	EG10276	accC	3.73
EG10839	rfaH	10.00	EG13023	mqsR	10.00	EG11985	wbbK	6.12	EG10044	osmE	3.72
EG10890	rpmF	10.00	EG13231	pgl	10.00	EG11722	yieE	6.08	EG12146	yhbJ	3.71
EG10898	rpoN	10.00	EG13319	rlmF	10.00	EG13183	ydbK	6.06	EG11407	dadA	3.71
EG10941	selA	10.00	EG13360	racR	10.00	EG10384	glnB	6.05	EG10774	prs	3.65
EG10962	speD	10.00	EG13703	ycbK	10.00	EG12320	yadG	6.05	EG12100	tktB	3.65
EG11002	thyA	10.00	EG14171	eutL	10.00	EG12459	rpiR	6.05	EG11428	sthA	3.64
EG11005	tnaA	10.00	EG14195	ypfH	10.00	EG12932	yhgF	6.02	EG11333	visC	3.59
EG11032	trxB	10.00	EG10558	malK	10.00	EG12944	yhhX	5.98	EG10966	spoT	3.54
EG11042	tyrR	10.00	EG11774	nuoF	10.00	EG11409	lpxK	5.93	EG10688	pck	3.53
EG11062	uvrB	10.00	EG13506	yeaT	10.00	EG12243	gadX	5.88	EG13110	ispD	3.53
EG11081	ispH	10.00	EG10105	atpH	9.76	EG10424	gyrB	5.81	EG11352	rfal	3.51
EG11218	creB	10.00	EG11890	slp	9.73	EG13391	yeeX	5.81	EG10649	ndh	3.44
EG11328	fdx	10.00	EG11060	ushA	9.72	EG11069	xerC	5.79	EG11121	yciA	3.43
EG11329	gabD	10.00	EG11552	hydN	9.61	EG10135	carB	5.78	EG12491	ulaR	3.39
EG11368	menB	10.00	EG10907	rpsH	9.59	EG12784	yhbO	5.76	EG10063	argA	3.30
EG11408	dadX	10.00	EG12798	yrbC	9.54	EG10618	mukB	5.63	EG10910	rpsK	3.27
EG11418	dcd	10.00	EG10447	hisD	9.51	EG14263	folX	5.62	EG10639	narH	3.26
EG11500	holB	10.00	EG10444	hisA	9.47	EG10211	dcm	5.60	EG12882	gsp	3.24
EG11517	glpX	10.00	EG13793	yddV	9.42	EG10079	aroG	5.60	EG11913	yijO	3.21
EG11530	fadD	10.00	EG12121	rssB	9.36	EG12309	yjtD	5.59	EG11357	dinG	3.14
EG11576	leuC	10.00	EG14038	dcyD	9.19	EG10339	ftsA	5.49	EG10913	rpsN	3.08

EG11578	greB	10.00	EG10759	pps	9.18	EG12110	ydcF	5.49	EG10619	murC	3.07
EG11751	otsA	10.00	EG12303	ycfH	9.10	EG11615	basR	5.43	EG10865	rplB	3.03
EG11932	dusA	10.00	EG11188	htrL	8.75	EG20151	nfsB	5.43	EG10911	rpsL	3.01
EG12098	rhuD	10.00	EG10633	nagB	8.66	EG40005	insE	5.43	EG11849	yihW	3.00
EG12114	prfC	10.00	EG10436	hflK	8.65	EG10566	manA	5.41	EG10382	glmS	2.89
EG12165	mukF	10.00	EG10796	purK	8.56	EG12904	yheT	5.41	EG11423	waaU	2.89
EG12184	nudF	10.00	EG12815	nanK	8.53	EG11353	rfaJ	5.41	EG11426	rfaZ	2.81
EG12245	treF	10.00	EG13492	mipA	8.52	EG10658	bamC	5.36	EG10917	rpsR	2.79
EG12307	mgsA	10.00	EG10817	rbsD	8.22	EG10901	rpsB	5.34	EG14033	cmoA	2.72
EG12531	yjgL	10.00	EG12078	nikD	8.18	EG10376	rsmG	5.32	EG10875	rplN	2.67
EG12669	solA	10.00	EG12840	rimN	8.17	EG13905	yciT	5.32	EG11819	purU	2.66
EG12794	yhbY	10.00	EG11983	wbbI	8.16	EG12622	adhP	5.24	EG11071	xerD	2.63
EG12807	yrbL	10.00	EG11606	kch	8.10	EG10380	glgP	5.24	EG10623	murG	2.58
EG12982	rdgB	10.00	EG10511	katG	8.08	EG10942	selB	5.20	EG50002	rpmA	2.57
EG13014	yqhD	10.00	EG10557	mall	8.07	EG10235	dnaA	5.18	EG10426	helD	2.53
EG13019	ygiQ	10.00	EG12399	dhaM	8.05	EG10283	fbp	5.16	EG12579	yjiR	2.39
									EG10621	murE	2.11

Supplementary Table S8 74 interactors are significantly decreased on DnaK upon the deletion of Trigger factor

Substrates significantly decreased on DnaK upon the deletion of Trigger factor are ordered alphabetically according to gene name. MW, molecular weight in kDa; pI, Isoelectric point; SP, signal peptide prediction by TargetP; E, essentiality;

EG	Gene Name	MW (kDa)	pI	SP	E	Fold change	EG	Gene Name	MW (kDa)	pI	SP	E	Fold change
EG10032	adk	23.5	5.76		E	0.79	EG10670	ompC	40.3	4.81	S		0.75
EG10061	arcA	27.2	5.32			0.68	EG10671	ompF	39.3	4.95	S		0.22
EG10068	argG	49.8	5.39			0.64	EG10673	ompT	35.5	6.05	S		0.68
EG12474	blc	19.8	8.76	S		0.64	EG11124	ompW	22.9	6.53	S		0.58
EG10130	btuR	21.9	6.54		E	0.21	EG11885	opgG	57.9	7.21	S		0.24
EG12319	can	25	6.65		E	0.80	EG10674	oppA	60.9	6.49	S		0.33
EG13443	cobB	31.4	7.93			0.72	EG10770	proS	63.6	5.24		E	0.71
EG10174	cydB	42.4	7.4	S	E	0.74	EG10828	recF	40.5	7.26			0.78
EG10248	dppA	60.2	6.65	S		0.19	EG10830	recJ	63.3	5.6			0.69
EG10260	entB	32.5	5.25			0.60	EG10831	recN	61.3	5.59			0.78
EG12606	fabF	43	6.09			0.78	EG10844	rhIB	47.1	7.68			0.80
EG11857	fdoH	33.1	5.32			0.73	EG11321	ribD	40.3	7.59		E	0.64
EG10300	ffh	49.7	9.51		E	0.61	EG10893	rpoA	36.5	5.06			0.41
EG10330	frdA	65.9	6.28			0.87	EG10894	rpoB	150.6	5.26		E	0.86

EG13226	ftsK	146.6	5.02			0.70	EG10895	rpoC	155.1	7.08		E	0.82
EG12419	gatY	30.8	6.34			0.49	EG11897	rpoE	21.6	5.49			0.59
EG10372	gdhA	48.5	6.4			0.80	EG10946	serC	39.7	5.59			0.78
EG10386	glnH	27.1	8.52	S		0.54	EG10961	speC	79.4	6.05			0.53
EG10389	glnQ	26.7	6.54			0.88	EG11000	thrC	47.1	5.41			0.54
EG14132	gtrB	34.6	8.16			0.79	EG11001	thrS	74	6.19		E	0.77
EG10422	guaC	37.3	6.54			0.52	EG12100	tktB	73	6.29			0.81
EG10428	hemB	35.6	5.39		E	0.24	EG11009	tolC	53.7	5.65	S		0.40
EG10456	hmp	43.8	5.76			0.77	EG11837	typA	67.3	5.33			0.86
EG40012	insL	40.9	8.53			0.71	EG11061	uvrA	103.8	6.64			0.73
EG12253	kdgK	33.9	5.03			0.75	EG11984	wbbJ	21.6	9.14			0.70
EG10532	leuS	97.2	5.3		E	0.75	EG11540	wrbA	20.8	5.86			0.88
EG10542	lon	87.4	6.39			0.65	EG13148	yafK	28	9.06	S		0.72
EG13690	ltaE	36.4	6.19			0.74	EG11241	ycaC	23.1	5.41		E	0.78
EG10552	lysS	57.6	5.24			0.70	EG12457	ydgA	54.6	5.17	S	E	0.50
EG10574	mcrB	53.1	5.6			0.74	EG13931	ydgJ	38.2	5.78			0.68
EG10589	metK	41.9	5.26		E	0.73	EG12347	yecC	27.6	8.93			0.83
EG11160	mscS	30.8	8.33	S		0.87	EG13385	yeeR	57.2	6.12	S		0.07
EG11358	murA	44.8	6.16			0.85	EG14199	yfgC	53.9	7.68	S		0.59
EG10649	ndh	47.3	8.85			0.78	EG11785	yfiE	33.2	6.77			0.85
EG12083	nuoB	25	5.75			0.57	EG12752	yhaM	45.3	5.33			0.84
EG12084	nuoC	68.2	6.42			0.73	EG12903	yheS	71.8	5.73			0.70
EG10669	ompA	37.2	6.42	S		0.50	EG12597	yjiU	39.8	8.49			0.58

Supplementary Table S9 71 interactors are significantly increased on DnaK upon the deletion of Trigger factor

Substrates significantly increased on DnaK upon the deletion of Trigger factor are ordered alphabetically according to gene name. MW, molecular weight in kDa; pI, Isoelectric point; SP, signal peptide prediction by TargetP; E, essentiality;

EG	Gene Name	MW (kDa)	pI	SP	E	Fold change	EG	Gene Name	MW (kDa)	pI	SP	E	Fold change
EG12867	ampH	41.8	9.52	S		2.13	EG10875	rplN	13.5	10.42		E	2.73
EG10135	carB	117.8	5.34	S		1.65	EG10879	rplR	12.7	10.42		E	1.82
EG11092	crI	15.6	6.78			1.44	EG10883	rplW	11.2	9.94		E	1.69
EG12739	exuR	29.8	5.63			2.06	EG10885	rplY	10.6	9.6		E	1.62
EG11318	fabG	25.5	7.41		E	1.62	EG10886	rpmB	9	11.42			1.59
EG11528	fabI	27.8	5.87		E	3.28	EG10888	rpmD	6.5	10.96			2.08
EG12686	flu	106.8	6.2			1.67	EG10890	rpmF	6.4	11.03			1.95
EG12414	gatA	16.9	5.28			1.62	EG10904	rpsE	17.6	10.11		E	1.47
EG12417	gatD	37.3	6.38		E	2.72	EG10906	rpsG	20	10.37			1.58

EG11198	glmU	49.1	6.54		E	1.51	EG10907	rpsH	14.1	9.42		E	1.95
EG11699	gpmA	28.5	6.18			1.72	EG10910	rpsK	13.8	11.33			2.09
EG11398	hdeA	11.8	5.25	S		2.70	EG10916	rpsQ	9.7	9.6		E	1.52
EG11485	hemG	21.2	9.67		E	1.62	EG10919	rpsT	9.6	11.18		E	1.80
EG10434	hemY	45.2	8.53	S		2.12	EG13937	rsxG	21.9	7.11	S		1.87
EG12930	hslO	32.5	4.49			1.45	EG11094	sbcD	44.7	5.89			1.41
EG10467	hupB	9.2	9.7			1.86	EG10455	skp	17.6	9.7	S		1.48
EG40003	insC	13.4	9.52			1.66	EG13409	slyB	15.6	9.3	S		1.69
EG11409	lpxK	35.5	8.54	S	E	1.99	EG10982	sucD	29.7	6.78			1.51
EG12712	luxS	19.4	5.36			1.42	EG11246	uspE	35.7	5.32			1.65
EG10567	manX	35	6.02			1.68	EG12674	uspF	16	5.96			1.67
EG10597	minD	29.6	5.37		E	1.46	EG12336	yaeh	15	7.19			1.65
EG10329	mutM	30.2	8.43			1.93	EG12851	ybeL	18.7	5.2			1.79
EG10639	narH	58	6.78			2.44	EG13716	ycbX	40.6	7.64			1.82
EG11391	osmY	21	6.82	S		2.68	EG13892	yegK	14.9	9.5	S		3.21
EG10684	pal	18.8	6.79	S		1.63	EG11128	yehH	11.3	9.29			1.62
EG10707	pheA	43.1	6.69			1.42	EG11132	ydiA	31.2	6.43			2.00
EG10771	proV	44.1	5.56			1.74	EG13022	ygiT	14.7	8.92		E	1.49
EG11314	purB	51.5	6.02			1.63	EG12784	yhbO	18.8	5.46			1.91
EG10803	pykA	51.3	6.68			2.30	EG12624	yiaG	11	8.16			1.96
EG11425	rfaY	27.4	9.68			1.67	EG11835	yihI	19	6.83			1.62
EG12207	rlmA	30.4	7.27			1.49	EG11913	yijO	32.1	8.25			1.56
EG10866	rplC	22.2	9.91		E	1.78	EG12171	yjil	58	6.09			1.53
EG10869	rplF	18.9	9.7		E	1.67	EG12779	yraN	14.7	9.86			1.84
EG10870	rplI	15.7	6.57			1.93	EG12838	yrdA	20.2	5.55			1.43
EG10873	rplL	12.2	4.65	S	E	1.52	EG12841	yrdD	19.8	8.19			1.58
							EG11969	zntR	16.1	6.38			1.51

Supplementary Table S10 40 proteins are significantly decreased in Trigger factor deleted cells

Significantly ($p < 0.05$) decreased proteins in the $\Delta T/K_{His}$ proteome compared to WT, ordered according to fold change from low to high. MW, molecular weight in kDa; pI, Isoelectric point; SP, signal peptide prediction by TargetP; E, essentiality;

EG	Gene Name	MW (kDa)	pI	SP	E	Fold change	EG	Gene Name	MW (kDa)	pI	SP	E	Fold change
EG10653	nirB	93.1	6.2			0.16	EG10174	cydB	42.4	7.4	S	E	0.64
EG10502	ilvN	11.1	6.1			0.19	EG13929	ydgH	33.9	9.3	S		0.64
EG10351	fucO	40.6	5.3			0.29	EG10670	ompC	40.3	4.8	S		0.64
EG12434	htrG	23	9.1	S		0.35	EG12532	yjgM	18.6	5.3			0.65

EG10463	degP	49.3	8.6	S		0.42	EG11035	tsx	33.5	5.3	S		0.67
EG12900	fkpA	28.8	8.5	S		0.43	EG14222	bamD	27.8	6.6	S		0.67
EG11291	yggG	26.8	6.1	S		0.48	EG12015	pbpG	33.8	9.9	S		0.68
EG14276	vacJ	28	5.1	S		0.49	EG13490	spy	18.2	9.7	S		0.68
EG10858	rnd	42.7	5.3			0.49	EG11914	yijP	66.6	7.4	S		0.69
EG10386	glnH	27.1	8.5	S		0.52	EG10389	glnQ	26.7	6.5			0.69
EG14199	yfgC	53.9	7.7	S		0.53	EG10362	galE	37.2	6.4			0.69
EG14166	yfeY	20.8	5.4	S		0.54	EG10173	cydA	58.2	6.8	S	E	0.70
EG14007	ynjE	48.2	6.7	S		0.58	EG12781	yraP	20	9	S		0.70
EG12676	bamA	90.5	5.1	S	E	0.58	EG12994	yghJ	164.8	5	S		0.70
EG10669	ompA	37.2	6.4	S		0.60	EG11011	tolR	15.3	5.6	S		0.72
EG11699	gpmA	28.5	6.2			0.61	EG12684	lolA	22.4	6.4	S		0.73
EG11009	tolC	53.7	5.7	S		0.61	EG11576	leuC	49.8	6.3			0.73
EG12705	yggN	26.4	8.9	S		0.61	EG10369	gcd	86.7	5.6	S		0.73
EG12254	yhjJ	55.5	6	S		0.62	EG11010	tolQ	25.5	7.1	S		0.74
EG12457	ydgA	54.6	5.2	S	E	0.63	EG10674	oppA	60.9	6.5	S		0.75

Supplementary Table S11 27 proteins are significantly increased in Trigger factor deleted cells

Significantly ($p < 0.05$) decreased proteins in the $\Delta T/K_{His}$ proteome compared to WT, ordered according to fold change from high to low. MW, molecular weight in kDa; pI, Isoelectric point; SP, signal peptide prediction by TargetP; E, essentiality;

EG	Gene Name	MW (kDa)	pI	SP	E	Fold change
EG13476	yliE	90	5.79	S		62.74
EG10771	proV	44.1	5.56			4.64
EG10927	sbcC	118.7	5.69			2.25
EG12686	flu	106.8	6.2			2.04
EG10158	clpP	23.1	5.8			1.88
EG10510	rpoS	37.9	4.95			1.78
EG13111	ftsB	11.6	7.26	S	E	1.70
EG10159	clpX	46.3	5.36			1.53
EG10936	secA	102	5.61		E	1.47
EG11534	ibpA	15.7	5.83			1.40
EG12419	gatY	30.8	6.34			1.40
EG10022	aceA	47.5	5.31			1.38
EG10241	dnaK	69.1	4.97		E	1.37

EG10240	dnaJ	41.1	7.84			1.31
EG10461	htpG	71.4	5.22			1.28
EG10600	groS	10.3	5.23		E	1.28
EG10599	groL	57.3	4.94		E	1.27
EG11797	talA	35.6	6.26			1.26
EG11881	hslU	49.5	5.34			1.26
EG10416	grpE	21.7	4.75		E	1.24
EG10157	clpB	95.5	5.52			1.24
EG10542	lon	87.4	6.39			1.23
EG11441	prlC	77.1	5.27			1.22
EG13656	ybeZ	39	5.97			1.21
EG10544	lpp	8.3	9.25	S		1.20
EG10731	phoP	25.5	5.26			1.17
EG10156	clpA	84.2	6.31			1.14

Supplementary Table S12 92 interactors are significantly increased on DnaK upon the deletion of GroEL

Substrates significantly increased on DnaK upon the deletion of GroEL are ordered alphabetically according to gene name. MW, molecular weight in kDa; pI, Isoelectric point; E, essentiality;

EG	Gene Name	MW (kDa)	pI	E	Fold change	EG	Gene Name	MW (kDa)	pI	E	Fold change
EG10056	araE	51.6	9.35		5.40	EG10710	pheT	87.3	5.3		2.86
EG10058	araG	55	6.37	E	2.44	EG10741	pmbA	48.3	5.61		7.21
EG11286	argE	42.3	5.9		1.75	EG13249	ppiD	68.1	5.08		3.11
EG10088	asd	40	5.58	E	48.65	EG12365	prkB	32.3	6.66		8.35
EG11407	dadA	47.6	6.62	E	1.72	EG10777	pspB	8.7	7.43		40.07
EG10205	dapA	31.2	6.44	E	3.64	EG10797	purL	141.4	5.42		7.35
EG10219	deoA	47.2	5.38		28.02	EG10806	pyrC	38.8	6.19		6.11
EG10238	dnaE	129.9	5.31	E	3.53	EG11492	qorA	35.1	8.31		5.29
EG10248	dppA	60.2	6.65		3.18	EG10815	rbsB	30.9	7.47		3.55
EG11415	dps	18.6	6.11		3.22	EG11979	rfbC	21.2	5.79		6.86
EG12606	fabF	43	6.09		21.16	EG10867	rplD	22	9.73	E	2.49
EG14062	fbaB	38.1	6.73		4.93	EG10875	rplN	13.5	10.42	E	1.98
EG12900	fkpA	28.8	8.47		2.05	EG10877	rplP	15.2	11.23		2.34
EG50011	folP	30.6	6.03		6.94	EG10883	rplW	11.2	9.94	E	4.53

EG10330	frdA	65.9	6.28		14.62	EG10884	rplX	11.3	10.21	E	3.89
EG12417	gatD	37.3	6.38	E	3.61	EG10897	rpoH	32.4	5.93	E	2.37
EG12419	gatY	30.8	6.34		4.77	EG10908	rpsI	14.8	10.94	E	4.28
EG10372	gdhA	48.5	6.4		2.68	EG10919	rpsT	9.6	11.18	E	1.73
EG10402	gltA	48	6.69		5.89	EG10932	sdhB	26.7	6.73		9.99
EG10428	hemB	35.6	5.39	E	9.85	EG10946	serC	39.7	5.59		18.92
EG10462	htpX	31.9	7.13		2.21	EG10455	skp	17.6	9.7		2.13
EG12434	htrG	23	9.11		2.19	EG10982	sucD	29.7	6.78		5.16
EG10370	ispG	40.6	6.22	E	12.57	EG14068	thiD	28.6	6.15		2.01
EG10518	kdsA	30.8	6.8		3.92	EG11589	thiG	26.8	5.57		11.56
EG14240	kefA	127.2	8.03		8.62	EG12826	tldD	51.3	4.96		19.20
EG11226	leuA	57.2	5.72		40.48	EG11009	tolC	53.7	5.65		2.13
EG10536	livF	26.3	5.88		5.68	EG12133	ucpA	27.8	5.27		15.73
EG12123	lrhA	34.5	5.54		2.77	EG12497	ulaE	32	5.32		3.40
EG13805	lsrR	33.7	6.69		8.14	EG12498	ulaF	25.2	6.66		5.37
EG10554	malE	43.3	5.7		4.76	EG12683	uspG	15.9	6.52		2.49
EG10559	malM	31.9	8.02		6.10	EG11650	yafD	29.9	9.6		3.27
EG10589	metK	41.9	5.26	E	18.54	EG11108	ybgA	20.2	9.56		2.45
EG10592	mglA	56.4	7.64		2.53	EG13892	ycgK	14.9	9.5		2.55
EG13625	mhpF	33.4	5.52		3.75	EG12967	yciO	23.2	6.35		3.95
EG10375	mmmG	69.5	6.63		11.36	EG13420	ydhF	33.6	6.18		8.22
EG11828	mobB	19.3	5.59		2.16	EG12041	yejF	58.7	9.01		61.83
EG12717	mug	18.6	9.08		12.87	EG14101	yfbQ	45.5	6.26		7.27
EG10648	narZ	140.2	6.67		4.86	EG11786	yfiF	37.7	8.78		3.17
EG12083	nuoB	25	5.75		5.55	EG12373	ygdH	50.9	6.48		3.94
EG12084	nuoC	68.2	6.42		29.34	EG13022	ygiT	14.7	8.92	E	2.26
EG12087	nuoG	100.3	6.25		4.58	EG12298	yibQ	35.3	9.62		2.21
EG12089	nuoI	20.5	5.48		7.28	EG12471	yjeI	11.9	5.77		2.26
EG10670	ompC	40.3	4.81		2.20	EG11436	yjgB	36.5	6.28		2.87
EG10674	oppA	60.9	6.49		3.05	EG13775	yncE	38.6	9.23	E	3.22
EG10677	oppD	37.1	6.1	E	2.46	EG12777	yraL	31.3	6.23		2.29
EG10698	pepQ	50.1	5.98		16.22	EG12678	znuA	33.7	5.98		1.68

Supplementary Table S13 54 interactors are significantly decreased on DnaK upon the deletion of GroEL

Substrates significantly decreased on DnaK upon the deletion of GroEL are ordered alphabetically according to gene name. MW, molecular weight in kDa; pI, Isoelectric point; E, essentiality;

EG	Gene Name	MW (kDa)	pI	E	Fold change	EG	Gene Name	MW (kDa)	pI	E	Fold change
EG10052	araA	56	6.6		0.46	EG10688	pck	59.6	5.7		0.36

EG10053	araB	61	5.4		0.71	EG10709	pheS	36.8	6.2		0.21
EG10054	araC	33.3	7		0.11	EG10752	potD	38.8	5.4	E	0.38
EG10055	araD	25.5	6.2		0.07	EG10770	proS	63.6	5.2	E	0.67
EG10095	aspA	52.3	5.3		0.43	EG10783	pstB	29	6.6		0.44
EG10103	atpF	17.2	6.2	E	0.57	EG10844	rhlB	47.1	7.7		0.64
EG10121	bioF	41.5	7.1		0.02	EG10869	rplF	18.9	9.7	E	0.70
EG12335	cdaR	43.6	6.8		0.03	EG10930	sdaA	48.9	5.3		0.04
EG10231	dld	64.6	6.7		0.55	EG10947	serS	48.4	5.5	E	0.44
EG10260	entB	32.5	5.3		0.39	EG10953	sodA	23	7		0.21
EG12686	flu	106.8	6.2		0.73	EG10954	sodB	21.2	5.9		0.44
EG10356	fumA	60.2	6.6		0.61	EG10981	sucC	41.3	5.5		0.23
EG50009	gadA	52.6	5.4		0.23	EG10989	tdcA	34.5	5.5		0.16
EG10379	glgC	48.6	6.1		0.23	EG10990	tdcB	35.2	6.1		0.11
EG10386	glnH	27.1	8.5		0.74	EG11333	visC	44.2	7.3		0.44
EG10409	glyQ	34.7	5	E	0.41	EG12855	ycbG	17.6	9.5		0.47
EG12181	grxD	12.8	4.8	E	0.54	EG13104	ygbJ	30.7	5.3		0.15
EG10426	helD	77.9	8.3		0.27	EG13060	ygfJ	21.5	6.2		0.05
EG10437	hflX	48.3	6		0.43	EG12729	ygjR	36.2	6.1		0.52
EG10453	hisS	47	5.9	E	0.07	EG12749	yhaJ	33.2	6.5		0.06
EG10495	ilvC	54	5.3		0.21	EG12614	yhcB	14.9	5.9		0.50
EG40008	insH	39.3	9.6		0.43	EG11467	yigl	17.1	6.9		0.10
EG12069	mgo	60.2	7		0.41	EG11849	yihW	28.5	6		0.68
EG10630	nadA	38.2	5.4		0.50	EG10021	yjiA	35.6	4.9		0.47
EG10649	ndh	47.3	8.9		0.28	EG13530	yqaB	20.7	5.9		0.35
EG13780	nhoA	32.2	6.3	E	0.33	EG13097	yqeF	41	5.9		0.07
EG10687	parE	70.2	5.7	E	0.55	EG13132	znuC	27.8	9.3		0.42

Supplementary Table S14 Significantly changed proteins upon depletion of GroEL at 30 °C and 37 °C

Significantly changed proteins in the GroEL-depleted cells compared to WT, ordered alphabetically according to gene name. EL: GroEL substrates classes (Kerner et al., 2005).

EG	Gene Name	EL	30 °C			37 °C			EG	Gene Name	EL	30 °C			37 °C			
			Dec	Inc	Agg	Dec	Inc	Agg				Dec	Inc	Agg	Dec	Inc	Agg	
EG12825	aaeR							19.18	EG10698	pepQ	III	0.36				0.17		25.23
EG11112	aat							3.74	EG11549	pepT								3.44
EG11647	accA	II						5.58	EG10699	pfkA								8.34
EG10022	aceA			2.18			4.92		EG10707	pheA	III							5.33
EG10023	aceB			2.21			5.64		EG10709	pheS								22.79
EG11095	acpH	III						10.25	EG10713	phnC								26.81
EG50003	acpP							2.12	EG10714	phnD							32.60	

EG12116	acrR				12.27				EG10716	phnG							9.11
EG11448	acs			2.19					EG10721	phnL							9.62
EG11942	actP				2.79				EG10723	phnN							23.55
EG10030	add	III	0.38						EG10727	phoA						26.39	
EG11501	adiA					0.26			EG10728	phoB			2.00			13.33	9.91
EG10035	aldA			2.13			2.90	5.50	EG10729	phoE						3.64	19.64
EG13616	allR							18.06	EG10731	phoP	II						4.93
EG10001	alr							4.24	EG10733	phoR						12.69	21.06
EG10039	amn					2.19		8.35	EG10735	phoU			1.57			10.96	4.90
EG11387	amyA							3.71	EG10741	pmbA	III	0.32			0.08		10.14
EG10048	apaH							5.63	EG10742	pncB							6.37
EG10049	appA					0.35			EG10752	potD			1.45				
EG11380	appC					0.17			EG11629	potF							2.56
EG10050	appY							7.43	EG11630	potG			1.39				2.80
EG10051	apt					0.59			EG11211	poxA					0.55		
EG10052	araA	III		20.12	91.35		5.64		EG10754	poxB							3.59
EG10053	araB			10.97					EG11510	ppk							5.81
EG10056	araE				48.31				EG12365	prkB		0.58			0.38		16.73
EG10057	araF			3.70					EG11441	prlC			1.80			2.07	
EG10064	argB			1.62			2.06		EG12449	prnB							2.31
EG10066	argD			1.47			1.77	5.43	EG10768	proB							2.10
EG11286	argE	III			2.10			15.78	EG10771	proV			1.50				4.78
EG10068	argG			1.42				4.83	EG10773	proX			1.67				
EG10490	argP	III						27.94	EG10774	prs	II				0.54		20.38
EG14091	arnA							9.78	EG12344	pspF							15.45
EG10074	aroB							5.76	EG10783	pstB	II	0.56					18.14
EG10077	aroE							4.46	EG10734	pstS						18.38	13.32
EG10080	aroH							6.93	EG10785	pth	II						10.77
EG11628	artJ						2.01		EG10793	purE							3.79
EG11624	artP		0.60			0.44			EG10797	purL	II				0.33		27.94
EG10088	asd	III	0.53			0.33		80.35	EG10800	purR							9.61
EG10091	asnA		0.48			0.30			EG11819	purU							12.44
EG10092	asnB					0.53			EG10803	pykA							2.70
EG10093	asnC							8.93	EG10805	pyrB					0.31		3.11
EG10096	aspC			1.43					EG10806	pyrC	II	0.46			0.15		23.00
EG11668	atoC							11.45	EG10807	pyrD	-	0.31			0.20		27.00
EG10113	bfr							15.28	EG10808	pyrE							3.17
EG10117	bioA							4.40	EG10809	pyrF	II	0.56			0.32		17.67
EG10118	bioB			1.43			1.84	4.31	EG11539	pyrH							3.78
EG10119	bioC							8.69	EG10811	pyrI					0.40		
EG10120	bioD							16.43	EG11492	qorA		0.55			0.41		16.13
EG10121	bioF	III				0.41		35.33	EG13173	queF							7.30

EG12319	can	II					5.82	EG14260	rbn							6.52
EG12335	cdsR						11.52	EG10815	rbsB	I		1.60				
EG11531	cfb						4.34	EG12982	rdgB							12.62
EG13993	cho						6.33	EG12158	rdgC							2.42
EG10157	clpB			2.71			3.05	5.04	EG10830	recJ						3.56
EG10158	clpP							40.07	EG10831	recN						4.22
EG14033	cmoA							7.19	EG10834	recR						4.03
EG14034	cmoB					0.44		17.52	EG11351	rfaB						5.70
EG14303	cnu		0.53						EG10838	rfaD						4.18
EG11190	coaD							6.78	EG11978	rfaA						26.63
EG13443	cobB							6.13	EG12412	rfaB						2.48
EG12151	cobT							7.89	EG11979	rfaC	III	0.50			0.24	28.70
EG13246	copA		0.39						EG12411	rfaD						7.17
EG11092	crl						2.51	EG11451	rffE							3.67
EG10164	crp	III						3.08	EG10465	ribB		0.36			0.16	
EG13082	csdA					0.17			EG11321	ribD						10.11
EG13410	csgD							6.16	EG11322	ribE						3.65
EG10166	espA		0.53						EG10852	rimK						20.87
EG10167	estA				2.78				EG11507	rlnE			1.42		1.78	11.94
EG12318	cueO		0.38					16.55	EG11254	rlnH					0.33	23.81
EG12956	cutC					0.40		19.53	EG13725	rlnI						2.88
EG10173	cydA		0.43						EG13717	rlnL	III					2.25
EG10174	cydB		0.49						EG12401	rlnN						2.99
EG10184	cysB	II						59.69	EG11118	rlnC	III					2.67
EG10192	cysK							2.46	EG12098	rlnD						12.49
EG11407	dadA	III	0.16			0.14		20.05	EG10857	rnc						4.02
EG11408	dadX	III						8.59	EG11299	rng						3.87
EG10204	dam							19.16	EG10861	rnhB						6.31
EG10205	dapA	III						123.61	EG13200	rnlA						11.11
EG10207	dapD							89.03	EG10862	rnpA						7.09
EG10208	dapE							5.52	EG11366	rob	II					4.58
EG20044	dctA						5.81		EG11960	rpe						30.31
EG12464	dcuR							9.95	EG11443	rpiA						9.01
EG14038	dcyD		0.32			0.26		29.99	EG10868	rplE						2.49
EG10219	deoA	III		28.15	12.17		11.35	52.76	EG10875	rplN						11.05
EG10220	deoB			11.61	3.94		10.08	12.36	EG10888	rplM						4.75
EG10221	deoC	I		64.88			32.42		EG10897	rpoH			1.60			
EG10222	deoD	I		4.87			4.56	29.70	EG10510	rpoS					2.01	4.93
EG10223	deoR					0.27			EG10904	rpsE						4.73
EG13015	dlkA		0.45			0.34			EG10906	rpsG						2.37
EG10231	dld							2.67	EG10911	rpsL						3.05
EG10236	dnaB							3.21	EG11879	rraA						11.91

EG10240	dnaJ	III		2.29			2.52	14.43	EG13177	rseB							2.50
EG10241	dnaK	II		2.78	2.67		3.22	8.33	EG10523	rsmA							5.57
EG10243	dnaQ							20.07	EG10376	rsmG							7.18
EG13161	dsdC							20.33	EG12120	rssA							10.69
EG11932	dusA	II	0.46		3.22	0.25		15.92	EG13190	rstA							7.02
EG12022	dusC	III						9.70	EG11247	rumA							6.59
EG12715	dxr		0.42			0.16			EG10924	ruvB							6.53
EG10256	eda						4.03	26.20	EG10925	ruvC							23.91
EG10257	edd			2.02			29.61		EG10926	sbcB					0.39		
EG13184	elaA							3.41	EG11623	sdaB							3.32
EG10261	entC	II				0.35			EG10931	sdhA	III				0.41		8.28
EG10368	epd							17.52	EG10932	sdhB			1.48				7.06
EG50006	eutB	III						10.43	EG10934	sdhD				4.44			3.98
EG14171	eutL							17.81	EG10935	sdiA							34.14
EG14031	exoX							26.56	EG10941	selA							4.04
EG12739	exuR							7.65	EG10944	serA	I						7.22
EG10273	fabA	I						3.46	EG10946	serC	II	0.53			0.23		47.62
EG10274	fabB	I						30.72	EG11890	slp		0.07			0.08		
EG12606	fabF	III	0.43			0.13		40.33	EG13408	slyA							7.07
EG11528	fabI							2.44	EG10954	sodB							4.09
EG11394	fabR							18.82	EG12669	solA							4.67
EG11284	fabZ			1.48				17.59	EG10957	soxR							18.95
EG10278	fadA	-						12.02	EG10958	soxS							88.10
EG11530	fadD							3.04	EG10960	speB							9.27
EG14128	fadI							6.99	EG10961	speC							5.21
EG10281	fadR							8.02	EG10962	speD							14.71
EG14062	fbaB	III						27.34	EG10963	speE							8.52
EG10283	fbp							3.95	EG12447	speG							4.08
EG10290	fecE							3.67	EG10966	spoT	II						6.05
EG12101	feoA							7.40	EG10977	sspA							4.00
EG10293	fepA					0.50			EG11428	sthA	II		1.43				7.11
EG12686	flu					0.18			EG10979	sucA	II		1.81				3.18
EG10325	fmr							15.87	EG10980	sucB	II		1.58				
EG10328	folD							3.82	EG10981	sucC			1.84				2.16
EG11375	folE	III		1.40			4.20	31.18	EG10982	sucD			1.82				3.19
EG50011	folP					0.37		69.97	EG13964	sufC							4.39
EG14263	folX							14.82	EG13963	sufD							2.95
EG11518	fpr							8.53	EG13962	sufS	III				0.18		14.83
EG10330	frdA	III						6.10	EG10983	suhB	III				0.66		
EG10334	fre							6.46	EG11372	tadA							18.84
EG50010	frmA							3.36	EG10986	tag							19.59
EG13295	frmB							5.43	EG11797	talA							15.65

EG10338	fruR							8.01	EG11556	talB			1.53				3.09
EG13471	fsaA							14.38	EG13093	tas	II						11.62
EG10921	ftnA						3.61		EG10994	tdk							8.72
EG10340	ftsE	III	0.36					0.30	EG11884	tehB	II						12.30
EG11376	ftsP		0.55					0.42	EG10995	tesB							44.60
EG10355	fucU							19.71	EG10996	tgt							14.35
EG10356	fumA			1.51					EG11585	thiC						3.43	5.00
EG12382	fxsA			1.69	2.24			2.84	EG14068	thiD		0.44			0.21		11.37
EG50009	gadA	II						0.07	EG11586	thiE	II						42.69
EG11490	gadB		0.10					0.07	EG11587	thiF							11.57
EG12242	gadW		0.42					7.04	EG11589	thiG	I				0.46		17.62
EG13578	galF							3.86	EG11590	thiH	III				0.39		10.02
EG10363	galK			1.65					EG20227	thiL							4.16
EG10366	galT			1.61					EG14069	thiM							4.04
EG10367	gapA	I		1.45					EG11572	thiQ							2.09
EG12414	gatA			33.15	6.60			30.48	50.86	EG14363	thiS						2.13
EG12415	gatB			9.77						EG12826	tldD	III	0.30			0.24	
EG12416	gatC			28.60	35.45			45.09	112.94	EG12302	tmk						5.44
EG12417	gatD	II		9.38				9.94	25.33	EG11005	tnaA	II		2.27			2.99
EG12419	gatY	III	0.42						38.86	EG12672	tpx	I					3.57
EG12418	gatZ	III		48.79				12.60	35.85	EG10967	trmH	II					10.70
EG10372	gdhA	-						0.41	13.99	EG13452	trmJ						6.60
EG11981	glf							15.91		EG11024	trpA					3.30	8.41
EG10379	glgC							7.21		EG11025	trpB					2.65	5.13
EG11553	glmM							6.10		EG11026	trpC					4.62	23.68
EG10383	glnA							0.43		EG11027	trpD						7.83
EG10389	glnQ		0.47					0.47		EG11028	trpE						9.61
EG10400	glpR							3.65		EG11030	trpS						6.80
EG11517	glpX							3.01		EG10454	truA				3.27		10.71
EG10402	gltA	II		1.42				28.58		EG13171	truC		0.51				19.63
EG10404	gltD							2.74		EG13109	truD						8.21
EG10407	gltX							3.08		EG11035	tsx			2.01	2.28		
EG10409	glyQ							5.23		EG11038	tus						21.49
EG12629	gntK							13.20		EG11040	tyrB						5.25
EG12630	gntR		0.37					30.32		EG11369	ubiC	III					18.62
EG12631	gntU							15.37		EG11396	ubiD						4.68
EG11699	gpmA	I						5.96		EG11473	ubiE					0.49	6.85
EG10414	gpt							11.21		EG13658	ubiF		0.63			0.35	13.15
EG10416	grpE	I		2.15				2.30		EG11143	ubiG						3.12
EG10419	gshB							2.41		EG11324	ubiH						8.55
EG12882	gsp							2.82		EG11044	ubiX						27.44
EG10422	guaC							8.54		EG11701	udk						3.51

EG13455	hcaR							3.66	EG13407	ugd			3.00	3.39			6.92
EG11398	hdeA		0.10						EG11047	ugpB						39.33	7.17
EG11399	hdeB		0.14			0.13			EG11048	ugpC						9.90	99.97
EG11449	hdfR							13.47	EG11050	ugpQ						4.27	
EG10426	helD							2.42	EG12493	ulaA							30.39
EG10428	hemB	III	0.39		2.12	0.24		46.89	EG12494	ulaB			67.05			12.72	46.99
EG11543	hemE	II	0.44			0.28		22.96	EG12495	ulaC			107.14			33.97	11.96
EG10431	hemH							4.16	EG12496	ulaD			58.54			54.40	48.84
EG11345	hflD							2.62	EG12497	ulaE			22.85			12.68	41.33
EG10437	hflX							9.82	EG12498	ulaF						5.41	58.18
EG10439	hha							34.61	EG12492	ulaG			189.01	45.52		25.00	24.82
EG10444	hisA							28.42	EG12491	ulaR							10.45
EG10445	hisB	III					2.03	3.08	EG11332	upp						0.61	
EG10446	hisC			1.39					EG11060	ushA				8.04			
EG10447	hisD			1.37			1.96	2.30	EG11140	uvrY	II						5.50
EG10448	hisF					0.31		33.23	EG12737	uxaC	III						8.05
EG10449	hisG							16.12	EG11333	visC							13.22
EG10450	hisH					0.42		41.99	EG11986	wbbL							13.96
EG10451	hisI							4.48	EG11540	wrbA							54.91
EG12124	hisJ			1.68					EG11146	xapR							3.77
EG20098	hpt							4.82	EG11072	xseA							6.08
EG10458	hsdM							3.55	EG11073	xthA		0.54			0.35		26.71
EG12930	hslO	II		1.88			1.90		EG20253	xylR							13.77
EG12929	hslR			1.82					EG10011	yaaA					0.52		18.97
EG11881	hslU			2.11			2.40	7.15	EG11649	yafC							15.31
EG11676	hslV			1.79			3.06	37.31	EG13272	yajL							9.47
EG13724	hspQ						3.15		EG13611	yajO	III	0.29					8.39
EG10461	htpG			2.73			3.25	2.92	EG11100	ybaB							5.66
EG12567	iadA							3.78	EG13247	ybaS						0.09	
EG11534	ibpA			1.83				7.19	EG13259	ybbL					0.44		14.79
EG11535	ibpB			1.55				18.32	EG13261	ybbN	II		1.71			2.04	
EG10441	ihfB							6.26	EG13629	ybcM							8.12
EG10494	ilvB							5.50	EG12692	ybdH						11.48	
EG10495	ilvC			1.57					EG11255	ybeB							5.87
EG10497	ilvE							11.09	EG11592	ybeD			2.01				
EG10498	ilvG							5.99	EG13655	ybeY			1.65				
EG10499	ilvH							21.39	EG13656	ybeZ	III		1.74			2.60	4.71
EG10500	ilvI							3.59	EG11776	ybfF	II	0.55			0.29		46.31
EG11422	inaA	II						6.37	EG11110	ybgC							7.20
EG40003	insC							15.57	EG13307	ybgK		0.56			0.31		15.23
EG40008	insH	II						12.20	EG13308	ybgL							10.38
EG40012	insL		0.41					12.30	EG11239	ybhA		0.33			0.16		9.45

EG11783	intA							11.87	EG13667	ybhK		0.51					8.80
EG12132	iscA							7.90	EG11580	ybiB	II						37.45
EG11816	ispF							8.44	EG11581	ybiC			1.39			2.48	14.96
EG10370	ispG		0.38			0.22		26.41	EG13316	ybiX					0.39		30.39
EG10518	kdsA	II	0.52			0.20		44.48	EG13678	ybjI							14.98
EG12803	kdsD							5.40	EG13688	ybjS	III				0.26		5.29
EG13898	ldcA							8.33	EG11241	yeaC							16.79
EG13186	ldhA				1.40				EG13703	yecK						2.40	63.28
EG11226	leuA		0.50					28.05	EG13704	yecL	II						5.54
EG11306	lipA	III	0.32			0.14		16.80	EG13715	yecW							11.11
EG10536	livF					0.44			EG13870	yedX							5.96
EG10537	livG		0.64			0.47			EG11116	yceA							3.19
EG10539	livJ				1.75				EG11438	yceF							15.65
EG11963	lldD	III	0.56			0.31			EG13879	yceM							16.85
EG10542	lon	II			1.87		2.26		EG12303	yefH	III	0.29			0.13		32.96
EG13146	lpcA							5.16	EG12444	yefJ					2.59		
EG11680	lptB							3.64	EG13434	yefP	III						13.18
EG10545	lpxA	II						5.62	EG13887	yegF							4.33
EG10265	lpxC							21.95	EG13905	yeiT							8.53
EG10316	lpxD							3.87	EG12870	yefF			1.82	2.54		2.47	2.93
EG12123	lrhA							12.10	EG13921	yecX			1.95			2.65	6.52
EG10547	lrp							3.92	EG13923	yecZ	II						25.30
EG13810	lsrF	III						5.60	EG13355	ydaM							5.45
EG13805	lsrR							23.74	EG11309	ydbC		0.49			0.28		28.02
EG13690	ltaE	III				0.36		15.02	EG12110	ydcF							21.22
EG10550	lysC						2.71	4.10	EG13752	ydcI							21.17
EG10551	lysR							60.64	EG13759	ydcP	II	0.38			0.47		5.97
EG14193	maeB			1.52		1.92			EG13820	ydfH							24.53
EG11288	mak							7.80	EG13838	ydfZ					0.18		
EG10554	malE			2.49					EG13931	ydgJ		0.33					5.40
EG10558	malK			5.69					EG12140	ydhB							10.36
EG10559	malM			2.27					EG13420	ydhF	II						49.26
EG10562	malT							7.12	EG11132	ydiA							32.85
EG10570	map							3.76	EG13969	ydiJ							3.99
EG11434	marA							10.09	EG11134	ydjA							3.12
EG10576	mdh			1.63					EG13489	yeaC						1.89	
EG12240	mdtE		0.09			0.11			EG12679	yeaD			1.58				
EG12241	mdtF		0.18			0.25			EG13506	yeaT	II						11.22
EG11368	menB							2.74	EG14020	yebR							3.66
EG10581	metA			3.97		33.89	67.18		EG13393	yeeZ							3.37
EG10582	metB			2.13		28.95	24.68		EG12200	yegD	II	0.43			0.28		
EG10583	metC			1.90		7.20	23.45		EG12105	yeiE							14.68

EG10584	metE			4.69	2.69		94.08	72.19	EG12045	yejH							6.89
EG10585	metF	III					9.67	55.54	EG14101	yfbQ	III	0.30			0.22		7.28
EG10587	metH			1.40			3.51	3.21	EG14108	yfcE							12.05
EG11737	metI			1.69			6.51	8.87	EG14109	yfcF							36.15
EG10588	metJ						2.69		EG14198	yfdZ			2.82				7.92
EG10589	metK	III	0.54					37.57	EG11784	yfiD		0.43			0.30		
EG10590	metL						6.81	5.05	EG11785	yfiE							56.17
EG11621	metN			1.64			6.25	8.02	EG13197	yfjK				5.60			
EG11504	metQ			1.63	2.11		4.32	8.05	EG13201	yfjO							7.82
EG10591	metR			1.83			7.83	21.15	EG12373	ygdH					0.25		
EG11619	mfd			1.53				2.36	EG11157	ygeA	II						18.48
EG10592	mglA	II			4.84				EG12971	ygfF							20.80
EG10593	mglB			2.78			2.88		EG12983	yggW							13.95
EG10594	mglC				3.20				EG12657	ygiN							12.53
EG13292	mhpE				3.13		9.14	82.67	EG13019	ygiQ							4.55
EG13625	mhpF						18.12	13.96	EG13022	ygiT							16.46
EG10595	miaA							12.43	EG12727	ygiP							12.53
EG10596	minC		0.51			0.43		8.62	EG12749	yhaJ							26.41
EG10375	mmnG	II				0.29		23.46	EG12752	yhaM			3.79	3.22	0.15		
EG11595	moaA	II						44.56	EG12754	yhaO				4.37			
EG11596	moaB	II		1.61			2.61	4.12	EG12146	yhbJ	III						3.91
EG11666	moaC	II		1.70			2.85	4.92	EG12788	yhbS							4.03
EG11597	moaD						2.64		EG12792	yhbW		0.58			0.18		20.25
EG11598	moaE			1.98			2.56		EG12820	yhcN		0.49			0.27		
EG11511	mog							3.75	EG12899	yheO							3.86
EG10603	mprA							3.20	EG12234	yhiR		0.49			0.36		14.94
EG12069	mqo			1.54					EG12247	yhjC							14.59
EG11085	mraW							3.14	EG12271	yiaD		0.55					
EG12394	msrB			1.58			2.00		EG12624	yiaG							15.35
EG10616	mtlD							7.03	EG11762	yibF							13.86
EG12717	mug	II	0.44			0.38		47.32	EG11888	yibK							9.37
EG12165	mukF							3.01	EG11192	yicC							3.62
EG11358	murA							9.21	EG11195	yidA							7.28
EG10329	mutM			1.66					EG11722	yieE							4.72
EG10630	nadA		0.47			0.28		4.16	EG11725	yieH							14.09
EG10631	nadB		0.49			0.48		5.87	EG11728	yieK							4.88
EG10663	nadE							3.97	EG11733	yieP							12.99
EG12192	nadK							14.78	EG11201	yigA							13.87
EG10633	nagB							5.03	EG11202	yigB		0.50					15.67
EG10634	nagD		0.42			0.22		18.70	EG11467	yigI		0.46					45.60
EG13442	nagK							4.99	EG11470	yigL							3.79
EG13433	nagZ	III	0.41			0.20		41.01	EG11870	yiiM					0.37		

EG11915	nfi						5.93	EG11935	yjbQ	II						8.44
EG10651	nfo	III	0.32			0.16	13.44	EG12473	yjeK					0.41		18.89
EG11740	nfrA			3.89				EG11436	yjgB							4.95
EG20151	nfsB						4.83	EG12528	yjgl							4.90
EG13780	nhoA						9.90	EG12545	yjhC							6.00
EG10662	nth						9.39	EG12604	yjhU					0.39		30.26
EG11702	nudC						6.38	EG10021	yjiA							3.80
EG12926	nudE						18.65	EG12579	yjiR							10.06
EG12693	nudL					0.37		EG12586	yjiY						3.49	3.46
EG12083	nuoB		0.41			0.30		EG12597	yjiU	III	0.13			0.21		
EG12084	nuoC	II	0.41			0.38		EG12598	yjiV	II	0.52			0.40		35.96
EG11774	nuoF	II	0.43			0.16		EG12600	yjiX							3.08
EG10670	ompC	I				0.66		EG12309	yjID							9.06
EG10671	ompF	II		2.11				EG14292	yngD						1.96	
EG10673	ompT					0.55		EG13775	yneE	I		1.79				
EG10674	oppA	I		1.55				EG13816	yneH							8.36
EG12480	orn						17.68	EG13850	ynfL							38.56
EG11751	otsA						3.82	EG13988	yniC							18.04
EG10681	oxyR	II					10.06	EG14150	ypdC							6.76
EG11493	pabC						19.60	EG14168	ypeA							13.08
EG11675	panB	I					22.71	EG13530	yqaB	III	0.23			0.19		10.41
EG11746	panC						4.43	EG13097	yqeF							11.03
EG11747	panD						8.58	EG12186	yqiA		0.55			0.46		27.96
EG10689	pem						17.70	EG12743	yqiD		0.59					
EG11088	pdhR						3.06	EG12783	yraR							3.80
EG10692	pdxB						8.35	EG12801	yrbF		0.63					
EG11487	pdxH						8.19	EG12838	yrdA							4.31
EG10693	pdxJ					2.13	8.57	EG12928	yrfG		0.47					7.80
EG13940	pdxY						17.83	EG12164	ytcC							7.94
EG10697	pepP						2.73	EG12878	zapA							6.62
								EG11969	zntR			1.66				

Supplementary Table S15 Proteins aggregated in Δ KJT cells

Significantly increased (> 2 fold) proteins in the Δ KJT insoluble fraction compared to WT are ordered according to the percentage of soluble protein depleted due to aggregation (Depl %).

EG	Gene Name	Depl (%)	EG	Gene Name	Depl (%)	EG	Gene Name	Depl (%)	EG	Protein Name	Depl (%)
EG11534	ibpA	74.89	EG11779	trml	4.60	EG10383	glnA		EG13940	pdxY	

EG12418	gatZ	67.85	EG11587	thiF	4.57	EG10868	rplE		EG14066	yegW	
EG10223	deoR	66.04	EG10960	speB	4.56	EG10867	rplD		EG14091	arnA	
EG12417	gatD	65.84	EG11031	trxA	4.56	EG11092	crl		EG14102	yfbR	
EG12473	yjeK	57.96	EG10431	hemH	4.54	EG10834	recR		EG14105	yfbU	
EG12210	rfaF	54.09	EG11964	yibL	4.53	EG10874	rplM		EG14114	mmnC	
EG11510	ppk	47.73	EG12826	tldD	4.49	EG10922	coaA		EG14127	fadJ	
EG13752	ydcI	47.08	EG10532	leuS	4.45	EG12044	rsuA		EG14149	ypdB	
EG11535	ibpB	46.90	EG11005	tnaA	4.45	EG10096	aspC		EG14159	yfeR	
EG10221	deoC	46.08	EG10375	mmnG	4.35	EG10213	ddlA		EG14162	murQ	
EG11540	wrbA	44.80	EG10045	ansA	4.31	EG10512	kbl		EG14023	rsmF	
EG10460	hsdS	42.79	EG10028	pflA	4.29	EG10805	pyrB		EG12528	yjgI	
EG12365	prkB	41.99	EG11119	yceD	4.28	EG10770	proS		EG12382	fxsA	
EG11511	mog	41.43	EG11345	hflD	4.23	EG10567	manX		EG12386	csiR	
EG10426	helD	40.47	EG14033	cmoA	4.12	EG10411	gnd		EG12396	yegE	
EG10380	glgP	39.78	EG10360	fusA	4.07	EG11442	gevT		EG12410	nudK	
EG10024	aceE	37.15	EG10796	purK	4.02	EG10948	maeA		EG12416	gatC	
EG10491	iclR	37.05	EG12207	rlmA	3.97	EG10643	narL		EG12432	ydiF	
EG11423	waaU	36.83	EG11407	dadA	3.93	EG10699	plkA		EG12444	ycfJ	
EG12690	rarA	36.77	EG10794	purF	3.91	EG12739	exuR		EG12459	rpiR	
EG10562	malT	36.41	EG10214	ddlB	3.85	EG10888	rpmD		EG13326	ybiU	
EG10264	entF	36.22	EG12114	prfC	3.82	EG10728	phoB		EG12516	ytP	
EG11061	uvrA	35.90	EG10081	aroK	3.47	EG10902	rpsC		EG12329	hrpB	
EG12319	can	34.44	EG13905	yciT	3.44	EG12683	uspG		EG12531	yjgL	
EG13183	ydbK	34.40	EG11268	fnt	3.38	EG11261	nfsA		EG12540	idnO	
EG11702	nudC	33.84	EG12401	rlmN	3.37	EG10231	dld		EG12579	yjiR	
EG12870	ycjF	33.74	EG12685	ygfZ	3.34	EG13261	ybbN		EG12595	fhuF	
EG10184	cysB	31.92	EG10159	clpX	3.24	EG10844	rhIB		EG12604	yjhU	
EG10212	dcp	31.58	EG11368	menB	3.23	EG10915	rpsP		EG12605	yacL	
EG13177	rseB	29.25	EG11784	yfiD	3.18	EG10330	frdA		EG12624	viaG	
EG11059	usg	29.18	EG10692	pdxB	3.18	EG10465	ribB		EG12642	pdxK	
EG10500	ilvI	28.39	EG10361	gabT	3.12	EG10095	aspA		EG12464	dcuR	
EG11470	yigL	28.19	EG10806	pyrC	3.10	EG12840	rimN		EG12223	rbbA	
EG11718	dgoR	27.73	EG10170	cyaA	3.08	EG12099	efp		EG12116	acrR	
EG10754	poxB	26.87	EG10967	trmH	3.00	EG10907	rpsH		EG12119	ychJ	
EG11045	udp	26.41	EG10118	bioB	2.99	EG11191	slmA		EG12121	rssB	
EG11132	ydiA	25.93	EG10418	gshA	2.88	EG13034	ygcF		EG12135	ompX	
EG12492	ulaG	25.70	EG10898	rpoN	2.84	EG12982	rdgB		EG12140	ydhB	
EG12878	zapA	25.64	EG11036	tufA	2.73	EG10419	gshB		EG12151	cobT	
EG11064	uvrD	25.48	EG13190	rstA	2.73	EG12309	yjtD		EG12184	nudF	
EG14087	yfaY	25.31	EG13657	miaB	2.71	EG11527	narP		EG12185	yqiB	
EG11335	nadR	24.67	EG10444	hisA	2.69	EG10985	surA		EG12378	yecD	
EG10959	speA	24.55	EG10857	mec	2.69	EG13357	ttcA		EG12198	chbG	

EG10966	spoT	24.27	EG11884	tehB	2.61	EG10187	cysE		EG12334	btuF	
EG11406	ribC	23.88	EG10504	infA	2.60	EG11675	panB		EG12229	yhiN	
EG12100	tktB	23.23	EG10043	cysQ	2.58	EG11153	rimM		EG12233	yhiQ	
EG10017	ispB	23.13	EG12415	gatB	2.51	EG11979	rfbC		EG12242	gadW	
EG11888	yibK	23.05	EG10265	lpxC	2.32	EG13259	ybbL		EG12247	yhjC	
EG11817	surE	22.79	EG12188	ptsP	2.32	EG13391	yeeX		EG12278	yiaJ	
EG13869	ghrA	22.22	EG10863	rph	2.31	EG10001	alr		EG12289	yiaU	
EG11985	wbbK	21.51	EG11100	ybaB	2.31	EG10326	folA		EG12307	mgsA	
EG11836	hemN	21.49	EG11187	yibA	2.28	EG11385	ahpF		EG12318	cueO	
EG10660	nrdA	21.38	EG10421	guaB	2.21	EG13716	ycbX		EG12693	nudL	
EG12433	rIuB	20.99	EG12048	yejK	2.21	EG10804	pykF		EG12192	nadK	
EG13086	amiC	20.61	EG11543	hemE	2.20	EG10356	fumA		EG13216	cof	
EG12930	hslO	20.32	EG11073	xthA	2.19	EG10944	serA		EG12657	ygiN	
EG10829	recG	20.02	EG10032	adk	2.17	EG12336	yaeH		EG13145	fadE	
EG11879	rraA	19.95	EG10446	hisC	2.15	EG13547	ivy		EG13147	yafJ	
EG10025	aceF	19.64	EG14193	maeB	2.13	EG10334	fre		EG13156	dgsA	
EG10561	malQ	19.44	EG10876	rplO	2.12	EG10545	lpxA		EG13181	hslJ	
EG10499	ilvH	19.20	EG11252	mukE	2.04	EG10980	sucB		EG13189	folM	
EG10510	rpoS	18.83	EG10774	prs	2.03	EG13870	yedX		EG13197	yfjK	
EG11062	uvrB	18.74	EG10511	katG	2.02	EG10911	rpsL		EG13198	yfjL	
EG10858	rnd	18.61	EG12672	tpx	2.02	EG12545	yjhc		EG13117	casC	
EG10425	hdhA	18.59	EG10862	rnpA	1.98	EG13393	yeeZ		EG13201	yfjO	
EG10238	dnaE	18.57	EG10316	lpxD	1.92	EG12132	iscA		EG13097	yqeF	
EG13967	ydiH	18.37	EG10453	hisS	1.88	EG11983	wbbI		EG13218	ybaO	
EG13079	bglA	18.33	EG10625	mutS	1.87	EG12627	dppD		EG13219	ldcC	
EG11411	glnD	18.32	EG10092	asnB	1.85	EG11202	yigB		EG13220	tilS	
EG10077	aroE	18.17	EG10398	glpK	1.82	EG10890	rpmF		EG13223	yaeQ	
EG10437	hflX	18.12	EG10740	plsB	1.76	EG12815	nanK		EG13227	modE	
EG10631	nadB	17.99	EG10885	rplY	1.69	EG10582	metB		EG13228	ycjG	
EG11002	thyA	17.97	EG12234	yhiR	1.68	EG14038	dcyD		EG13289	yqgE	
EG10219	deoA	17.65	EG10694	pepA	1.66	EG11849	yihW		EG13292	mhpE	
EG11485	hemG	17.34	EG10581	metA	1.64	EG11916	yjaG		EG13295	frmB	
EG11296	radA	17.25	EG10447	hisD	1.60	EG10931	sdhA		EG13200	rmlA	
EG11246	uspE	16.98	EG11701	udk	1.56	EG14111	yfcH		EG12879	ybcJ	
EG11226	leuA	16.96	EG11325	acnA	1.50	EG10591	metR		EG10204	dam	
EG11519	nikR	16.96	EG12795	obgE	1.43	EG11204	murI		EG12698	ygaD	
EG13434	ycfP	16.83	EG11090	mtn	1.42	EG11731	ravA		EG12710	yedJ	
EG11436	yjgB	16.37	EG10088	asd	1.29	EG50003	acpP		EG12717	mug	
EG10895	rpoC	16.35	EG10904	rpsE	1.17	EG10767	proA		EG12729	ygiR	
EG10587	metH	16.31	EG10838	rfaD	1.17	EG13019	ygiQ		EG12754	yhaO	
EG10743	pnp	16.19	EG10762	prfB	1.14	EG11870	yiiM		EG12798	yrbC	
EG10546	lpxB	16.12	EG13186	ldhA	1.05	EG11422	inaA		EG12816	nanE	

EG12253	kdgK	16.06	EG12352	ppiC	1.04	EG11453	rffG		EG13120	queD	
EG11782	smpB	15.87	EG10924	ruvB	0.98	EG10157	clpB		EG12859	opgD	
EG10661	nrdB	15.87	EG11881	hslU	0.97	EG12310	pepB		EG12691	yciM	
EG11795	gevA	15.59	EG10382	glmS	0.93	EG10776	pspA		EG12902	kefG	
EG11083	hepA	15.52	EG10755	ppa	0.82	EG11506	ftsH		EG12913	frlR	
EG10894	rpoB	15.46	EG20227	thiL	0.79	EG12480	orn		EG12944	yhhX	
EG11783	intA	15.33	EG13951	ydhQ	0.75	EG10123	birA		EG12979	yggS	
EG11294	ispE	15.28	EG11797	talA	0.74	EG11428	sthA		EG12983	yggW	
EG10896	rpoD	15.16	EG10937	secB	0.72	EG12332	erpA		EG12998	glcC	
EG10494	ilvB	15.15	EG10636	nagC	0.70	EG11676	hslV		EG13010	yghZ	
EG12817	nanR	15.09	EG13578	galF	0.66	EG10612	mrr		EG13013	yqhC	
EG12882	gsp	14.98	EG12567	iadA	0.60	EG10598	minE		EG13093	tas	
EG12176	yjdC	14.75	EG11682	ptsN	0.54	EG10882	rplV		EG12825	aaeR	
EG13717	rlmL	14.67	EG12596	rsmC	0.51	EG10954	sodB		EG11801	hybC	
EG11603	ygiF	14.52	EG10808	pyrE	0.51	EG13493	yeaG		EG11714	cbrA	
EG13699	ycaO	14.45	EG13535	dsbG	0.50	EG50011	folP		EG11963	lldD	
EG10600	groS	14.42	EG10686	parC	0.48	EG10412	gor		EG11942	actP	
EG14198	yfdZ	14.38	EG11085	mraW	0.48	EG10569	manZ		EG11929	zur	
EG13546	nemA	14.35	EG13725	rlmI	0.44	EG10117	bioA		EG11926	yjbH	
EG10543	lpd	14.18	EG11319	galU	0.43	EG10400	glpR		EG11915	nfi	
EG10407	gtX	14.10	EG13329	ispU	0.41	EG10807	pyrD		EG11858	fdoG	
EG11026	trpC	13.91	EG10893	rpoA	0.40	EG10363	galK		EG11853	yiiD	
EG11649	yafC	13.87	EG10061	arcA	0.40	EG12971	ygfF		EG12006	yehT	
EG12788	yhbS	13.73	EG10420	guaA	0.38	EG10761	prfA		EG11831	rdoA	
EG13988	yniC	13.72	EG11254	rlmH	0.38	EG10390	glnS		EG12022	dusC	
EG11437	plsX	13.69	EG10823	recA	0.37	EG10165	crr		EG11796	lplA	
EG13901	dhaK	13.50	EG10710	pheT	0.29	EG10428	hemB		EG11794	ygdE	
EG10423	gyrA	13.47	EG10129	btuE	0.25	EG10075	aroC		EG11787	gmd	
EG10317	fis	13.40	EG12447	speG	0.23	EG10785	pth		EG11785	yfiE	
EG10403	glfB	13.17	EG10282	fbaA	0.23	EG13290	yqgF		EG11749	yadE	
EG10235	dnaA	13.13	EG10795	purH	0.22	EG11507	rlmE		EG11747	panD	
EG10438	hfq	12.98	EG11819	purU	0.19	EG12069	mgo		EG11735	efeB	
EG12164	ytjC	12.97	EG20098	hpt	0.15	EG10941	selA		EG11241	ycaC	
EG10039	amn	12.63	EG10781	pssA	0.14	EG10547	lrp		EG11850	yihX	
EG13900	dhaL	12.54	EG10866	rplC	0.14	EG10663	nadE		EG11369	ubiC	
EG11030	trpS	12.53	EG10759	pps	0.11	EG11663	slyD		EG10913	rpsN	
EG10458	hsdM	12.49	EG13148	yafK		EG11286	argE		EG11284	fabZ	
EG11600	sseA	12.48	EG11088	pdhR		EG10506	infC		EG10162	cpsG	
EG11577	leuB	12.45	EG13319	rlmF		EG10164	crp		EG11323	ygfB	
EG12133	ucpA	12.44	EG12688	grxB		EG10258	eno		EG11324	ubiH	
EG10031	adhE	12.33	EG10596	minC		EG13252	queC		EG11350	rfaS	
EG13408	slyA	12.29	EG10758	ppiB		EG12669	solA		EG11351	rfaB	

EG13931	ydgJ	12.27	EG10205	dapA		EG10616	mtlD		EG11352	rfaI	
EG10222	deoD	12.14	EG13613	yajQ		EG10909	rpsJ		EG11986	wbbL	
EG10963	speE	12.04	EG10158	clpP		EG11517	glpX		EG11383	elbB	
EG13173	queF	11.89	EG10875	rplN		EG14132	gtrB		EG11679	aas	
EG10318	fldA	11.84	EG10048	apaH		EG10977	sspA		EG11375	folE	
EG10801	putA	11.73	EG10696	pepN		EG10035	aldA		EG12110	ydcF	
EG11358	murA	11.68	EG10965	gmk		EG14049	yodA		EG12108	norR	
EG14060	yegQ	11.67	EG10097	aspS		EG13656	ybeZ		EG12105	yeiE	
EG10496	ilvD	11.44	EG10402	gltA		EG12926	nudE		EG12094	sgrR	
EG11089	yacC	11.17	EG10746	polA		EG10688	pck		EG12093	nuoN	
EG13616	allR	11.02	EG12146	yhbJ		EG10415	greA		EG12045	yejH	
EG11001	thrS	11.01	EG11430	ycfD		EG10703	pgk		EG12024	yohK	
EG13759	ydcP	10.83	EG10497	ilvE		EG10274	fabB		EG11357	dinG	
EG11198	glmU	10.71	EG10803	pykA		EG11247	rumA		EG11322	ribE	
EG14165	yfeX	10.71	EG11070	dsbC		EG10709	pheS		EG11730	viaA	
EG13478	rimO	10.62	EG10947	serS		EG11058	ung		EG11394	fabR	
EG14263	folX	10.58	EG11072	xseA		EG11810	gevP		EG11408	dadX	
EG10034	alaS	10.44	EG10445	hisB		EG10789	ptsI		EG11396	ubiD	
EG12302	tmk	10.42	EG10903	rpsD		EG12303	ycfH		EG12316	acnB	
EG10666	nusB	10.39	EG13395	iscU		EG10918	rpsS		EG10912	rpsM	
EG10599	groL	10.35	EG10905	rpsF		EG10622	murF		EG12172	hinT	
EG11619	mfd	10.23	EG10900	rpsA		EG10552	lysS		EG10108	bcp	
EG10618	mukB	10.22	EG10113	bfr		EG12679	yeaD		EG11426	rfaZ	
EG10570	map	10.20	EG12479	rsgA		EG10230	dksA		EG10542	lon	
EG10788	ptsH	10.12	EG12163	rsmB		EG12866	proQ		EG11438	yceF	
EG12749	yhaJ	9.99	EG10790	purA		EG10901	rpsB		EG11786	yfiF	
EG11492	qorA	9.98	EG10283	fbp		EG11932	dusA		EG10237	dnaC	
EG11648	dkgB	9.92	EG11314	purB		EG11333	visC		EG10052	araA	
EG12777	yraL	9.91	EG10192	cysK		EG11203	yihA		EG12115	yjiG	
EG10409	glyQ	9.82	EG10368	epd		EG20091	gpsA		EG13481	yliJ	
EG12532	yjgM	9.81	EG11366	rob		EG10576	mdh		EG10583	metC	
EG13325	ybiT	9.77	EG20080	glcB		EG10450	hisH		EG12013	bglX	
EG11063	uvrC	9.71	EG10690	pcnB		EG10621	murE		EG10211	dcm	
EG11042	tyrR	9.67	EG10873	rplL		EG10910	rpsK		EG10700	pfkB	
EG10339	ftsA	9.67	EG10870	rplI		EG10978	sspB		EG11548	lhr	
EG11609	evgA	9.57	EG10786	ptrA		EG11620	rnb		EG11673	folB	
EG13376	mppA	9.49	EG12957	glk		EG10914	rpsO		EG11668	atoC	
EG11118	rhuC	9.42	EG11032	trxB		EG11759	yciK		EG11650	yaD	
EG11259	mr	9.40	EG10022	aceA		EG10021	yjiA		EG11643	ydeH	
EG12165	mukF	9.39	EG11235	rhIE		EG12752	yhaM		EG11602	glnE	
EG11487	pdxH	9.36	EG10242	dnaN		EG10416	grpE		EG11601	sseB	
EG11205	murB	9.24	EG10448	hisF		EG13969	ydiJ		EG11597	moaD	

EG11592	ybeD	9.22	EG12726	rlmG		EG10422	guaC		EG11595	moaA	
EG10236	dnaB	9.10	EG10651	nfo		EG10814	rbsA		EG11425	rfaY	
EG10066	argD	9.10	EG10916	rpsQ		EG10811	pyrI		EG11580	ybiB	
EG10074	aroB	9.04	EG12686	flu		EG10384	glnB		EG11244	yggE	
EG10372	gdhA	9.01	EG10899	rpoZ		EG10461	htpG		EG11539	pyrH	
EG10079	aroG	8.86	EG11553	glmM		EG11217	creA		EG11516	ycgB	
EG10529	lepA	8.74	EG10595	miaA		EG11443	rpiA		EG11503	yaeB	
EG11549	pepT	8.60	EG10441	ihfB		EG10553	lysU		EG11500	holB	
EG13109	truD	8.58	EG10358	fumC		EG12362	menF		EG11472	rmuC	
EG13273	thiI	8.44	EG10359	fur		EG11403	ppx		EG11467	yigI	
EG11531	cfa	8.26	EG11043	tyrS		EG50001	rplU		EG11449	hdfR	
EG12899	yheO	8.24	EG11255	ybeB		EG10207	dapD		EG11440	def	
EG11265	cmk	8.21	EG10335	frt		EG10731	phoP		EG11591	lipB	
EG13690	ltaE	8.14	EG10379	glgC		EG10630	nadA		EG10637	nanA	
EG10953	sodA	8.09	EG10566	manA		EG13305	ybgI		EG10752	potD	
EG11452	rffD	7.96	EG12130	hscA		EG11448	acs		EG10503	ilvY	
EG13968	ydiI	7.95	EG12483	rlmB		EG12366	rsmE		EG10519	kdsB	
EG10196	cysS	7.82	EG13146	lpcA		EG10328	fold		EG10523	rsmA	
EG12936	hrpA	7.75	EG11195	yidA		EG10872	rplK		EG10568	manY	
EG11022	trmA	7.72	EG10518	kdsA		EG11178	rbfA		EG10574	mcrB	
EG10697	pepP	7.72	EG11033	tsf		EG13382	yeeN		EG10579	menD	
EG11067	valS	7.72	EG10011	yaaA		EG11596	moaB		EG10592	mglA	
EG10560	malP	7.66	EG12144	pgm		EG10908	rpsI		EG10498	ilvG	
EG10741	pmbA	7.65	EG10981	sucC		EG13921	ycjX		EG10633	nagB	
EG10327	folC	7.63	EG10188	cysG		EG11015	tpiA		EG10482	zraR	
EG10208	dapE	7.60	EG10880	rplS		EG10881	rplT		EG10648	narZ	
EG12453	rraB	7.59	EG10946	serC		EG10883	rplW		EG10677	oppD	
EG11299	rng	7.58	EG10665	nusA		EG13850	ynfL		EG10678	oppF	
EG10996	tgt	7.52	EG10220	deoB		EG13688	ybjS		EG10679	osmB	
EG12600	yjx	7.51	EG12419	gatY		EG13689	ybjT		EG10683	pabB	
EG10810	pyrG	7.50	EG11746	panC		EG13701	ycaQ		EG11288	mak	
EG12098	rhuD	7.33	EG10367	gapA		EG13703	ycbK		EG10738	pldA	
EG11451	rffE	7.27	EG12606	fabF		EG13718	ycbZ		EG11212	nsrR	
EG12181	grxD	7.14	EG12158	rdgC		EG13761	ydcR		EG10594	mglC	
EG12860	yebK	7.14	EG10864	rplA		EG13766	prf		EG10357	fumB	
EG10797	purL	7.13	EG11556	talB		EG13780	nhoA		EG10209	dapF	
EG10073	aroA	6.96	EG12613	gst		EG13322	mntR		EG10225	dgt	
EG13654	ybeX	6.96	EG10871	rplJ		EG13798	ydeP		EG10239	dnaG	
EG10076	aroD	6.95	EG11699	gpmA		EG13577	wcaK		EG10246	mltD	
EG13433	nagZ	6.94	EG12803	kdsD		EG13851	cusR		EG10273	fabA	
EG11102	gsk	6.91	EG13915	ycjR		EG13879	yceM		EG10278	fadA	
EG13226	ftsK	6.91	EG10533	lexA		EG13885	iraM		EG10279	fadB	

EG11344	mnmA	6.83	EG10698	pepQ		EG13886	ycgE		EG10281	fadR	
EG10681	oxyR	6.83	EG10793	purE		EG13887	ycgF		EG10502	ilvN	
EG12440	mpl	6.74	EG11134	ydjA		EG13898	ldcA		EG10331	frdB	
EG10586	metG	6.71	EG13678	ybjI		EG13902	dhaR		EG10747	polB	
EG10094	asnS	6.70	EG11376	ftsP		EG13920	ycjW		EG10381	glgX	
EG10742	pncB	6.64	EG12272	ghrB		EG13793	yddV		EG10394	glpD	
EG11081	ispH	6.57	EG10632	nagA		EG13469	yphH		EG10413	gpp	
EG13612	dxs	6.53	EG10932	sdhB		EG10167	estA		EG10414	gpt	
EG14018	kdgR	6.47	EG13693	ybjX		EG13327	ybiV		EG10427	hemA	
EG14034	cmoB	6.46	EG12449	prnB		EG13330	gloB		EG10439	hha	
EG10370	ispG	6.37	EG10979	sucA		EG13372	pinR		EG10451	hisI	
EG10845	rho	6.36	EG20151	nfsB		EG13407	ugd		EG10454	truA	
EG11528	fabI	6.36	EG11586	thiE		EG13413	csgG		EG10329	mutM	
EG11091	frsA	6.23	EG11040	tyrB		EG13415	gmr		EG11050	ugpQ	
EG11981	glf	6.17	EG11415	dps		EG13446	nudJ		EG10763	priA	
EG11139	yecA	6.16	EG11666	moaC		EG13683	ybjN		EG10994	tdk	
EG11590	thiH	6.14	EG20173	pta		EG13451	caiF		EG10736	phr	
EG10769	proC	6.10	EG10459	hsdR		EG13658	ubiF		EG11014	topB	
EG11306	lipA	6.01	EG10993	tdh		EG13482	ydjF		EG11019	trkA	
EG10004	dfp	5.98	EG10051	apt		EG13489	yeaC		EG11023	trmD	
EG11574	thiB	5.98	EG12678	znuA		EG13497	yeaK		EG11028	trpE	
EG11317	fabD	5.95	EG10362	galE		EG13502	yeaP		EG11038	tus	
EG10702	pgi	5.93	EG10489	ied		EG13506	yeaT		EG10976	ssb	
EG14104	yfbT	5.75	EG13861	efeO		EG13513	yoaA		EG11044	ubiX	
EG11757	yjeE	5.70	EG10879	rplR		EG13514	yoaB		EG10986	tag	
EG10080	aroH	5.58	EG13084	ygdL		EG13566	wza		EG11078	nhaR	
EG10799	purN	5.57	EG12411	rftD		EG13942	anmK		EG11080	fkpB	
EG10982	sucD	5.54	EG12903	yheS		EG13447	rluE		EG11109	mngR	
EG11837	typA	5.53	EG10865	rplB		EG11387	amyA		EG11165	ygiC	
EG11315	yhdH	5.50	EG13324	ybiS		EG13923	ycjZ		EG11188	htrL	
EG10071	argS	5.48	EG10975	srmB		EG14196	tmcA		EG11201	yigA	
EG11320	nrdR	5.42	EG10376	rsmG		EG14201	hda		EG11210	yjdA	
EG11329	gabD	5.40	EG12197	seqA		EG14224	yfiQ		EG11211	poxA	
EG12343	yjjK	5.40	EG11585	thiC		EG20249	uxuR		EG11039	tyrA	
EG11221	zwf	5.40	EG11024	trpA		EG40007	insG		EG10897	rpoH	
EG12179	cspE	5.33	EG12412	rftB		EG40008	insH		EG10816	rbsC	
EG12204	cspC	5.30	EG10906	rpsG		EG50006	eutB		EG10820	rcsA	
EG10121	bioF	5.16	EG13820	ydfH		EG14168	ypeA		EG10822	rcsC	
EG10662	nth	5.14	EG10701	pflB		EG10338	fruR		EG10824	recB	
EG11177	truB	5.13	EG10492	ileS		EG14164	yfeW		EG10825	recC	
EG12792	yhbW	5.07	EG10284	fdhE		EG10036	puuC		EG10826	recD	
EG10270	era	5.03	EG12838	yrdA		EG10093	asnC		EG10828	recF	

EG14207	der	5.00	EG10695	pepD		EG10119	bioC		EG10830	recJ	
EG11537	yceH	4.96	EG10983	suhB		EG10130	btuR		EG10831	recN	
EG11623	sdaB	4.94	EG12695	azoR		EG10140	chbB		EG10833	recQ	
EG10756	ppc	4.91	EG10792	purD		EG10142	chbA		EG10837	rep	
EG12296	gpmM	4.90	EG10707	pheA		EG10144	chbF		EG10995	tesB	
EG12399	dhaM	4.87	EG10800	purR		EG10161	cpsB		EG10861	rmhB	
EG10277	fabH	4.87	EG11581	ybiC		EG10869	rplF		EG10962	speD	
EG10215	deaD	4.79	EG11921	rluF		EG40012	insL		EG10921	ftnA	
EG10942	selB	4.74	EG11978	rfbA		EG14062	fbaB		EG10933	sdhC	
EG11427	tktA	4.74	EG10650	ndk		EG13307	ybgK		EG10934	sdhD	
EG13452	trmJ	4.73	EG11079	ribF		EG13948	yobD		EG10935	sdiA	
EG12414	gatA	4.70	EG10248	dppA		EG13962	sufS		EG10957	soxR	
EG12935	nfuA	4.67	EG10815	rbsB		EG13963	sufD		EG10958	soxS	
EG10926	sbcB	4.67	EG11960	rpe		EG13965	sufB		EG10851	rimJ	
EG11441	prlC	4.65	EG10877	rpIP		EG13974	ydiO		EG11192	yicC	
EG50002	rpmA	4.63	EG11384	ahpC		EG13980	ydiU		EG11013	topA	
EG12503	flkIB	4.62	EG11589	thiG		EG13993	cho		EG11199	mioC	
EG11321	ribD	4.61	EG10256	eda		EG14172	intZ		EG10961	speC	
			EG10589	metK		EG14045	yedW		EG11098	xseB	

7.2 List of abbreviations

Units are expressed according to the international system of units (SI). For the amino acids, one and three letter codes were used.

AA	acrylamide
ADP	adenosine 5'-diphosphate
Amp	ampicillin
AMP	adenosine 5'-monophosphate
APS	ammonium peroxodisulfate
ATP	adenosine 5'-triphosphate
BSA	bovine serum albumin
BG	background
CID	CID
Clp	caseinolytic protease
Cm	chloramphenicol
COG	Clusters of Orthologous Groups of proteins

Δ (delta)	deletion
NBD	nucleotide-binding domain
DNA	deoxyribonucleic acid
DnaJ	bacterial Hsp40 chaperone
DnaK	bacterial Hsp70 chaperone
DTT	dithiothreitol
ECL	enhanced chemiluminescence
<i>E. coli</i>	<i>Escherichia coli</i>
EDTA	ethylenediaminetetraacetic acid
emPAI	exponentially modified protein abundance index
FA	formic acid
FDR	false discovery rate
FPR	false positive rate
FT ICR	fourier transform ion cyclotron resonance
FRET	fluorescence resonance energy transfer
GFP	Green fluorescent protein
GRAVY	grand average of hydropathy of protein sequences
GroEL	large <i>growthE</i> gene product
GroES	small <i>growthE</i> gene product
GrpE	Growth P-like gene E
HEPES	N-(2-hydroxyethyl)piperazin-N'-2-ethanesulfonic acid
His6	histidine tag
HPLC	high-performance liquid chromatography
HRP	horseradish peroxidase
Hsc	heat shock cognate protein
HSF	heat shock factor
Hsp	heat shock protein
IMAC	immobilized metal ion affinity chromatography
IPTG	isopropyl- β -D-1-thiogalactopyranoside
<i>k</i>	rate
Kan	kanamycin

K _D	dissociation constant
kDa	kilodalton
LB	Luria Bertani
LTQ	linear quadrupole ion trap
Luc	Luciferase
MAD	median absolute deviation
MS	mass spectrometry
MW	molecular weight
NAC	nascent chain-associated complex
NBD	nucleotide binding domain
NEF	nucleotide exchange factor
NMR	nuclear magnetic resonance
OD	optical density
PAGE	polyacrylamide gel electrophoresis
PBS	Phosphate buffered saline
PBD	peptide binding domain
PD	pulldown
PEP	posterior error probability
PCR	polymerase chain reaction
PDB	protein data bank
PFD	prefoldin
pI	isoelectric points
PPIase	peptidyl-prolyl <i>cis/trans</i> isomerase
REF	relative enrichment factors
RAC	ribosome-associated complex
RNA	ribonucleic acid
rpm	revolutions per minute
RT	room temperature
<i>S. cerevisiae</i>	<i>Saccharomyces cerevisiae</i>
SBD	substrate binding domain
SD	standard deviation

SDS	sodium dodecylsulfate
SILAC	stable isotope labeling with amino acids in cell culture
SRP	signal recognition particle
TBS	Tris-buffered saline
TFA	Trifluoroacetic acid
TTBS	Tween / Tris-buffered salt solution
TEMED	<i>N,N,N',N'</i> -tetramethylethylenediamine
TF	trigger factor
<i>Tm</i>	<i>Thermotoga maritime</i>
TPR	tetratricopeptide repeat
Tris	trishydroxymethylaminomethan
UV	ultraviolet
v/v	volume per volume
WT	wild type
w/v	weight per volume
YPD	yeast extract peptone dextrose

7.3 Publication

Shao-Jun Dai, **Taotao Chen**, Kang Chong, Yongbiao Xue, Tai Wang. Proteomics identification of differentially expressed proteins associated with pollen germination and tube growth reveals characteristics of germinated *Oryza sativa* pollen. Mol Cell Proteomics 2007 6, 207-230.

Shao-Jun Dai, Lei Li, **Taotao Chen**, Kang Chong, Yongbiao Xue, Tai Wang. Proteomic analyses of *Oryza sativa* mature pollen reveal novel proteins associated potentially with pollen germination and tube growth. Proteomics, 2006 Proteomics 6, 2504-2529.

Giulia Calloni*, **Taotao Chen***, Sonya Schermann, Hung-chun Chang, Pierre Genevaux, Manajit Hayer-Hartl and F.Ulrich Hartl. DnaK functions as a central hub in the E. coli chaperone network. Submitted to Cell.

* Equal contribution

7.4 Oral presentations

“Analysis of the DnaK (Hsp70) interactome: Interplay of the two main chaperone principles in *Escherichia coli*” Proteomic in Time and Space (PROSPECTS), 2nd Plenary European Union Projects Meeting, November 2010, Taormina, Sicily, Italy.

7.5 Posters

Taotao Chen, Giulia Calloni, Sonya Schermann, Manajit Hayer-Hartl, and Ulrich Hartl. “Analysis of the DnaK (Hsp70) interactome: Interplay of the two main chaperone principles in *Escherichia coli*” EMBO conference series, the biology of Moleculare Chaperones May 2011, Grundlsee, Austria.

Taotao Chen, Giulia Calloni, Sonya Schermann, Manajit Hayer-Hartl, and Ulrich Hartl. “Analysis of the DnaK (Hsp70) interactome: Interplay of the two main chaperone principles in *Escherichia coli*” Proteomic in Time and Space (PROSPECTS), 2nd Plenary European Union Projects Meeting, November 2010, Taormina, Sicily, Italy.

Taotao Chen, Giulia Calloni, Sonya Schermann, Manajit Hayer-Hartl, and Ulrich Hartl. “Identification and Characterization of the Substrate Proteome of the Chaperone DnaK” Interaction proteome, sixth framework programme European Union Projects Meeting, Sep 2009, Majucar, Spain.

7.6 Curriculum vitae

Name:	Taotao Chen
Date of birth:	10, December, 1982
Nationality:	China

Dissertation

February 2007 – Present	Ph.D. dissertation directed by Prof. Dr. F. Ulrich Hartl in Department of Cellular Biochemistry, Max-Planck Institute of Biochemistry, Martinsried: “ <i>Analysis of the DnaK (Hsp70) interactome: Interplay of the two main chaperone principles in Escherichia coli</i> ”
-------------------------	---

Education

September 2003 – December 2006

Master of Science

Institute of Botany, the Chinese Academy of Sciences, and Graduate University of the Chinese Academy of Sciences, Beijing, China

September 1999 – June 2003

Bachelor of Life Science


College of life science, Henan Normal University, Henan, China

Prize

EMBO Poster Prize May 2011

“Analysis of the DnaK (Hsp70) interactome: Interplay of the two main chaperone principles in *Escherichia coli*” EMBO conference series, the biology of Moleculare Chaperones May 2011, Grudlsee, Austria.

Munich, 12. 12. 2011



Tatoao Chen